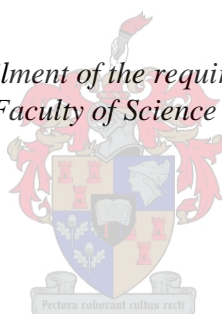


The Synthesis of Novel Kinase Inhibitors using Click Chemistry

by
Luke Hodson

*Thesis presented in fulfilment of the requirements for the degree of
Master of Science in the Faculty of Science at Stellenbosch University*



Supervisor: Prof Willem A. L. van Otterlo
Co-supervisor: Dr Stephen C. Pelly
Faculty of Natural Science
Department of Chemistry and Polymer Science

"

"

"

"

"

"

.....Cr tki'4236"

DECLARATION

By submitting this thesis electronically, I declare that the entirety of the work contained therein is my own, original work, that I am the sole author thereof (save to the extent explicitly otherwise stated), that reproduction and publication thereof by Stellenbosch University will not infringe any third party rights and that I have not previously in its entirety or in part submitted it for obtaining any qualification.

February 2014

Copyright © 2014 Stellenbosch University

All rights reserved

ABSTRACT

Cancer is the leading cause of death on the planet, killing an estimated 8.2 million people in the year of 2012. The disease is associated with two families of genes, namely oncogenes and tumour suppressor genes. The hallmarks of cancer pathogenesis include gene amplification, point mutations or chromosomal rearrangements within these genes. Kinases are responsible for the reversible phosphorylation of proteins, which plays a significant and extensive role in cellular signal transduction. Aberrant kinase activity provokes overexpression, mutations and chromosomal translocation and results in the onset of onco- and tumorigenesis, ultimately leading to cancer.

Inactivation of this class of enzyme is thus critical as it would result in the suppression of these unwanted activities. For this, researchers have developed kinase inhibitors, specifically targeting these proteins and thus inhibiting signal transduction pathways and tumour growth. This has resulted in great successes, particularly in the case of the commercial inhibitor, imatinib. However, resistance to approved therapeutic agents through mutations has resulted in the search for more potent and selective inhibitors to overcome these obstacles.

This project involved the synthesis of bioactive heterocycles linked to 1,2,3-triazoles using either a C-C or C-N bond forming strategy. The synthetic methodology followed included the use of Sonogashira coupling reactions between 3-bromoquinoline, 7-chloro-4-iodoquinoline, 4-bromoisoquinoline and 5-bromoisoquinoline and trimethylsilylacetylene (TMSA), followed by deprotection of the TMS group to yield heterocycles bearing terminal alkynes. The synthesis of both benzyl azide and 2-(azidomethyl)pyridine as azide fragments, allowed for subsequent coupling of the synthesized azide and alkyne fragments through copper-mediated click chemistry, affording a library of 1,4-substituted 1,2,3-triazole based reversible kinase inhibitors. Synthesis of a second library of *o*-, *m*- and *p*-substituted nitro benzyl azides, allowed for both copper- and ruthenium-mediated click reactions, between the alkynes and nitro benzyl azides synthesized, to yield 1,4- and 1,5-substituted 1,2,3-triazoles, respectively. Finally, reduction of the incorporated *o*-, *m*- and *p*- substituted nitro group, and acylation of the resultant amine with acryloyl chloride, resulted in the incorporation of the important Michael acceptor moiety required for irreversible inhibition. This afforded a library of both reversible and potential irreversible triazole-based kinase inhibitors through efficient copper- and ruthenium-mediated click chemistry.

Biological screening and activity assays against the wildtype, and two mutated forms of the EGFR kinase, were undertaken with these synthesized compounds. A number of synthesized inhibitors showed good selectivity for the mutated forms of the EGFR kinase only. The most potent inhibitor *N*-{2-([4-(isoquinolin-4-yl)-1*H*-1,2,3-triazol-1-yl]methyl}phenyl}acrylamide, displayed efficacy in the low μM range - comparable to that of the FDA approved drug, gefitinib.

The synthetic methodology derived in this project could be applied to the use of biological space probes with further investigatory research. Furthermore, from the biological screening results obtained, and the selectivity profile shown by these inhibitors, the synthesis of a second generation library of compounds is an additional research possibility.

UITTREKSEL

Kanker is die hoof oorsaak van sterftes ter wêreld, wat verantwoordelik is vir die dood van ongeveer 8.2 miljoen mense in die jaar 2012. Die siekte word geassosieer met twee geenfamilies, naamlik onkogene en gewasonderdrukkingsgene. Die kenmerke van kanker pathogene behels geenversterking, puntmutasies of chromosomale herrangskikking binne in die gene. Kinase is verantwoordelik vir die omkeerbare fosforilering van proteïene wat 'n uiters belangrike rol in sellulêre sein transduksie speel. Abnormale kinase aktiwiteit lei tot ooruitdrukking, mutasies en chromosomale translokasie wat tot die ontwikkeling van onkogene groei en wat eindelik tot kanker lei.

Deaktivering van die klas van ensieme is dus krities want dit sal die ongewenste abnormale aktiwiteite onderdruk. As gevolg van die bogenoemde, het navorsers kinase inhibeerders ontwikkel wat die spesifieke proteïen teiken en hiermee die sein transduksie roete asook gewas groei inhibeer. Hiermee het die sukses van inhibeerders veral die kommersiële inhibeerder, imatinib, grootliks toegeneem. Oor die afgelope jare het die belangstelling in die ontwikkeling van meer selektiewe en kragtige inhibeerders toegeneem as gevolg van die weerstand wat goedgekeurde terapeutiese middels opbou.

In hierdie projek is daar gebruik gemaak van 'n C-C of C-N bindingsvorming strategie om bioaktiewe heterosikliese molekules te sintetiseer wat gekoppel is aan 1,2,3-triasool funksionele groepe. Die sintetiese metode maak gebruik van Sonogashira reaksies vir die 3-bromo-kwinolien, 7-chloro-4-iodokwinolien, 4-bromoisokwinolien en 5-bromoisokwinolien met trimetielsilielasetileen (TMSA), gevolg met die ontskerming van die TMS-groep om die terminale alkyn op die heterosiklus te ontbloot. Die asied fragmente, bensiel asied en 2-(asidometiel)piridien, was toe gesintetiseer om met die gevormde heterosiklus alkyne 'n koper ondersteunende kliek chemie te ondergaan. 'n Reeks van 1,4-digesubstitueerde 1,2,3-triasool gebaseerde omkeerbare kinase inhibeerders is toe gevorm. 'n Tweede reeks met *o*-, *m*-, en *p*- gesubstitueerde nitro bensiel asiede was gesintetiseer om 1,4- en 1,5- digesubstitueerde 1,2,3-triasole te sintetiseer met behulp van koper- en ruthenium ondersteunende kliek chemie. Laastens was die *o*-, *m*-, en *p*- nitro groepe gereduseer om 'n primêre amien te vorm. Die gevormde amien het 'n asileringsreaksie met akriloiel chloried ondergaan om die kern, die Michael akseptor, te inkorporeer. Die Michael akseptor word benodig om 'n onomkeerbare inhibitiese aktiwiteit te kan uitvoer. Die projek het dus met behulp van kliek chemie, twee

1,2,3-triasool reekse gelewer wat omkeerbare en onomkeerbare inhibitiese aktiwiteit kan uitvoer.

Die verbindings gesintetiseerd in hierdie projek het keuringstoetse ondergaan teen die wilde tipe en teen twee gemuteerde forme van die EGFR kinase ensiem. Van hierdie verbindings het goeie selektiwiteit vertoon teenoor die gemuteerde EGFR kinase ensiem. Die mees aktiewe inhibeerder, *N*-{2-[4-isokwinolin-4-iel)-1*H*-1,2,3-triasool-1-iel]feniel}akrielamied, het aktiwiteit in die lae μM reeks vertoon. Dié inhibisie waarde is vergelykbaar met die FDA goedgekeurde medikasie, gefitinib.

In hierdie projek is sintetiese metodes ontwikkel wat toegepas kan word op meer intensiewe biologiese ondersoeke en asook meer navorsing. Die resultate verkry van die biologiese aktiwiteit, asook die verbindings se selektiwiteit, gee die moontlikheid vir die ontwikkeling en sintese van 'n tweede generasie verbindings.

ACKNOWLEDGEMENTS

Personal Acknowledgements

It is with a fond and gracious heart that I look back on the years of 2012 and 2013. I can't think of a time that I've learnt more about life than in the span of these last two years. Throughout this time I've acquired a great deal of memories, experiences, triumphs and losses. I've learnt that in chemistry, a passion and love for what you do is not enough. A stalwart determination and patience is required in this field, something I am grateful to have learnt. I like to think I am an adult now, or at least approaching that landmark. The very toughness and unforgiving nature of research in organic chemistry - which has caused an abundance of frustration and vexation in my life to put it mildly - has consequentially taught me that nothing in life worth having, is not achieved through hard work. Smooth sailing never made a skilled sailor, and it is through these hardships and trials and tribulations that we learn and grow as human beings. I have my sweetest mistress, organic chemistry, to thank for this.

At the top of my list I would like to thank my supervisor Professor Willem van Otterlo. You have been a father figure to me in the time I have known you since 2011. You are a role model not only in academia, but in the diplomatic and fair way you treat everyone, no matter what their title or role. I have so much respect for the love you have for your family, and how you put them first. It really does shine through. I am grateful for all the opportunities and guidance you have given me and I look forward to working with you for the next few years. This luckily equates to more biltong for you.

To my co-supervisor Dr Steven Pelly, there are two things in this world you have a colossal knowledge of - beer and molecular modelling. I would thus like to thank you for the fine beer that you brew and the complete education you have given me in molecular modelling. It is a fine skill to possess and I believe I have learnt from the best teacher on the continent.

I would like to especially thank Dr Gareth Arnott - you reached this kid! Thank you for all the advice and input in my project and always having a free minute to talk to me any time during the day. You are a metaphorical well of synthetic information and you inspire me to want to always inspect and question the finer details, which really is the beauty of science.

For all the NMR analytical data I would like to thank Dr Jaco Brand and Ms Elsa Malherbe. For the MS data I would like to acknowledge CAF and Dr Marietjie Stander. Elsa cheered me

up on numerous occasions upon days of experiencing that dreaded feeling of not acquiring the correct spectra. I would also like to thank Dr Daniel Rauh and Julian Engel at the Technische Universiteit Dortmund for their work on the biological screening assays. I look forward to further collaboration and perhaps sampling some of your world renowned beer in the future.

To the group of medicinal and organic chemistry, I find myself extremely privileged and grateful to work with such an amazing, if not slightly weird, assembly of people. The best people are the crazy ones and for this I must single out Leon Jacobs. Thank you for teaching me how to do my first column, I like to think I have come a long way from my humble beginnings. Derik Wilbers, the epitome of a true gentleman, thank you for being such a loyal friend. To Jacques Vogeli, my oldest friend, we've seen quite a lot since we met in 1999. Here's to the next 15 years.

I am a person that believes family comes first. So I feel extremely blessed to be able to call the most extraordinary people I know, my family members. Thank you for always being so strong mom. Words would never be able to express the gratitude and respect I have for you. For all the sacrifices you have made and putting your children in front of yourself in all things. You are the best person I know. I call myself lucky to such a good relationship with my sister. Thank you for always looking after me Loreen. You know me better than anyone else, and only we can laugh the way we do. Thank you dad for all the words of wisdom and fatherly advice you've given me sitting around a fire at many hunting trips.

Lastly, but most certainly not least, I would like to thank my best friend, who just so happens to be my girlfriend and soulmate. Thank you Alet, for being the beautiful person you are. You've taught me what life is all about. Thank you for always wanting what's best for me, and more importantly showing me to want it for myself as well.

Im sure the piano would have started playing by now if I were at the Emmys or Oscars, but I feel very blessed and privileged to be able to say that when I wake up in the morning the first thing I think and look forward to, is getting into the lab to start working. Even on Mondays. Every day brings challenges but most importantly to me, it brings something new to learn. I count myself very lucky and amongst and rich in the world to have this.

Acknowledgements for Funding

Money makes the world go round and this is no more evident than in the field of science. Without proper funding, this MSc project would not have been possible.

Therefore I would like to extend my thanks to The National Research Foundation (NRF) for their generous contribution in the form of a bursary.

Declaration	2
Abstract.....	3
Uittreksel	5
Acknowledgements	7
Personal Acknowledgements	7
Acknowledgements for Funding.....	8
List of Abbreviations	13
CHAPTER 1 – CANCER AND TARGETED TREATMENT	14
1.1 Cancer.....	14
1.1.1 Statistics, Definition and History	14
1.1.2 Causation of Cancer and Prevention	20
1.1.3 The Evolution of Cancer Treatment.....	27
1.2 Targeted Therapy.....	35
1.2.1 The Revolution of Targeted Therapy	35
1.2.2 Molecular-Targeted Treatments – Successes and Challenges.....	36
1.2.3 The Scope of Targeted Therapy and the 21 st Century.....	41
CHAPTER 2 – KINASES AND KINASE INHIBITORS	47
2.1 Kinases	47
2.1.1 The Origins and Mechanism of Protein Phosphorylation	47
2.1.2 The Eukaryotic Protein Kinase Superfamily and the Protein Kinase Complement of the Human Genome.....	50
2.1.3 Oncogenic Kinase Signalling.....	54
2.2 Kinase Inhibitors.....	57
2.2.1 Protein Kinase Inhibitors – an Overview.	57
2.2.2 Design, Synthesis and Modes of Binding.	60
CHAPTER 3 – 1ST GENERATION REVERSIBLE INHIBITOR LIBRARY.....	64
3.1 Synthetic Methodology, Target Strategy and Driving Group.....	64
3.1.1 The Paper that started it all.	64
3.1.2 Rationale of Target Kinase: EGFR	66
3.1.3 Choice of Heterocyclic Driving Groups and Side Chains.....	68

3.2 Synthesis of Alkyne Fragments	70
3.2.1 Sonogashira Coupling and Silyl Deprotection.	70
3.2.2 Optimization of Reaction Conditions.....	72
3.3 Synthesis of Azide Side Chain Fragments.....	76
3.3.1 Synthesis of benzyl azide and 2-(azidomethyl)pyridine.	76
3.4 Generation of Combinatorial Library from Azide and Alkyne Fragments	78
3.4.1 Defining “Click” Chemistry.....	78
3.4.2 The 1,4-Copper Catalysed Azide Alkyne Cycloaddition (CuAAC).	79
3.4.3 Catalytic Cycle and Mechanism.	80
3.4.4 Synthetic Optimization and Generation of Library of Novel Reversible Inhibitors	81
CHAPTER 4 – 1ST GENERATION IRREVERSIBLE INHIBITOR LIBRARY	86
4.1 Motivation, Rationale and Strategy for Synthesis of Irreversible Inhibitor Library	86
4.1.1 Irreversible Inhibitors – Successes and Advantages.	86
4.1.2 Rationale and Proposed Synthetic Strategy for Irreversible “Space Probing” Inhibitor Library.	89
4.2 Synthesis of Library of 1,5- Substituted Potential Irreversible Inhibitors.	91
4.2.1 Synthesis of Nitrobenzyl Azide Fragments.....	91
4.2.2 The Ruthenium Catalysed Azide Alkyne Cycloaddition Reaction.	91
4.2.2 Catalytic Cycle and Mechanism.	93
4.2.3 Synthetic Optimization and Generation of Library of Novel Irreversible Inhibitors	94
4.2.4 Reduction of Aromatic Nitro and Addition of Acryl Amide Moiety to Clicked Compounds.	98
CHAPTER 5 – BIOLOGICAL EVALUATION OF SYNTHESIZED POTENTIAL KINASE INHIBITORS AND CONCLUSIONS	102
5.1 Biological Screening Methodology	102
5.1.1 Professor Daniel Rauh’s Research Focus – Fluorescent Labelling in Kinases.	102
5.1.2 Methodology Used in Screening of Reversible and Irreversible Inhibitors against EGFR.....	104
5.2 Results and Discussion	105
5.3 Conclusions	108
CHAPTER 6 – FUTURE WORK	110
6.1 Future Work.....	110
6.1.1 2 nd Generation Library Based on Compound AT5.....	110
6.1.2 Biological Space Filling and Cysteine Targeting Probes	112

CHAPTER 7 – EXPERIMENTAL	114
7.1 General procedures	114
7.1.1 Purification of solvents and reagents.	114
7.1.2 Chromatography	114
7.1.3 Spectroscopic and physical data	114
7.1.4 Other general procedures	115
7.2 Synthesis Pertaining to Chapter 3.	115
7.2.1 Compounds 2a-b.	115
7.2.2 Compounds 2c-d.	117
7.2.2 Compounds 3a-b.	118
7.2.2 Compounds 4a-d.	119
7.2.3 Compounds 5a-d.	122
7.3 Synthesis Pertaining to Chapter 4.	124
7.3.1 Compounds 6a-c.	124
7.3.1 Compounds 7a-l.	126
7.3.2 Compounds 8a-l.	133
CHAPTER 8 – REFERENCES	142

LIST OF ABBREVIATIONS

AAC – Azide alkyne cycloaddition	mAbs – Monoclonal antibodies
Abl – Abelson murine leukemia viral oncogene homolog 1	MAP – Mitogen-activated protein kinases
ADP – Adenosine diphosphate	NCI – National Cancer Institute
ALL – Acute lymphoblastic leukemia	NGF – Nerve growth factor
ALK – Anaplastic lymphoma kinase	NSCLC – Non-small-cell lung carcinoma
aPK – Atypical lymphoma kinase	PARP – Poly ADP ribose polymerase
ATP – Adenosine triphosphate	PDB – Protein data bank
BCR – Breakpoint cluster region	PDGF – Platelet derived growth factor
BRM – Biological response modifier	PDK1 – Phosphoinositide-dependent kinase-1
cAMP –Cyclic adenosine monophosphate	PKA – Protein kinase A
CMCK – Calcium -dependent protein kinase	PKC – Protein kinase C
CML – Chronic myelogenous (or myeloid) leukemia	PTK – Protein tyrosine kinase
COD –Cyclooctadiene	RPTK – Receptor protein tyrosine kinase
Cp –Cyclopentadiene	Ser – Serine
CuAAC – Copper catalysed azide alkyne cycloaddition	SERM – Selective estrogen-receptor modulator
Cys – Cysteine	Src – Sarcoma
EGF – Epidermal growth factor	SVCP – Special virus cancer program
EGFR –Epidermal growth factor receptor	T790M – Threonine790 mutation
ePK –Eukaryotic <i>protein kinases</i>	TAF – Tumour angiogenesis factor
EPR – Electron paramagnetic resonance	TBAF – Tetrabutyl ammonium fluoride
FLiK – Florescent labelling in phosphatases	TBAI – Tetrabutyl ammonium iodide
FLiP – Florescent labelling in phosphatases	TGF – Transforming growth factor
FRET – Fluorescence resonance energy transfer	Thr – Threonine
GIST – Gastrointestinal stroma tumors	TK – Tyrosine kinase
Glu– Glutamic acid	TMSA – Trimethylsilyl acetylene
HBV –Hepatitis B	Tyr – Tyrosine
HER2 – Human epidermal growth factor	VEGF – Vascular endothelial growth factor
HGP – Human Genome Project	
HPV – Human papillomavirus	
IARC - International Agency for Research on Cancer	
JAK – Just another kinase	
KSP – Kinesin spindle protein	
L858R – Leucine 858 mutation	
LK – Lipid kinase	

CHAPTER 1 – CANCER AND TARGETED TREATMENT

1.1 CANCER

1.1.1 Statistics, Definition and History

Cancer is the chief cause of death worldwide, leading mortality causation in economically developed countries and second in developing countries.¹ In 2002, the inaugural GLOBOCAN series of the International Agency for Research on Cancer (IARC) estimated that there were 10.9 million new cases and 6.7 million deaths in the year due to cancer.² In 2004, deaths due to cancer amounted to 12.6% of total deaths worldwide, coming second only to heart disease related deaths with 15.1%.³ In 2008, the number increased to an estimated 12.7 million new cases and 7.6 million deaths for the year. This translates to approximately 21000 deaths per day and 13% of all deaths worldwide per annum. Globally, cancer is the culprit for one in eight deaths and is the cause of more deaths than AIDS, tuberculosis and malaria combined.⁴

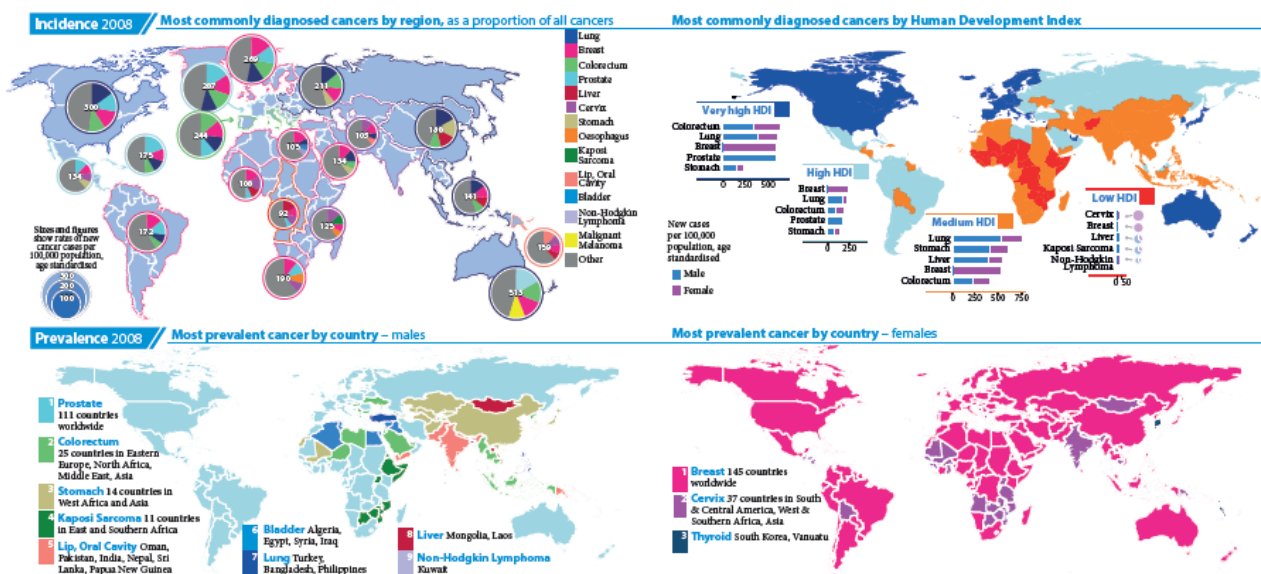


Figure 1

Illustration of worldwide statistics gathered from GLOBOCAN 2008.⁵

Most recently, in 2012, 14.1 million new cases and 8.2 million deaths were estimated in the year – an 11% and 7.8% increase, respectively, since 2008. Prevalence estimates exhibited that there were 32.6 million people alive, above the age of 15, who had been diagnosed with cancer in the last 5 years. 57% (8 million) of new cancer cases, 65% (5.3 million) of the cancer deaths and 48% (15.6 million) of the 5-year prevalent cancer cases occurred in the less

Chapter 1 – Cancer and Targeted Treatment

developed regions. The most commonly diagnosed cancers worldwide illustrated in Figure 1, were those of the lung (1.8 million, 13.0% of the total), breast (1.7 million, 11.9%), and colorectum (1.4 million, 9.7%). The most common causes of cancer death were cancers of the lung (1.6 million, 19.4% of the total), liver (0.8 million, 9.1%), and stomach (0.7 million, 8.8%).⁶ Projections based on these estimations display a substantial increase to 19.3 million cases by the year 2025, and 21.4 million cases and 13.2 million deaths by 2030.⁷ These increases can largely be attributed to the growth and aging of the human population, a consequence of reductions in childhood mortality and deaths due to infectious diseases in developing nations. As developing countries advance through accelerated societal and economic transitions, they are ultimately more likely to become “Westernized”. With Westernization and the adoption of Western lifestyles - which includes the use of tobacco, poor diet choice and lack of physical activity – it can be deduced that the pattern of cancer incidences, especially that of lung, breast and colorectal cancer, so evident in developed countries, will follow.⁸

Closer to home, these predictions and evaluations are becoming a reality. With over 715 000 newly recorded cancer cases and 542 000 deaths occurring in the year 2008 on the African continent due to cancer, a significant number which is estimated to double in the next 20 years, the burden of cancer is becoming heavier every day.

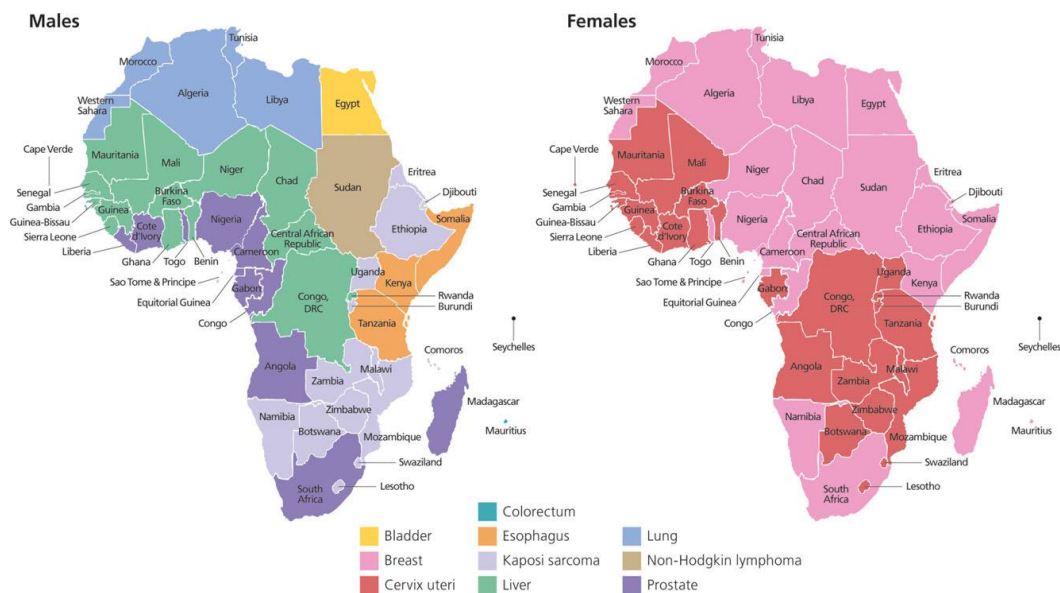


Figure 2

Illustration of most common cancers by gender and country in Africa gathered from GLOBOCAN 2008.⁹

Furthermore, an increasing number of lung, female breast and prostate cancer cases are being documented as shown in Figure 2.⁹ In the face of these daunting statistics and harsh realities, opportunities for cancer prevention and control on our native soil, as well as worldwide, must be undertaken.

Cancer, which is medically termed *malignant neoplasm*, is the collective name given to an expansive group of diseases which are mainly characterised by unregulated cellular division and growth. In cancer, the rapid division of abnormal cells leads to the formation of malignant tumours which grow beyond their usual capacity and boundaries. This results in the invasion of adjoining body parts and possibly vital organs.¹⁰ Cancer may also spread via the lymphatic system and bloodstream to other remote areas of the body. This process is referred to as metastasis, and if the spread is not controlled or regulated it can result in death. Metastases are the major cause of death from cancer. Cancer can evolve from almost any type of cell and you can develop cancer in any organ of the body. There are over 200 different types of cancer known and over 60 different organs in the human body where cancer can grow.¹¹

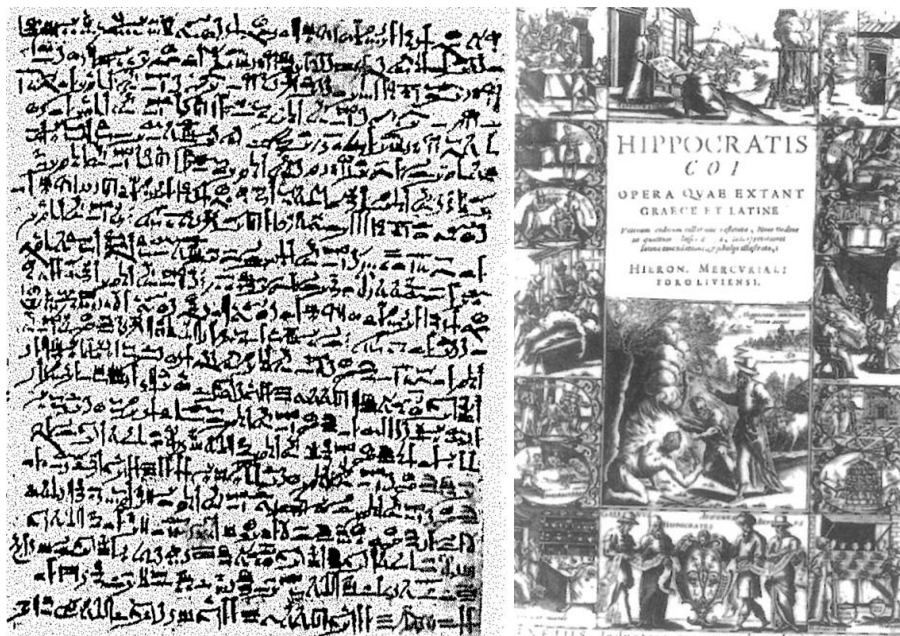


Figure 3

a) (left) The Edwin Smith Papyrus and b) (right) The printed collected writing of Hippocrates circa 1588 in Venice.¹²

It has been said that cancer is as old as the human race; however discoveries in the field of paleopathology indicate the existence of tumours in prehistoric animals, predating the advent of man. The oldest medical description of what we call cancer, dates back to approximately

3000 BC and can be found written in the Edwin Smith Papyrus, an ancient Egyptian manual for surgery illustrated in Figure 3a. It recounts 8 incidents of tumours or ulcers in the breast area, with the writer concluding that there is no treatment or cure for the disease. The attempted treatment entailed cauterisation by making use of a fire drill. It is interesting to note that the Egyptian manner of remedy for tumours and cancerous growths using arsenic paste, known as “Egyptian ointment,” remained in use up until the 19th century. Fast forwarding approximately 2600 years brings us to the time of the Greek physician Hippocrates (460-375 BC), considered the “Father of Medicine.” Hippocrates is credited with the coining of the term “cancer” from the Greek words *carcinos* and *carcinoma*, names Hippocrates gave to describe non-ulcer- and ulcer- forming tumours respectively. The Greek words translate to crab - what the bulging, finger like protrusions of tumours reminded him of. Treatment at the time included salves and ointments and cautery for surface lesions, whilst deep tumours were removed by knife or regarded as untreatable.¹² A printed collection of his writings, still effective at the end of the 16th century, is pictured in Figure 3b.

With the incorporation of Greece into the Roman Empire in 146 BC, Greek physicians now became Roman citizens. Among these was Aulus Celsus (25 BC-AD 50), an authoritative physician who modelled Latin as the language of medicine and transcribed the Greek terms Hippocrates used, to the Latin name for crab – *cancer*. Another native of Greece, Claudius Galen (130-200), used the Greek term for swelling, *oncos*, to describe tumours. Both the terms that Hippocrates, Celsus and Galen brought into existence are still used today – to describe the study malignant growths and cancer specialists respectively, namely oncology and oncologists.^{12,13}

The Renaissance was a time of great development in scientific thinking and the application thereof. Thinkers such as Galileo Galilei (1564-1642) and Isaac Newton (1643-1727) introduced the use of scientific method which was later applied to study diseases. William Harvey (1578-1657), who shed light on human circulation by performing autopsies.¹² The pioneering work of Giovanni Batista Morgagni (1682-1771) also propelled cancer research forth. He is remembered as a giant of the time because of the relations he drew from patient’s conditions and post-mortem conclusions derived from autopsies, and the importance of persuading his colleagues - and the medicinal field in general – that the further advancement of medicine lay in clinicopathologic correlation. His published work in 1761, *De Sedibus, et*

Causis Morborum, connected and linked analytic and post-mortem data from over 700 autopsies.¹⁴

Significant advances were made in anatomy, pathology and surgical techniques which served as a foundation for the modern advancements in the 18th and 19th centuries. Despite the innovation and improvement achieved at the time, surgery was used as a last ditch remedy to save the patient's life. This was predominately due to the pain subjects had to endure *sans* anaesthesia. It is noted that during these centuries most patients would rather die than go through the agony of surgery. William T.G. Morton (1819-1868) is considered the founder of modern anaesthesia, and administered the anaesthetic (sulphuric ether), in the first surgical operation under general anaesthetic. The surgery - removal of a large vascular tumour on the neck - was carried out by John Collins Warren on 16 October 1846 in the Massachusetts Hospital in Boston.¹⁵ It is important to note that were it not for the introduction of "germ theory" by Louis Pasteur (1822-1895), and its ensuing utilization in the operating theatre by Joseph Lister (1827-1912), patients that survived operations would almost certainly have become stricken with infection, and death by sepsis would ensue. Lister was one of the first to see the link between Pasteur's findings on the fermentation and decomposition of meat by microscopic living organisms and the infection suffered by patients. Surgeons were now able to operate with a considerably diminished chance of infection.¹⁶ The combination of these two milestones in medicine allowed surgery to flourish, leading to the development of long-established cancer operations such as the radical mastectomy which was devised by William Stewart Halsted (1852-1922), the first to perform such an operation in the United States in 1882. This revolutionary operation remained the standard for breast cancer treatment surgery, until the 1970s which ushered in the use of a modified radical mastectomy.¹⁷

The 19th century saw the employment of the modern microscope in the field of oncology. Pathologists, or sometimes surgeons who assumed the role of pathologists, would perform preoperative and postoperative microscopic investigation on the tumours of their patients. From this was born the field of surgical pathology, of which Rudolf Virchow (1821-1902) of Germany was a colossus. Rudolf coined a number of terms including chromatin and leukaemia, deduced that cancer cells are abnormal in comparison to benign cells and proposed that all cells arise from the division of pre-existing cells. He presented the first microscopic description of benign and malignant tumours and very importantly speculated that cancer in fluids of the body is caused by a growth-stimulating substance.¹⁸ In short, he

deciphered the cellular origin of cancer¹⁹ and like Morgagni before him, conceived a correlation between the microscopic pathology of the patient with cancer. This paradigm shift aided in the progression of cancer surgery and allowed for precise prognosis for patients and a way of knowing whether operations were successful in the removal of tumours.

In the early decades of the 20th century, two major breakthroughs provided impetus for the use of animals in cancer research.²⁰ These were the discovery of the Rous sarcoma virus,²¹ a retrovirus that cause sarcoma in chickens and the first oncovirus to be described, by Francis Peyton Rous (1879-1970). There was also an important proposal by Theodor Boveri (1862-1915) that cancerous tumours arise from chromosomal mutation, the causation of cells to grow and divide uncontrollably, which was later proved correct by Thomas Hunt Morgan in 1915.²²

Year	Discovery or Event	Relative Survival Rate
1863	Cellular origin of cancer (Virchow)	
1889	Seed-and-soil hypothesis (Paget)	
1914	Chromosomal mutations in cancer (Boveri)	
1937	Founding of NCI	
1944	Transmission of cellular information by DNA (Avery)	
1950	Availability of cancer drugs through Cancer Chemotherapy National Service Center	
1953	Report on structure of DNA	35%
1961	Breaking of the genetic code	
1970	Reverse transcriptase	
1971	Restriction enzymes Passage of National Cancer Act	
1975	Hybridomas and monoclonal antibodies Tracking of cancer statistics by SEER program	50%
1976	Cellular origin of retroviral oncogenes	
1979	Epidermal growth factor and receptor	
1981	Suppression of tumor growth by p53	
1984	G proteins and cell signaling	
1986	Retinoblastoma gene	
1990	First decrease in cancer incidence and mortality	
1991	Association between mutation in APC gene and colorectal cancer	
1994	Genetic cancer syndromes Association between <i>BRCA1</i> and breast cancer	
2000	Sequencing of the human genome	
2002	Epigenetics in cancer MicroRNAs in cancer	
2005	First decrease in total number of deaths from cancer	68%
2006	Tumor stromal interaction	

Figure 4

Table illustrating the discoveries and events in the field of cancer and the effects on patient survival rates in the United States.¹⁸

Following the timeline illustrated in Figure 4, a number of colossal discoveries throughout the 20th century, including the deciphering of structure of DNA, the breaking of the genetic code, and an array of advances in the understanding of molecular biology of cancer itself – which will be divulged in full - have led to an ever increasing survival rate and the first decrease in the total number of deaths from cancer in human history. Building on the path that brought us to this milestone, further scientific research and experimental evaluation will be paramount in bringing an end to the war on cancer.

1.1.2 Causation of Cancer and Prevention

Since the dawn of medicine and medical science, physicians were perplexed and pondered the causes of cancer. Humorism, or humoralism, was a theory postulated by the ancient Egyptians, but only established and adopted by Hippocrates, and the ancient Greek and Roman physicians and philosophers, *circa* 400 BC. This theory stated that the human body held within it four humours or bodily fluids, namely: black bile, yellow bile, phlegm and blood. For a healthy person, these humours would be in balance. Diseases and illness were believed to originate from an excess or deficiency of any one or more humours. Galen promulgated this theory and it is largely due to his influence and writings - and the religious prohibition of autopsies and studying of the body – that humorism remained undisputed for many years.¹³In 1858, Rudolf Virchow conclusively discredited this theory with his published work on cellular pathology.¹⁸

Opposition to the humoral theory was founded by the discovery of lymph and the absence of black bile by numerous dissections of animals, conducted by Andreas Vesalius (1514-1564). His published work provoked rivalry antagonism from the devotees of Galen. Lymph eventually replaced black bile in the world of medicine and it was believed that the flow of blood and lymph throughout the body was essential for life. With this knowledge, the French philosopher and mathematician René Descartes (1596-1650) put forward his “lymphatic theory of cancer.” This theory hypothesized that leakage of lymph through the lymph ducts resulted in benign tumours, whilst local fermentation and deterioration of lymph resulted in a malignant tumour. Lymph theory was endorsed by the German duo of Georg Ernst Stahl (1659-1734) and Friedrich Hoffman (1660-1742), who further expounded that the etiology of cancer was as result of the degeneration of lymph, with variable density, acidity and alkalinity.²³The renowned Scottish surgeon, John Hunter (1728-1793), a pioneer in work of

the lymphatic system, agreed that tumours were formed as a result of lymph being thrown out by the blood.¹³

In 1838, the German pathologist Johannes Müller (1801-1858) determined the cellular nature of tumours. According to his research, cancerous growths did not consist of lymph but rather of cells and that the makeup of these growths was virtually identical to that of normal tissue. However, Müller speculated that the origin of cancer cells were not from normal tissue, but grew from blastema – analogous cells between normal tissue – giving rise to “Blastema Theory” as the cause of cancer. Müller also propounded that the basis for cancer was the accumulation of cells in diseased organs that could be potentially harmful in growing and spreading to other organs. His student, Rudolf Virchow, later showed that all cells, including cancerous cells, are copied from other cells.^{14, 23}

In the 18th century, the birth of the field of cancer epidemiology – the study of the patterns, causes, distribution and control of the disease - can be attributed to three major findings. The first was in 1713 by the Italian physician Bernardino Ramazzini (1633-1714), who noticed the almost entire absence of cervical cancer and higher frequency of breast cancer in nuns, in comparison to that of married woman at the time. He speculated whether this was due to their celibacy, an important observation in advancing the understanding the role of hormones, especially during pregnancy, as well as STDs and their contribution towards cancer risk.²⁴ His work also divulged the hazards of metals in certain occupations and dangers of occupational disease.²⁵ Secondly, in 1761 the London surgeon John Hill (1716-1775) confirmed in his book, *Cautions against the Immoderate Use of Snuff*, the correlation between the use of tobacco snuff and the formation of swellings and polyps in the nose. This confirmed the concerns of Thomas Venneron the threat of excessive use of tobacco 150 years earlier.²⁵ These conclusions eventually led to further research years later, which found that smoking causes lung cancer and the United States Surgeon General’s warning of the hazards of tobacco use in 1964.²⁶ Lastly, Percival Pott (1714-1788) noticed a considerable number of cases of scrotal cancer in chimney sweeps, caused by the chronic exposure to soot collecting in the area of the scrotum. This is not surprising as chimney sweeps of the time would “buff it” or proceed to work in the nude. Pott identified the association between the soot being the causation of the cancer and in so doing, became the first scientist to demonstrate a work-related link to cancer and that cancer may be caused by an environmental carcinogen.¹⁴ This

led to the induction of the Chimney Sweepers Act of 1788, which attempted to stop child labour.²⁷

In 1915, Katsusaburo Yamagiwa (1863-1930), a Tokyo pathologist, and his associates were the first to invoke cancer in laboratory animals. By applying a solution of crude tar to the rabbit's ears daily for two years, Yamagiwa and co-workers were able to induce invasive skin cancer in seven of the 137 rabbits – demonstrating for the first time experimentally that chemicals can be carcinogenic.²⁰

In the decades of, and following 1940, a nationwide fervour in researchers in the United States searching for chemical carcinogens was witnessed. Amongst others, oils, tar, petroleum, rubbers and other chemicals were irrefutably shown to lead to cancer. By the 1960s, a lengthy list of organ-specific cancer-causing agents had been identified by experimental evaluation.²⁸ Preceding the 1950s, only a handful of viruses were known to cause malignant neoplasm in laboratory animals. In less than 20 years, the field of viral oncology exploded with the identification of a myriad of viruses being the causative agent of cancer. This included the discovery of the origin of Rous chicken sarcoma, the first cancer seen in animals, to be a virus through electron microscopy. Rous chicken sarcoma is shown on a hen in Figure 5, induced through the virus. In addition, an unusually high number of leukaemia cases in radiologists were attributed to continua exposure to X-rays.²⁸



Figure 5

Rous sarcoma that was induced by a filterable virus is shown on a hen.¹⁸

Diet and nutrition was determined to be the responsible factor in a large proportion of molar pregnancies in Asia.²⁸ The discovery that external amounts of oestrogen were able to induce mammary cancer across a range of species of laboratory animals, and that oestrogen was responsible for breast cancer in both female and male humans, was also achieved in this period.²⁸

With the onset of the 1950s, scientists were far more capable of tackling the intricate enigmas of chemistry and biology, owing largely to a number of experiments carried out in the period of two decades. The misconception that genetic information was contained and transmitted by cell proteins was experimentally abolished by Oswald Avery (1877-1955) in 1944. His work with pneumococcal bacillus, indicated that DNA was the carrier of cellular information and contributed principally to the colossal revelation, that was the unravelling of the structure of DNA, by Francis Crick (1916-2004) and James Watson (1928-) in 1953.¹⁹ In the same year, the Finnish researcher Carl Nordling (1919-2007), first postulated the multi-mutation theory of cancer in his publication in the *British Journal of Cancer*.²⁹ Nordling observed that the occurrence of cancer in industrialised nations increased with age, and theorized that cancer cells contain mutations in a number of various genes which amass with age. This work was the first to associate cancer with ageing and would later become known as the “Knudson Hypothesis”, after Alfred G. Knudson’s (1922-) work confirming that the accumulation of mutations in cellular DNA is a causation of cancer. His statistical analysis on instances of retinoblastoma in children, found that inherent retinoblastoma occurs at an earlier age and in both eyes of patients, in comparison to the sporadic disease. This was linked to a genetic propensity for cancer and Knudson further suggested that multiple mutations to DNA were necessary to induce cancer.³⁰

The discovery of two significant families of genes associated with cancer, namely oncogenes and tumour suppressor genes, occurred in the 1970s. With the proposal of the oncogene hypothesis of cancer and the coining of the term oncogene by Robert Huebner (1914-1998) and George Todaro (1937-) in 1969,³¹ it was postulated that oncogenes were genes that could cause uncontrolled cellular growth in other cells, resulting in cancer. The discovery of the first oncogene, Src (short for sarcoma), by J. Michael Bishop (1936-) and Harold E. Varmus (1939-), who found that DNA in normal chicken cells contained the gene responsible for avian sarcoma, a source for the causation of cancer in chickens, followed shortly thereafter in 1976. This suggested that the gene that regulated cell growth and differentiation could also be

responsible for the formation of malignant tumours.³² The origin of oncogenes was identified as the alteration or over expression of normal cellular genes called proto-oncogenes, a process known as activation. Proto-oncogenes provide the blueprint for their corresponding onco-proteins, which oversee cell growth and differentiation and play a role in cellular signal transduction pathways.³³ Activation of proto-oncogenes to become oncogenes can occur through mutations, an increase in protein concentration or over expression and chromosomal translocations. These processes are illustrated in Figure 6. Bishop and Varmus' work on oncogenes led directly to the discovery of the first human proto-oncogene, c-Src, for which they were awarded the Nobel Prize in Physiology or Medicine in 1989.³²

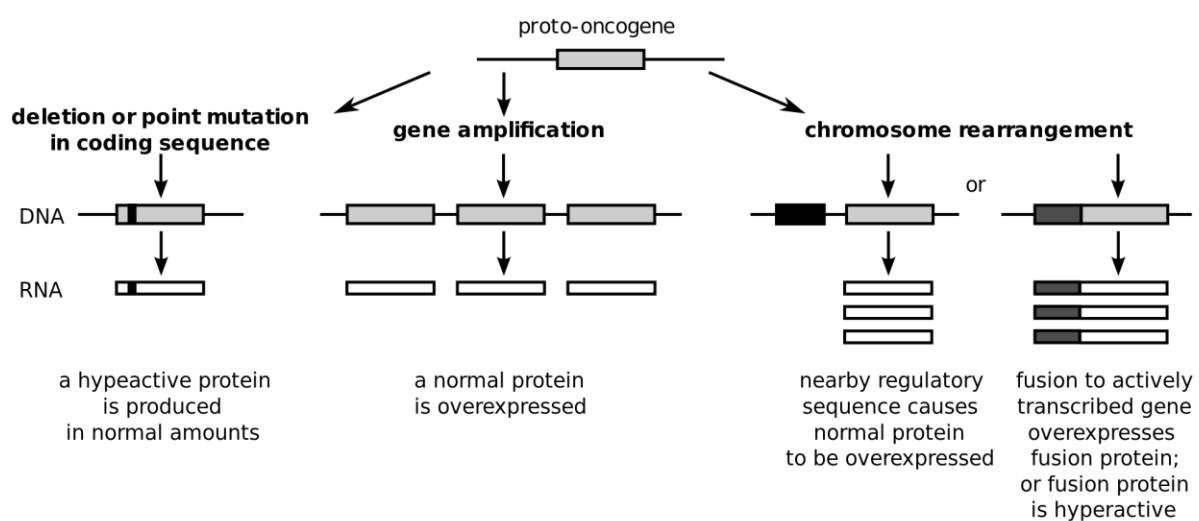


Figure 6

Representation of the various mechanisms of proto-oncogene activation.³⁴

Examples of proto-oncogenes include the protein subfamily rat sarcoma or RAS – found in ~20-25% of all carcinomas and in up to 90% of pancreatic cancer tumours, myelocytomatosis viral oncogene homolog or MYC – a regulator gene that codes for transcription factors - and the WNT signal transduction pathways which are responsible for cell proliferation and embryonic development.³⁵

Genes that could inhibit tumorigenicity were first reported to exist in experiments conducted by Stanbridge in 1976, and later confirmed by Klinger and co-workers.³⁶ Molecular genetic studies identified and subsequently characterized the role of tumour suppressor genes and their involvement in cancer. It is now known that these genes regulate an array of cellular activities including the retardation of cellular growth, repair of damaged DNA, differentiation and apoptosis.³⁷ Defective tumour suppressor genes can lead to uncontrolled cellular growth and have been associated with the cause of multiple cancers.³³ With the aid of research, a

number of tumour suppressor genes have been identified which include p53, RB, INK4a and ARF – all of which have been linked to the causation of many tumour types.³⁷

Scientists had now discovered that the causation of cancer by carcinogens or viruses was in fact damage by chemicals and radiation to DNA, or the addition of new DNA sequences by viruses respectively. It was understood that defective genes or mutated DNA in cells could be inherited, and that these hereditary anomalies were similar to mutations caused by carcinogens and could result in further instances of cancer with additional mutations. Regardless of the cause of mutation, inherent, sporadic or environmental, cells that arose through activation of proto-oncogenes to form oncogenes led to the growth of clusters of irregular cells named clones of the abnormal cell. Through cell differentiation and division, mutant clones would evolve and become more damaged with more mutations over time, causing the cancer to grow and spread. The most notable difference between normal cells and cancerous cells, is that regular cells with mutations undergo apoptosis whilst cancerous cells with damaged DNA do not, a discovery that shed light on the mystery that was the etiology of cancer. The 6 hallmarks of cancerous cells, what differentiates them from normal cells, is displayed in Figure 7. The identification of oncogenes and tumour suppressor genes is ongoing in genetic research and information from these findings can be used to identify people who are at a higher risk and more vulnerable to certain cancers.

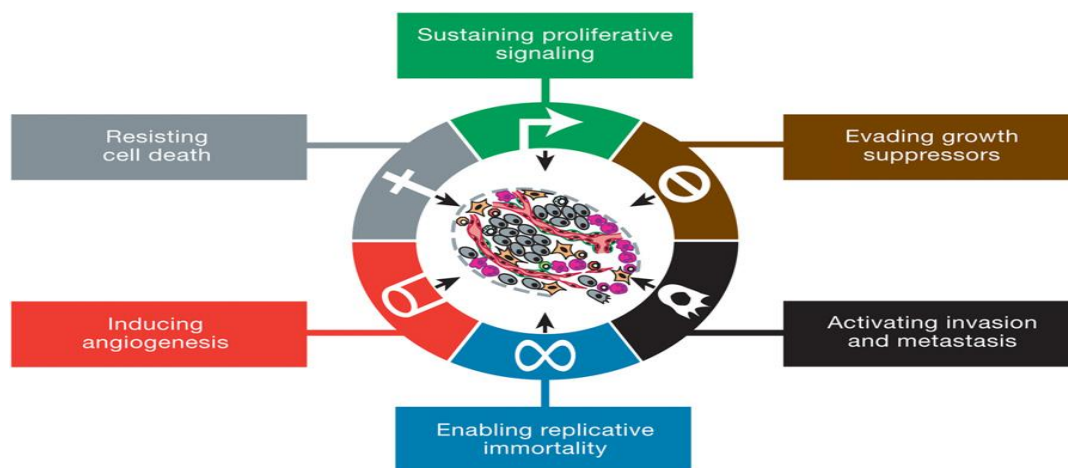


Figure 7

The acquired and functional capabilities of cancer.³⁸

Today, we know that cancer is caused by both internal aspects such as inherent genetic mutations, hormones, immune conditions and metabolic mutations, as well as external or environmental factors.³⁹ These external or environmental factors can be subdivided

into three categories, namely physical carcinogens such as UV radiation, chemical carcinogens such as tobacco, asbestos and arsenic and biological carcinogens, such as infectious organisms and viruses.¹⁰

As is clearly evident in the graphic representations of Figure 8, tobacco is one of the main cancer risk factor in the world, increasing risk of developing at least 14 different types of cancer, containing at least 50 carcinogens and being the culprit for 22% of global cancer mortalities and 72% of lung cancer deaths worldwide. It has been estimated that poor diet can be linked to 30-35% of all cancer deaths in United States, up to 70% of these being colorectal cancers. Chronic alcohol consumption has been connected to a multitude of cancers, including those of the upper aerodigestive tract, liver, pancreas and even breast. Persistent infections of amongst others, the Human Papilloma virus (HPV), hepatitis B (HBV), hepatitis C and HIV, have been related to cervical, anogenital and skin cancer, as well as Hodgkin's Lymphoma and T-cell leukaemia to name a few. Infections are associated with 17.8% of all cancer cases internationally and in up to 20% in the United States as shown in Figure 8.^{10, 39}

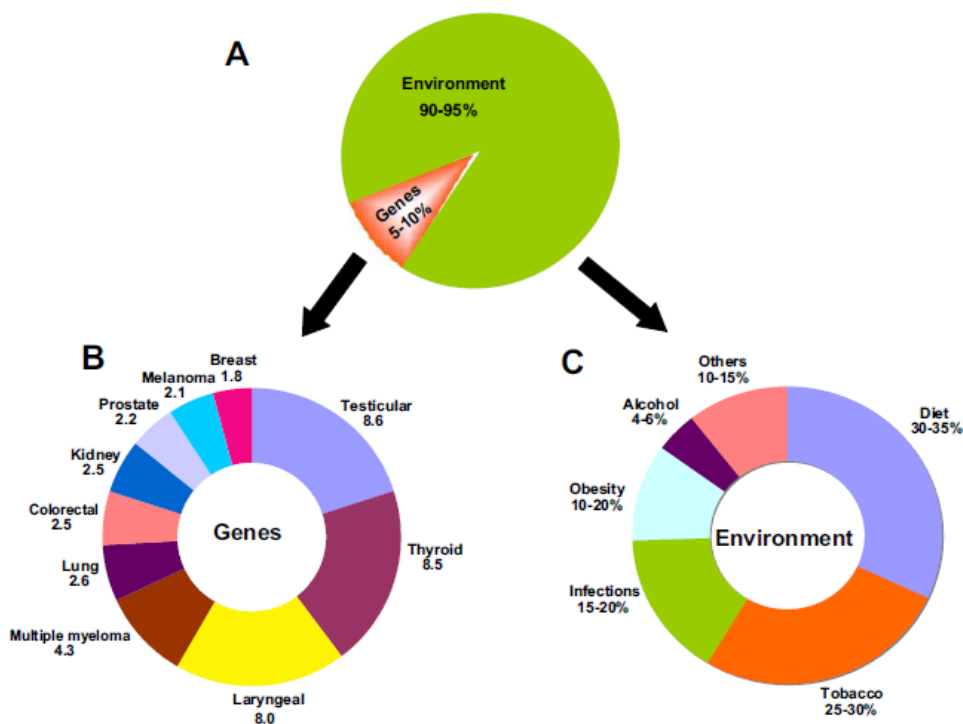


Figure 8

The role of genes and the environment in the development of cancer. A is the percentage contribution of each factor. B is familial risk ratios for certain cancers. C is the percentage contribution of each environmental factor.³⁷

It is estimated that more than 30% of all cancer incidents can be prevented. This can be achieved by avoiding known carcinogens such as tobacco, alcohol and other chemical carcinogens, a healthy diet and lifestyle, vaccinations against HPV and HBV and reduced exposure to UV radiation. It is a case of cancer prevention is better than cure and if detected early and treated effectively a large number of cancers have a high probability of going into remission. Awareness of early signs and symptoms and undergoing screening at regular intervals when older, can both decrease the cancer mortality rate.¹⁰ As an important example, the invention of the “pap smear” or “pap test” by George Papanicolaou (1883-1962) and its implementation as test in the 1960s by the American Cancer Society (ACS) has led to a decline of about 70% in cervical cancer.¹³ A greater understanding of the pathogenesis and causation of malignant neoplasm has enabled researchers to develop effective therapeutic treatments for the disease. From humble beginnings, these treatments now make use of state of the art technology and cutting edge research techniques to halt the advance of cancer.

1.1.3 The Evolution of Cancer Treatment

Similar to ascertaining and understanding the cause and diagnosis of cancer, the progression and development of cancer treatment has been a slow endeavour. In antiquity, putting under the knife and cautery remained the best method for removal of tumours and remedy of cancer. Since 1500 BC, and for 300 years afterwards, various concoctions of herbal remedies containing boiled cabbage, tea or fruit amongst other things, as well as elixirs and pastes of assorted metals like mercury, lead, iron and copper, were made use of internally or externally in different concentrations. Galen, as Hippocrates did, held firm beliefs that cancer was incurable and considered the patient untreatable. With his prolific writings and influence at the time, progress in the comprehension and treatment of cancer was brought to a standstill for an age, as others throughout history adopted his approach.¹² Surgery, the only real tool of cancer treatment at the time, was a primeval and ghastly affair with many complications, the main obstacle being blood loss. As discussed previously, it wasn't until the 19th and early 20th century with the pioneering introduction of antiseptic practice, use of anaesthesia and surgical pathology that cancer surgery, and surgery in general, blossomed. So much so, that the subsequent 100 years were named, “the century of the surgeon.”¹³

A surge of surgical prototypes followed in this century, with a number of them being accomplished by Theodor Billroth (1829-1894). His repertoire included the first esophagectomy, laryngectomy and the first successful gastrectomy or treatment of gastric

cancer.¹⁸ However, the most monumental moment in cancer surgery transpired in 1882, with the introduction of the radical mastectomy technique by William Halsted. Halsted believed that cancer radiated from the primary tumour to adjacent points. Figure 9 shows the *en bloc* abscission of all neighbouring tissue technique he endorsed, to ensure removal of all cancerous cells.¹⁹ The surgery entailed removal of the full breast, axillary lymph nodes and the pectoralis major and minor in one piece under his recommendation.

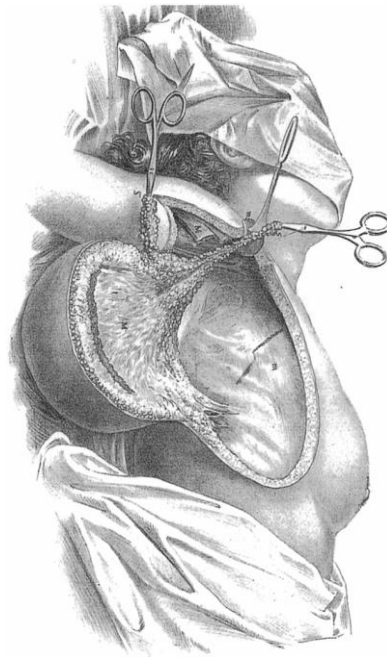


Figure 9

A diagram of Halsted's showing his technique for the radical mastectomy.¹⁸

Halsted's radical mastectomy remained the cream of the crop of cancer operations for a century with only slight alterations being made by others.¹⁸ Stephen Paget (1855-1926) made an important contribution to the knowledge of how cancer spreads by the bloodstream to all organs, but could only develop in particular organs, with his "seed and soil" theory of metastasis.⁴⁰ This appreciation of metastasis was truthful and aided physicians in ascertaining the limits of cancer surgery and the development of systemic therapy – the future of cancer treatment. Cancer surgery eventually evolved into a combinational therapy with chemotherapy and radiation. With the vast escalation in superior technology of today, the use of ultrasound, computed tomography (CT scans), magnetic resonance imaging and positron emission tomography (PET scans) has become standard procedure and replaced the need for investigative surgery. In addition, through the use of fibre optic technology, the endoscope,

cryosurgery, radiofrequency ablation and laser technology, surgeons have been devising lesser invasive ways of eliminating tumours.¹³

The foundation of hormone therapy, among the most prominent of modern approaches of cancer treatment, was laid by George Thomas Beatson (1848-1933) and his inquisitive nature. Beatson perceived, and concluded experimentally, that removal of the ovaries in rabbits led to fatty degeneration in normal cell division. In work he published in 1896, a paper entitled, “On Treatment of Inoperable Cases of Carcinoma of the Mamma: Suggestions for a New Method of Treatment, with Illustrative Cases,” Beatson showed improvement of advanced breast cancer after bilateral oophorectomy (removal of the ovaries) in 3 patients. Beatson surmised that the ovaries were indeed the cause of breast cancer and had unknowingly correlated the hormone oestrogen and its complications in cancer causation even before it had been discovered. He has been named the “father of endocrine ablation” in cancer treatment.⁴¹ 45 years later Charles Huggins (1901-1997) established the validity of this relationship with hormones and cancer, by experimental removal of the testicles (orchiectomy) in male patients with prostate cancer. Striking reversion of metastatic prostate cancer through this surgical procedure, as well as with dispensing of oestrogen, was witnessed by Huggins.⁴² The combined work of these two giants in their field led to the use of modern hormonal therapy used to treat breast cancer today, such as tamoxifen and aromatase inhibitors. The development of new hormone therapeutic agents is on-going and this, combined with research in understanding how hormones manipulate cancer growth, has revolutionized cancer risk and treatment, especially in prostate and breast cancer.¹³

The German physics professor Wilhelm Röntgen (1845-1923) became the first man to produce and detect X-rays in 1895, whilst experimenting with gaseous discharge tubes. In fact, the first x-ray image is that of his wife’s hand. He later held a lecture disclosing his discovery, generating excitement worldwide. His work earned him the first Nobel Prize in physics in 1901,⁴³ and coupled with the discovery of the radioactive elements radium and polonium in 1898 by Pierre and Marie Curie, the era radiation therapy for cancer had emerged. The first physician to use X-rays to treat cancer was Emil Grubbe (1875-1960), only months after Röntgen’s discovery, on Gordon Isaacs for retinoblastoma as pictured in Figure 10.⁴⁴ Radiotherapy showed marked success in skin cancer, as well breast cancer and cervical cancer.²⁰ Fractionated radiation treatment, where the doses of radiation are spread out over time, became a landmark in the field, and in 1928 it was shown to treat head and

neck cancers.¹⁹ Modern radiation oncology can be traced back to the introduction of cobalt therapy and medical linear accelerator technology as treatment. The first patient that received radiotherapy from a clinical linear accelerator was in 1953.⁴⁵ Henry Kaplan (1918-1984) was hugely influential in the design and development of these machines, which has become a cornerstone in cancer radiotherapy.⁴⁶ As with surgery, breakthroughs in technology, especially in the field of computation, have in recent years allowed radiologists to deliver accurate and precise energy to tumours, limiting damage to adjacent regular tissue.¹⁹



Figure 10

The first patient treated with a linear accelerator for retinoblastoma, Gordan Isaacs, who lived to adulthood with normal vision after radiotherapy.⁴⁷

It became clear to surgeons, radiologists and all individuals involved in the field of oncology that regardless of the quality of surgery or radiotherapy treatment, or the combination of the two, cure rates had levelled and progression had thus halted. In the 1950s only a third of cancers could be treated successfully with the methods and techniques available.¹⁹ The closing of the 19th century saw Paul Ehrlich (1854-1915) postulate his “side chain theory” of 1897 - the origin of targeted therapy and the introduction of the notion that chemicals could be used to fight cancer.⁴⁸ Ehrlich coined the term “chemotherapy”¹⁹ and later won the Nobel Prize in

Physiology or Medicine in 1908, for his work on immunology, a field he brought into being.⁴⁸ His proposition that the human immune system stems tumour growth, gave impetus for research directed at exploiting the immune system in cancer treatment, as well as the widespread search for vaccines and chemicals to extinguish cancer. Animal models of transplantable tumours were developed at the dawn of the 20th century and a basis of being able to consistently predict the antitumour effect of these agents for humans from these models was thoroughly investigated. This research remained largely fruitless, mostly due to a restricted clinical trial for humans.¹⁹ This changed however, after examination of soldiers exposed to mustard gas in World War I and II showed acute reduction and harmful changes in bone marrow that developed in blood cells. During this period, experimental evaluation showed that nitrogen mustard, an analogue of mustard gas, had beneficial effects in treating lymphoma, as well as leukaemia. Nitrogen mustard was the first of its kind, an alkylating agent that damaged the DNA of abnormal, rapidly growing cells, effectively killing them, and the blueprint for the design of a series of similar but more efficacious compounds.⁴⁹ In addition, folic acid, a vitamin present in leafy vegetable, was shown to be associated with bone marrow function and its associated deficiency in megaloblastic anaemia.⁴⁹ Sidney Farber (1903-1973) and colleagues, probed the effects it had on leukaemia patients, during which it surprisingly showed to accelerate proliferation of the cancerous cells. Joining forces with medicinal chemists at Lederle Laboratories, a series of similar compounds were generated which included aminopterin and amethopterin, now known as methotrexate, which acted as folate antagonists.⁵⁰ Farber dispensed these drugs to children with acute lymphoblastic leukaemia (ALL) and remarkably, by blocking the folate-needing enzymes activity, induced remission of ALL. Methotrexate proved to show inhibition across a wide range of cancers, including breast, bladder and choriocarcinoma, a malignancy inherent in trophoblastic cells of the placenta, and formed the basis for the first cure for metastatic cancer.⁴⁹ With the knowledge that chemotherapeutic agents could act by inhibiting a vital chemical reaction for DNA duplication, researchers discovered inhibitors of other critical cellular functions. The early activity and success of nitrogen mustard and methotrexate, resulted in the founding of the National Cancer Chemotherapy Service Center (NCCSC) in 1955, of which Farber became a director.²⁸ This heralded the age of chemotherapy.

The migration to the pioneering use of combination chemotherapy, where multiple drugs with different modes of action are used collectively, can be traced back to the long term remissions and even curing of ALL developed by Emil Frei (1924-2013) and colleagues, and the

extension of this to Hodgkin's and non-Hodgkin's lymphoma by Vincent DeVita (1935-) and co-workers.⁴⁹ In the case of Hodgkin's lymphoma, a combination of nitrogen mustard, oncovin, procarbazine and prednisone administered as treatment, lead to remission rates of effectively zero to 80%, with 60% of these patients never relapsing. Today, this cancer is curable 90% of the time, with treatment consisting of integration of radiotherapy and chemotherapy.⁵⁰

The success of combination therapy had a positive effect use of chemotherapeutic agents as an adjuvant to surgery and radiotherapy.¹⁹ Physicians became more lenient and tolerable to using drugs after surgical resection, with no greater success than in that of breast and colorectal cancer. As a result of the long but ever improving methodology and techniques used in the treatment of cancer, shown in Figure 11, the breast cancer mortality rate began to fall in 1991 - a trend that has been maintained – and a drop of 40% in the mortality rate of colorectal cancer patients has been witnessed in the last 4 decades.¹⁹

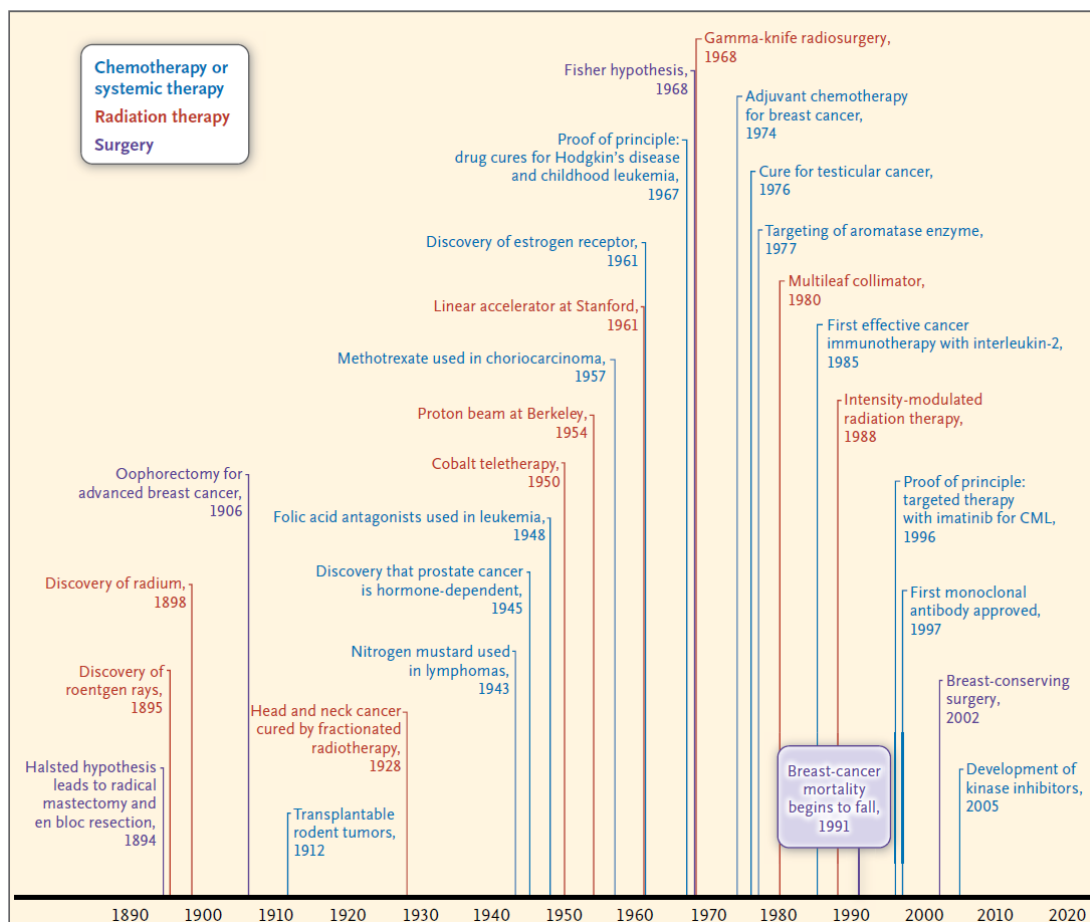


Figure 11

Timeline of pivotal events in cancer treatment.¹⁹

Research today in chemotherapy, mainly involves improving the activity and reducing the side effects these drugs have. This includes the search and use for new drugs and drug combinations, the development of liposomal therapy⁵¹ which increases selectivity towards cancer cells and decreases side effects, and chemo protective agents such as amifostine which reduces renal injury in chemo patients.⁵²

The great Paul Ehrlich did put forward the idea that the human immune system could halt and prevent tumour growth.⁵³ With scientists growing understanding of the biology of cancer cells, biological agents that could imitate natural cellular signals that are responsible for cell growth, were developed and unveiled. The isolation, synthesis and application of these agents in treatment, is known biological response modifier (BRM) therapy or immunotherapy. These agents are administered to patients in order to either emulate or manipulate a natural immune response. This can be achieved by directly changing abnormal cellular growth or indirectly by aiding normal cells bring the cancer under control.¹³ The first real embodiment of Ehrlich's vision was the production of monoclonal antibodies (mAbs) by Georges Köhler (1946-1995) and César Milstein (1927-2002), for which they won the Nobel Prize in Physiology or Medicine in 1984.⁵³ Scientists recognized and identified certain tumour targets, name antigens, which bind specifically to certain antibodies. With technological advancements in the 1970s, mass production of mAbs could be undertaken and used to target specific antigens.¹³ With the accessibility to substantial amounts of mAbs with singular specificity, developments and enhancement of this method by making use of recombinant DNA technology improved efficacy and diminished side effects and resulted in the first Food and Drug Administration (FDA) approved monoclonal antibody, rituximab, in 1997, for the treatment of B-cell lymphoma.¹⁹ Since then eleven other antibodies have obtained approval for cancer immunotherapy for a wide variety of cancers, which include trastuzumab in 1998 for the treatment of breast cancer.⁵³ It became clear that cellular, rather than hormonal, immunity played a much larger role in the immunotherapy of cancer. A name synonymous with immunotherapy is that of Steven Rosenberg(1940-) who first introduced immuno cell therapy in 1985, after the description of T-cell growth factor or interleukin-2 in 1976. By administering interleukin-2 to patients with metastatic melanoma and renal cancers, regression was witnessed in an invasive metastatic disease for the first time by immune therapy.¹⁹ This became known as adoptive cell transfer treatment.⁵⁴ Immunotherapy has also been shown to increase survival probability, regress malignant tumour growth⁵⁵ and result in regression and disease free periods.⁵⁶ It has also been shown to be more efficacious as a

combination or adjuvant therapy.⁵⁷ Therapeutic vaccines that treat cancer by aiding the human body's immune system in attacking cancer cells - not unlike preventative vaccines which prevent infectious diseases - have been researched and developed. Sipuleucel-Tor Provenge, is an example of this, and received FDA approval in 2010 for treatment of metastatic hormone refractory prostate or prostate cancer that no longer responds to immunotherapy and is castration resistant.⁵⁸

The signing of the National Cancer Act of 1971 by Richard Nixon and the subsequent declaration of the “war on cancer” was explosive for the development of chemotherapy. The act effectively quadrupled the budget of the National Cancer Institute (NCI) by the end of the decade.¹⁹ Clinical evaluation of novel drugs and innovative programs of chemotherapy improvement were broadened.⁵⁰ This led to the development of a new series of screening techniques, as throughout the 1960s and 70s, screening was done strictly *in vivo* in mouse models. However, these screening evaluations proved inadequate and in 1976 human xenografts were introduced either by implantation or inoculation of mice. Today, over 300 xenografts have been established, including all the key human tumour types. Regrettably, these newly implemented screening systems are yet to accurately predict the outcome of clinical trials correctly.⁴⁹

In the 1980s, chemotherapy research and development decelerated, due to extended periods of time required for trials which afforded only minor increases in efficacy against malignant tumours, coupled with the dismal performances of screening methods. Whilst endeavours to recover the development and progression of cytotoxic drugs continued, new insights in cellular biology revealed brand new cellular signal transduction pathways that regulate cell growth and differentiation. These new signal networks were also found to be fundamentally modified in cancerous cells. Researchers set out on amending these inherent flaws by targeting growth factors, signalling molecules, cell-cycle proteins, apoptosis regulators and angiogenesis catalysts.⁴⁹ Until the 1990s, virtually all drugs employed in cancer therapeutics - excluding that of hormonal therapy - operated by destroying proliferating abnormal cells. At this very time, an outbreak of novel drug targets revolutionized the cancer industry, from a government funded research program to a multi-billion dollar enterprise.⁴⁹ The last two decades has seen a transition from the use of cytotoxic agents and immunotherapy, to the rational design of anticancer drugs, which are mechanism based.⁵⁹ This shift can best be described as the dawn of the era of targeted therapy.

1.2 TARGETED THERAPY

1.2.1 The Revolution of Targeted Therapy

The past two decades has witnessed a metamorphosis in our understanding of cancer epidemiology and our approach to the treatment thereof, a statement no more evidently substantiated with a recent study showing a 20% decline in cancer mortality in the United States since its peak in 1991. In the period from 1991-2010 this accounts for 1.3 million lives being saved, a decline of more than 30% in the death rate of colorectal cancer, breast cancer in woman and lung cancer in men, and more than 40% in prostate cancer. In the five year period of 2006-2010, an annual decrease of 1.8% in men and 1.4% in woman has been observed.⁶⁰ These statistics can largely be attributed to tremendous advancements in the fields of molecular and cellular biology which has led to improved insight into the neoplastic cellular mechanisms of proliferation, differentiation, apoptosis, tumour immunology and causation of cancer in viral and chemical carcinogens.⁶¹

The origin of identification of these novel signalling pathways, or molecular targets, can be traced back to the 1960s Special Virus Cancer Program (SVCP), a program dedicated to identifying viruses linked to cancer. When this project failed, it altered its research program to study genes that were co-opted by tumour viruses, which led to the description of numerous oncogenes, suppressor oncogenes and signal transduction pathways critical in formative biology.⁵⁰ This scientific knowledge led to the identification of the majority of contemporary drug targets that are currently the focal point of targeted therapy.⁵⁰ It also expedited the Human Genome Project (HGP) and the complete sequencing of the human genome in 2001,⁶² a milestone in advancing our understanding of cancer.⁶³ A flash flood of small biotechnology firms were founded during this time, filled with researchers intent on rectifying the molecular faults in cancer cells. Today there are over 1300 of these enterprises, with more than half concerned with cancer research and treatment.⁴⁹ In 2013, the worldwide market for oncology-related products was estimated to be approximately \$77.3 billion and it is projected to reach an estimated \$143.7 billion by 2023.⁶⁴ The targeted cancer therapy market value is expected to double from \$25 billion in 2008 to \$51 billion by the year 2015.⁶⁵ Biochemist Stanley Cohen (1922-) and neurologist Rita Levi-Montalcini (1909-2012) discovered and isolated nerve growth factor (NGF), for which they received the Nobel prize in 1986.⁶⁶ Cohen went on to discover epidermal growth factor (EGF),⁶⁷ a fundamental discovery in our understanding of cancer for the design of modern cancer therapeutics. Research was

also beginning to reveal the importance of signal transduction in cancer translation. Signal transduction is the conversion of extracellular signalling such as hormones, growth factors, neurotransmitters and cytokines which elicit a specific internal cellular response such as gene expression, proliferation or even apoptosis.⁶⁸ The transformation of cancer treatment from sweeping, non-tailored, large dose chemotherapy with undesirable side effects, to the exploration and hunt for inhibitors that maintained negligible adverse effects with superlative anticancer activity was thus desired.⁶⁹ In addition the required features of auspicious drugs became apparent - a high metabolic stability which meant a long half-life and slow decomposition rate by enzymes such as cytochrome-P450, high specificity, good bioavailability and low toxicity.⁴⁹

1.2.2 Molecular-Targeted Treatments – Successes and Challenges.

Tamoxifen (Nolvadex; AstraZeneca) has been hailed as the foundation of targeted therapy and was the first of its kind - a selective oestrogen receptor modulator (SERM).⁷⁰ Tamoxifen was originally developed as a prospective contraceptive some 40 years ago in the era of discovery and application of chemotherapy.⁷¹ Prompting its failure as the post coital prophylactic ICI 46474, it was reinvented as tamoxifen – the first targeted therapeutic for breast cancer.⁷⁰ Its first clinical trials in 1971 showed encouraging effects in advance breast cancer⁷² and subsequent oestrogen-assay evaluations and further experimentation shed light on its mechanism of action. It was found that tamoxifen itself was a prodrug, having little affinity for its target, the oestrogen receptor. Metabolic breakdown of tamoxifen in the liver yielded its active compound 4-hydroxytamoxifen, an anti-oestrogenic metabolite with a 100 fold higher affinity for the oestrogen receptor.⁷¹ This metabolite acts as an antagonist of the oestrogen receptor in breast tissue, blocking gene transcription and preventing proliferation of cancerous cells.⁷³ This breakthrough in the understanding of anti-oestrogen activity further advanced structure-activity relationship studies and led to the synthesis of nearly all other SERMs including raloxifene. It has been estimated that over 400 000 woman have their lives today because of tamoxifen therapy which has remained the benchmark in treatment for endocrine treatment of all stages of oestrogen-receptor positive breast cancer, and is one of the most widely used anticancer agents today. Although tamoxifen has been shown to have an excellent risk benefit ratio in midlife and older woman, it has also been shown to augment the risk of some positive events, such as prevention of osteoporosis, and others negative, such as an increased risk of endometrial cancer in woman.⁷¹

The first monoclonal antibody to match the criteria of a targeted therapeutic agent was trastuzumab (Herceptin; Genentech). Human epidermal growth factor receptor type 2 (HER2), also known as HER2/neu and ErbB-2, is over expressed in up to 30% of early stage invasive breast tumours and a noteworthy association between this aberrant gene activity and a diminished rate of survival in patients has been found.⁷⁴ The receptor consists of an extracellular binding domain, a transmembrane lipophilic segment and a functional intracellular tyrosine kinase domain.⁷⁵ HER2 signalling is responsible for certain cellular responses and processes which include cell proliferation, differentiation, apoptosis and migration. Activation of the tyrosine kinase domain occurs by homo- or heterodimerisation, usually brought about by ligand binding; however, in the case of HER2, dimerisation may occur without a ligand. Upon activation, the signal transduction pathways of HER2 stimulate cell growth and survival. In some types of cancer this mechanism is utilized, as mutations or over expression of this class of receptor has been known to result in uncontrolled cellular growth, ergo leading to tumour formation.⁷⁵ Trastuzumab prevents the activation and thus dimerisation of the HER2 receptor, thus inhibiting tumour growth and inducing cell death. It has also been suggested that trastuzumab may enlist immune effector cells accountable for antibody-dependant cytotoxicity, which results in increased tumour assault by lymphoid cells.⁷⁵ Trastuzumab received FDA approval in 1998, shows mild adverse effects and when coupled with chemotherapy, has shown considerable improvements in response, duration and survival time of therapy in contrast to chemotherapy only. Furthermore, studies have shown that trastuzumab might enhance the effects of radiotherapy, as well as the action of tamoxifen.⁷⁴

If tamoxifen and trastuzumab shed light on the capability and efficacy of these molecular targeted therapeutic agents in cancer treatment, imatinib mesylate (Gleevec, Novartis) – used in the treatment of chronic myeloid leukaemia (CML) - was the monumental paradigm shift in exhibiting the potential and power of rationally designed inhibitors in a number of facets. It graced the cover of Time magazine as shown in Figure 12, hailed as the new cure for cancer. With tremendous advancements in technology, the first step to identifying the pathogenesis of CML was taken by Peter Nowell (1928-) and David Hungerford (1927-1993) whilst studying human cellular mitosis. They detected a persistent chromosomal abnormality, namely a shortening in chromosome 22, which would later become known as the Philadelphia chromosome (Ph).



Figure 12

Time magazine cover of 28 May 2001 detailing Glivec as a 'cure' for cancer.⁷⁶

It was later deduced that the abnormality of the Ph chromosome arose from a reciprocal translocation, which entailed the long arms of both chromosome 9 and 22 being exchanged, entitled $t(9;22)(q34;q11)$.⁶³ Chromosome 9 and 22 transmit the Abelson murine leukaemia viral oncogene homologue 1 (ABL or ABL1) and the breakpoint cluster region (BCR) gene respectively, which encode for a standard correctly formed tyrosine kinase.⁶⁹ By utilizing cloned ABL oncogenes and genes, it was elucidated that a fusion of these two genes, termed BCR-ABL, was evident in the Ph chromosome.⁷⁷ This union spawns a blueprint for the formation of a tyrosine kinase which signals unrestrained cellular proliferation and non-apoptotic behaviour in myeloid cells leading to tumour growth.⁷⁸ Experimental evaluations later showed the presence of the chimeric BCR-ABL fusion gene in CML cells,⁶³ as well as its demonstration as the singular oncogenic event that brought about CML in murine models, acknowledging the BCR-ABL gene to be the causation of CML.⁷⁸ CML is characterised by uncontrolled growth of myeloid cells and comprises of 3 phases, namely the chronic, accelerated and blastic phase.⁶⁹

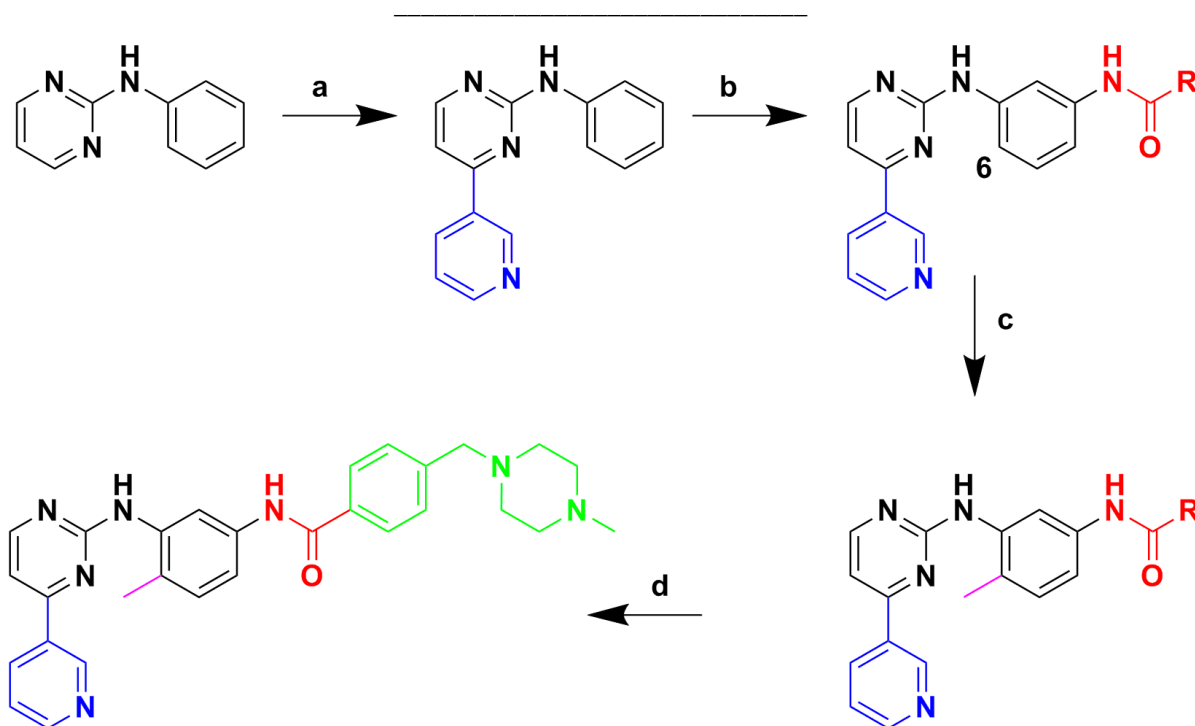


Figure 13

Illustrative summary of the chemical optimization of imatinib.⁷⁸

With the identification of the molecular pathogenic event for CML, an attractive drug target had been exposed in the BCR-ABL tyrosine kinase and its enzymatic activity.⁷⁸ This resulted in CIBA–Geigy, now Novartis, establishing a kinase inhibitor development program in 1984.⁶³ Following screening for inhibitors of protein kinase C (PKC), a lead compound was identified with a phenylaminopyrimidine backbone which can be seen in Figure 13a. PKC inhibitions were markedly increased with the addition of a 3-pyridyl group at the 3 position of the pyrimidine (Fig. 13a, blue). Furthermore, tyrosine kinase inhibitory activity benefitted largely from the inclusion of an amide group on the phenyl ring of the lead structure (Fig. 13b, red). Interestingly, substitution at the 6 position of the diaminophenyl ring completely nullified any PKC inhibitory activity, but the addition of a methyl, increased activity against tyrosine kinases whilst sacrificing loss of PKC inhibition (Fig. 13c, pink). Lastly, to combat poor solubility and oral bioavailability, an extremely polar, hydrophilic side chain was attached (Fig. 13c, green). STI571, or what is now imatinib, was selected as the most encouraging candidate for further development. With the aid of molecular modelling and crystallographic data, the binding mode in the ATP active site was further understood. A crystal structure of imatinib in complex with the c-ABL kinase domain can be seen in Figure 14. *In vitro* screening of the candidate compound against a number of kinases showed

inhibitory activity of phosphorylation for three target kinases, namely BCR–ABL, c-KIT and the platelet-derived growth factor (PDGF) receptor.⁷⁸



Figure 14

Crystal structures of the kinase domain of c-Abl in complex with imatinib (PDB_ID:1IEP)

The candidate compound was found to not only inhibit the growth of CML and BCR-ABL cells in cultures, but also *in vitro*.⁶³ Following this, *in vivo* experiments with mouse models showed continuous inhibition of the fundamentally active p210^{BCR-ABL} tyrosine kinase phosphorylation, and resulted in tumour free existence of the mice. The first clinical trials carried out by Brian Druker (1955-) showed a remarkable response of 98% of the patient's blood counts returning to normal.⁷⁸ This propelled imatinib's FDA approval application forward and in 2001 it received FDA approval for treatment of CML. A disease that was regarded as untreatable, and thus inevitably fatal before –with an estimated survival of 15 months for patients - is now treatable with a survival expectation of 15 years.⁶³ In a 5 year evaluation of patients treated with imatinib, 89% of these patients survived with complete remission after 60 months.⁷⁹ Imatinib is not as selective as previously thought, but fortunately this promiscuity extends to treatment and inhibition of other kinases as previously stipulated. Imatinib has undergone clinical trials for the inhibition of c-kit in which overexpression can lead to the formation of gastrointestinal stromal tumours (GIST), as well as being effective in treatment of proliferative premalignant hematopoietic diseases such as hypereosinophilia syndrome and chronic eosinophilia leukaemia, associated with the expression of an activated form of PDGFR.⁶³ Imatinib is a champion for targeted therapy and through its development

by identification of its molecular pathogen and drug target, medicinal chemistry endeavours, as well as biological assays and application to human clinical trials, has shown that it is possible to produce a rationally designed, molecularly-targeted agent for the treatment of a specific cancer. Importantly, success was attained in the predictive quality of *in vitro* and animal model trials, as the results obtained in these trials agreed well and substantiated the results obtained in the clinical trials.⁶³ In its success; it presented a proof of principle and concept, following a more traditional route of drug discovery which had never before been successful for this target – cancer. This was a definitive advancement in the campaign of targeted therapy.

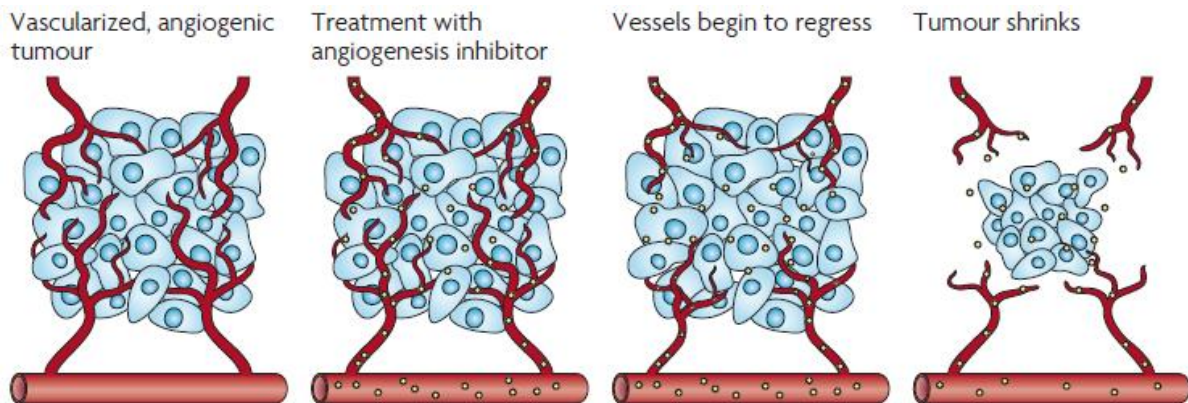
1.2.3 The Scope of Targeted Therapy and the 21st Century.

Although examples of growth factor receptor inhibitors - which target signal transduction pathways to bring a halt to aberrant and uncontrolled cellular growth - have been discussed, there are various other mechanisms that are focussed and exploited and different ways in which targeted therapeutic agents are implemented in the treatment of cancer. Angiogenesis is derived from the two Greek words *angio*, meaning “blood vessel,” and *genesis*, meaning “origin” or “beginning.” From this it is clearly deduced that the term describes the physiological process by which new blood vessels are created. The creator and titan of the field of angiogenesis, Judah Folkman (1933-2008), first postulated in 1971 that tumour growth is angiogenesis dependant and correctly predicted that the inhibition of angiogenesis or the concept of “antiangiogenesis” could be used as a possible future cancer therapeutic.⁸⁰ Whilst conducting research on different solutions of haemoglobin as possible blood transfusion substitutes, Folkman determined the viability of this hypothesis by perfusing canine thyroid glands in these solutions. The glands subsisted for up to two weeks. To ascertain whether or not these glands could support growth, they were implanted with murine melanomas. Tumour development was witnessed, but only to about 1-2mm in size whereupon growth was halted, even though both the tumour and thyroid gland remained alive. Upon transplantation back to the mice, the tumour underwent accelerated vascularisation and swelled to sizes of up to 1cm³. It was on these experiments that Folkman based his deductions divulged in his landmark paper.⁸¹ The paper he wrote provided a schematic and the foundation for the rest of his research based on a number of observations. Folkman recognized that solid tumours were much more reliant and possibly dependant on the enlistment of new blood vessels for growth. Another crucial perception made during experimentation with resting endothelial cells of blood vessels was that tumours

were capable and readily made use of dispersing factors, termed tumour angiogenesis factor (TAF) by Folkman, which promoted and stimulated endothelial cell proliferation, a mechanism implemented by tumours for tumour angiogenesis.

Figure 15

The principle of anti-angiogenesis therapy.⁸²



Logically, Folkman rationalized that antiangiogenesis therapy by inhibition of TAF, could provide control on the growth of malignant neoplasms, effectively cutting it off from resources for further proliferation – the principal of angiogenesis inhibitors as illustrated in Figure 15. This would not lead to complete tumour removal, but rather withdrawal to a dormant state and a diminutive size of the tumour. Folkman recognized this fragile instrument necessary for tumour growth and saw a target for future cancer therapeutics, foreseeing the evolution of anti-angiogenic antibodies in use today, decades prior to their arrival onto the scene.⁸²

Today, it is universally acknowledged that oncogene activation leads to carcinogenesis.⁸³ The use of *in vitro* bioassays, which were later extended to murine models, displayed evidence that the conditional expression of activated oncogenes in cells resulted in a heightened rate of proliferation and a marked reduction in apoptosis, resulting in rapid tumour growth leading to the death of the host. Oncogene deactivation resulted in the tumours receding, leaving either shrunken malignancies or no trace of them at all. This verified the reliance of tumour proliferation and survival on oncogene activation, what is today known as oncogene addiction.^{83, 84} Further studies and experiments have been undertaken indicative that this is not the only requisite for the conceiving of a malignant tumour. The omission of angiogenesis in tumour growth results in inert, miniscule malignancies of $\sim 1\text{mm}^3$ or less, in a dormant like state, shown to be innocuous to patients. In addition, transformation of oncogenes in tumour

cells have shown to considerably escalate angiogenic activity by means of abnormal expression of vascular endothelial growth factor (VEGF) – one of many signal proteins produced by cells that act as a mitogen for endothelial cells, promoting angiogenesis and vasculogenesis. A decrease in the expression of antiangiogenic proteins was also witnessed. Combined with experiments conducted by Fernandez *et al.*⁸⁵, which showed tumour growth restriction by an angiogenesis inhibitor, led to the premise that formation of a malignant mass is unachievable without both tumour and endothelial cell proliferation, a requirement and component of angiogenesis.⁸³

The discovery of the existence of factors promoting endothelial cell proliferation, coupled with the notion of tumour growth dependency on angiogenesis, led to various scientific endeavours to identify and isolate these angiogenic mitogen factors. It was not until 1989 that Ferrara *et al.* became the first to isolate VEGF, an endothelial cell specific factor, from the follicular cells of bovine thyroids.⁸⁶ Arrays of *in vivo* and *in vitro* models have displayed VEGF to prompt a potent angiogenic reaction, as well as the dependency of cells of newly formed blood vessel on VEGF in malignancies. Overexpression of this factor has been documented in a myriad of cancers including lung, breast, gastrointestinal tract, renal and ovarian carcinomas.⁸⁷ It is estimated that in the order of 60% of the roughly 200 different types of human cancers express VEGF.⁸³ This led to the development of bevacizumab (avastin, Genentech/Roche), a humanized monoclonal antibody which is known as a ‘direct’ angiogenesis inhibitor. Its mode of action entails blocking signalling from the pro-angiogenic protein VEGF and thus thwarting vascular endothelial cell proliferation, migration and evasion of apoptosis.⁸⁸ Clinical trials of avastin ensued, where it passed with flying colours, showing great efficacy, especially in cases of colorectal cancer.⁸⁷ In February 2004, FDA commissioner Mark McClellan declared that, in conjunction with surgery, radiotherapy and chemotherapy, “antiangiogenic therapy can now be considered the fourth modality of cancer treatment.” Avastin subsequently received FDA approval for colorectal cancer. With the closing stages of 2007, 23 therapeutic agents with antiangiogenic activity were in phase III and 30 were in phase II clinical trials.⁸⁹ The challenges faced with antiangiogenic therapy is mainly concerned with the recognition that tumours may generate a range of angiogenic molecules, and depending on the stage of development may be dependent on different factors for angiogenesis. Thus the inhibition of a singular angiogenic factor may have little to no effect of halting tumour growth. Antiangiogenic agents are now used in combination with other angiogenesis inhibitors, as well as in adjuvant therapy to greater effect.⁸¹

Apoptotic and non-apoptotic mechanisms of cellular death have been acknowledged to be conducive to the growth of cancer and the development of resistance to anticancer therapeutics. Irregularities in DNA maintenance and preservation facilitate genetic mutations and ultimately causation of cancer. Regular cells possess vital mechanisms to disrupt and ensure that these inherent anomalies do not perpetuate, leading to carcinogenesis. The tumour suppressor gene p53, aptly labelled the “guardian of the human genome”, plays an essential role in this defence of normal tissue and prevention of cancer. P53 stands sentry to cellular strain, hypoxia and DNA deterioration and following detection of any of the aforementioned stresses, the suppressor gene becomes stabilized, inducing cell cycle arrest or apoptosis.⁹⁰ The nature of this response is to destroy deviant cells undergoing uncontrolled cellular growth, discontinuing the progression to malignancies. It is now understood that cells can also be eradicated following DNA impairment by necrosis, mitotic catastrophe and autophagy.⁹⁰ It is not surprising that researchers have found ways to utilize these processes in bringing about the programmed cellular death of tumours. An example would be bortezomib (Velcade, Millennium Pharmaceuticals), a boronic acid dipeptide and novel reversible proteasome inhibitor, which was shown to be effective amongst patients with multiple myeloma which was obstinate to conventional chemotherapy.⁹¹ It has been determined that the mechanism of action of this new class of anticancer therapeutic involves induction of apoptosis, the reversal of resistance to therapy of multiple myeloma cells, and blocking angiogenesis *in vivo*.⁹² The ubiquitin-proteasome signal transduction pathway is extensively involved in the removal of damaged or redundant proteins in the cells of eukaryotic organisms. It has been shown that proteasome inhibition is associated with sensitization to apoptosis and more importantly, that cancerous cells are significantly more receptive to proteasomal obstruction than are normal cells.⁹³ Following success in clinical trials, bortezomib received FDA approval and it has been shown to be superior to other available treatments in cases of multiple myeloma.⁹²

In addition to the expansion of monoclonal antibodies and small molecule signal transduction pathway inhibitors available, researchers have identified new classes of molecules and therapies such as small interfering RNA (siRNA) and poly (ADP-ribose) polymerase enzyme (PARP) inhibitors. The involvement of siRNA in the RNA interference (RNAi) pathway, where the expression of specific genes can be tampered with or even dismantled, has led to sparks of interest in targeted therapy and more recently clinical trials of patients with advanced liver metastasized cancer through lipid nanoparticles targeting VEGF and kinesin

spindle protein (KSP). The trials were a success, halting the growth of the metastases or even promoting remission in certain patients.⁹⁴ PARP activation plays a critical role in DNA harm response processes or the ability of cells to maintain damaged DNA, and has been shown to enhance the cytotoxicity of anticancer therapeutics by tumour chemo and radio sensitization.⁹⁵ The exploitation of defects in these DNA repair pathways has generated considerable interest in the targeted inhibition thereof, spawning a number of inhibitors in clinical phase III and phase II trials.⁹⁶

With the steady and continual innovation of state-of-the-art, superior technology and a greater understanding of the biological process of cancer at the molecular level, researchers will gain, and keep gaining, additional novel targets for promising therapeutic agents. The precise targeting of specific inhibitors to a distinct breed of tumour, increasing the effectiveness and lowering adverse events, has always been problematic. The use of gene expression profiling by DNA microarrays has facilitated in the comprehensive identification of new cancer classes (class discovery) and the classification and assignment of known tumours to classes (class prediction), a powerful new tool to be sharpened for use in target therapy.⁹⁷

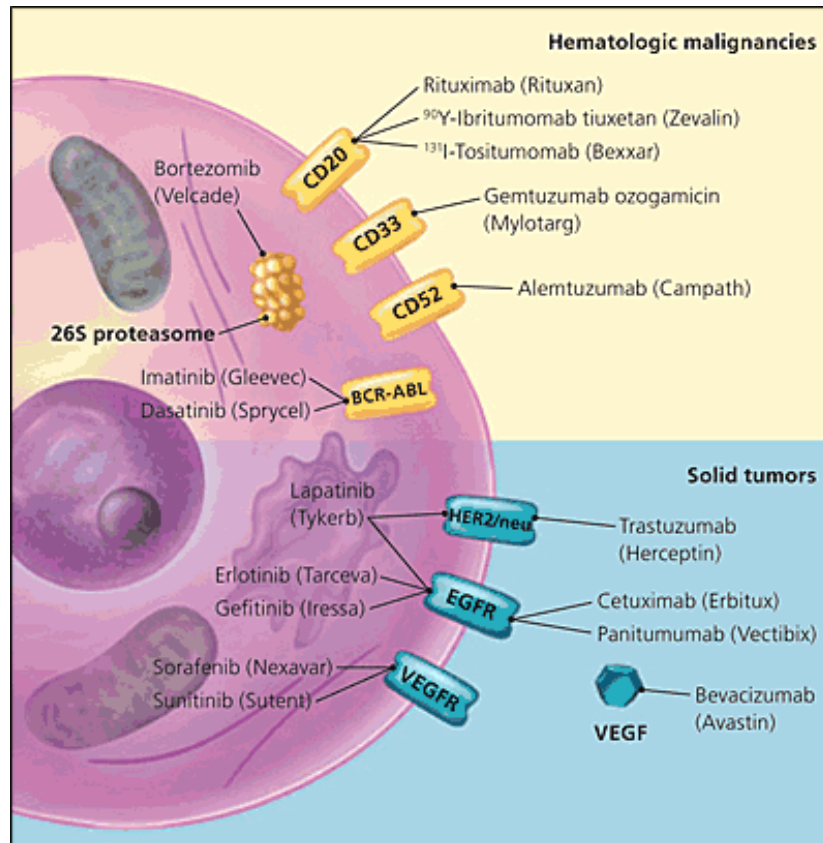


Figure 16**Targeted therapeutic agents, their targets and mechanisms.⁹⁹**

Proteomics, or the extensive study of proteins structure and functions, has found its footing in cancer research as biomarkers for certain cancers and early cancer prognosis.⁹⁸ Specificity, fewer and milder adverse effects, greater efficacy and lower toxicity is the trademark of targeted therapy. The future of research in this area will see the pursuit of improvement of these qualities as anticancer agents, as well as the identification and understanding of new therapeutic targets.

The field of targeted therapy has grown enormously over the last twenty years, targeting a host of different cancer through an assortment of disease mechanisms. A few of these therapeutic agents with their corresponding targets are shown in Figure 16. Of all the targeted treatments, none have shown as much promise and delivered as many results, both clinically and in gaining an understanding of oncogenesis as that of the targeted inactivation of kinases through kinase inhibitors. With a collection of FDA approved drugs being used to treat cancer and a variety of other disorders, an impetus has been provided for further research in this area of cancer treatment and the development of new and improved kinase inhibitors.

CHAPTER 2 – KINASES AND KINASE INHIBITORS

2.1 KINASES

2.1.1 The Origins and Mechanism of Protein Phosphorylation

The collaboration of spouses Carl (1896-1984) and Gerti Cori (1896-1957) and their work on carbohydrate metabolism, the discovery of the “Cori Cycle,” “Cori Ester” and glycogen synthesis earned them the Nobel Prize in physiology or medicine in 1947, as well as illuminating the presence of phosphorylation as a regulatory process. Experimentation with diced skeletal muscle tissue of frogs revealed an intermediate from glycogenolysis – the breakdown of glycogen – designated glucose-1-phosphate, which would later be termed the “Cori Ester.” Further studies elucidated its structure and the enzyme glycogen phosphorylase, which catalyses the rate-determining step of this process.^{100,101} Phosphorylase was seen to have two forms, namely a and b, and the inter-conversion of these two enzymes from a to b, by another enzyme discovered in 1943 by Gerty Cori, was the first example of allosteric activation.¹⁰¹ However, it was not until many years later that the real significance of this reaction was grasped.

It was in the middle of the 1950s that Edwin Krebs (1918-2009) and Edmond Fischer (1920-) determined that the processes of phosphorylation and dephosphorylation were implicated in the mutual conversion of phosphorylase a into phosphorylase b, work for which they received the Nobel Prize for physiology or medicine in 1992. They exposed that this interconversion, or more specifically the conversion of form b into form a, occurred readily in the presence of magnesium adenosine triphosphate (Mg-ATP or ATP) and phosphorylase kinase, an enzyme they discovered and coined.^{101,102,103} This enzyme was later shown to facilitate the conversion from b into a by assignment of a γ - phosphoryl group of ATP to an explicit serine residue of phosphorylase b, an example of phosphorylation.¹⁰⁴ Dephosphorylation, or the reversion from a back to b, was activated by removal of this γ - phosphoryl group by a phosphate releasing (PR) enzyme known today as phosphatase 1.¹⁰¹ The first example of a protein kinase cascade -the activation of one protein kinase by another – was identified with the revealing of 3', 5'-cyclic adenosine monophosphate (cAMP) dependant protein kinase A (PKA) and its activation of phosphorylase kinase. PKA was subsequently shown to suppress another enzyme, namely glycogen synthase, the first example to display the inhibitory activity of phosphorylation.¹⁰¹ Phosphorylation however, remained dormant in research – owing to the

belief that it was exclusive to the regulation of only the glycogen metabolic pathway – until the 1970s and 80s.

A number of the most notable serine/threonine specific protein phosphatases and their regulatory mechanisms were identified during decades of the 1970s and 80s.¹⁰⁵ The unravelling of the amino-acid sequence for the first protein kinase PKA was accomplished in 1981.¹⁰⁶ The amalgamation of these and other discoveries, led to insight into the target of cyclosporin, the immunosuppressant drug that made organ transplants possible. Multisite phosphorylation, the phosphorylation of two or more residues by two or more protein kinases, was observed in the 1970s.¹⁰¹ Perhaps the greatest milestone in these 20 years was the discovery by Ray Erikson (1936-) that v-Src, a gene found in Rous sarcoma virus, encoded a protein kinase.¹⁰⁷ This led Tony Hunter (1943-), or the “kinase king,” to uncover that the v-Src gene was responsible for phosphorylation of tyrosine kinase residues in 1980.¹⁰⁸ Within a year, the realization that tyrosine phosphorylation played a role in regular cellular preservation was grasped, and in the following years the magnitude of phosphorylation as an extensive, complex and crucial cellular activity regulatory mechanism was revealed.¹⁰⁹ The discovery of epidermal growth factor receptor (EGFR) as a protein kinase,¹¹⁰ shed light on its activation by epidermal growth factor (EGF) interacting with the receptor itself. The exposure that this was the case with a number of other growth factor receptors provided an impetus for researchers to find the natural substances these enzymes acted upon.¹⁰¹ This led to the peculiar finding that the receptors themselves were becoming repeatedly phosphorylated at multiple tyrosine residues - being the most prominent suitable cellular substrates themselves - and the discovery of receptor autophosphorylation, which today is recognized as pivotal in downstream signal transduction and mediation of these signals.¹⁰¹ It was not long thereafter that the first protein tyrosine phosphatase (PTP1B) was purified, as well as the cloning of the family of “just another kinase” (JAK) which were shown to play a role in signal transduction and activation of transcription.¹⁰¹ The 1990s have been conferred the title of “decade of protein kinase cascades”¹⁰¹ and the unearthing of an insulin activated protein kinase that phosphorylates microtubule-associated protein 2 (MAP2), later changed to mitogen-activated kinase (MAP) kinase - a family of protein kinases that are activated in response to diverse mitogens, stresses and developmental signals.¹¹¹ Both tyrosine and threonine residues are phosphorylated – activated by a dual specific MAP kinase. Further experimental evaluation on these MAP kinases showed their importance in cellular protection against stress, damaging agents and infection.¹⁰¹

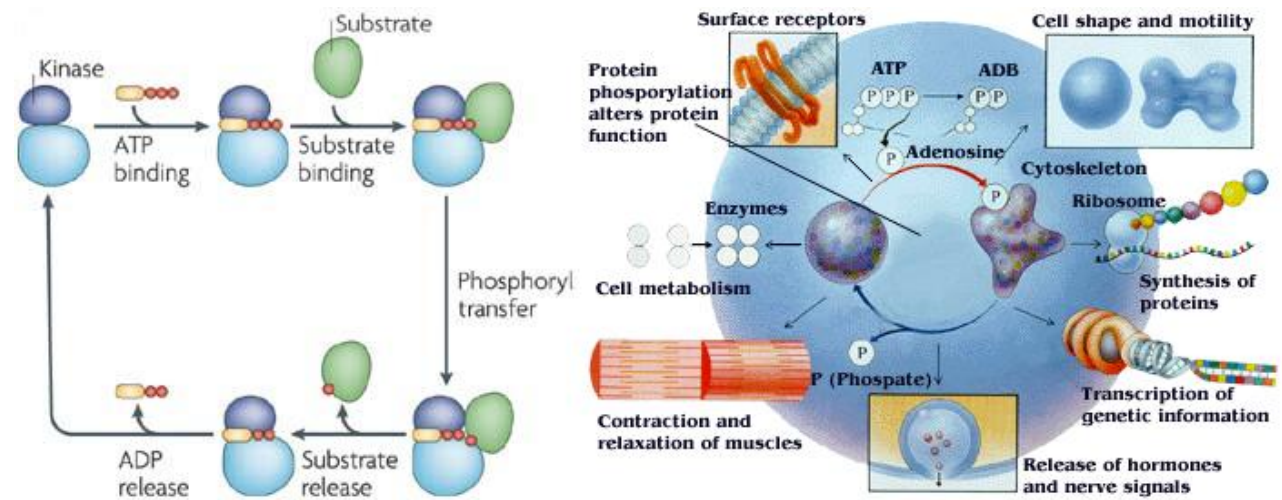


Figure 17

The basic catalytic cycle for substrate reversible phosphorylation by a kinase and its regulation in aspects of cellular processes and life.^{111, 112}

Our comprehension of reversible protein phosphorylation today, recognizes its central and essential role encompassing almost every regulatory process in cells and proteins. Philip Cohen captures it quite eloquently in his review on the subject, with the statement that “the reversible phosphorylation of proteins regulates nearly every aspect of cell life”.¹⁰¹ Copious volumes of published works have either paraphrased or echoed these words in one way or another.^{111, 113} Phosphorylation by protein kinases is the most extensive mechanism for cellular signal transduction. Referring to Figure 17, protein kinases activate the transfer of a γ -phosphoryl group from ATP to generate phosphate monoesters, using a specific residue in proteins in eukaryotes, namely protein alcohol groups on serine (Ser) and threonine (Thr) and/or protein phenolic groups on tyrosine (Tyr) amino acids as phosphate acceptors.¹¹⁴ This is accomplished by ATP binding to the active site of the protein kinase, after which the substrate follows suit. Once constrained, the γ -phosphate of ATP (red) is transferred to an explicit residue of the substrate, changing its enzymatic activity, cellular location, or association with other proteins. The substrate and adenosine diphosphate (ADP) is then released.¹¹¹ Reversible phosphorylation, or the dephosphorylation of these specific substrates, would be undertaken by protein phosphatases in a similar manner. This would catalyze removal of the γ -phosphate group, yielding the unmodified substrate once again available for phosphorylation.^{113c} As can be seen in Figure 17, phosphorylation and dephosphorylation can alter the activity or behaviour of a protein in essentially every imaginable way, thus playing a cardinal role in virtually all cellular process and every aspect of cell life. This includes metabolism, proliferation, differentiation, motility, membrane transport, apoptosis, immunity,

learning and memory.^{101,111} The selection of reversible phosphorylation as the universal cellular regulative mechanism utilized by eukaryotic cells lies in its simplicity, adaptability and the large concentration of ATP as a γ -phosphate donor.¹⁰¹ It has been predicted that phosphorylation takes place on at least one suitable residue of up to 30% of all proteins. If there are approximately 10000 different proteins in a normal cell, with an average length of roughly 400 amino acids, of which 17% are Ser (8.5%), Thr (5.7%) and Tyr (3.0%) residues, then there are a staggering 700 000 potential locations for phosphorylation to take place for any given kinase.^{111, 115,116} The knowledge of phosphorylation, and its role, propelled extensive research into protein kinases to answer questions pertaining to the specificity of phosphorylation and its regulatory roles and its involvement in disease.

2.1.2 The Eukaryotic Protein Kinase Superfamily and the Protein Kinase Complement of the Human Genome

With the last piece of the human genome sequence puzzle fitted in 2001, an opportunity to determine the complete accompaniment of human protein kinases presented itself. Bioinformaticians at SUGEN, Inc. - a drug discovery company focused on development of protein kinase inhibitors - led by Gerard Manning and Sucha Sudarsanam and including Tony Hunter and Greg Plowman, embarked on a comprehensive effort to classify, characterise and describe the full eukaryotic protein kinase (ePK) complement from genomic sequence data.^{113a} The group exhausted all available human genome sequence sources - including all those publicly available, Celera genomic databases, Genbank and many others not publicly available - with a hidden Markov model profile to detect fragments bearing any similarity to any known kinase. Following this, the use of homology modelling, predictive software and verification of the accuracy of these techniques by DNA cloning, resulted in a complete catalogue of 518 putative protein kinase genes. This eukaryotic superfamily, or kinome, consisted of 478 ePK and 40 atypical protein kinases (aPK) – that is a variety of protein kinases that do not share a substantial sequence overlap to the ePK domain, but have proven kinase activity – approximating to 1.7% of all predicted human genes. Their efforts also identified 106 kinase pseudogenes.^{113d} Classification of an extensive and intricate group such as the human kinome, and the addition of model organism's kinases, meant division into a hierarchy of groups, families and sub-families as can be seen in Fig 16. There are two main subdivisions within the superfamily: the protein-serine/threonine kinases and the protein-tyrosine kinases.¹¹⁴ This superfamily contains 9 broad groups including tyrosine kinase (TK), tyrosine kinase like (TKL), calcium/calmodulin-dependent protein kinase (CMCK), and

Chapter 2 – Kinases and Kinase Inhibitors

others shown in large on Figure 18. The 9th group is not displayed and contains the aPK family. Each of these broad groups is further sub-divided into a total of 134 families and 196 subfamilies. The classification of these kinases was carried out according to a number of fundamental criteria, by sequence correlation of the active catalytic domains, supported by sequence similarity outside the catalytic domain and physiological function.^{113d} The knowledge acquired with the full complement of the ePK superfamily provided a colossal impact on further research on kinases and kinase inhibitors.^{113a}

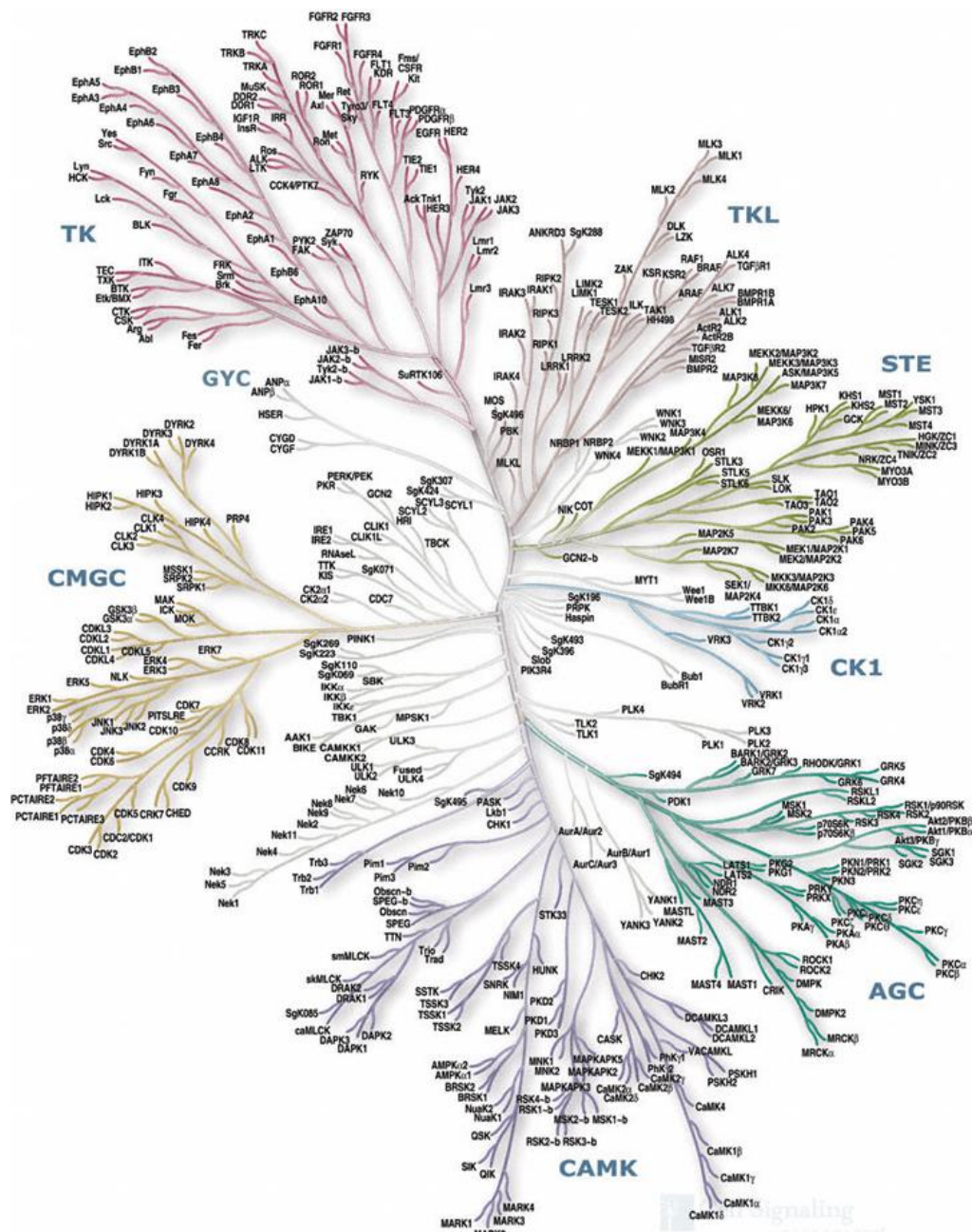
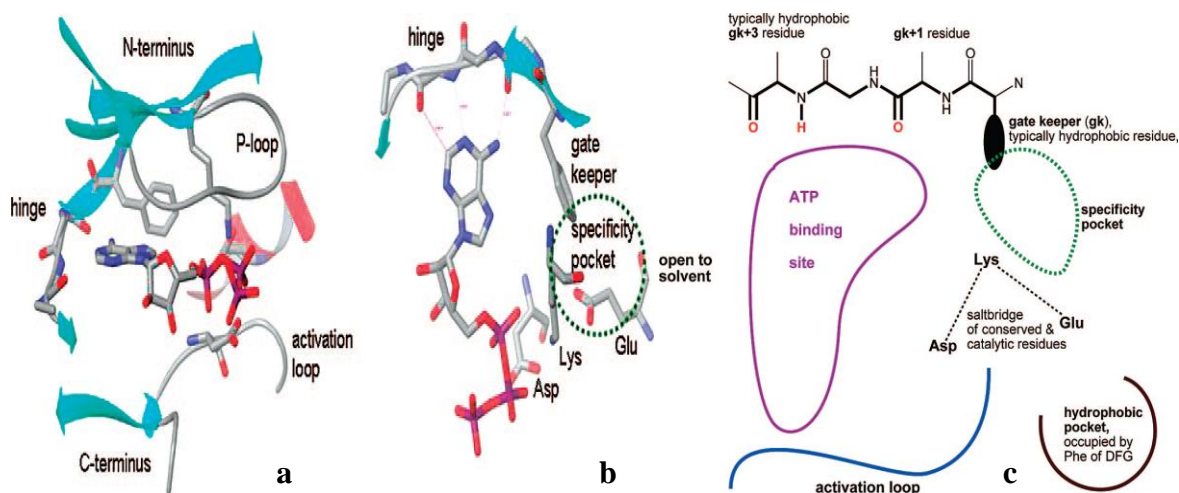


Figure 18

An overview of the human kinome.¹¹⁷

Figure 19
3D and 2D representation of the kinase ATP binding site, illustrating structure and nomenclature.¹¹⁸



Most ePKs are structurally similar and are analogous by their canonical, homologous catalytic domains consisting of approximately 250 – 300 amino acid residues.¹¹⁴ The majority of kinases possess a common fold composed of two lobes, a smaller N-terminus lobe consisting of 5 antiparallel β -sheets and 1 helix and the C-terminus lobe consisting of α -helices as can be seen in Figure 19a.^{111,118} A cleft or narrow hydrophobic pocket situated between these two lobes houses the ATP binding site, where ATP resides with its phosphate backbone protruding into the solvent tail – the area of the protein exposed to the solvent. The ATP binding site is linked by a flexible hinge region which commonly consists of one hydrogen bond donor flanked by two hydrogen bond acceptors arising from the protein spine as can be seen in a 2D schematic in Figure 19c.¹¹⁸ The activation loop of the kinase represents Ser, Thr and Tyr residues which may be phosphorylated and occupy a sector of the binding site when not phosphorylated. After activation, this hydrophilic charged loop moves into the solvent to expose the ATP catalytic domain allowing the protein or substrate to bind along the cleft of the active site whereby transfer of the terminal γ -phosphate of ATP to the hydroxyl oxygen of the Ser, Thr or Tyr residue of the substrate occurs.¹¹¹ These substrates can be seen in Figure 20. A large role in this phosphate transfer is played by the aspartate residue which typically engages in a salt bridge interaction with a conserved lysine residue shown in Figure 19c. The gatekeeper (gk) residue plays a significant role in defining kinase inhibitor selectivity with the specificity pocket shown in Figure 19b. The size/volume of this side chain governs entrance to the hydrophobic pocket located behind it as seen in Figure 19b and c.¹¹⁸

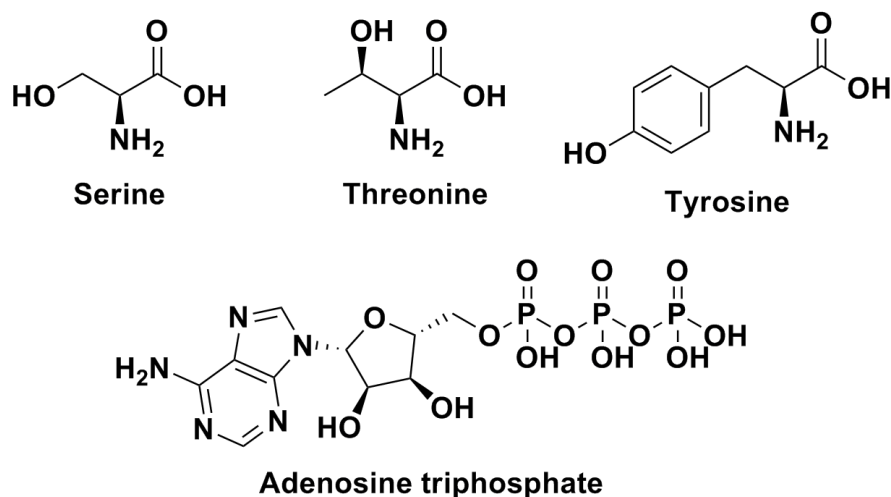


Figure 20

Chemical structures of amino acids and ATP involved in protein phosphorylation.

Although protein kinases share a common fold and many structural affinities, differences in relation to charge and hydrophobicity in the surface area of the active site result in distinct kinase specificity.¹¹¹ A number of structural relationships kinases have in common with one another reflect in related cell regulatory functions.¹¹⁴ Neighbouring determinants in and around the ATP binding site play a large role in determining substrate specificity and particular phosphorylation sequences which take place in the protein kinase.¹¹⁴ Exemplification of this is the difference in the depth of the catalytic cleft between the two major classes of kinases namely the Ser/Thr - specific kinases, which constitute about 80% of protein kinases, and the Tyr-specific kinases.¹¹⁴ The difference in depth allows a Tyr residue to traverse the length amid the protein backbone and the γ -phosphate of ATP, whilst Ser/Thr residues cannot. This attribute is instrumental not only for the specificity of Tyr and Ser/Thr kinases, but also their phosphatase counterparts.¹¹⁴ Distal binding motifs and docking sites or additional binding sites, which are often spatially isolated from the catalytic domain, provide supplementary binding interactions and sometimes allosteric regulation and localization – leading to an increase in the affinity of kinases for particular substrates. Various other mechanisms, such as competition and multisite phosphorylation, ensure proper phosphorylation of corresponding substrates selectively to maintain the specificity that is observed in signalling pathways.¹¹⁴ An understanding of these differences in selectivity and specificity of phosphorylation and the regulatory effects thereof, as well as the catalytic domain of the vast number of kinases, has increased the understanding in designing increasingly efficacious and selective kinase inhibitors.

2.1.3 Oncogenic Kinase Signalling

Work undertaken by Stanley Cohen in the 1980s with EGF responsive malignant cells indicated an operative relationship between oncoprotein activity and receptor phosphorylation signalling.^{110, 119} Shortly thereafter, the successful cloning of the first oncogene - cellular homologues of the *ras* genes – and subsequent molecular genetic studies, showed a single amino acid change in the c-Ha-RAS1 gene and its malignant analogue, namely a transformation from glycine to valine. Further experimental evaluation showed that this single alteration transformed the *RAS* protein, promoting aberrant activity. Not only was the first cellular oncogene identified and confirmed, its active mutation was also singled out and recognized. This was a monumental step in our understanding of genetic mutations, oncogenes, oncoproteins and their involvement in cancer.¹²⁰

	Kinase	Tumor/Cancer Types	Oncogenic Alteration
RTK	EGFR	Breast, lung, glioma	Extracellular domain deletions & point mutations(L858R, G719S, & deletions)
	HER-2/ErbB2	Breast, ovarian, colon, lung, gastric	Overexpression
	IGF-1R	Colorectal, pancreatic, breast, ovarian, MM	Overexpression
	PDGFR- α	Glioma, glioblastoma, ovarian, HES	Overexpression & translocation
	PDGFR- β	CMML, glioma, DFSP	Translocation Tel-, COL1A1
	c-Kit	GIST, seminoma, mastocytosis	Point mutations: D816V
	Flt-4, Flt3	AML	Internal tandem duplication
	FGFR1	CML, Stem cell myeloproliferative disorder	Translocation BCR-, FOP-, ZNF198-, CEP110-
	FGFR3	Multiple myeloma	Translocations & point mutations (S249C)
	FGFR4	Breast, ovary	Overexpression
	c-Met	Glioblastoma, Colorectal, Hepatocellular carcinoma, renal carcinoma, HNSCC metastases	Overexpression, translocation Tpr-, & point mutations(Y1253D)
	RON	Colon, hepatocellular carcinoma	Overexpression
	c-Ret	Thyroid carcinoma, MEN2A, MEN2B, FTMC familial & sporadic	Translocations & point mutations
	ALK	Anaplastic large cell lymphoma, lung, neuroblastoma	Translocations NPM-, EML4; point mutations
CTK	c-SRC	Lung, colon, breast & prostate	Overexpression, C-terminal truncation
	c-YES	Lung, colon, breast & prostate	Overexpression
	Abl	CML	Translocation Bcr-
	JAK-2	CML, T-ALL, solid	Translocation Tel-, point mutation V617F
S/T Kinase	Akt	Multiple	Overexpression
	ATM	Ataxia telangiectasia	Point mutations
	Aurora A & B	Multiple	Overexpression
	CDKs	Multiple	Overexpression
	mTOR	Multiple	Overexpression
	PKC δ	Non-small cell lung, ovarian	Overexpression
	PLKs	Multiple	Overexpression
	b-Raf	Colon, thyroid, melanoma	Point mutation (V599M)
	S6K	Multiple	Overexpression
STK11/LKB1	Peutz-Jeghers syndrome	Point mutations	
LK	PI3K	Prostate, colorectal, breast	Overexpression, point mutations (H1047R)
	SK1	Breast, prostate	Overexpression

Figure 21

Kinases implicated in human cancer, their variety and oncogenic role.¹²¹

Fast forward 20 years – with the unravelling of the full human kinome complement and chromosomal mapping, 244 protein kinases were revealed to map to disease loci or cancer amplicons.^{113d} 164 of these were seen to be implicated with tumour amplicons - or replicative genes, whilst 80 kinases mapped to loci associated with other diseases.^{113d} Figure 21 illustrates known kinase targets that has been intensely investigated and shown to be involved in carcinogenesis, where RTK is receptor tyrosine kinase, CTK is cytoplasmic tyrosine kinase, S/T Kinase is serine/threonine kinase and LK is lipid kinase.¹²¹ With the incredible amount of regulatory activity and responsibility protein kinases have with regards to all cellular processes, it is not surprising that perturbations of these signal transduction pathways by mutations and other genetic alterations results in deregulation of kinase activity and malignant neoplasm transformation.¹²² Certain classes of signalling proteins, i.e. those that oversee cellular proliferation, differentiation and development, are targeted much more sporadically by oncogenic mutations.¹²² Receptor protein tyrosine kinases (RPTK) represent a significant allocation of all oncoproteins that are responsible for causation of a variety of cancers as can be seen in Figure 21. Protein tyrosine kinases (PTK) phosphorylation activity in resting, untransformed cells is usually tightly controlled by the antagonizing effect of tyrosine kinase and phosphatases.¹²³ However, with even slight genetic or structural mutations, these PTK change into powerful oncoproteins which can wreak cellular havoc.¹²² Oncogenic deregulation or transforming functions acquired by PTK can principally be attributed to disruption or constitutive activation of one or more of the signalling pathways which are regulated by PTKs to ensure conservation of catalytic domains and cellular function. This results in activation of further signalling pathways, proteins and messengers impeding regular cellular processes.^{122, 123} Aberrant activity may be brought about by a variety of mechanisms; however, there are four main principals to oncogenesis or oncogene addiction in PTKs.

Firstly, abnormal or over-expression of PTKs, or an over expression of its associated ligand, is concomitant with autocrine-paracrine stimulation which has been linked to array of human cancers. Overexpression of EGFR is reported in 40-80% of non-small cell lung cancer (NSCL) and up to 50% of primary lung cancer. EGFR and ligand over-expression is depicted in panel A of Figure 22, with PTKs known to be activated through that mechanism listed on the right. Secondly, gain of function (GOF) mutations or mutations within the extracellular domain of RPTKs and CTKs has been associated with several neoplastic malignancies, e.g mutations in EGFR amino acids have led to uncontrolled cellular growth of ovarian tumours and non-small cell lung carcinoma.

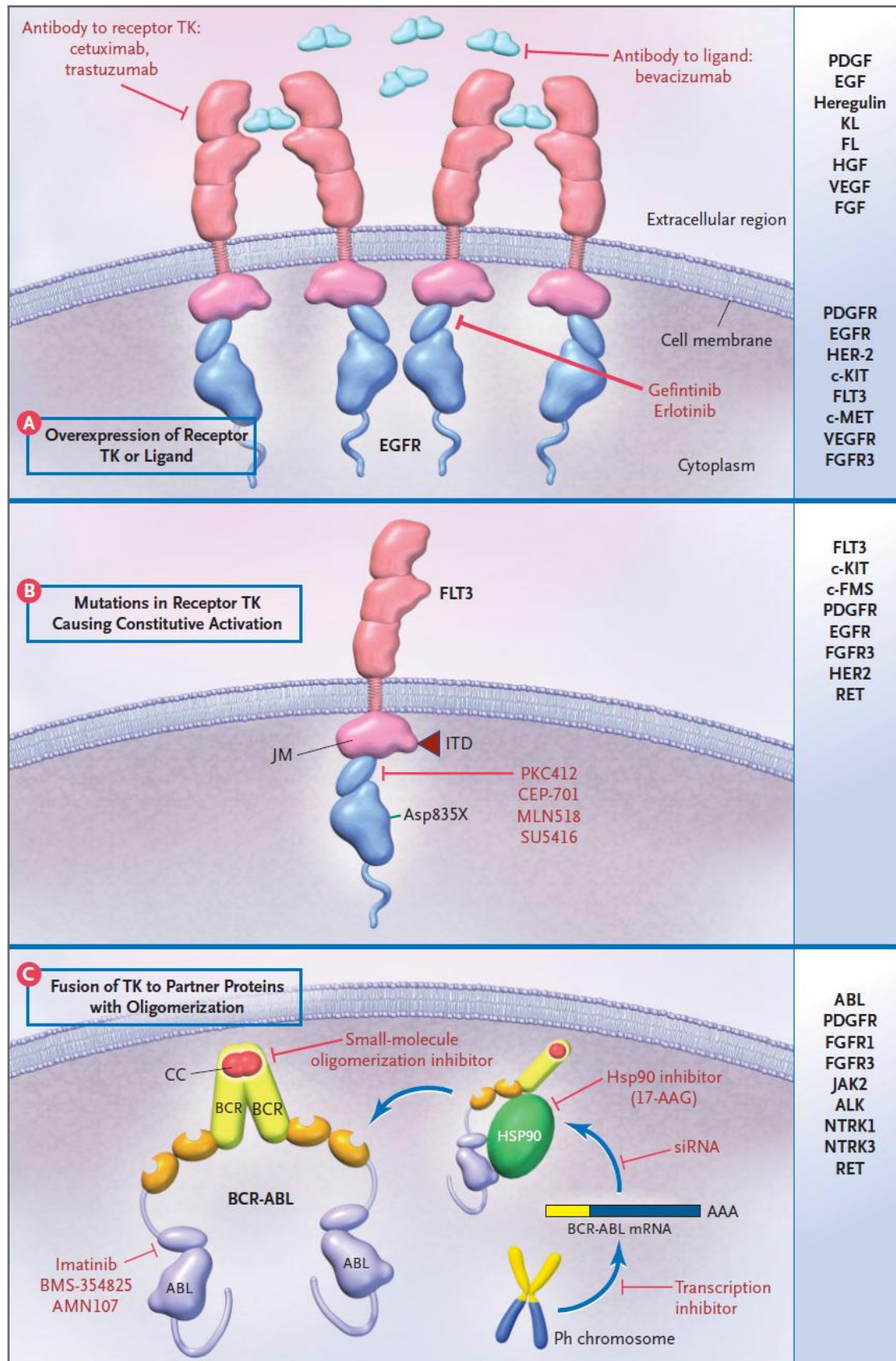


Figure 22

Mechanisms of PTK deregulation and oncogenic activation.¹²⁴

Panel B of Figure 22 shows constitutional activation of Fms-like tyrosine kinase 3 (FLT3) through a point mutation. Thirdly, abnormal chromosomal translocation and genomic rearrangements may result in the cancerous fusion of proteins and resulting in irregular functionality. A representation of this is CML, which arises from a reciprocal translocation between chromosomes 9- and 22, as highlighted in Section 2.1.2. This fusion is illustrated in panel C of Figure 22. Lastly, in rodents and chickens, retroviral transduction of proto-oncogenes related to a PTK leads to constitutional transitions – resulting in malignant activity.^{122, 123,124} With deregulation of signalling, mutation and over expression of PTKs playing a colossal role in the molecular pathogenesis of cancer, as well as the wealth of knowledge on the enzymes themselves and their congruency as drug targets, the design and synthesis of kinase inhibitors as targeted therapeutic agents of the PTKs has been a very successful and attractive endeavour for the last 20 years.

2.2 KINASE INHIBITORS

2.2.1 Protein Kinase Inhibitors – an Overview.

A search on Scifinder for the term “kinase inhibitor” yields ~90 000 references containing the word as entered and ~310 000 containing the concept. To date 26 protein kinase inhibitors have received FDA approval of which 17 are small molecules, with the remainder consisting of both anti-angiogenic and monoclonal antibody inhibitors of Ser/Thr and Tyr kinases.¹²⁵ Approximately 142 inhibitors, ranging over 42 different kinase targets have progressed to some phase of clinical assessment.¹²⁶ Although the vast majority of these are related to the treatment of cancer, kinase inhibition has been implicated in the remedy of an array of ailments inclusive of immunological, neurological, metabolic and infectious disease.¹²¹ With protein kinases comprising a large share of all oncoproteins and aberrant cellular activity playing such a pivotal role in the pathogenesis of a myriad of diseases, it is not surprising that widespread interest and impetus into the targeted inactivation of this class of enzyme has been witnessed. This has resulted in a tremendous investment of resources, especially from the pharmaceutical sector, towards the development of numerous efficient strategies for designing potent and selective kinase inhibitors for suppression of these unwanted cellular processes and treatment of these disorders.^{121, 123}

The prominence of kinases as one of the most intensively pursued classes of drug targets may be attributed to a number of factors. Standing true to the adage, “kinases are responsible for the regulation of nearly every aspect of cellular life,” and with 518 kinases in the human

kinome, almost every signal transduction pathway goes via a phosphotransfer cascade, meaning the inactivation of this target is viable and will yield a real biological response.¹²⁴ As was discussed before, the emergence of imatinib and its success displayed this aspect of kinase inhibition and was the herald for a proof of principle of this targeted therapy.⁷⁸ Despite a high degree of similarity and preservation in the active site of kinases, highly selective inhibitors with positive therapeutic characteristics can and have been developed.¹²⁷ Moreover, and quite surprisingly, inhibition of regular cell kinase activity is well tolerated in the human body, allowing for the selective felling of malignant cells. This is illustrative in dasatinib, an inhibitor of BCR/Abl and Src tyrosine kinases and used in the treatment of imatinib resistant CML, which potentially inhibits all 9 members of the Src family, and possibly others, whilst showing minimal adverse events and a favourable side effect profile.¹²⁴ Targeting and inhibition of genetically mutated or activated kinases has been fortuitous in the relative ease of designing mechanistically relevant cellular assays, as these kinases are promptly identified by DNA sequencing due to their inherent anomalies. This gives a distinct advantage in inhibitor discovery and optimization.¹²⁴ Kinase inhibitors have shown marked success in clinical trials and as approved therapeutic agents. In an evaluation of 974 anticancer drugs, kinase inhibitors shone with a clinical attrition rate of 53% from phase I to approval, considerably lower in contrast to the 82% achieved for other antitumour remedies.¹²⁶ Besides imatinib, exhibiting up to 80% reduction in tumour growth in chronic phase CML patients,⁷⁹ other FDA approved inhibitors have shown beneficial effects in patients. Crizotinib, an inhibitor of an anaplastic lymphoma kinase (ALK) fusion protein linked with carcinogenesis, showed tumour shrinkage and growth halt in 90% of 82 patients carrying this ALK fusion gene.¹²⁸ Lapatinib is associated with the inhibition of two oncogenes namely, EGFR and HER2. Overexpression of HER2 has been shown to be conducive to breast cancer and in combination therapy with capecitabine, showed 51% reduction in the risk of disease progression.¹²⁹ Erlotinib is an inhibitor of EGFR, which is over expressed in certain malignant cells such as those of breast and lung carcinoma. In combination with the use of cytotoxic drugs, erlotinib has shown improved overall survival in patients by 19%, whilst progression free survival (cancer is not exacerbated) was increased by 29%, in comparison to the use of cytotoxic drugs alone.¹³⁰

However, despite the inspiring successes and advantages of this branch of targeted therapy, the field of kinase inhibition faces a number of challenges. These include drug resistance due to further mutations, lack of inhibitor selectivity and efficacy and challenges in drug target

validation associated with its particular disease.¹²⁴ Kinase inhibitors are very efficacious for patients with single genetic alteration type cancers, in contrast to those carcinomas that carry a large number of different mutations where treatment by kinase inhibition is limited. Thus, proper subject selection has become a main concern in kinase drug discovery.¹²⁶ Resistance to small molecule kinase inhibitors is best exemplified with gefitinib, which targets EGFR which is over expressed in 40-80% of NSCLC and other epithelial malignancies.¹³¹ Tumours of patients that exhibited strong responses to therapy usually contained abnormalities in the EGFR gene. These genetic mutations were found to most frequently be either deletions in the amino acid chains between 747 – 750 (delL747-S752), or a point mutation - a replacement of one gene with another. These consist virtually always of substitution of arginine with leucine at codon 858 (L858R) and methionine which is substituted for threonine at position 790 (T790M).¹³² These mutations lead directly to an increase in alteration of signalling pathways and carcinogenesis and thus facilitate oncogenic activity. Patients with the delL747-S752 mutation were seen to show increased tumour susceptibility to gefitinib, which resulted in interim regression of tumour growth and successful treatment. However, following a remission period a second mutation was seen to develop, in this case the T790 mutation, which shows high level resistance to the anilinoquinazoline inhibitor. This showed that relapses in patients with NSCLC usually contained mutations in EGFR which conferred resistance to gefitinib.¹³² In another example, mutations in BCR-ABL associated with imatinib resistance usually result in replacement of threonine with isoleucine at position 315, which corresponds structurally to a very similar change to that of the T790 mutation.¹³² A greater understanding of the mechanisms of resistance in CML has resulted in the development of a 2nd generation library of inhibitors.¹³³ With the advancement of large selectivity screening platforms, it has been shown that the majority of approved kinase inhibitors show inadequate selectivity and are promiscuous in targeting multiple kinases. With the exception of lapatinib, this places restrictions on the applicability of late stage cancer treatment and its use as therapeutic agents in general.¹²⁶ Accessibility of high-resolution crystal structures has markedly expedited the design of increasingly selective inhibitors and coupled with the development of allosteric and irreversible inhibitors, has done much to combat these issues.¹³⁴ Target validation remains problematic in kinases and has resulted in a constricted selection of kinase targets. More than 50% of all inhibitors in clinical evaluation target kinases with already approved drugs on the market. This suggests that a proof of concept is necessary in kinase drug discovery. Almost the same percentage of kinases are

uncharacterized with nearly 25% having completely unknown function, with little to no explanation as to their implication in signalling pathways.¹²⁶ However, the introduction of specificity screening platforms and chemical probes that target a number of these unknown kinases have shown that current clinical and preclinical candidates display inhibitory activity of these kinases.¹²⁶ The use of modern cytogenetics to identify chromosomal transformations and array comparative genomic hybridization techniques may also be utilized for the identification of new tyrosine kinase drug targets.¹²⁴

2.2.2 Design, Synthesis and Modes of Binding.

In modern drug discovery, advances in technology, protein ligand interactions and cellular based assays and screening methods, has resulted in the design, development, synthesis and optimization of hugely successful anti cancer agents.^{59,123} A search for the term “kinase” in the protein data bank (PDB), yields 6540 crystal structure with nearly 2700 ligand hits. The importance of structural biology in the campaign of kinase inhibitor drug discovery is no more evident than in these numbers. Technological leaps in x-ray crystallography and related disciplines has facilitated the rapid and low cost solution of *de novo* compounds and structures, yielding important protein:drug interactions in a typically cheaper and faster method than that of compound synthesis and *in vitro* evaluation.^{113b} The world wide protein data bank (wwPDB) acts as a deposition for all protein related data, and thus a plethora of crystal structures are available for scrutiny and research. This provides structural insight into kinase inhibitors and their specific binding modes in the active site and assists in the structure-guided design of specific kinase inhibitors.¹³⁵ Thorough profiling of kinase inhibitors through biochemical, cell base assays such as fluorescent polarization assay and nonradioactive high throughput assays, have provided insight into target validation and selectivity.¹²³ Pharmacophore and molecular modelling, docking and structure-aided ligand design tools of increasing refinement have also found a place in drug design and optimization.¹¹⁸ The combined and cumulative usage of 2D NMR spectroscopy, *in silico* computer-assisted methods, structural biology, enzymatic and cellular based assays, medicinal chemistry and synthetic experimental evaluation efforts together, can be defined as structure assisted design and optimization in modern drug discovery.⁵⁹

Kinase inhibitors consist of different classes which are distinguished by their mode of binding in the ATP active site, as well as their location in the enzyme itself. This class of anticancer agents can thus be divided into three types, namely: type I or ATP

competitive, type II or allosteric and type III or covalent inhibitors. In spite of the large amount of conservation in the sequencing of the ATP binding site of kinases, the majority of reported and approved inhibitors are ATP competitive or reversible inhibitors.^{113b}

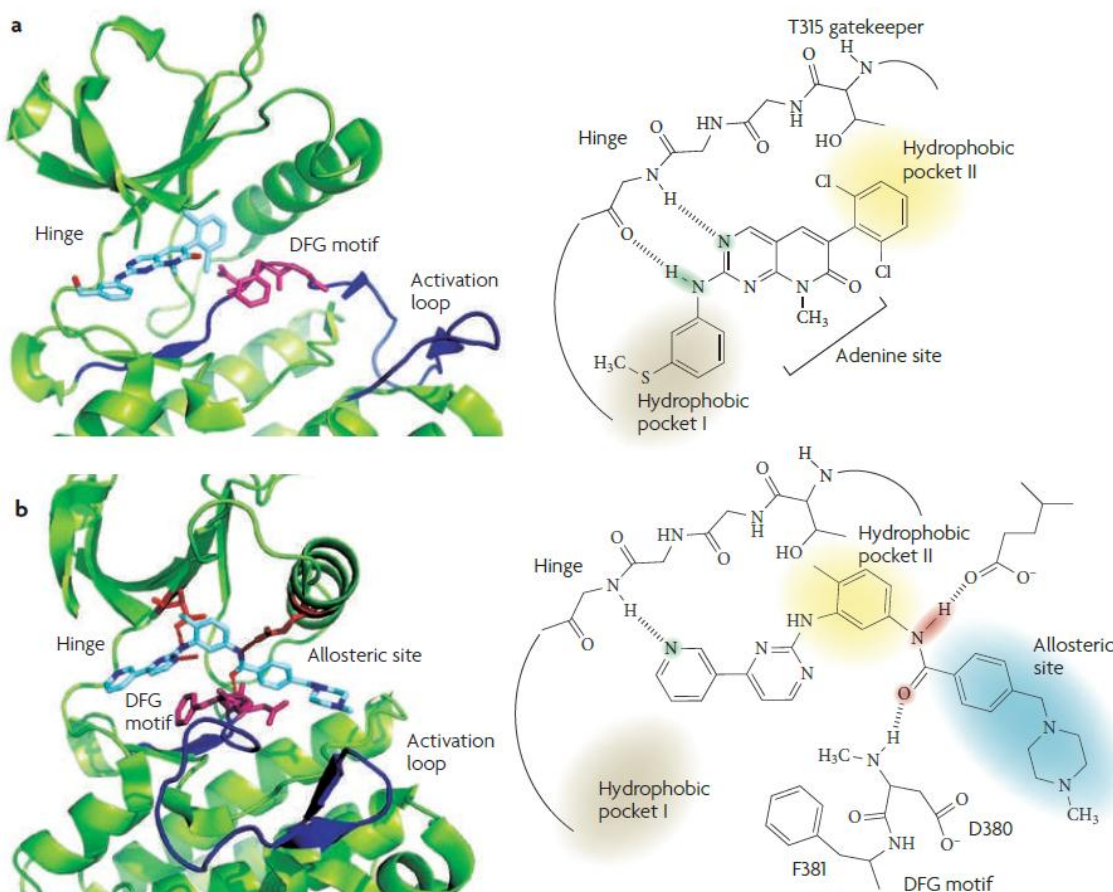


Figure 23

Kinase inhibitor type I and II binding modes.¹²¹

These type I inhibitors exploit the active conformation of the kinase. These inhibitors usually consist of a heterocyclic core, which serves to form weak non-covalent hydrogen bond acceptor/donor interactions with the hinge binding region in the active site, as can be seen in Figure 23a. Furthermore, this heterocyclic system acts as a scaffold for side chains which are used to fill the hydrophobic pockets located in the active site seen shaded in grey and yellow in Figure 23a. This provides further hydrophobic interactions and increases selectivity in the inhibitors. Examples of these inhibitors include imatinib and nilotinib.

Type II or allosteric inhibitors in contrast, target the inactive form of the kinase, also known as the DFG out conformation due to the configuration of this chain.¹²¹ This configuration of the DFG out motif, from movement of the activation loop, bares a peripheral hydrophobic binding site flanking the ATP active site, where type II inhibitors reversibly inhibit the

protein kinase as illustrated in Figure 23b (the blue shaded area defines this additional hydrophobic binding site.)¹²¹ Allosteric inhibitors bind outside the ATP binding site, at an allosteric site separate from the enzyme active site, where ligand binding takes place to effect kinase activity. They are non ATP competitive as they block ATP phosphorylation remotely from the active site.^{113b} Allosteric inhibitors are thus highly selective as they target explicit binding sites that are unique to certain kinases.¹²¹

The last class of kinase inhibitors, type III, are irreversible or covalent inhibitors. This class of drug inhibits irreversibly, by forming a covalent bond to a specific cysteine residue located in the ATP active site.¹²¹ Irreversible inhibitors, like their reversible counterparts, consist of a heterocyclic core or “driving group” which fulfils the same role as in reversible inhibitors, forming weak hydrogen bond interactions with the hinge region. However, covalent inhibitors carry at a designated position a suitable electrophilic functionality known as a “warhead.” It is this “warhead” that forms a covalent bond with a nucleophilic cysteine residue located inside the binding site, usually through a Michael addition reaction as an example. The mechanism of this covalent bond formation and structure of the irreversible inhibitor canertinib, which has shown activity against EGFR and HER2, can be seen on Figure 24 below. In this reaction the electron rich sulphur group of the cysteine residue reacts at the electrophilic β -carbon of the acrylamide warhead. The intermediate enolate then forms the 1,4- addition product.¹³⁶

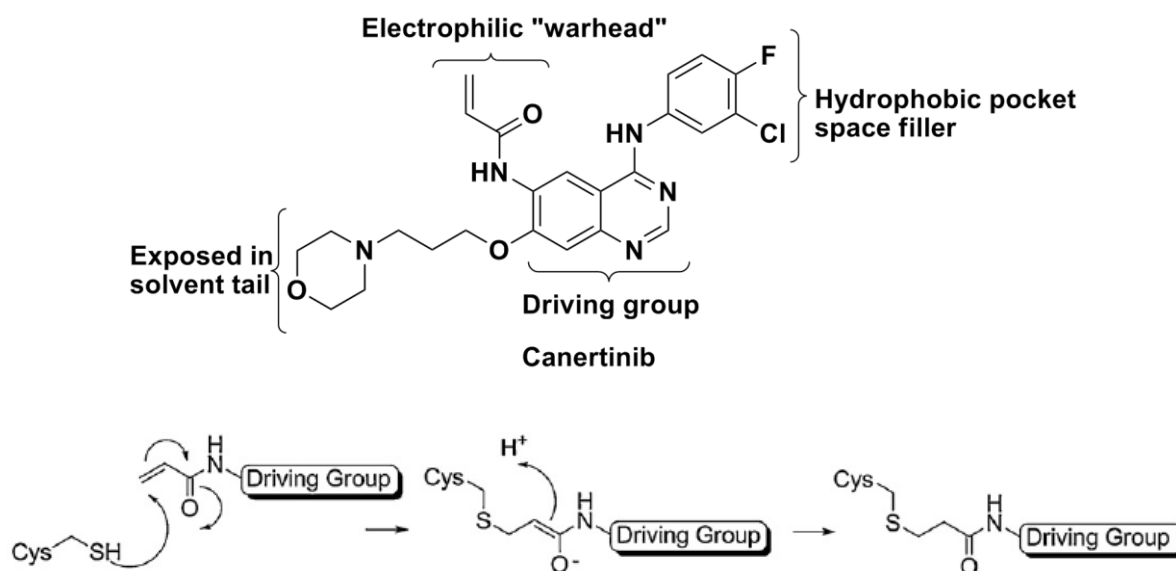


Figure 24

Notable structural moieties and mechanism of covalent inhibition with Canertinib as example.¹³⁶

Irreversible inhibition holds a number of advantages over ATP competitive inhibition. Firstly, irreversible inhibitors contain the structural motifs necessary for reversible inhibition, thus irreversible inhibitors benefit from weak hydrogen bond interactions in the active site, as well as stronger covalent bond interactions. Irreversible inhibitors are not in competition with high endogenous concentrations of ATP in cells. This also means irreversible inhibition is unaffected by changes in the ATP binding affinity of the kinase through point mutations, a mechanism to overcome some forms of drug resistance. Irreversible inhibition has a longer duration of effect and has been shown to persist in deactivation of the enzyme even after the free inhibitor has left circulation. Lastly, a high selectivity profile is associated with these inhibitors as only kinases with the appropriate cysteine residue in the correct place should undergo covalent bond formation and irreversible inhibition.^{134b, 136} Of the 518 kinases in the human kinome only 43% (or 211) have at least one cysteine residue in the ATP binding site spread over 27 different positions. This means that a finite number of these candidates are druggable, which brings about an increased chance of developing potent and selective inhibitors.¹³⁷ However, promiscuity and toxicity remain the biggest challenges in the development of irreversible inhibitors. Selectivity, amongst not only the kinome, but also other cell constituents becomes an issue. However, with a vast library of inhibitor kinase co-crystal structures, refinement of driving portions, as well as proper placement of warheads, has resulted in overcoming these complications.¹³⁶

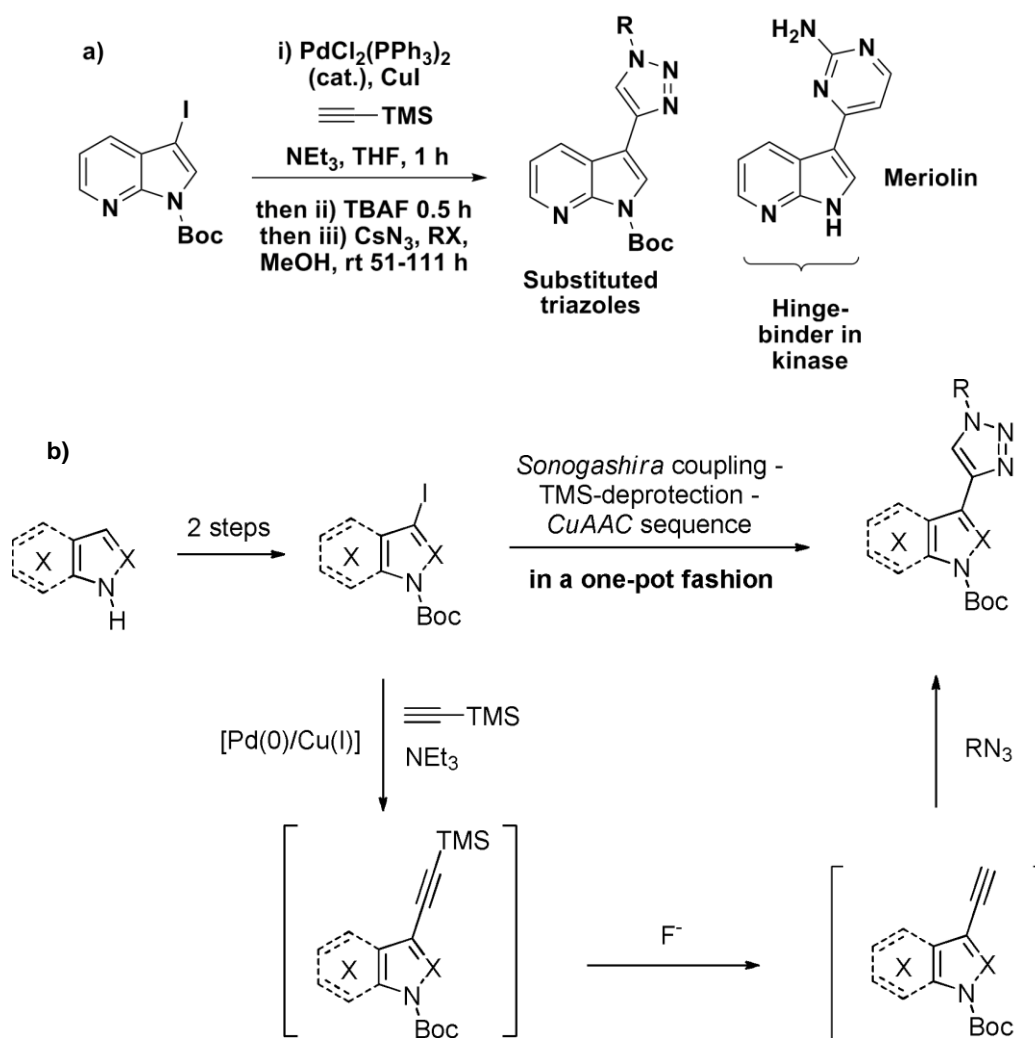
Protein kinases and kinase inhibitor design, development and synthesis has become one of the most significant drug discovery categories in oncology.¹²⁶ Technological advancements, developments in high throughput sequence screening for target validation and innovation in structural biology all aid the rational design and synthesis of novel kinase inhibitors, thereby increasing the viability and opportunities for drug discovery development in this field. This is therefore an attractive area for medicinal chemists to investigate and has become the main focus of many research groups.

CHAPTER 3 – 1ST GENERATION REVERSIBLE INHIBITOR LIBRARY

3.1 SYNTHETIC METHODOLOGY, TARGET STRATEGY AND DRIVING GROUP

3.1.1 The Paper that started it all.

Recently, Müller and co-workers described an innovative way to prepare mimics of naturally-occurring kinase inhibitors, such as meriolin, by following synthetic methodology they developed.¹³⁸ This synthetic procedure, which can be seen in Scheme 1b, involved a one pot Sonogashira coupling, followed by a TMS deprotection and a copper-mediated click reaction to afford 1,2,3-substituted triazoles, in good yields, from the corresponding halogenated precursors shown as in Scheme 1a.¹³⁸



Scheme 1

Synthetic concept and methodology used by Müller for N-Boc protected heterocycles.¹³⁸

A library of these triazolyl NH-heterocycles was synthesized and not surprisingly, as these mimics contain a heterocyclic core with a hinge binding motif corresponding with reversible kinase inhibition, the group found that a number of the compounds were excellent inhibitors of pyruvate dehydrogenase lipoamide kinase isozyme 1 (PDK1). To determine whether the triazole moiety simply acted as a linker or retained additional functionality important for inhibition an analogue of the most efficacious compound was prepared whilst substituting the triazole moiety with a pyrazole ring. Interestingly, the triazole-bearing compound **8f** was shown to act as more than just a simple linker, displaying a pharmacophore character essential for biological activity. It was shown that the pyrazole compound **11** was significantly less active with an IC_{50} value of 2.6 μM for PDK1 compared with 0.8 μM for the triazole as can be seen in Figure 25. Furthermore, an isomeric compound **10** was synthesized, varying only in the positioning of the triazole moiety's carbon and nitrogen, which showed no activity against PDK1. A crystal structure of compound **8f** with kinase PDK1 indicated the presence of hydrogen bond interactions between the triazole nitrogen **N3** with Thr222 and a bridging interaction between **N2** and H₂O and Lys111.¹³⁸

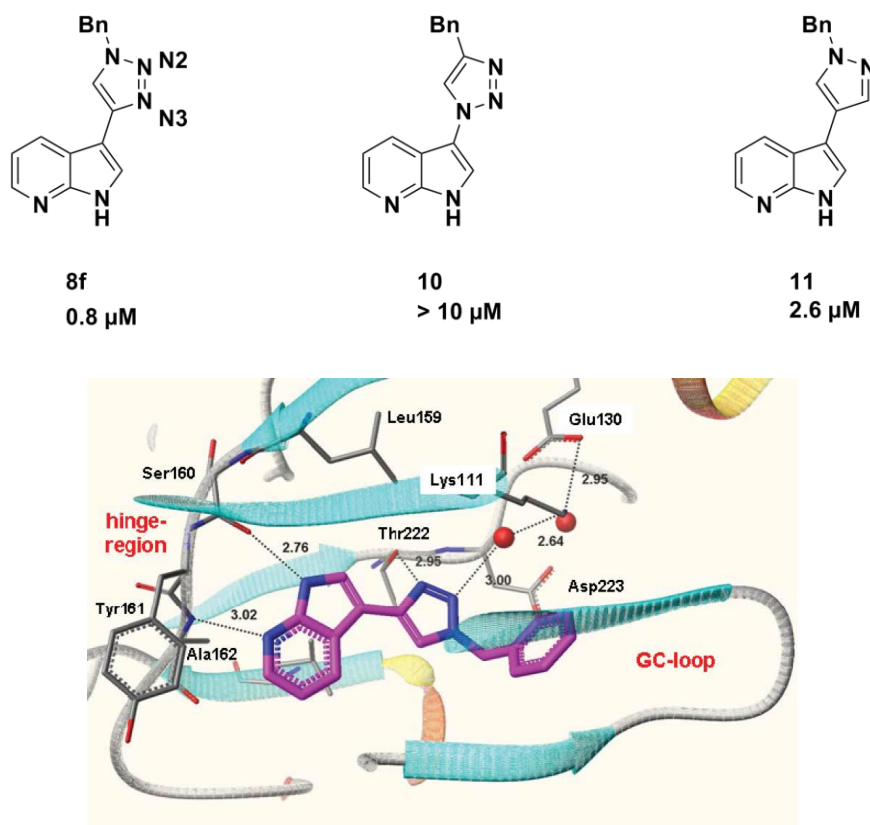


Figure 25

Comparison of IC_{50} values of PDK1 inhibition between triazole, isomeric and pyrazole compounds and crystal structure of compound **8f** in PDK1.¹³⁸

Heterocycles containing 1,2,3-triazole systems have been reported to possess various biological activities including anti-HIV, anti-allergic, anti-fungal, anti-viral and anti-microbial activity.¹³⁹ 1,2,3-Triazole moieties have also been shown to be useful building blocks in chemistry and have been modified to play important roles in pharmacological applications due to their stability towards light, moisture, oxygen and metabolism in the body.¹⁴⁰ Moreover, these moieties have found a range of applications in industry as dyes, corrosion inhibitors, photographic materials and agrochemicals.¹⁴¹ In 1,4-disubstituted 1,2,3-triazoles, N2 and N3 have been shown to act as H-bond acceptors.^{142, 143} Their resistance to hydrolytic cleavage and oxidative transformations has also earned them their ability to act as bioisosteres for moieties sensitive to these conditions, such as esters, thioesters, and thioamides.¹⁴³ Triazoles used as linkers have been shown to form planar structures, which would promote eligibility for the narrow ATP binding site.¹⁴⁴ This has generated considerable interest in the development of new and more efficient synthetic pathways for the design of a diverse array of 1,2,3-triazole-containing heterocycles as possible drug candidates, as well as investigation of their ability as pharmacophores. Thus, on this basis, it was our endeavour to adopt the synthetic methodology formulated by Müller and his team, to be applied to various halogenated heterocyclic analogues of our choosing, which also contained the important hinge binding motif for kinases. This would be an excellent platform to determine the triazole's ability to act as a hydrogen bond acceptor with the hinge region or within the active site of the target kinase and to generate a 1st generation library of novel potential reversible inhibitors and determine their efficacy.

3.1.2 Rationale of Target Kinase: EGFR

Lung cancer accounts for over a third of all cancer deaths and is the leading cause of death in men worldwide, coming second in woman only to breast cancer.^{145,146} It can be seen as a miscellany of diseases largely divided into two groups namely: small cell lung cancer (SCLC) accounting for ~20% of lung cancers and non-small cell lung cancer (NSCLC) comprising of the remaining ~80% of lung cancers.¹⁴⁶ NSCLC is postulated to originate in lung epithelial cells, and is made up of a large variety and number of cellular malignancies such as adenocarcinoma, bronchioloalveolar, squamous, anaplastic and large-cell carcinomas.¹⁴⁶ The EGFR family or ErbB tyrosine kinase receptors, constitutes four homologous receptors namely: the epidermal growth factor receptor (ErbB1/EGFr/HER1), ErbB2 (HER2/neu), ErbB3 (HER3), and ErbB4 (HER4), whose functions has been investigated and studied extensively.¹⁴⁷ The role of EGFR driven signalling in the aetiology

of human cancer is well known¹⁴⁸ and as has been elaborated and clarified before. Over expression of these receptors is abundant in tumours, as well as autocrine or paracrine-stimulated growth in malignancies.^{147a} EGFR has been correlated to a multitude of cancers, including that of the head and neck, brain, colorectal, bladder, breast and lung.¹⁴⁶ Recent analyses have shown that EGFR is over expressed in 62% of NSCLC patients. Also, the chromosomal region of EGFR, 7p12, was found to be augmented in genomic examinations. Additional to over expression and chromosomal transformations, the receptor ligands epidermal growth factor (EGF) and transforming growth factor (TGF) have also been found to be commonly over expressed in NSCLC. This leads to aberrant autocrine functionality and uncontrolled activity and growth of the receptor.¹⁴⁶ Approximately 40% of patients diagnosed with NSCLC today are at an advanced stage. First line therapy for this disease consists of platinum-based combination chemotherapy; however prognosis is poor with median survival rates of 8-11 months, 1 year survival rates of ~35% and 2 year survival rates of 10-20% being reported.¹⁴⁵ The treatment of NSCLC is thus an on-going struggle and new therapeutic targets of the molecular mechanisms that govern the growth of these malignancies are desperately needed.

A range of drug discovery strategies has been developed to address this need, including the use of monoclonal antibodies such as cetuximab and bevacizumab and small molecule kinase inhibitors such as gefitinib, erlotinib and lapatinib whose molecular structures can be seen in Figure 26 below. Gefitinib, a reversible inhibitor, has increased our understanding of NSCLC and mutations of EGFR through specific resistance mechanisms to this treatment. Erlotinib, as discussed before in Section 2.2.1, has shown a benefit to patients with advanced lung cancer, some showing complete response, whilst others only partial to the treatment.¹⁴⁵ Lapatinib is seen as a dual tyrosine kinase inhibitor as it interrupts both the HER2 and EGFR signalling pathways and is used primarily for the treatment of breast cancer where it has shown marked success.¹²⁹

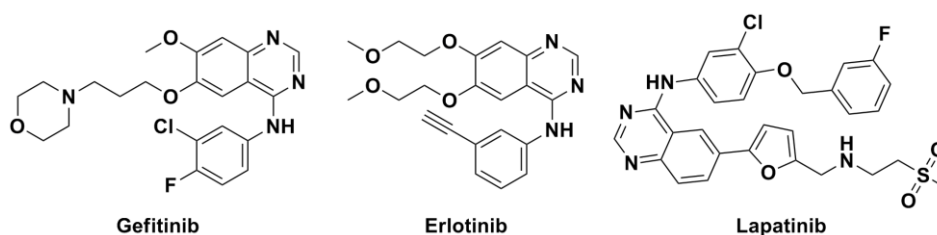


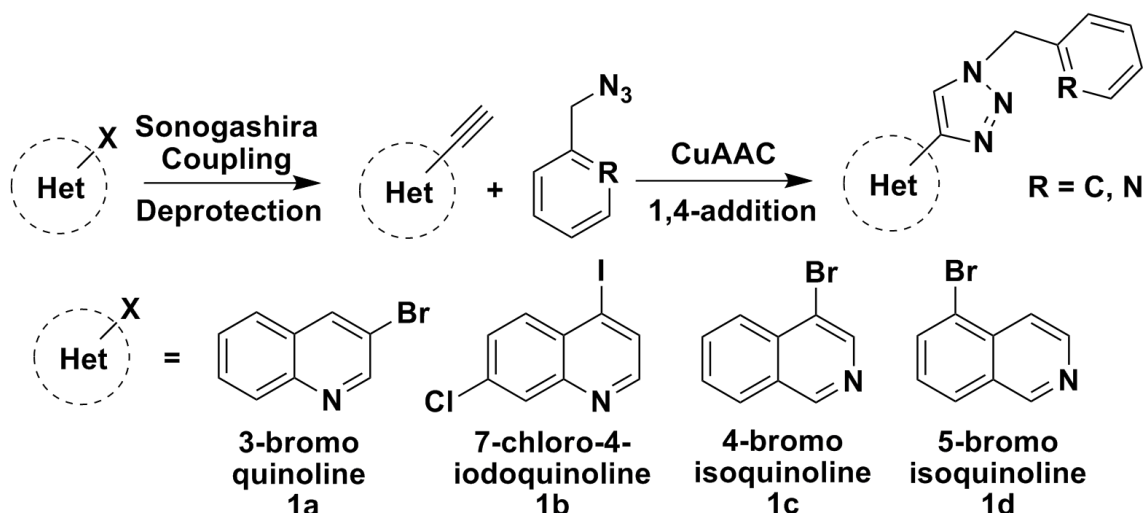
Figure 26
Molecular structures of gefitinib, erlotinib and lapatinib.

Following the lead of these FDA approved drug candidates, the EGFR kinase domain would seem a logical and attractive target for drug discovery. For this project we would be collaborating with a team of German biochemists from the Technische Universiteit Dortmund, led by Prof. Daniel Rauh. A student in Prof. Rauh's group, Julian Engel, would be responsible for carrying out the biological assays and determining the potency and efficacy of our library of potential inhibitors. Julian's main focus of research is that of EGFR, which was accordingly selected as our target kinase for this project as screening could be facilitated.

3.1.3 Choice of Heterocyclic Driving Groups and Side Chains.

Quinoline, a heterocyclic aromatic compound, was first extracted from coal tar in 1834, which still remains the primary source for its industrial usage. Although the heterocycle itself has limited application, derivatives thereof have been shown to possess an enormous variety of uses in extensive fields, and it also occurs in a number of natural products and alkaloids.¹⁴⁹ A natural product derivative, quinine, and further synthetic analogues thereof such as chloroquine,¹⁵⁰ primaquine¹⁵¹ and mefloquine,¹⁵² have been extensively researched and found great success in the treatment of malaria. Biological activity of compounds containing a quinoline backbone has been found in anti-tuberculosis,¹⁵³ anti-microbial,¹⁵⁴ anti-convulsant,¹⁵⁵ anti-inflammatory,¹⁵⁶ cardiovascular¹⁵⁷ and most importantly, anticancer applications. Quinoline as a privileged anticancer scaffold shows activity in a number of different target sites such as topoisomerase I, telomerase, farnasyl transferase, Src tyrosine kinase, protein kinase CK-II and others.¹⁴⁹ As protein tyrosine kinase inhibitors, quinoline-based driving groups have shown potent IC₅₀ values for a range of kinases and different types of cancers.^{61, 158}

Isoquinoline, a benzopyridine derivative like quinoline, was also first isolated from coal tar 51 years after its structural isomer. This heterocycle is the structural spine of a large number of natural alkaloids. Isoquinoline analogues have found a variety of uses as anaesthetics, antihypertension agents and vasodilators.¹⁵⁹ A number of derivatives have been applied in anti-malarial, anti-HIV, anti-tumour, anti-microbial and anti-bacterial usage.¹⁶⁰ Most importantly, isoquinoline-derived drugs have shown protein tyrosine kinase inhibitory activity against a number of kinases including EGFR.¹⁶¹



Scheme 2

Synthetic scheme illustrating choice of heterocyclic driving group, side chains and reactions.

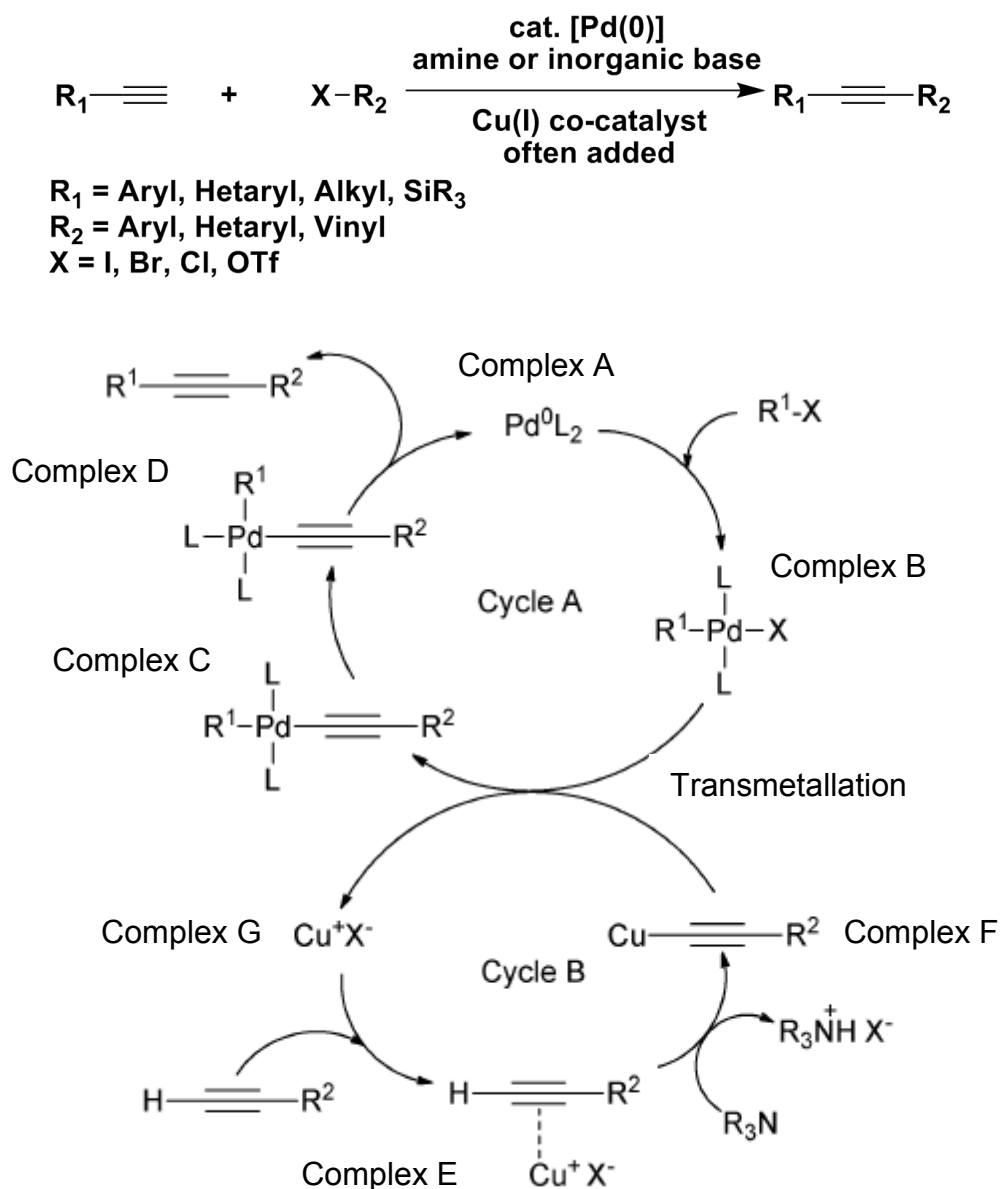
On the premise of these findings and research already carried out using these heterocyclic cores, we decided to make use of two halogenated structures of both quinoline and isoquinoline which can be seen in Scheme 2 above (**1a-d**). Following the synthetic approach devised by Müller, Sonogashira coupling and deprotection would afford heterocyclic alkynes which could subsequently undergo a copper catalysed azide alkyne cycloaddition (CuAAC) with appropriate azides, affording a library of reversible, 1,4 1,2,3- triazole-based potential kinase inhibitors. A number of molecular modelling and docking calculations were undertaken making use of Acclerys Discovery Studio software. The investigation visually showed promising results and binding modes adopted by these compounds. A number of hydrogen bond acceptor/donor interactions were seen between the quinoline and isoquinoline moieties, and the methionine and threonine hinge binding region. The choice of benzyl azide and 2-(azidomethyl)pyridine (Scheme 2) as suitable side azide side chain fragments to undergo this CuAAC was made on the grounds of simplicity, as well as potential hydrophobic interactions, as seen in the molecular modelling and docking calculations. As both moieties were predicted to fit in the hydrophobic pocket of the active site, an aromatic core with a flexible methyl linker for rotation was logically chosen. The addition of nitrogen in the pyridine moiety, and a lack thereof in the benzyl variation, would give an indication as to whether the heterocyclic counterpart took part in any favourable hydrogen bond interactions, possibly increasing efficacy and selectivity. This provided further encouragement for the use of these driving groups and side chain linkers for the synthesis of our potential reversible inhibitors.

3.2 SYNTHESIS OF ALKYNE FRAGMENTS

3.2.1 Sonogashira Coupling and Silyl Deprotection.

The palladium-catalysed coupling of aryl or vinyl halides (or triflates) with terminal acetylenes is generally referred to as a Sonogashira coupling reaction.¹⁶² Garnering its name from Kenkichi Sonogashira, Yasuo Tohda, and Nobue Hagihara, who first reported usage of the reaction in 1975,¹⁶³ it was an extension of the work done by Heck but allowed for much milder conditions to be used.¹⁶² Nearly 30 years on, the robust Sonogashira coupling has transitioned to one of the most central and well established methods for sp²-sp carbon-carbon bond formation in organic synthesis,¹⁶² finding widespread application in the preparation of arylalkynes and conjugated enynes, a lynchpin in natural product synthesis and in heterocyclic chemistry.¹⁶⁴ This has also extended to use in the synthesis of molecular electronics, dendrimers and conjugated polymers or nanostructures.¹⁶² Conventionally, a copper co-catalyst is added, which provides increased reactivity, but copper-free Sonogashira synthetic methodology has been explored and developed.¹⁶⁵ Standard Sonogashira reaction conditions employ some source of palladium such as PdCl₂(PPh₃)₂ as catalyst, in conjunction with a co-catalytic amount of Cu(I) such as CuI, with an amine as solvent or an inorganic base as shown in scheme 3.¹⁶²

The precise mechanism for the Sonogashira coupling is not yet accurately understood, due to complications in analysis as two metal catalysts are present, which sheds doubt on certain intermediates that are formed. However, it is generally accepted that the reaction progresses through two separate catalytic cycles, namely the palladium and copper cycle as illustrated in Scheme 3. Firstly, the palladium cycle is well agreed upon as it is derived from classical carbon-carbon cross-coupling reactions.¹⁶⁶ The cycle begins with the inactive Pd(II) catalyst, such as PdCl₂(PPh₃)₂, being reduced to the active 14 electron palladium species [Pd(0)L₂], shown as complex **A** in scheme 3. This complex then undergoes oxidative addition of the aryl or vinyl halide, which is reasoned to be the rate-limiting step of the reaction, forming the adduct [Pd(II)R₁L₂X], or complex **B** in Scheme 3. This adduct then undergoes transmetallation with the copper acetylide complex **F**, formed during the copper cycle, which in turn results in complex **C** after expulsion of the copper halide complex **G** which is regenerated. The *trans* organic ligands of complex **C** undergo *cis/trans*-isomerisation, yielding complex **D**, following subsequent reductive elimination affording the alkyne product and regenerating the [Pd(0)L₂] catalyst.¹⁶²



Scheme 3

Standard Sonogashira coupling reaction conditions and catalytic cycle adapted from Chinchilla *et al.*¹⁶²

In comparison to the palladium cycle, the copper cycle is unexplored and esoteric, with most of the mechanistic details hypothesized. It is believed that the presence of base promotes copper acetylide formation through the formation of an intermediate π -alkyne copper complex **E**, which in turn makes the terminal alkyne's proton more acidic, resulting in the copper acetylide complex **F** which undergoes transmetalation in the palladium cycle, regenerating the copper halide catalyst.¹⁶²

The use of silyl protecting groups in organic synthesis has become a routine procedure.¹⁶⁷ The utilization of these groups in organic synthesis has extended across a wide variety of

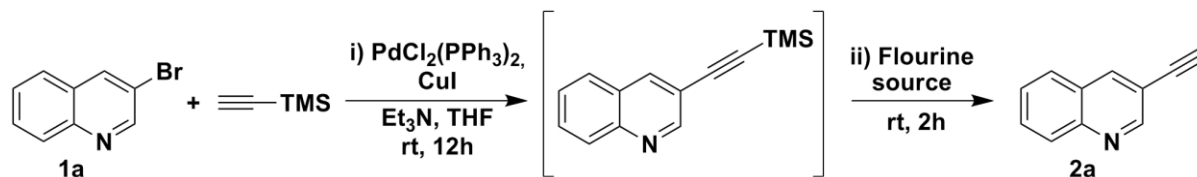
functional groups including formation of silyl ethers in protection of hydroxyl groups, as well as acetylene hydrogen protection. In the case of acetylene, the use of a protecting group for an acetylenic hydrogen is often necessary due to its acidic nature.¹⁶⁸ In addition the steric bulk of these silane moieties prohibits catalytic hydrogenation.¹⁶⁹ The use of trialkylsilylacetylenes in organic synthesis is convenient as they tend to be liquids or solids, as opposed to the unprotected gaseous counterparts.¹⁶⁸ These protecting groups are frequently cleaved or removed through a fluoride source, the driving force of this reaction being the formation of the stronger Si-F bond (564.8 kJ/mol) in comparison to that of the Si-C bond (451 kJ/mol). Trimethylsilylacetylene (TMSA) is frequently used in Sonogashira coupling reactions with aryl or vinyl halides.¹⁶²

3.2.2 Optimization of Reaction Conditions.

For the synthesis of our alkyne fragments, the halogenated heterocyclic scaffold of 3-bromoquinoline (**1a**) was selected for optimization of this synthetic procedure. As this reaction sequence had not been previously applied to quinoline or isoquinoline scaffolds, the one pot methodology was provisionally abandoned and products were isolated and purified at various steps throughout the synthesis of this alkyne fragment. The reaction sequence that followed would entail a Sonogashira coupling of the heterocyclic halide with TMSA followed by *in situ* deprotection of the silyl protected alkyne intermediate. This was done via an appropriate source of fluoride, namely tetrabutyl ammonium fluoride (TBAF) as the trihydrate, as can be seen in Table 1. Our first attempt entailed recreating conditions as used by Müller and co-workers,¹³⁸ using appropriate inert Schlenk and degassing techniques. However, the yields initially obtained were poor and the results obtained by Müller could not be reproduced under these conditions. A number of optimization modifications were undertaken, including increasing the amount of catalyst and co-catalyst, the amount of base added, as well as the source and amount of fluoride for deprotection which can be seen summarized in Table 1. THF was kept as solvent and reaction times were kept constant at 12 h for the optimization process. As can be deduced from this experimental evaluation, changing of the parameters afforded little profit in the yield obtained, with exception to the use of liquid TBAF as fluoride source and longer degassing periods. It was only after employing the freeze-pump-thaw cycling technique for degassing of liquids that the alkyne heterocyclic compound was afforded in very good yields.

Table 1

Optimization of Sonogashira coupling for 3-bromoquinoline.

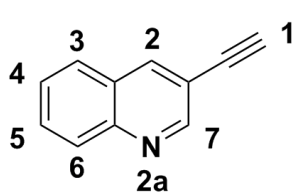


Attempt	PdCl ₂ (PPh ₃) ₂ (mol. %)	CuI (mol. %)	Et ₃ N (equiv.)	Fluoride source (equiv.)	Degassing (min) ^a	Yield (%)
1	2	4	2	TBAF.3H ₂ O (1.5)	-	37
2	4	4	2	TBAF.3H ₂ O (1.5)	15	50
3	4	6	3	TBAF.3H ₂ O (2)	30	52
4	4	4	2	Liquid TBAF (1.5)	30	64
5 ^b	4	4	2	Liquid TBAF (1.5)	30	85

a = Performed by passing N₂ through reaction.

b = Freeze-pump-thaw technique was also applied for degassing.

This laboratory-scale technique, involves the flash freezing of the fluid to be degassed in a Schlenk tube usually with liquid nitrogen and the application of a vacuum thereafter. Upon subsequent thawing, bubbles of gas are seen to form and escape to the top head space of the flask. This process is typically repeated between 3-6 times until all air is removed from the reaction vessel and fluid.¹⁷⁰ This afforded our first alkyne fragment **2a** in good yield.



Subsequent ¹H NMR spectroscopic analysis confirmed formation of the unprotected alkyne product. The acetylenic proton **1** was identified as a singlet at 3.28 ppm integrating for 1H. The aromatic proton peaks of **4** and **5**, were seen as a triplet of doublets

integrating for 1H each at 7.56 and 7.63 ppm. Peaks corresponding to proton **6** and **3**, were witnessed as doublets at 7.77 and 8.09 ppm, both integrating for 1. Proton **2** was seen as a singlet at 8.27 ppm integrating for 1H and proton **7** could also be seen as a singlet at 8.94 ppm, integrating for 1H.

Application of these synthetic conditions and parameters for 7-chloro-4-iodoquinoline (**1b**) did not afford the yields obtained for the 3-bromoquinoline (**1a**) counterpart. After experimentation with different sources of fluorine, including potassium fluoride (KF) and caesium fluoride (CsF), it was determined that the use of CsF facilitated the maximum yield obtained for this specific heterocycle. Similar application of the optimized synthetic conditions to both 4- and 5-bromoisoquinoline scaffolds (**1c-d**) resulted in no reaction taking place.

After scouring the literature for halogenated isoquinolines and metal-mediated coupling reactions and further experimental evaluation, it was found that Et₃N was required as solvent and elevated temperatures were necessary for the reaction to proceed.¹⁷¹ This afforded both heterocyclic alkynes **2c** and **2d** in very good yields. The necessity of these conditions could possibly be explained by the isoquinoline moieties higher pK_a value of 5.46, and thus increased basicity, in comparison to that of the quinoline moieties pK_a value of 4.85.¹⁷² Studies on the basicity of these heterocycles, in both the liquid and gaseous phase, have been indicative of a “peri” steric effect - hindering protonation in aqueous media of both quinoline and acridine that is absent in isoquinoline. This is displayed in Figure 27, where the presence of two peri hydrogens results in a more pronounced steric hindrance effect, which in turn is reflected in a lower pK_a value in comparison to quinoline, with one peri hydrogen, and pyridine with none.¹⁷² Basicity measurements undertaken in the gas phase showed the trend of increasing basicity in the order pyridine < isoquinoline ~ quinoline < acridine, a complete reversal in the trend seen in solution.¹⁷²

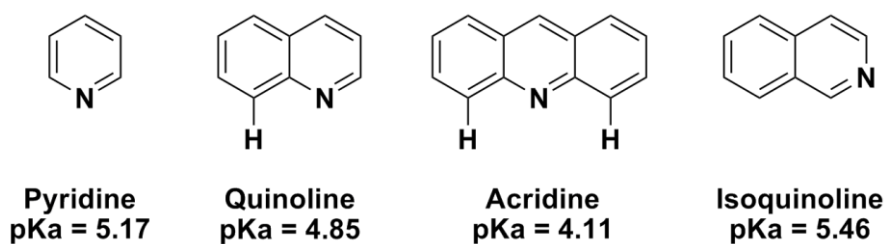
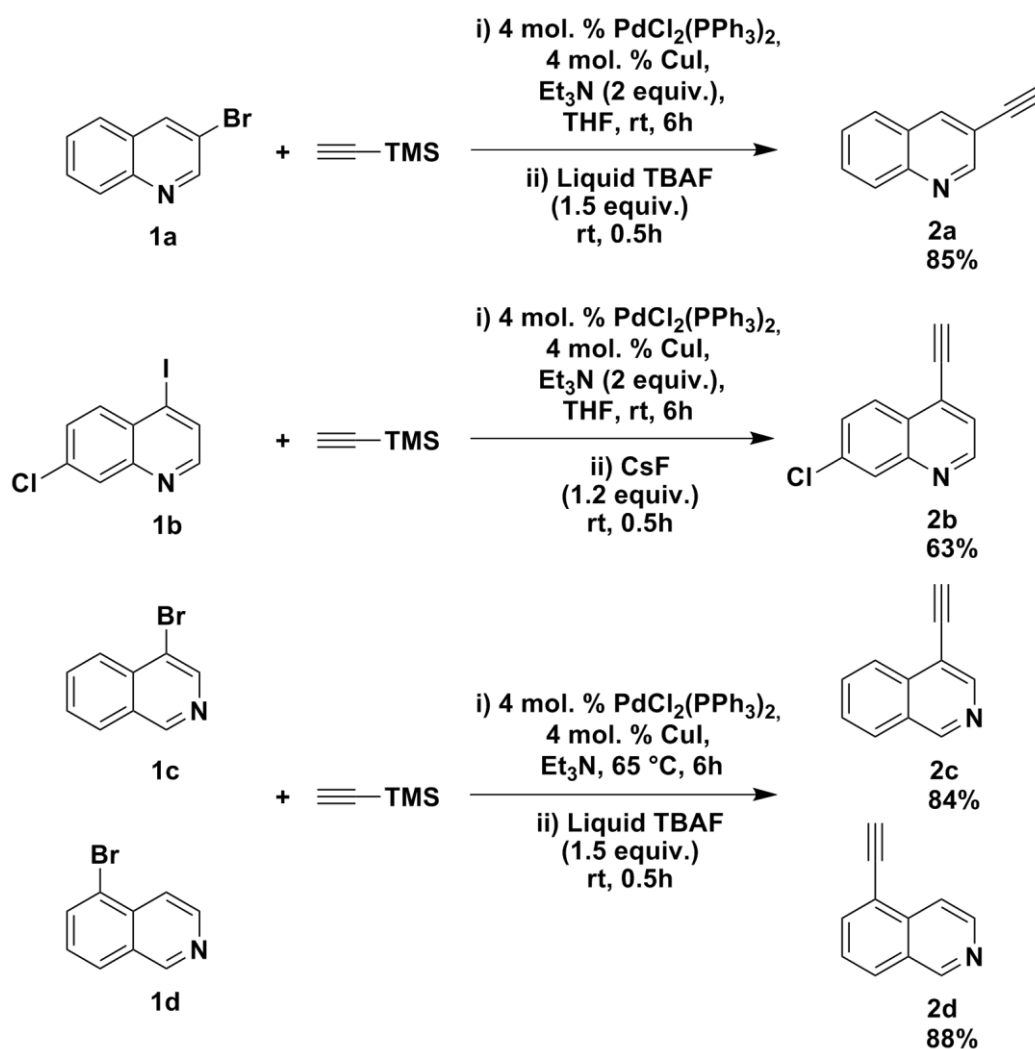


Figure 27

Peri steric effects on various heterocyclic scaffolds and their corresponding pK_a values in solution.

The solvent free values support the hypothesis of this peri steric effect. With the lack of this peri steric effect in the isoquinoline moiety, coordination to the copper catalyst could be occurring more freely, hindering formation of the π -alkyne copper complex and in turn the reaction itself. Furthermore, with a higher pKa value and increased basicity, the isoquinoline moiety could be acting as a base. The use of excess triethylamine and increased temperatures in the reaction could be counteracting these factors. A summary of the final optimized reaction conditions for each halogenated heterocycle, as well as the best yield obtained, can be seen in Scheme 4. All heterocyclic alkyne compounds **2a-d** were fully characterized and product formation was confirmed through the analysis thereof. This furnished our fully characterized alkyne heterocycle fragment library, compounds **2a-d**, and allowed us to continue in the synthesis of the azide fragments.



Scheme 4

Optimized conditions for Sonogashira coupling and *in situ* deprotection for all heterocycles.

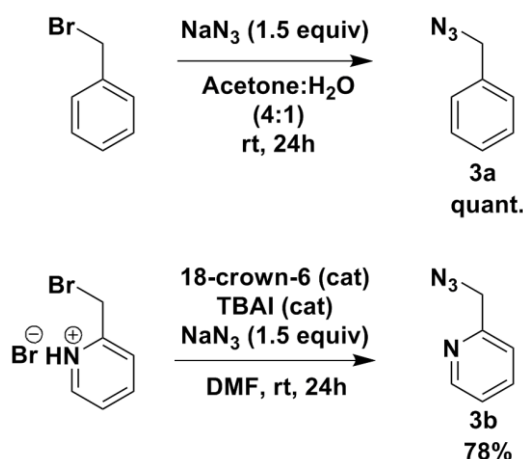
3.3 SYNTHESIS OF AZIDE SIDE CHAIN FRAGMENTS

3.3.1 Synthesis of benzyl azide and 2-(azidomethyl)pyridine.

The azide side chain fragments chosen to undergo the CuAAC reaction with our already synthesized alkyne fragment library, consisted of benzyl azide and 2-(azidomethyl)pyridine. As the halogenated precursors, benzyl bromide and 2-(bromomethyl)pyridine hydrobromide, were commercially available and a number of literature procedures for the synthesis of these fragments were accessible, few complications arose.

The conversion of benzyl bromide into benzyl azide is a well-documented, simple reaction. Sodium azide undergoes a simple nucleophilic substitution reaction with benzyl bromide. The azide group acts as the nucleophile and salt formation of NaBr is the driving force behind the reaction. Our reaction conditions entailed the use of acetone and water as solvents in a 4:1 ratio at ambient temperature, as can be seen in scheme 5.¹⁷³ This afforded a quantitative yield of benzyl azide as a brown oil (**3a**).

The synthesis of 2-(azidomethyl)pyridine was not as straight forward. A first attempt at the synthesis of this fragment using the procedures for compound **3a**, afforded the product in a very poor yield. Further research on the literature of these compounds unearthed a procedure which made use of a catalytic amount of both 18-crown-6 and tetrabutylammonium iodide with DMF as solvent, as can be seen in Scheme 5.¹⁷⁴



Scheme 5

Reaction conditions for azide fragment synthesis.

The reaction proceeded smoothly at ambient temperature and afforded the product **3b** in a good yield of 78%. The role of 18-crown-6 and tetrabutylammonium iodide (TBAI) in this

reaction is as a phase transfer catalyst. 18-crown-6 has been known to accelerate various substitution reactions through suppression of ion pairing.¹⁷⁵ The anions, or in this case the azide moiety, become naked nucleophiles – increasing the nucleophilicity and reaction rate.

FTIR analysis confirmed the successful conversion of the reaction and the presence of the azide moiety in both fragments, with a characteristic strong asymmetric stretch at 2089 cm⁻¹ and symmetric stretch at 1282 cm⁻¹ for **3a** and at 2093 cm⁻¹ and 1270 cm⁻¹ for **3b**, as can be seen in Figure 28.

With both our alkyne and azide fragment precursors synthesized, the synthetic path was now clear to attempt the CuAAC reaction to obtain a 1st generation, combinatorial library of potential reversible kinase inhibitors from these fragments.

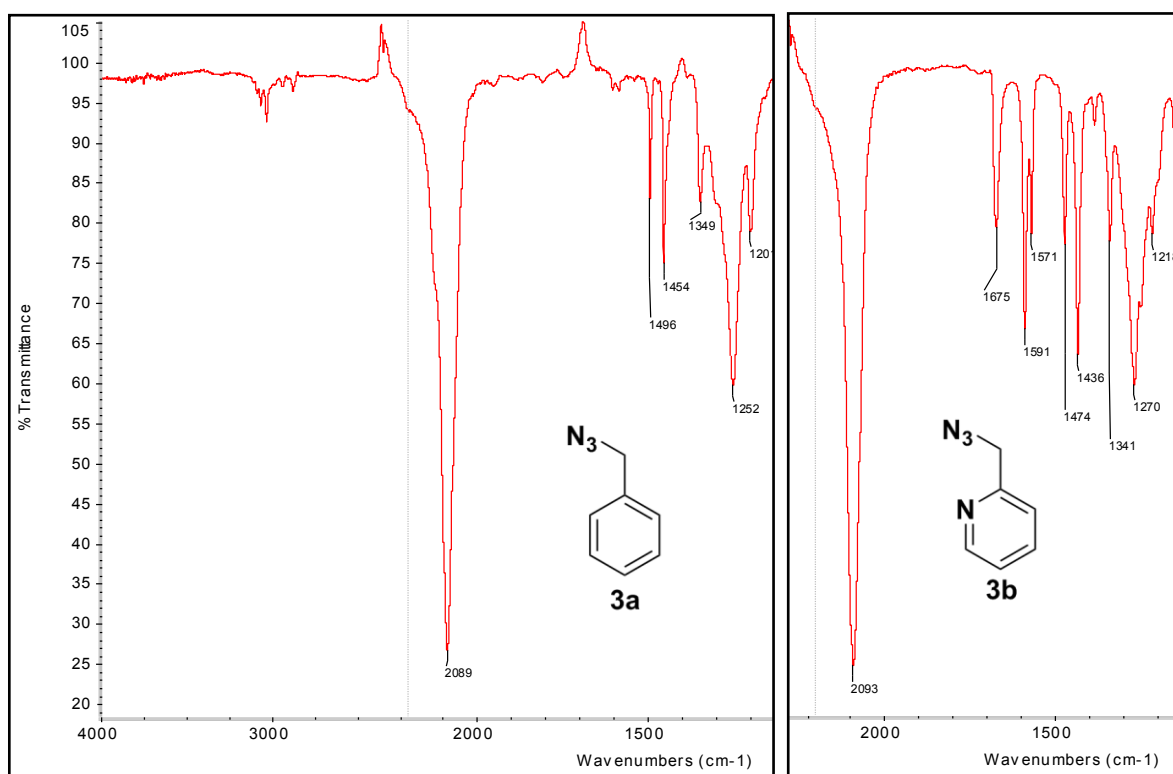


Figure 28

IR spectra of compound **3a** and **3b** illustrating prominent azide stretches.

3.4 GENERATION OF COMBINATORIAL LIBRARY FROM AZIDE AND ALKYNE FRAGMENTS

3.4.1 Defining “Click” Chemistry

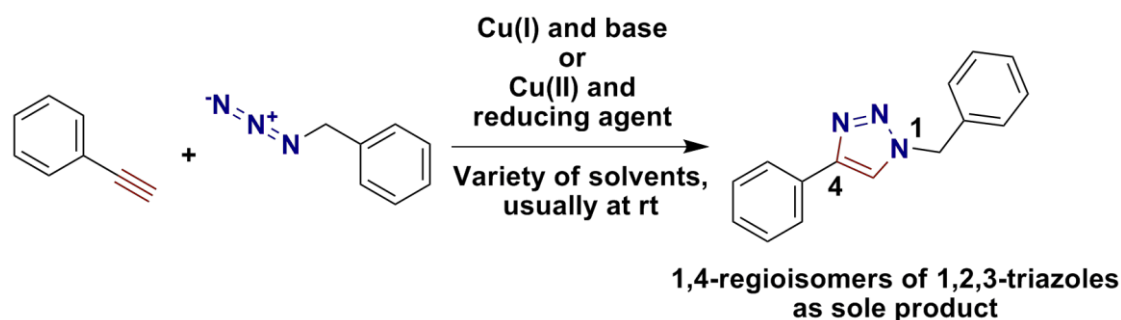
The term “Click” chemistry was coined by K. Barry Sharpless and his group in a landmark paper in 2001.¹⁷⁶ With particular emphasis on following the strategy adopted by nature in generating large molecules built from smaller components via heteroatom to carbon linkers, a rigorous and stringent set of criteria was defined which must be observed by a process, to fall within this category. Thus a click chemistry reaction is delineated and exemplified best as one that is modular, broad in application, affording high yields with minimal and innocuous by-products, stereospecific and have a high atom economy. Furthermore, the reaction should proceed under ambient reaction conditions, using commercially and readily available reagents and starting materials, in a solvent that is benign to the environment and easily removed with simple separation, isolation and purification.¹⁷⁶

A number of reactions have been found to satisfy these criteria exceptionally and have become benchmark click reactions. These include: thiol-ene click reactions,¹⁷⁷ Diels-Alder and inverse electron demand Diels-Alder reactions,¹⁷⁸ nucleophilic substitutions to strained epoxides,¹⁷⁹ and cycloaddition reactions such as the [4+1] cycloaddition between isonitriles and tetrazines¹⁸⁰ and the [3+2] Huisgen 1,3-dipolar cycloadditions, frequently called “click” reactions, including the copper-¹⁸¹ and ruthenium-catalysed variants.¹⁸²

Click chemistry has found a plethora of applications in chemistry, biochemistry, supramolecular chemistry, polymer and materials science.¹⁸³ This has extended to its use in 2D gel electrophoresis, macromolecular or nanostructures,¹⁸⁴ peptidomimetics or its peptide chains,¹⁸⁵ macrocyclizations,¹⁸⁶ dendrimer design,¹⁸⁷ nanotechnology and drug discovery.^{183,188} Click chemistry has also been used to label biomolecules within systems, through biorthogonal click reactions. This means that these reactions possess good selectivity and biocompatibility,¹⁸⁹ overcoming toxicity such that their participating reagents can form covalent bonds within abundantly functionalized biological systems - in some cases, living organisms.^{195, 196} This has won click chemistry world recognition as a household term for chemists.

3.4.2 The 1,4-Copper Catalysed Azide Alkyne Cycloaddition (CuAAC).

The azide alkyne Huisgen cycloaddition has been referred to as the “cream of the crop” of click chemistry by Sharpless himself.¹⁷⁶ In particular, the copper-catalysed cycloaddition has become one of the most popular and recurrently used reactions in click chemistry today.^{183,188} It was discovered simultaneously and separately by the groups of Sharpless and Valery V. Fokin,¹⁹⁰ as well as the Meldal group in Denmark.¹⁹¹ Whilst the Meldal group were the first to document and report the reaction in the synthesis of peptidotriazoles on solid support, they did not fully appreciate the potential of the reaction and its applicability as a click reaction. Sharpless on the other hand, lauded it as a reliable and robust catalytic process, bringing unparalleled selectivity, consistency and broad spectrum utilization in the organic synthesis for the formation of covalent linkers between assorted components.¹⁹⁰



Scheme 6

General reaction conditions and product formed for CuAAC.

The copper-catalysed azide alkyne cycloaddition reaction occurs between organic azides and terminal alkynes which are united to exclusively form 1,4-regioisomers of 1,2,3-triazoles as product, shown in scheme 6.¹⁹² Although commercial sources of copper(I) such as cuprous bromide or iodide may be used for the cycloaddition, the reaction has been found to proceed more efficiently with the use of a copper(II) source such as copper sulphate and an applicable reducing agent such as sodium ascorbate or ascorbic acid, as seen in scheme 6. This is due to Cu(I) species being unstable in aqueous solvents, which can be overcome with the addition of stabilising ligands. An advantage of generating the Cu(I) species *in situ*, whereby the Cu(II) complex is reduced from the +2 oxidation state to the +1, is the non-requirement of a base. If copper(I) sources are used directly, triethylamine (Et₃N) or N,N-diisopropylethylamine (DIPEA) are frequently used as bases.

This economical reaction excels in a variety of solvents. Whilst water without organic co-solvent or a mixture of water/alcohol such as methanol, *iso*-propanol or *tert*-butanol is most

commonly used, organic solvents such as dimethyl sulfoxide, tetrahydrofuran, acetone, dimethylformamide and acetonitrile are also effective.¹⁹² The reaction functions in a wide pH range, from 4-12, with pH 7-9 yielding best results. Reactions have been shown to proceed at 0 °C and as high as 160 °C. The isolation and purification is also simple, usually requiring filtration of product or extraction, avoiding laborious and time consuming chromatographical methods or recrystallization.¹⁹² A huge boon of this reaction is its inertness to many of the most common functional groups without protection.¹⁸⁸ For these reasons, it is clear to see why this reaction has gained such relevance and esteem in organic synthesis.

3.4.3 Catalytic Cycle and Mechanism.

The current proposed mechanism for the CuAAC is based on density functional theory (DFT) calculations undertaken by Sharpless and his group.¹⁹² Although there was a deficiency in certain aspects of chief transitions and intermediates, the study elucidated much in understanding, through qualitative and quantitative analysis, of the mechanistic path followed in this reaction as shown in Figure 29. Nevertheless, the exact DFT calculations agree and overlap with a number of experimental observations and evidence. These include a lower activation barrier calculated in comparison to related cycloadditions, which accounts for a dramatic increase in reaction rate observed in the CuAAC. Secondly, the regioisomer obtained in the experimental reaction, the 1,4-substituted variant, is predicted by DFT. Lastly, the DFT calculations successfully predicted the reaction to proceed with other dipoles such as nitrile oxides, which is observed experimentally adhering strictly to the regioselectivity. This enforces the mechanism put forward by Sharpless and his group.¹⁹²

The reaction mechanism begins with either the Cu(I) catalyst or the Cu(I) species generated *in situ* through reduction of a suitable Cu(II) pre-catalyst. This alkyne coordinates to the Cu(I) species, which results in the expulsion of a ligand from the copper complex and formation of the copper acetylide as shown in step **A** Figure 29. This conversion proceeds through the formation of a π -alkyne copper complex as has been seen in various other copper mediated coupling reactions.¹⁶² Thereafter, step **B** involves the replacement of the previously expelled ligand with the coordination of the azide to the copper through the nitrogen proximal to the carbon forming the copper-azide-acetylide complex. Subsequent attack, in step **C**, from the distal nitrogen of the azide of the alkyne carbon bonded to R¹ affords the six-membered copper(III) metallacycle. From this point the barrier for ring formation is very low, which furnishes the triazolyl-copper derivative through step **D**.

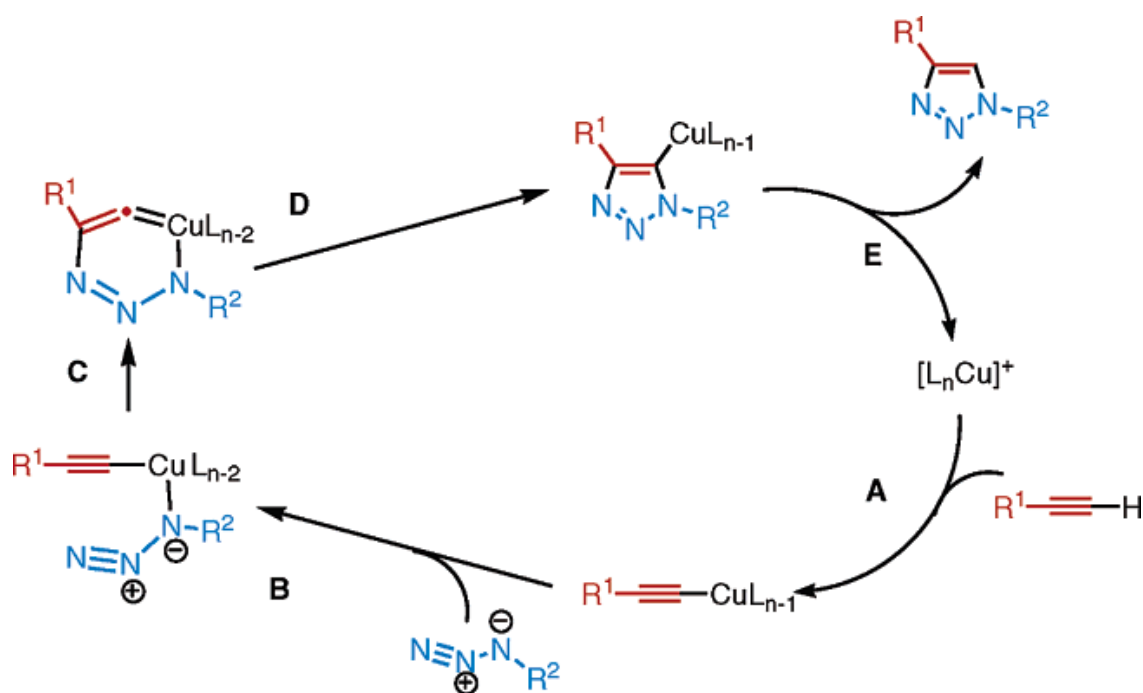


Figure 29

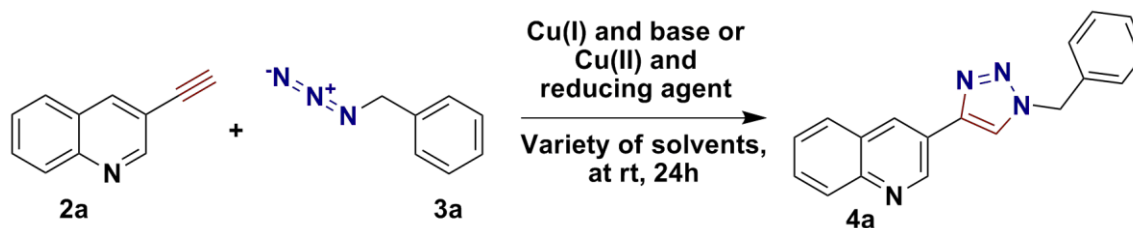
Proposed reaction mechanism and catalytic cycle for CuAAC adapted from Sharpless *et al.*¹⁹²

Subsequent release of the triazole through step E affords the 1,4-substituted 1,2,3,-triazole and regeneration of the copper catalyst.¹⁹²

3.4.4 Synthetic Optimization and Generation of Library of Novel Reversible Inhibitors

With our alkyne and azide side chain moieties in hand, it was our intention to generate a small “combinatorial” library derived from these previously synthesized fragments, through the use of the CuAAC. As can be imagined, a large amount of literature procedures and reaction conditions have been reported for this reaction, which resulted in a number of experimental evaluation and optimization reactions being performed, in order to determine what conditions afforded the highest yield in the most efficient manner as can be seen in Table 2. For this, compound **2a** and benzyl azide (**3a**) were selected and examined against an assortment of different sources of copper, including Cu(I) and Cu(II) species with reducing agents, and a variety of different solvents in different ratios. The reaction time was kept constant at 24h and all reactions were carried out at rt.

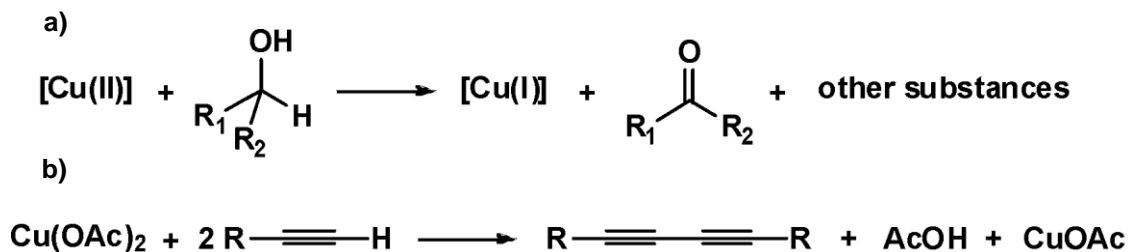
Table 2
Optimization of CuAAC for compound 4a.



Attempt	Source of copper	Amount (mol. %)	Reducing agent	Amount (mol. %)	Solvents used	Solvent ratio	Yield (%)
1 ¹⁹³	CuSO ₄ ·5H ₂ O	2	Sodium ascorbate	5	H ₂ O:t-BuOH	1:1	18
2 ¹⁹³	CuSO ₄ ·5H ₂ O	5	Sodium ascorbate	5	H ₂ O:t-BuOH	1:3	20
3 ¹⁹³	CuSO ₄ ·5H ₂ O	5	Sodium ascorbate	5	H ₂ O:MeOH	1:1	28
4 ¹⁹⁴	CuI	5	DIPEA	1 equiv.	ACN	-	12
5 ¹⁷⁴	Cu(OAc) ₂	10	-	-	H ₂ O:t-BuOH	1:1	62
6 ¹⁷⁴	Cu(OAc) ₂	10	-	-	H ₂ O:MeOH	1:4	73

Our initial reactions condition were based on the one of the most popular and frequently used copper sources, CuSO₄, with the equally as prominent sodium ascorbate as reducing agent in aqueous medium – a procedure which often affords quantitative yields as outlined by one of the co-discoverers and founder of the principle of click chemistry, Valery V. Fokin.¹⁹³ Sodium ascorbate, a mild reductant, is a suitable and advantageous alternative to oxygen free conditions as any dissolved dioxygen is reduced, eliminating the appearance of by-products from copper catalysed oxidative side reactions.¹⁹³ Water is a conducive solvent for the formation of reactive copper acetylides, especially when formed *in situ*.¹⁹³ However, as shown above in attempt 1-3 in Table 2, use of these reagents and conditions with a variety of solvents and ratios and amount of catalyst loadings afforded very poor yields. This led us to evaluate the use of a Cu(I) halide species in an organic solvent, such as CuI in acetonitrile with the use of DIPEA as base (attempt 4). However this afforded an even lower yield which

can be explained by the formation of oxidative by-products, which seemingly halted progression of the reaction and destroyed the catalyst. With this methodology, elimination of oxygen in the reaction vessel is a priority, but with the proclaimed robust nature of this reaction we sought out other synthetic conditions which would afford a reasonable yield.



Scheme 7

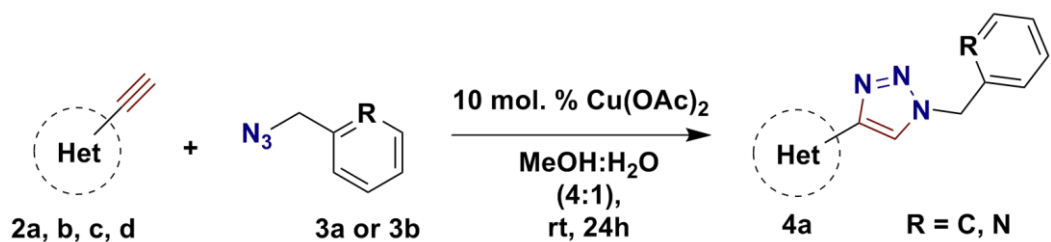
General reaction conditions and product formed for CuAAC.¹⁷⁴

After combing through the literature, a procedure was found which makes use of copper (II) acetate without inclusion of a reducing agent as devised by Zhu and co-workers.¹⁷⁴ The group found that the CuAAC proceeds with a number of Cu(II) salts, without the need for a reducing agent, in readily oxidizable alcohols such as MeOH, EtOH and *i*-PrOH, but not *t*-BuOH. This led to the hypothesis that a Cu(I) species was generated via the reduction of the Cu(II) catalyst through oxidation of these alcohol solvents as shown in Scheme 7a below. However, the reaction was seen to proceed with a very high yield with Cu(OAc)₂ in *t*-BuOH which is not inclined to oxidation. This led to the group putting forward a second postulation, that a Glaser-type reaction - or in the case of copper (II) acetate salts, a related Eglinton-type reaction, shown in Scheme 7b - was taking place. This furnished the catalytically active Cu(I) species, which has been shown to be generated in these reactions,^{195, 196} which in turn facilitated reaction of the azide alkyne cycloaddition (AAC). According to the authors, electron paramagnetic resonance (EPR) and absorption spectroscopy both supported these hypotheses.¹⁷⁴

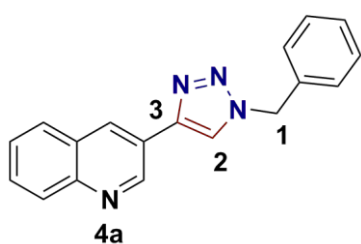
Use of Cu(OAc)₂ in a mixed solvent system H₂O:*t*-BuOH afforded a satisfactory yield and with replacement of MeOH a yield of 73% was found to be acceptable for the optimization of this reaction, as seen in Table 2. With a suitable synthetic procedure optimized, we applied these parameters to the rest of our heterocyclic alkyne and azide fragments in a “combinatorial” fashion, generating a library of clicked compounds in good yield as shown in Table 3.

Table 3

Combinatorial library generated through CuAAC with yields.



Alkyne	Azide	1,4- CuAAC products	Yield (%)
			R = C: 4a = 73 N: 5a = 70
			R = C: 4b = 71 N: 5b = 68
			R = C: 4c = 66 N: 5c = 69
			R = C: 4d = 68 N: 5d = 66



These novel compounds were fully characterized using ¹H NMR, ¹³C NMR, FTIR spectroscopy and HRMS-TOF MS. This confirmed the formation of the clicked products. Showing compound **4a** as example, both the benzylic protons and the

CH₂ proton in the triazole ring were clearly accounted for in the ¹H NMR spectra, with proton **1** showing up as a singlet at 5.61 ppm integrating for 2H and proton **2** being observed as a singlet at 7.86 integrating for 1H as was expected. All other protons were accounted for in the spectra. For the ¹³C NMR spectra, carbon**1** was at 54.5 ppm and the triazole formation was confirmed by both carbons **2** and **3** showing on the spectra at and 129.36 and 145.49 ppm. All other corresponding carbon peaks were accounted for. The [M+H]⁺ ion found in the MS spectra was 287.1297, which matched identically with the calculated 287.1297 for C₁₈H₁₅N₄.

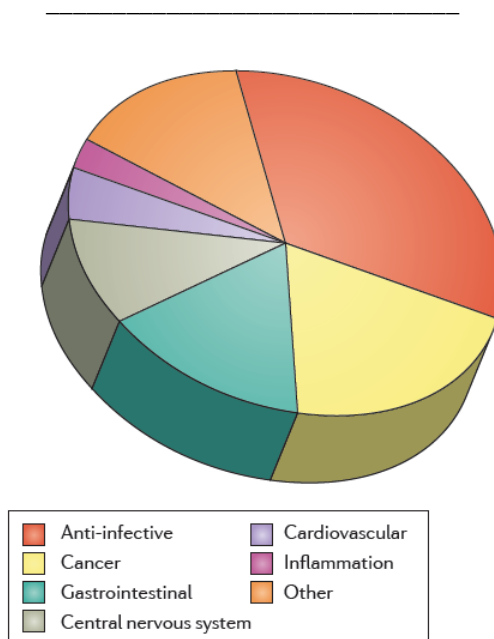
Through use of the CuAAC we were able to generate 8 novel, 1,4-substitued 1,2,3,-triazole based potential reversible kinase inhibitors. These compounds would later be sent for biological assays to determine efficacy and potency. With the synthetic methodology adopted and developed in the synthesis of our potential reversible inhibitor library, we set our sights on utilizing this click chemistry approach in the synthesis of potential irreversible inhibitors. Irreversible kinase inhibitors have been shown to possess a number of distinct advantages over their ATP competitive counterparts, and thus it was our endeavour to move one step forward in the design of potent and selective inhibitors.

CHAPTER 4 – 1ST GENERATION IRREVERSIBLE INHIBITOR LIBRARY

4.1 MOTIVATION, RATIONALE AND STRATEGY FOR SYNTHESIS OF IRREVERSIBLE INHIBITOR LIBRARY

4.1.1 Irreversible Inhibitors – Successes and Advantages.

The successes attained by reversible, ATP competitive kinase inhibitors as anticancer agents, brought drug discovery in kinase inhibition to the forefront of the targeted therapeutic treatment of cancer. However, challenges met in the clinical and approved phases of these drugs, which include promiscuity across the widely conserved human kinome, high intracellular concentrations of endogenous ATP, the competitive substrate in reversible inhibition and resistance to prescribed drugs due to mutations in the enzyme, has sparked a search for alternative therapeutic mechanisms to combat these challenges.¹⁹⁷ A resurgence in the field of covalent drugs or irreversible inhibitors,¹⁹⁸ has been paramount to addressing and overcoming these challenges. This revival has been brought on by a greater understanding of the advantages and disadvantages of irreversible inhibition and the approval of a number of potent and non-toxic covalent drugs.¹⁹⁹ Covalent drugs, in general, have been an extremely lucrative and successful class of treatment for the pharmaceutical sector, with 3 of the top ten selling drugs in the United States in 2009 being covalent drugs, \$33 billion dollars in worldwide sales from the 26 covalent drugs for which there is data and the most used irreversible drug globally, aspirin, having 80 million tablets consumed per year in the United States alone.¹⁹⁸ A breakdown of the 39 drugs that had received FDA approval in mid-2011 shows that ~33% are used as anti-infectives, 20% as anti-cancer agents, 15% for gastrointestinal disorders and 10% and 5% for cardiovascular and central nervous system disorders respectively as can be seen in Figure 30. Inflammation targets make up 3% of these FDA approved drugs with 13% targeting other disorders.¹⁹⁸ This has shown irreversible inhibition to be a successful, proven approach in many classes of drug targets.¹⁹⁷ In the last decade, the distinct advantages of targeted, irreversible kinase inhibitors include benefits such as extraordinary efficacy and IC₅₀ profiles in biological assays, success in overcoming ATP competition, an inherent selectivity that is exclusive to its mechanism of action and very importantly, an ability to retain efficacy against resistance mutations in target kinases.¹⁹⁷ This has resulted in a number of irreversible kinase inhibitors undergoing clinical investigation and this field of research can be considered the vanguard of protein kinase inhibition.

**Figure 30**

Pie chart illustrating the spread of covalent inhibitors in treatment.¹⁹⁸

With no greater PTK are these benefits greater exemplified than with EGFR. Figure 31 shows the chemical structure of 6 irreversible inhibitors in particular, all targeting the EGFR/HER2 pathway and in clinical trials, that have shown the promise and potential of this mechanism of treatment. IC₅₀ values in nM, based on preclinical *in vitro* EGFR and HER2 kinase assays, are indicated below each compounds name.^{197, 200} Not only do these inhibitors show remarkable antitumour activity and efficacy in *in vitro* and *in vivo* assays, they also exhibit potent selectivity and the ability to overcome mutations that have sparked resistance to approved ATP competitive inhibitors on the market.^{134b, 200-201} The compound WZ4002, as example, has shown remarkable selectivity in targeting the T790M specific mutation within the EGFR kinase domain.^{201c, 201d} This secondary mutation at the gatekeeper residue, which occurs by substitution of the threonine 790 amino acid with methionine, is one of the most common causes of resistance to known therapeutic agents.^{134b} The result of this substitution is a bulkier side chain at the gatekeeper residue which restricts and hinders access to the active site by the inhibitor through sterics, thus lowering efficacy. It has also been shown that this mutation increases affinity for the natural substrate ATP, thus meaning an increased dosage of inhibitors are needed to remain competitive.^{134b} Drug discovery stratagems targeting this mutation through irreversible inhibition have resulted in failure due to a unacceptable toxicity profile which is linked to simultaneous inhibition of the wildtype EGFR.^{201c}

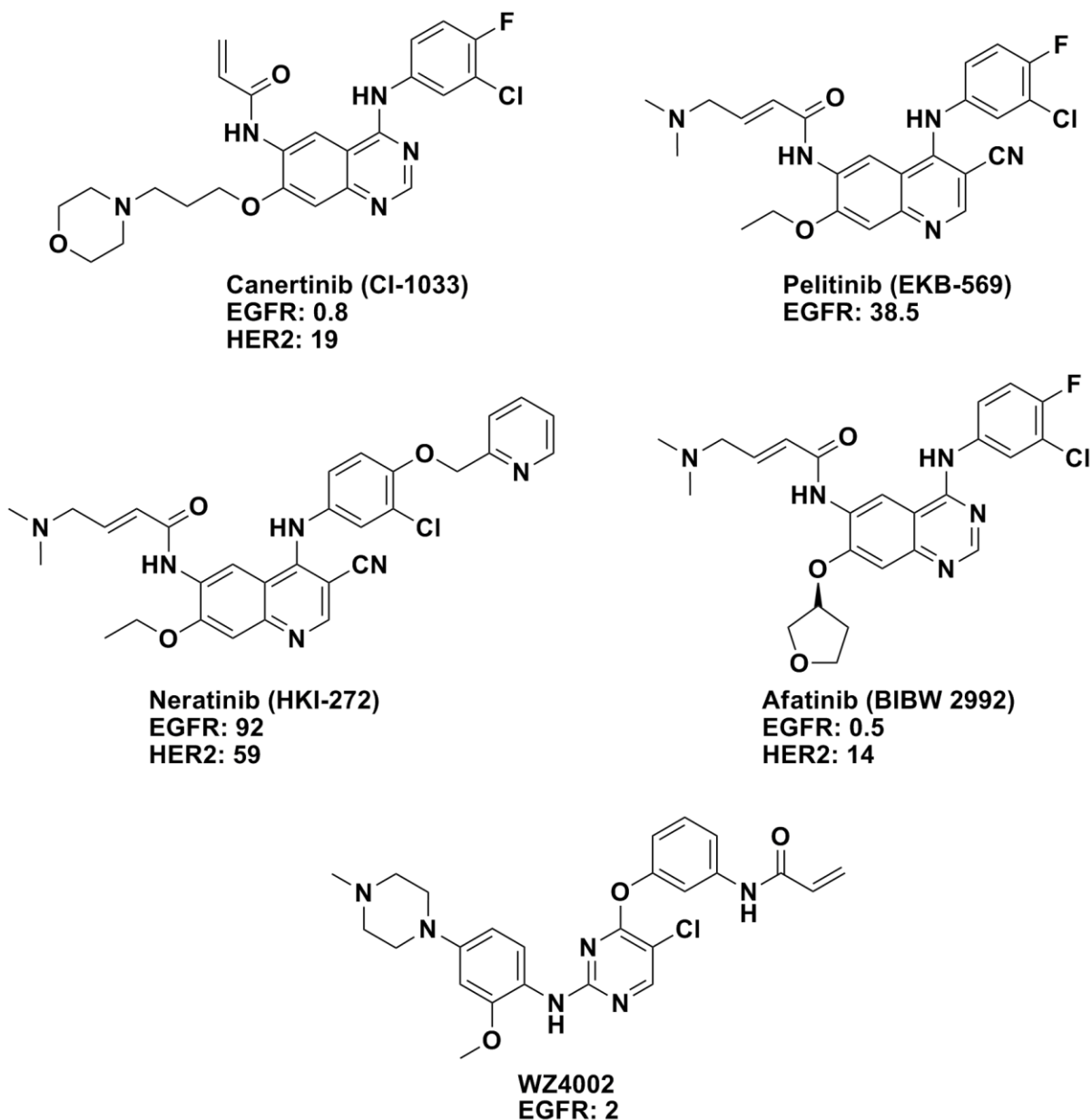


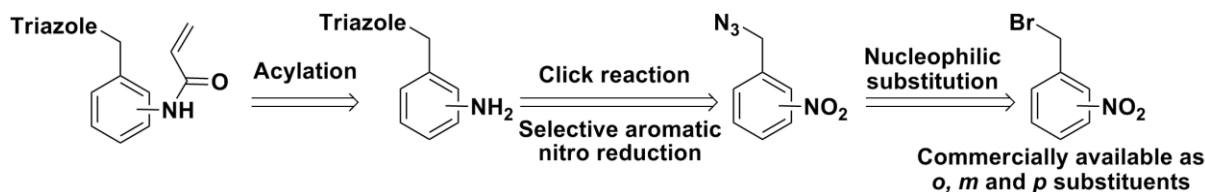
Figure 31

A number of irreversible inhibitors currently in clinical trials with IC₅₀ values shown in nM.

The wild type can be thought of as the normal or phenotypic enzyme, a product of standard alleles, present in the body. However, WZ4002 has shown an incredible selectivity for this mutated form of the EGFR kinase, being 30-100 fold more potent against EGFR T790M, and up to 100- fold less potent against the wildtype EGFR, in comparison to other quinazoline-based EGFR inhibitors *in vitro*.^{201c} With these results it is clear to see why the field of irreversible inhibition has generated so much interest and has opened up a dominant approach to identifying new classes of mutant-selective kinase inhibitors.

4.1.2 Rationale and Proposed Synthetic Strategy for Irreversible “Space Probing” Inhibitor Library.

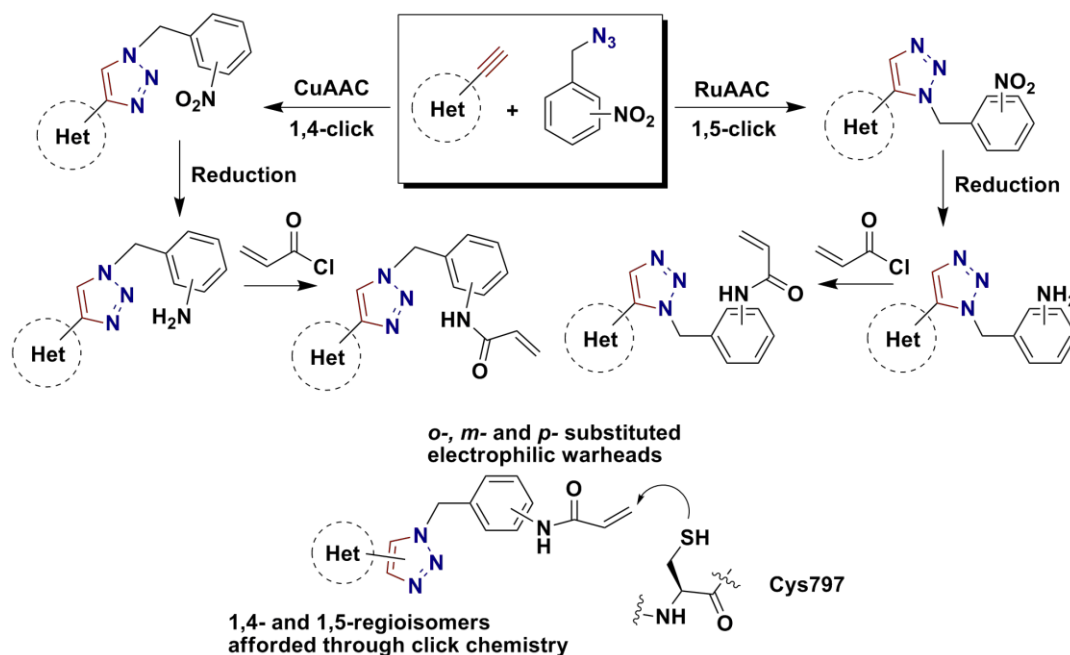
With the clear advantages inherent in irreversible inhibitors and synthetic methodology already laid out incorporating click chemistry in the design of reversible inhibitors, it was our endeavour to apply this to the design and synthesis of a library of irreversible inhibitors. A retrosynthetic analysis of possible ways of incorporating an electrophilic “warhead”, in combination with our already synthesized heterocyclic alkynes, led us to the azide moiety shown in Scheme 8. From the commercially available *o*-, *m*- and *p*- substituted nitrobenzyl bromides, a simple nucleophilic substitution reaction would afford the corresponding nitrobenzyl azides. These compounds would be coupled with our heterocyclic alkynes through click chemistry, followed by subsequent selective reduction of the aromatic nitro group to afford the aromatic amine. Coupling with acryloyl chloride in an acylation reaction, would present a suitable electrophile, or Michael acceptor motif, necessary for covalent bond formation. For the generation of our library of irreversible inhibitors, the use of the acryloyl amide moiety as electrophile was chosen. This was due to its ease of synthetic availability and its known capacity for participation in irreversible inhibition interactions, and its experimentally shown ability to form covalent bonds with cysteine residues.²⁰²



Scheme 8

Retrosynthetic breakdown of electrophilic “warhead” space probes.

An important factor to bring to the reader’s attention is that by utilizing *ortho*, *meta* and *para* substituted nitrobenzyl azides, a large amount of conformational space could be probed in the ATP binding site, increasing the chances for this electrophilic “warhead” to form a covalent bond with the conserved cysteine residue present in the EGFR active site – namely Cys797.¹³⁷ A logical choice to make in the generation of this library of irreversible inhibitors would be to utilize both the copper- and its ruthenium-catalysed click counterpart.



Scheme 9

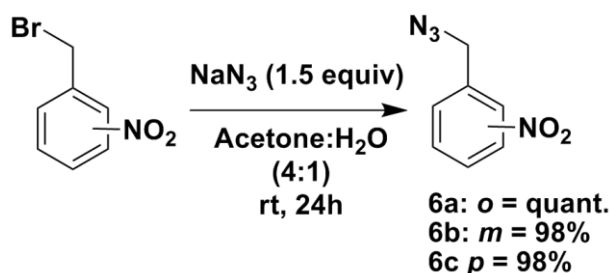
Proposed synthetic route to potential irreversible inhibitors and illustration of space probing effect of these compounds.

This would allow the generation of 1,4- and 1,5- substituted CuAAC and ruthenium catalysed azide alkyne cycloaddition (RuAAC) products respectively (see Section 4.2.2 for more information), affording two different regioisomers – thus expanding the conformational space filled and effectively augmenting the probing affect brought on by the use of *o*-, *m*- and *p*-substituted electrophiles. An illustration of the proposed synthesis for this library of space probing potential irreversible inhibitors can be seen in Scheme 9 above. A copper- or ruthenium-mediated click reaction between the quinoline and isoquinoline heterocyclic alkynes and synthesized azides would afford the corresponding triazole carrying an aromatic nitro group. Reduction of this moiety and subsequent coupling with acryloyl chloride would provide our fully furnished 1,4- and 1,5-, *o*-, *m*- and *p*-substituted library of potential irreversible inhibitors. To fully show the space probing effect of these compounds, and illustrated example is shown at the bottom of Scheme 9. This shows that for each heterocyclic alkyne undergoing this reaction sequence, six potential irreversible inhibitors, adopting unique spatial conformation and thus occupying a different volume of space in the active site, will be generated. This can be seen as a powerful tool for generating a large library of compounds targeting the cysteine residue and irreversible inhibition. The generation of the 1,4-substituted library through CuAAC was carried out and completed by a postdoc researcher in our labs, Dr. Abu Taher and will not be discussed here.

4.2 SYNTHESIS OF LIBRARY OF 1,5- SUBSTITUTED POTENTIAL IRREVERSIBLE INHIBITORS.

4.2.1 Synthesis of Nitrobenzyl Azide Fragments.

With the heterocyclic alkynes synthesized already in hand the first step in the generation of the irreversible inhibitor library was to synthesize the *o*-, *m*- and *p*-substituted nitrobenzyl azide fragments. This was accomplished with relative ease as conditions used for the synthesis of compound **3a** were utilized, affording quantitative or near quantitative yields. The reaction conditions and yields are summarized in Scheme 10 below.



Scheme 10

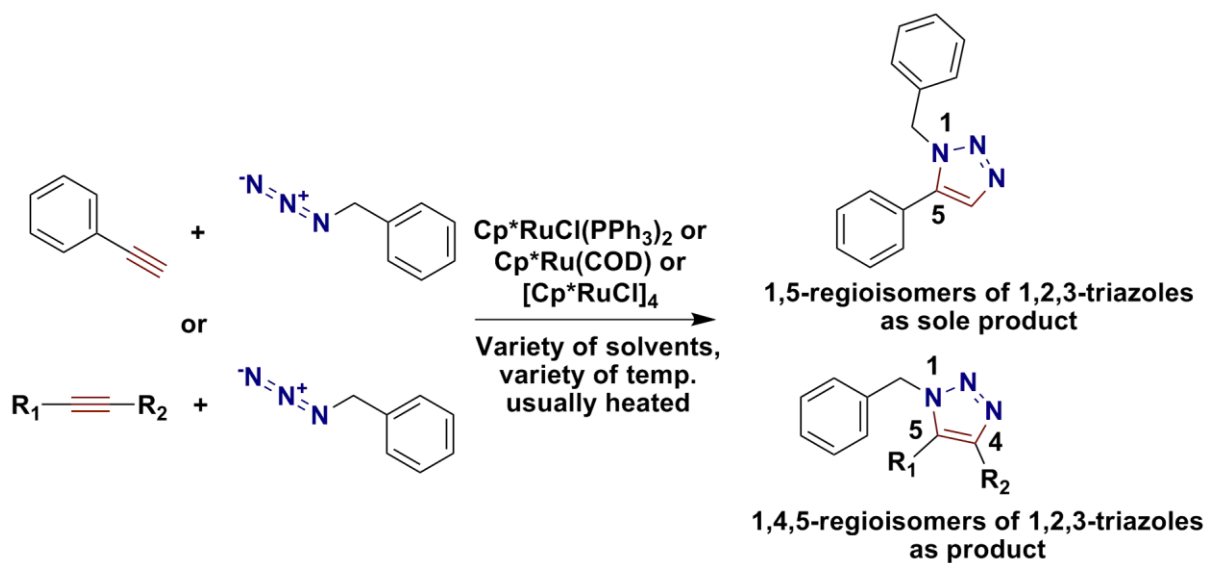
Synthesis of nitrobenzyl azide fragments **6a-c**.

Subsequent FTIR analysis confirmed the presence of the azide species in compounds **6a-c**. As an example, compound **6a** showed a characteristic strong asymmetric stretch at 2091 cm^{-1} and symmetric stretch at 1254 cm^{-1} . This afforded the nitrobenzyl azide fragments and allowed us to move on to synthesizing a combinatorial library of these fragments and the previously synthesized alkyne fragments, through RuAAC reactions.

4.2.2 The Ruthenium Catalysed Azide Alkyne Cycloaddition Reaction.

The success, popularity and applicability attained by the regioselective 1,4-substituted triazole CuAAC reaction demanded a viable synthetic route and methodology to be crafted for its corresponding regioisomer, the 1,5-substituted triazole.²⁰³ Although synthetic procedures to these 1,5-substituted regioisomers are available, which include the use of stabilized phosphonium ylides,²⁰⁴ the addition of bromomagnesium acetylides to organic azides²⁰⁵ and the use of enamines with aryl azides,²⁰⁶ they lack the simplicity, scope and directness of the CuAAC.^{182, 203} This led to the development of a ruthenium-mediated azide alkyne cycloaddition reaction by the groups of Fokin and Jia.²⁰³ By making use of ruthenium-based catalysts such as such as $\text{CpRuCl}(\text{PPh}_3)_2$ and $\text{Cp}^*\text{RuCl}(\text{PPh}_3)_2$, the groups found a regioselective catalytic route to these 1,5-substituted triazoles.²⁰⁷ A notable dampener on the

scope of the CuAAC was its inability to catalyse cycloaddition reactions on internal alkynes. In contrast to the CuAAC, the group of Fokin found that these ruthenium catalysts were indeed able to induce cycloaddition on both terminal and internal alkynes.²⁰³ Weinreb *et al.*,²⁰⁸ investigated the synthesis of these 1,4,5-substituted triazole products with some interesting results as well as the group of Huang and co-workers,²⁰⁷ who deduced that the factors governing the regioselectivity of the reaction are due to electronic effects of the substituents. Although a number of ruthenium based catalysts and their activity in promoting the cycloaddition have been investigated, η^5 -pentamethylcyclopentadienyl ruthenium [Cp*RuCl] variants have been shown to be the most successful in doing this. These include Cp*RuCl(PPh₃)₂, the cyclooctadiene variant Cp*RuCl(COD) and [Cp*RuCl]₄. The effectiveness of these complexes can be attributed to stabilisation of higher oxidation states of the ruthenium centre by the electron rich Cp* ligand, evident in complexes lacking this ligand showing little to no effect in driving the cycloaddition forward. Aprotic solvents are well tolerated including toluene, THF, dioxane, benzene and DMF, with a temperature range from ambient to 110 °C. Interestingly, the presence of water in the reaction flask usually did not affect the catalytic activity of the complexes, leading to the conclusion that incredibly dry conditions are not necessary.¹⁸² Scheme 11 gives an outline of the general synthetic procedures used and products afforded from this reaction. The RuAAC has found applicability in synthesis of glycoconjugate carbonic anhydrase inhibitors,²⁰⁹ mimics of vancomycin²¹⁰ and other synthetic applications such as one pot reaction methods.²¹¹



Scheme 11

General reaction conditions and products formed for the RuAAC.

4.2.2 Catalytic Cycle and Mechanism.

Ruthenium-mediated catalytic transformations of alkynes have been well established in the literature and confirmation of the existence of intermediates such as ruthenium(II) acetylides,²¹² vinylidenes²¹³ and ruthenametalacyclic complexes²¹⁴ have been presented.²⁰³ This and a number of DFT calculation projects have laid the ground work to deciphering the mechanism of the RuAAC. This includes work done by the Fokin group,¹⁸² and most recently an investigation done by Tüzün from Istanbul.²¹⁵ The mechanistic proposal outlined by these groups which proceeds via a 6-membered ruthenacycle intermediate, is supported by the DFT calculation data observed. This proposed mechanism is shown in Figure 32. The catalysts ability to be involved in both terminal and internal alkynes, suggests it is unlikely that a ruthenium acetylide is present in the catalytic cycle. The specific catalysts that are most competent in this cycloaddition point to $[\text{Cp}^*\text{RuCl}]$ being the catalytically active species, a hypothesis supported by a lower catalytic activity seen in both the $[\text{Cp}^*\text{RuBr}]$ and $[\text{Cp}^*\text{RuI}]$, whilst removal of the anionic chloride through Ag^+ , to form $[\text{Cp}^*\text{Ru}]^+$ cationic complexes, results in complete loss of activity.¹⁸²

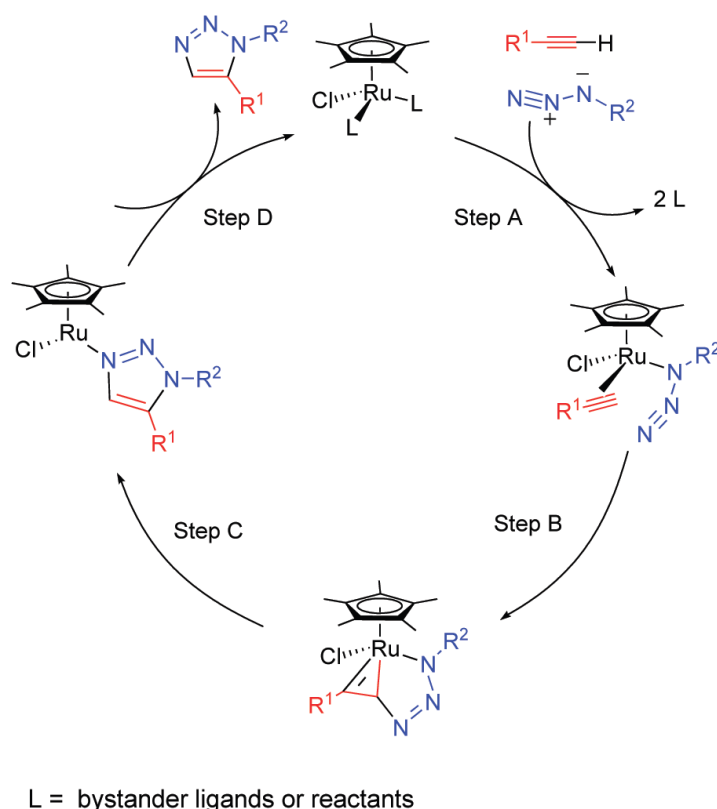


Figure 32

Proposed reaction mechanism and catalytic cycle for RuAAC adapted from Sharpless *et al.*¹⁸²

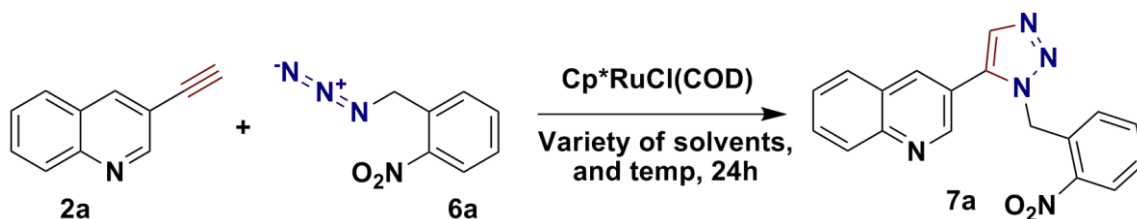
The group hypothesized that the reaction mechanism begins with displacement of the spectator ligands to form an activated complex as shown in step A of Figure 32. This complex is converted, via oxidative coupling of the alkyne and azide, to the ruthenacycle illustrated by step B in Figure 32. The regioselectivity is determined by this step or the first new carbon-nitrogen bond formed, which can be seen as a nucleophilic attack of the activated alkyne at the electrophilic terminal nitrogen of the azide. Computational studies support the irreversible configuration of this ruthenacycle. Subsequent reductive elimination (step C) releases the 1,5 substituted triazole product and the catalyst is regenerated in as shown in step D. DFT studies also indicate that the reductive elimination is the rate determining step in the catalytic cycle.¹⁸²

4.2.3 Synthetic Optimization and Generation of Library of Novel Irreversible Inhibitors

With both the heterocyclic alkyne fragments (**2a-d**) and the newly synthesized nitrobenzyl azide fragments (**6a-c**) in hand, the synthesis of the exclusively 1,5-substituted, RuAAC-mediated library of potential irreversible kinase inhibitors could be undertaken. For this purpose, the catalyst Cp**RuCl(COD)* was chosen and purchased for all reactions on the grounds that it is the most labile catalyst, with the cyclooctadiene group being more easily displaced than say that of the phosphine ligands, and proceeds in the least demanding reaction conditions.¹⁸² Following suit as was previously done in the synthetic endeavours of our reversible library, the coupling between the heterocyclic alkyne **2a** and *ortho* substituted nitrobenzyl azide **6a** was chosen to be optimized, as can be seen in Table 4. The Cp**RuCl(COD)* has been shown to be active at catalytic amounts of 2 mol. % at ambient temperatures producing high yields and 100% regioselectivity.¹⁸² Thus our first reaction conditions implemented a minimum amount of catalyst at rt with anhydrous tetrahydrofuran as solvent. Careful consideration was taken to keep conditions inert and a period of 45min of degassing with nitrogen was implemented. This however, resulted in very poor yields which were solely attributed to the incomplete consumption of both starting reagents as determined by TLC. The reaction was seen not to proceed to completion, and after 24h the reaction was stopped and both the starting materials were salvaged and the product isolated. This meant that whilst we were not losing both our heterocyclic alkyne and azide fragment reagents, the amount of product afforded in this reaction was unacceptable (<20%). Thus it was decided to make use of more catalyst in the second attempt², but again to no avail, it was seen to have little effect on the yield and more importantly not successful in driving the reaction to completion.

Table 4

Optimization of RuAAC for compound 7a.



Attempt ¹⁸²	Cp*RuCl(COD) (mol. %)	Solvent	Temp (°C)	Yield(%)
1	2	THF ^a	rt	18
2	4	THF ^a	rt	19
3	4	THF ^b	rt	23
4	4	Dioxane ^a	rt	18
5	4	Toluene ^a	Gradually to 80	71
6	4	Toluene ^a	80	85

^a = Nitrogen was passed through reaction for 45min for degassing

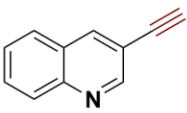
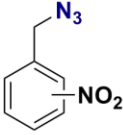
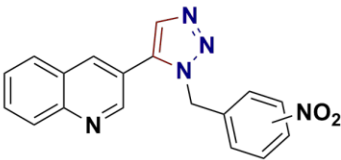
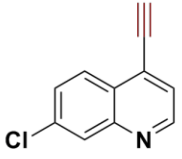
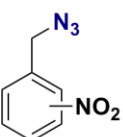
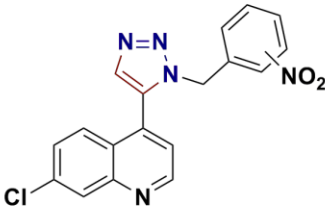
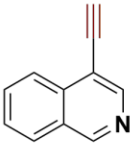
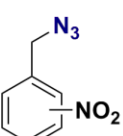
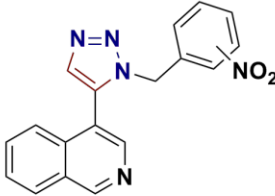
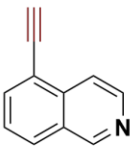
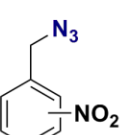
^b = Freeze-pump-thaw technique and nitrogen was passed through for 45min for degassing of reaction.

At this point we investigated whether or not the catalyst was being deactivated due to contaminants such as molecular oxygen or water in the reaction flask and so a freeze-pump-thaw technique, in combination with passing nitrogen through the reaction, was applied for attempt 3.

This had little effect on the yield and the next variable to investigate was that of solvents. Attempt 4 saw the utilization of anhydrous dioxane, which resulted in a lower yield than that obtained for attempt 3 – the main culprit still being incompleteness of the reaction. Finally it was decided to make use of a high boiling point solvent and by increasing the temperature of the reaction, give external energy to drive the reaction to completion. For this purpose, toluene was chosen as solvent and the reaction was gradually heated to 80 °C, starting at rt in 20 °C increments every hour for attempt 5. Satisfyingly, this resulted in the reaction going to completion and a good yield of 71% being obtained for the reaction. The reason we delayed with increasing the temperature to allow it to go to completion, was that the Cp*RuCl(COD)

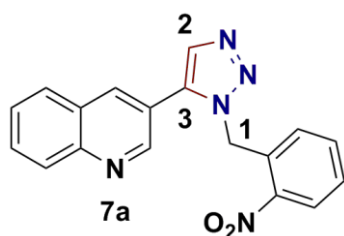
catalyst has specifically been shown to proceed better at ambient conditions and that elevated temperatures are actually detrimental to the reaction, resulting in deactivation, decomposition and low yields.¹⁸² Interestingly, this was not the case for our reactions and the final attempt **6** kept the temperature of the reaction constant at 80 °C from start to finish, resulting in our optimized yield of 85% for compound **7a**. These reaction conditions were then applied to the rest of the heterocyclic alkynes **2a-d** and our *o*-, *m*- and *p*- substituted nitrobenzyl azides **6a-c**, the results of which are summarized below in Table 5.

Table 5
Summary of synthesis of 1,5- substituted triazole compounds 7a-l.

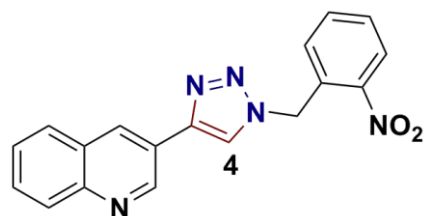
Alkyne	Azide	1,5- RuAAC products	Yield (%)
			7a <i>o</i> = 85 7b <i>m</i> = 92 7c <i>p</i> = 83
			7d <i>o</i> = 81 7e <i>m</i> = 83 7f <i>p</i> = 82
			7g <i>o</i> = 54 7h <i>m</i> = 55 7i <i>p</i> = 60
			7j <i>o</i> = 53 7k <i>m</i> = 54 7l <i>p</i> = 60

It is interesting to note that the products formed from the isoquinoline alkynes resulted in far lower yields than those products built from the quinoline alkynes. A number of control reactions, changing the solvent, temperature and the use of freeze-pump-thaw techniques, similar to those done in the optimization reactions, were undertaken to determine whether these had any effect on the yield. As was the case with our optimization results, the reactions

did not proceed to completion with a lowering of the temperature and other variables altered only worsened the afforded yield. The difference in yields between these two scaffolds could be attributed to coordinative and basic effects of the isoquinoline driving group as discussed in Section 3.2.2. In the end the yields obtained were very good for the quinoline backbone products and acceptable for those containing isoquinoline as the driving group.



The compounds synthesized were fully characterized using ¹H NMR, ¹³C NMR, FTIR spectroscopy and HRMS-TOF MS. This confirmed the synthesis thereof. Using compound **7a**, as example, ¹H NMR spectroscopic analysis showed the benzylic peak of protons **1** at 6.07 ppm integrating for 2H and proton **2** in the triazole ring being witnessed as a singlet at 8 ppm integrating for 1H, as was expected. All other protons were accounted for in the spectra. ¹³C NMR spectroscopy also confirmed product formation as the benzylic carbon **1** was witnessed at 49.6 ppm and both triazole carbons **2** and **3** were seen at 129.6 and 136.1 ppm respectively. The remaining carbon peaks were all accounted for in the spectrum. MS analysis and spectra showed the [M+H]⁺ ion as 332.1156, which correlates well with the calculated 332.1147 for C₁₈H₁₄N₅O₂.



Confirmation of the synthesis of both the 1,4- and 1,5-regioisomers was gained through comparison of the peaks obtained in both the ¹H NMR and ¹³C NMR spectra of the appropriate CuAAC analogues synthesized by Dr. Abu Taher, and the library synthesized through the RuAAC. For example, the triazole proton **4** of the analogue of compound **7a**, shown above on the left, was observed at 8.17 ppm, a notable shift from that seen for proton **2** of compound **7a** (8.00 ppm). A similar trend was observed for all compounds synthesized and on the basis of these findings, it was deduced that both the 1,4- and 1,5-regioisomer series had been synthesized. It should be noted that these correlations do not confirm which regioisomer is which; however, there is significant literature precedent concerning the regiochemical outcomes of CuAAC and RuAAC reactions.^{190, 203} It is thus our assumption that the 1,4-regioisomer was furnished through the CuAAC reaction, whilst the 1,5-regioisomer was provided under the RuAAC conditions. It should also be noted that 2D NMR spectroscopy, such as Nuclear Overhauser effect spectroscopy (NOESY), or the obtaining of a crystal structure, could be used to confirm the absolute structure of each click reaction.

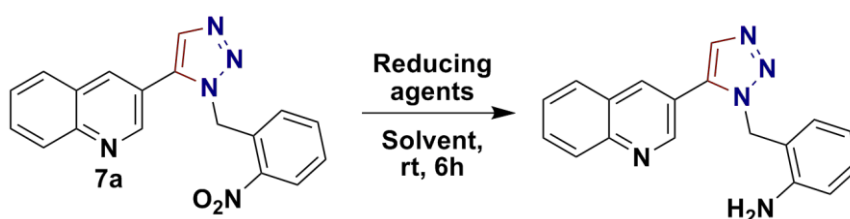
This afforded a range of 1,5-substituted triazole compounds that were ready to have the electrophilic warhead moiety incorporated for irreversible inhibition introduced.

4.2.4 Reduction of Aromatic Nitro and Addition of Acryl Amide Moiety to Clicked Compounds.

With the formation of our twelve 1,5-substituted 1,2,3-triazole-based core driving portions, with *o*-, *m*- and *p*- substituted aromatic nitro groups attached to them, the next step in the synthesis of the library of potential irreversible kinase inhibitors would be the introduction of the electrophilic warhead or Michael acceptor moiety. This would enable the inhibitors to potentially undergo a Michael addition reaction with the nucleophilic cysteine residue present in the kinase active site. This would involve two synthetic steps, namely the reduction of the aromatic nitro group followed by a subsequent acylation reaction with acryloyl chloride.

A trove of synthetic methods is known for the reduction of nitroarenes using a variety of reagents, catalysts and reaction conditions. These include the use of catalytic hydrogenation by making use of palladium on activated charcoal and a source of hydrogen,²¹⁶ platinum(IV) oxide,²¹⁷ Raney nickel,²¹⁸ stannous or tin(II) chloride²¹⁹ and zinc²²⁰ or iron in aqueous media.²²¹ This left us with a variety of options in the reduction of the *o*-, *m*- and *p*- substituted nitro group on each clicked compound. Once again to remain consistent the compound **7a** was chosen for optimization reactions for this synthetic procedure. Our synthetic endeavours resulted in the use of a couple of different reagents and conditions in the reduction of this aromatic group. A summary of these experimental efforts can be seen below in Table 6.

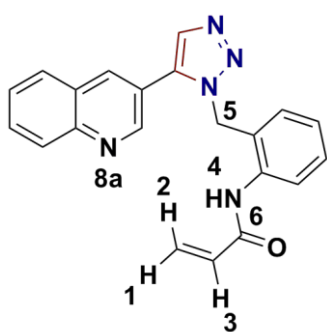
Table 6
Optimization of reduction of aromatic nitro compound **7a**.



Attempt	Catalyst (mol. %)	Secondary Reducing agent (equiv.)	Solvent	Yield(%)
1 ²²²	Raney Nickel (10)	NaBH ₄ (2)	EtOH	14
2	Pd/C (5)	H ₂	DCM	81

For attempt **1**, we synthesized our own Raney nickel following a procedure set out by Mozingo.²²³ The use of this reducing agent in tandem with NaBH₄ as outlined by Litvić and co-workers,²²² resulted in a very poor yield and discouraged us from further use of these reducing agents. Our next choice of reductant system, in attempt **2**, made use of palladium on activated charcoal with hydrogen gas. DCM was chosen as solvent purely for solubility issues and the reaction was seen to proceed smoothly and effectively with a simple filtration through Celite required for product isolation. This afforded the aniline in a good yield and became our choice for the further reduction of all aromatic nitro groups.

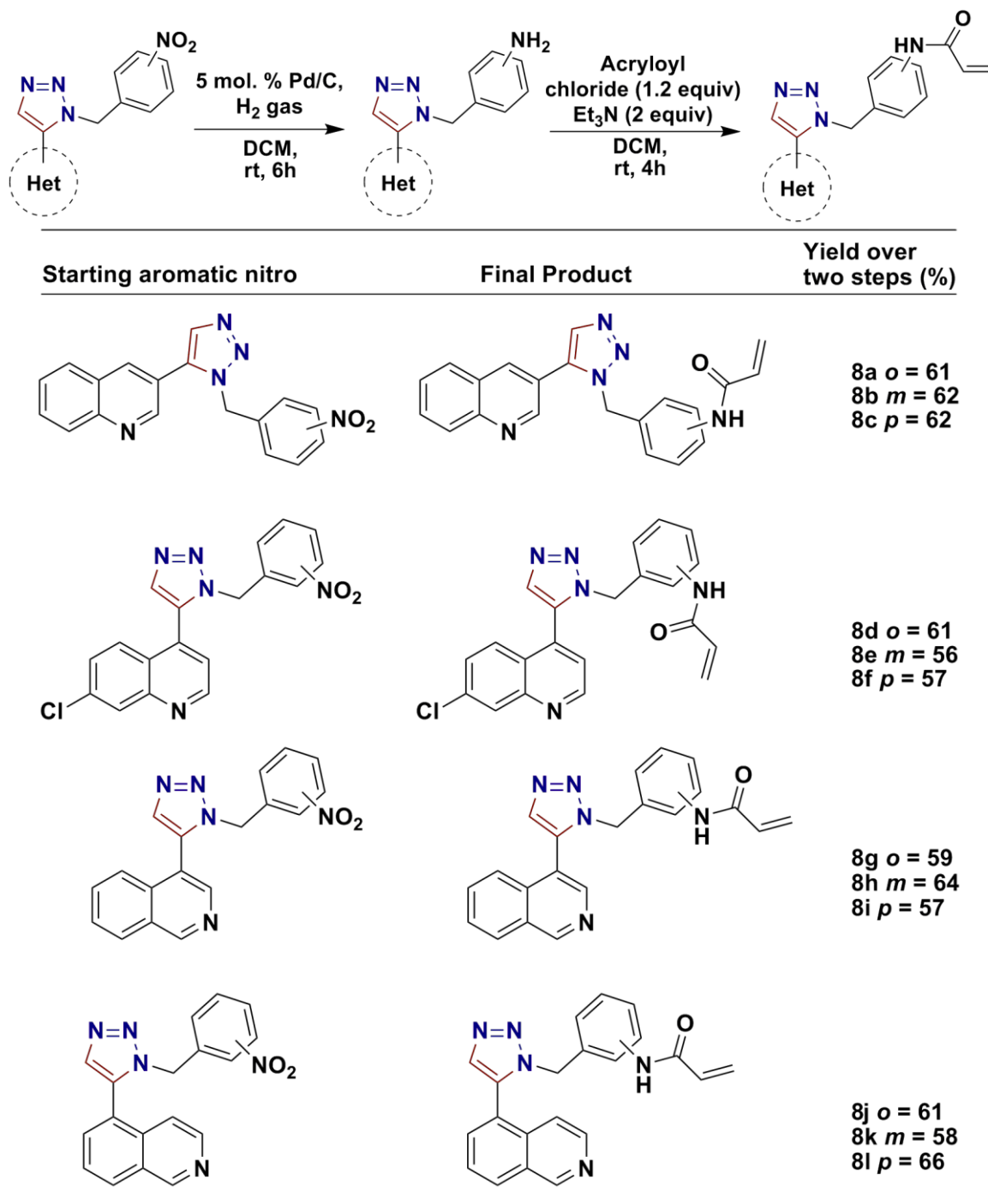
It was deemed unnecessary to purify the product obtained after reduction, due to the lack of formation of by-products and simple isolation procedure, and thus the acylation reaction was performed directly on the aromatic amine afforded after reduction. The reaction of acryloyl chloride with triethylamine as base in DCM, proceeded smoothly with acceptable yields between 56 and 66%. It is important to note that the yields obtained were calculated over two steps. As this reaction afforded our final product, it was seen as redundant to labour further on optimization of the reaction conditions. The formal reaction conditions used for both the aromatic nitro reduction and acylation reaction can be seen below in Table 7, as well as a full summary of yields obtained over the two steps for products **8a-l**.



A full characterisation of all synthesized compounds was completed. The spectral data obtained from this confirmed the formation of our desired products. With compound **8a** as example, analysis of the ¹H NMR spectra obtained clearly showed the ethylene protons **1** and **2** both as doublets of doublets at 6.12 and 5.64 ppm respectively, each integrating for 1H. The 3rd ethylene proton **3** was also witnessed as a doublet of doublets at 6.28 ppm integrating for 1H. The amide proton **4** could be seen far downfield at 9.84 ppm integrating for the required 1H. Lastly, the benzyl protons of **5** were observed as a singlet at 5.77 ppm, integrating for 2H and indicative of the triazole and driving portions still being attached to the molecule. All other protons were accounted for in the spectra. The ¹³C NMR spectrum for compound **8a** clearly showed the benzyl carbon of **5** at 48.8 ppm and that of carbon **6** further downfield at 163.4 ppm. All other carbons were observed as expected in the spectra. Finally, the HRMS spectra for compound **8a** showed agreement between the [M+H]⁺ ion 356.1510 and that calculated for C₂₁H₁₈N₅O as 356.1511.

Table 7

Reaction conditions and yields obtained for products 8a-l.



This afforded our twelve potential irreversible kinase inhibitors and furnished our 1st generation library of potential irreversible inhibitors. With both a 1st generation library of eight reversible and twelve 1,5-substituted potential irreversible inhibitors synthesized and another twelve 1,4-substituted irreversible inhibitors synthesized by Dr. Abu Taher, we were ready to send these compounds to our collaborators at the Technische Universiteit Dortmund

in Germany for biological screening. The assays results could determine efficacy, selectivity and other important factors and data that could be analysed to provide further knowledge on these potential kinase inhibitors. Further use of molecular modelling could be used to rationalize the results obtained and determine where the most feasible and profitable synthetic modifications could be made in the possible synthesis of a 2nd generation library based on the most efficacious potential inhibitors. The methods and results of these biological assays will be discussed in full in the following chapter.

CHAPTER 5 – BIOLOGICAL EVALUATION OF SYNTHESIZED POTENTIAL KINASE INHIBITORS AND CONCLUSIONS

5.1 BIOLOGICAL SCREENING METHODOLOGY

5.1.1 Professor Daniel Rauh's Research Focus – Fluorescent Labelling in Kinases.

Professor Daniel Rauh is the head of chemical biology at the Technische Universiteit Dortmund and has filled this post since the end of 2010. With nearly 70 publications in journals such as Nature Chemistry, Nature Chemical Biology, Nature Genetics, Journal of the American Chemistry Society and the American Chemistry Society Chemical Biology, he has distinguished himself in his field. His research focus is mainly on the development of biological assays for protein kinases and phosphatases, which is why we have been privileged to collaborate with him and his group. Prof. Rauh's group were the first to develop detection methods in biological assays called fluorescent labels in kinases (FLiK) or the FLiK approach,²²⁴ and for their phosphatase counterparts fluorescent labels in phosphatases (FLiP).²²⁵

The active reversible phosphorylation of a protein kinase may change the enzyme conformation and thus its state of activity towards further phosphorylation or biological processes.²²⁶ Important residues in this reversible process are the conserved triplet of the activation loop in the kinase domain, consisting of aspartate (D), phenylalanine (F), and glycine (G) residues – making up the DFG motif. This can be seen on the right of Figure 33. The aspartate residue (D) in particular, plays a catalytic role in phosphate transfer.¹¹⁸ Two important conformations protein kinases may adopt is the DFG-out, or inactive state, and the DFG-in or active state. The reversible transition between these two conformations is controlled by the rotational movement of the aspartate residue (D), accompanied by corresponding rotation of both the adjacent phenylalanine (F) and glycine (G) residues. In the DFG-out conformation the aspartate residue (D) is rotated out of the ATP binding pocket, exposing a large hydrophobic pocket for ligands or inhibitors to utilize.¹¹⁸ For the DFG-in conformation the opposite is true, with the aspartate residue (D) moving back into the ATP active site. This reversible process is illustrated on the left side of Figure 33.

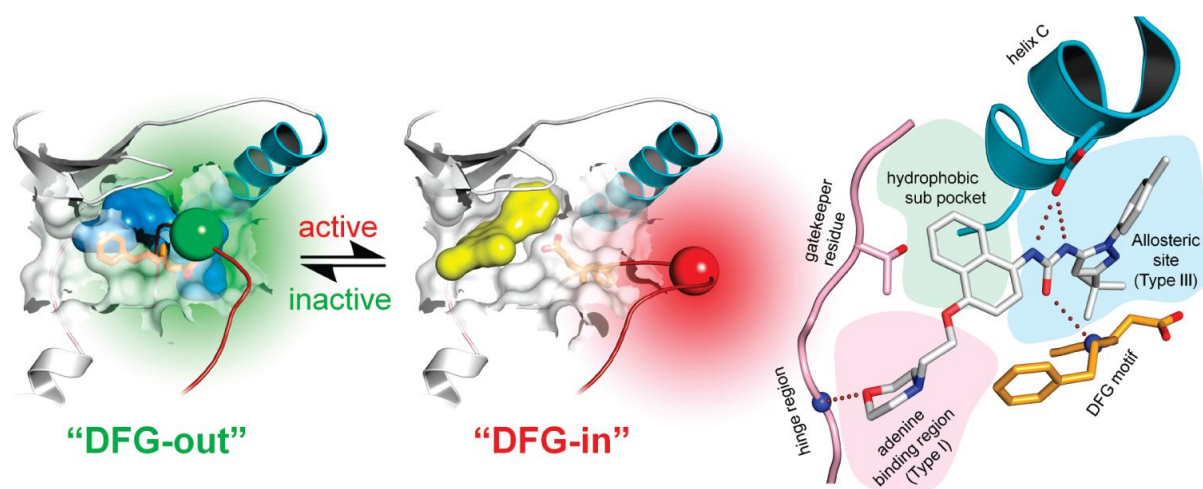


Figure 33

Illustration of reversible conformational transition of kinases and the DFG motif.²²⁴

Certain inhibitors make use of, and in doing so stabilize, a specific conformation of a protein kinase for ligand binding. Type II, or allosteric inhibitors and type III, non ATP competitive or irreversible inhibitors – shown in blue - make use of and stabilize the inactive or DFG-out conformational state, whilst classic ATP competitive, reversible or Type I inhibitors – shown in yellow - make use of and stabilize the DFG-in or active state.²²⁶ It is this precise mechanism and conformational preference and stabilization of the protein kinase by ligands and inhibitors that the FLiK biological assay exploits.

The FLiK assay makes use of the environmentally sensitive, thiol-reactive fluorophore acrylodan, which is attached to a specific site of the target kinase – shown as a green and red sphere in the DFG-out and DFG-in conformation respectively in Figure 33 above. During ligand or inhibitor binding, the protein kinase undergoes a conformational change. This conformational change and stabilization brought on by the inhibitor binding, produces an alteration in the microenvironment, which may change the solvent shell of the fluorophore acrylodan, seen as a change between the red and green sphere illustrated in Figure 33. This alteration is witnessed as a significant change in its emission spectra, which is characterised by two emission maxima ($\lambda_{em,max}$) at ~470 and ~510 nm. Conformational transitions bring about changes in the total intensity of these two emission maxima relative to each other, resulting in an attractive ratiometric fluorescence readout, which has been shown to be superior to its monochromic counterpart.^{224,226} The FLiK assay is thus a conformation-specific binding assay and has been shown to be viable for a number of kinases including p38 α kinase,²²⁷ abl²²⁸ and cSrc,²²⁹ to name a few. This methodology has been used in high

throughput screening and in cooperation with the pharmaceutical industry,²²⁶ and is especially significant when deducing the relative binding modes and specificity of potent inhibitors. The ratiometric fluorescence readout explained above is also made use of in activity-based assays for kinases.

5.1.2 Methodology Used in Screening of Reversible and Irreversible Inhibitors against EGFR.

For the biological assays and IC_{50} values determined for our compounds, a student in Prof. Rauh's group, Julian Engel, made use of the HTRF KinEASE-TK assay from Cisbio. For our specific biological screening, this technique involved use of the wildtype form of the kinase and the two medicinally relevant mutant deviants, more specifically the inhibitor-sensitizing mutation EGFR Leu858Arg (L858R) and the double mutant drug resistant variant, EGFR Leu858Arg-Thr790Met (L858R_T790M). As a control reaction these kinases were each incubated in the presence or absence of our potential reversible and irreversible inhibitors, followed by the addition of a biotinylated poly Glu-Tyr substrate peptide which is phosphorylated by the EGFR kinase. Completion of the reaction allows for subsequent introduction of an antiphosphotyrosine antibody labelled with europium cryptate, and streptavidin which is labelled with a fluorophore XL665. The fluorescence resonance energy transfer or FRET is then measured between europium cryptate and XL665 to quantify the phosphorylation of the substrate peptide. This allows for a control experiment and value for kinase activity and following this, ATP concentrations were set at their respective K_m values (30 μ M for the EGFR-WT, 60 μ M for EGFR-L858R, and 30 μ M for EGFR-L858R_T790M). Our synthesized inhibitors were then preincubated with the specific kinase and peptide for 2h, where after ATP was added to initiate the reaction and the fluorescence of these samples were documented at 620 nm (Eu-labelled antibody) and 665 nm (XL665 labelled streptavidin) 60 μ s after excitation at 317 nm by a Tecan Safire plate reader. The quotient of these two readings, done in an eight fold dilution series and carried out in triplicate, were then plotted against inhibitor concentrations and fitted to a Hill 4-parameter equation to determine relevant IC_{50} values.²³⁰ The principle of the FRET analysis, using the attached europium cryptate and streptavidin groups, as well as the data acquired and an example of IC_{50} value determination in these biological assays is shown in Figure 34.

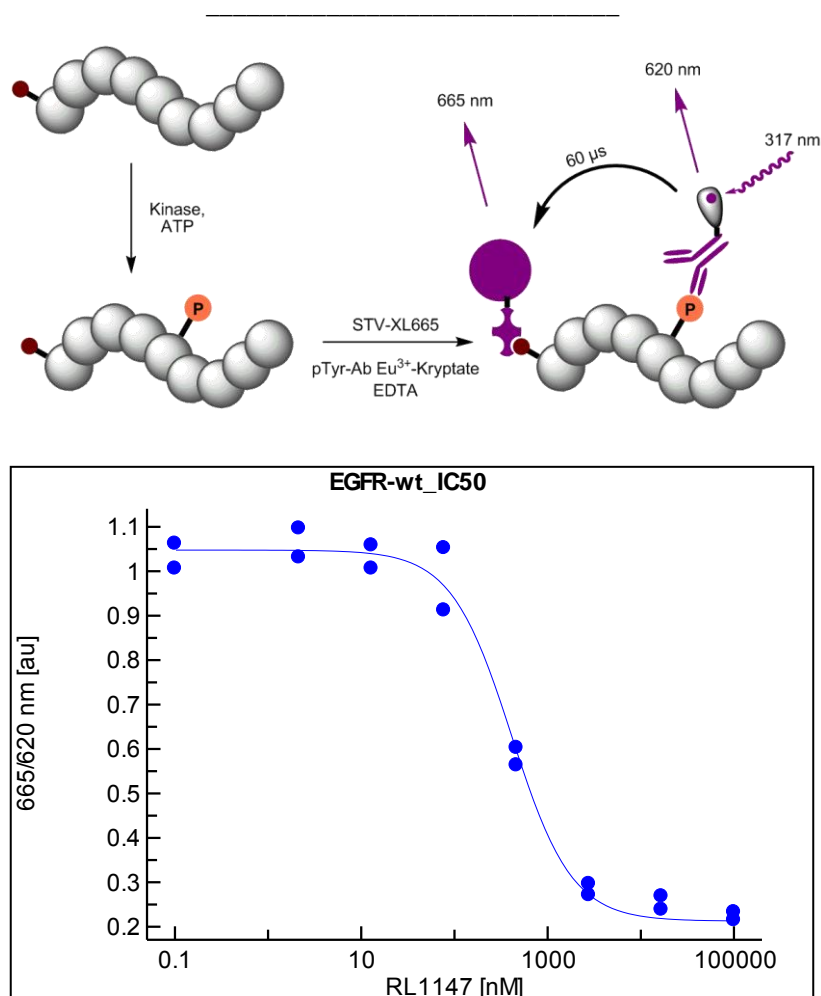


Figure 34

Principle of FRET analysis as well as IC_{50} value through use of this technique and plotting of 8-fold dilution series.

Gefitinib and WZ4002 were used as control groups for the kinase inhibitory activity tests and in determination of the IC_{50} values. A total of 33 inhibitors were sent to our collaborators and the kinase inhibitory activity results against the EGFR wildtype, L858R and L858R_T790M mutation can be seen in Figure 35.

5.2 RESULTS AND DISCUSSION

The biological screening yielded a few important and interesting results. The first point is evident in the screen against the wildtype. Whilst the control inhibitors exhibit very potent inhibition of the wildtype EGFR kinase at low concentrations, it is encouraging to see that our synthesized inhibitors showed little to no activity against the phenotypic kinase, even at high concentrations of $50\mu\text{M}$. This can be interpreted as a very good result as high inhibitory activity against the wildtype kinase is usually linked to a high toxicity profile, as it targets the unmutated form of the kinase.

Chapter 5 – Biological Evaluation of Synthesized Potential Kinase Inhibitors and Conclusions

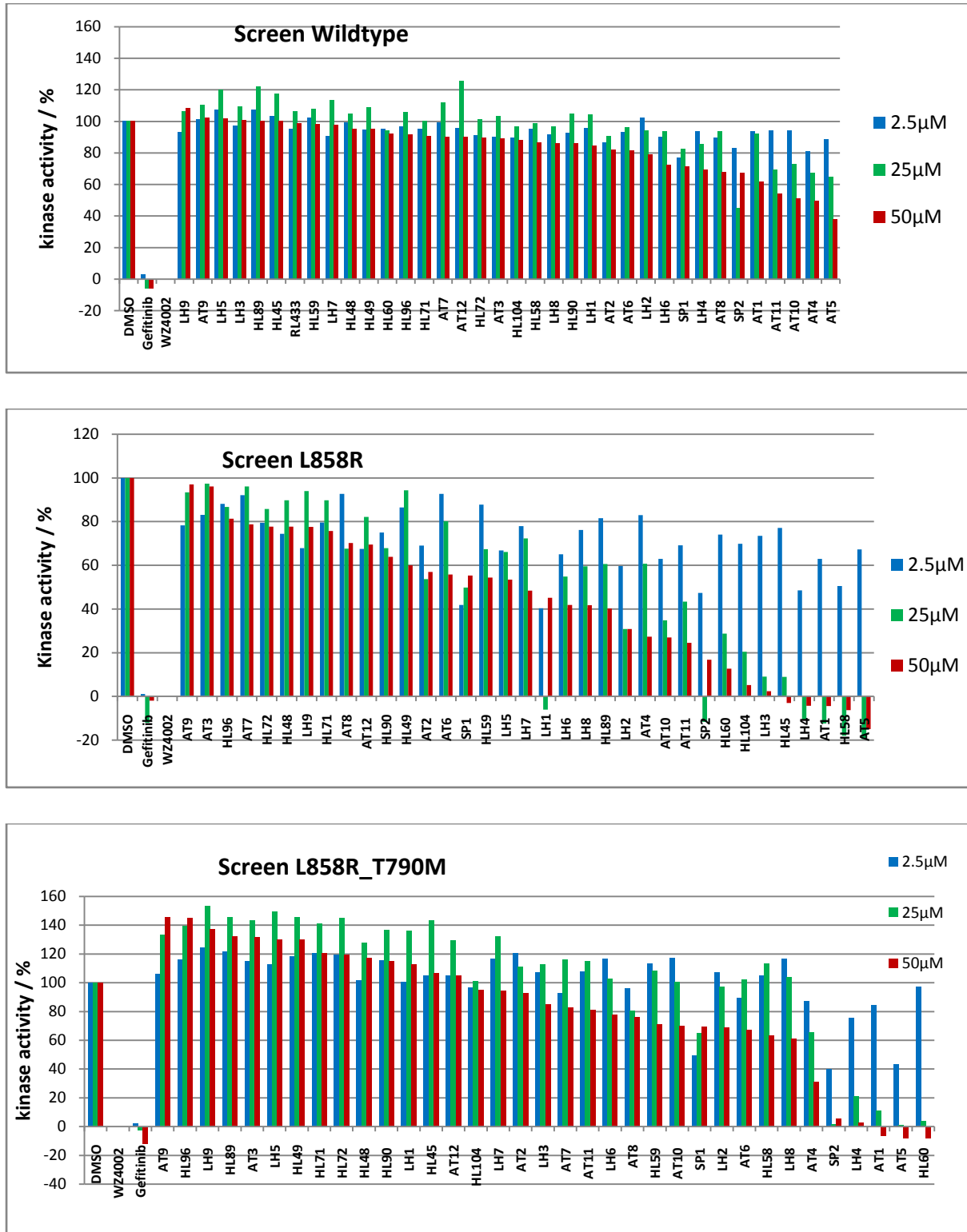


Figure 35

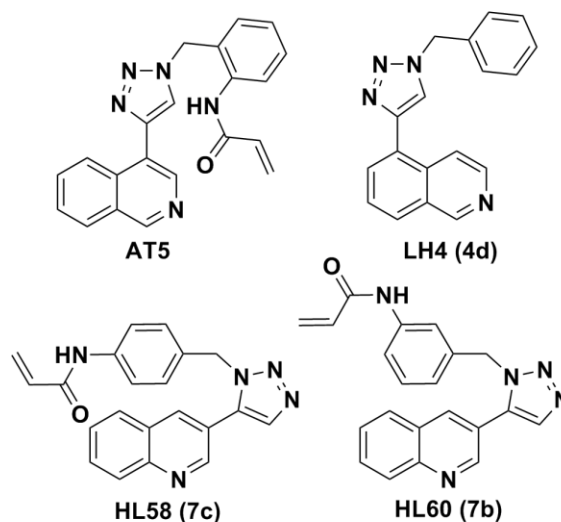
Kinase inhibitory activity results against wildtype, L858R and L858R_T790M mutation EGFR kinases.

Looking at both mutated forms of the EGFR kinase and the biological screening data, it is encouraging to see that not only are the inhibitors active, but in the case of the L858R screen, a number compounds including **AT5**, **HL58 (8c)**, **AT1** and **LH4 (4d)** are seen to be similarly active to the FDA approved drug gefitinib, used specifically for treatment of breast and lung cancer as an EGFR inhibitor. This is also the case for the double mutant variant L858R_T790M, where compounds **HL60 (8b)**, **AT5** and **AT1** show comparable activity to the control group. An important conclusion to draw from this data is that whilst our synthesized inhibitors are not effective in inhibiting the wildtype variant, they show promise and efficacy against the mutant strains. This indicates a positive selectivity profile for our inhibitors, in contrast to that found for gefitinib and WZ4002, which show activity across the board for all the EGFR screens. This shows promise for our synthesized inhibitors as a high selectivity and moderate to good inhibition trend and profile was witnessed.

Table 8

IC₅₀ values in μM of most efficacious and selective synthesised inhibitors.

Inhibitor	IC ₅₀ EGFR Kinase [μM]		
	Wildtype	L858R	L858R_T790M
WZ4002	0.00458	0.00021	0.00016
Gefitinib	>0.1	1.91	2.20
AT5	>100	4.53 \pm 0.94	1.85 \pm 0.59
LH4	>100	4.29 \pm 0.54	7.65 \pm 1.36
HL58	n.i	6.99 \pm 4.37	>10
HL60	n.i	>10	5.43 \pm 1.44



From these results corresponding IC₅₀ values were derived for each of our inhibitors. A summary of the most efficacious and selective inhibitors is shown in Table 8. Whilst the IC₅₀ values of these compounds are not inside of the nanomolar range and cannot compete with WZ4002, a number of interesting conclusions and future work can be derived from these results. Compound **AT5**, highlighted in red in Table 8, was shown to be the most efficacious inhibitor of those synthesized, in this case by Dr Taher. This was based on the isoquinoline scaffold with the 1,4-substituted regioisomer of the triazole and the Michael acceptor in the

ortho position and thus an irreversible inhibitor. **AT5** showed good inhibitory activity and an excellent selectivity profile for the mutated kinases. Its IC_{50} value was comparable to gefitinib and lower in the case of the double mutant variant. The very impressive selectivity could be investigated further with molecular modeling, as well as the determination of whether synthetic tweaking to the molecule could result in a lower IC_{50} value whilst still retaining the selectivity. Compound **LH4**, highlighted in green in Table 8, was a reversible inhibitor synthesized in this project and showed slightly higher IC_{50} values, yet retained the selectivity seen for compound **AT5**. With further investigation into this compound through molecular modeling, a suitable position for an electrophilic warhead to be placed on the molecule could be found, perhaps increasing its efficacy. Lastly, compounds **HL58 (7c)** and **HL60 (7b)** showed remarkable selectivity for the L858R and L858R_T790M mutations alone respectively. This is highlighted in blue in Table 8. The use of molecular modelling to further determine the differences in selectivity and their binding modes is definitely a venture worth pursuing.

5.3 CONCLUSIONS

The aim of this project was to synthesize a library of reversible and potential irreversible kinase inhibitors. This project has seen the synthesis of 20 of the 32 potential inhibitors including eight reversible inhibitors, compounds **4a-d** and **5a-d**, as well as twelve irreversible inhibitors, compounds **8a-l**. The synthesis of these compounds made use of palladium, copper and ruthenium metal-mediated chemistry including Sonogashira coupling reactions, CuAAC and RuAAC. All novel compounds were fully characterized using a range of analytical techniques.

Biological screening assays against the wildtype, and two mutant forms of the EGFR kinase – L858R and L858R_T790m – were undertaken by our collaborators at the Technische Universiteit Dortmund in Germany. The potential kinase inhibitors synthesized showed good inhibitory activity and a favourable selectivity profile for both the mutated strains of the EGFR kinase. Compound **AT5** showed the greatest inhibitory activity and was the most efficacious inhibitor with an IC_{50} value of 4.53 and 1.85 μ M L858R and L858R_T790M mutants respectively. This inhibitor shows greater activity against the double mutant variant L858R_T790M than the FDA approved drug, gefitinib. Compound **AT5** is exceedingly selective towards the mutant forms of the EGFR kinase as it is essentially non-active against the EGFR wild type. Compound **LH4(4d)**, shows similar efficacy, being slightly less potent,

and a similar selectivity profile. Compounds **HL58 (7c)** and **HL60 (7b)** showed selectivity for the L858R and L858R_T790M mutation respectively.

With the encouraging results obtained from the biological screening assays, molecular modelling and docking studies could be undertaken to determine the synthetic alterations that are required to generate a 2nd generation library of compounds. Based on compound **AT5**, **LH4(4d)**, **HL58 (7c)** and **HL60 (7b)**, this library would build on the inherent selectivity of these molecules for the mutant EGFR kinase variations and explore the origin of this selectivity. This could possibly lead to more potent inhibitors with an even higher selectivity profile.

The synthetic methodology developed in this project could also be utilized in the synthesis of possible biological space and cysteine probes. With the synthesis of these probes, large libraries could potentially be synthesized quickly and efficiently, allowing for a large scale, broad range kinase screening.

CHAPTER 6 – FUTURE WORK

6.1 FUTURE WORK

6.1.1 2nd Generation Library Based on Compound AT5.

Molecular modelling calculations and docking studies were undertaken to postulate the specific binding mode of AT5, and inspection of the conformation adopted by the compound provided insight into possible synthetic modifications. Scrutiny of the inhibitor in the active site and its adopted spatial arrangement revealed two possible sites for further investigation shown in Figure 36 below. The first of these promising sites is the introduction of another, secondary hydrogen bond interaction with the hinge region at Glu791.

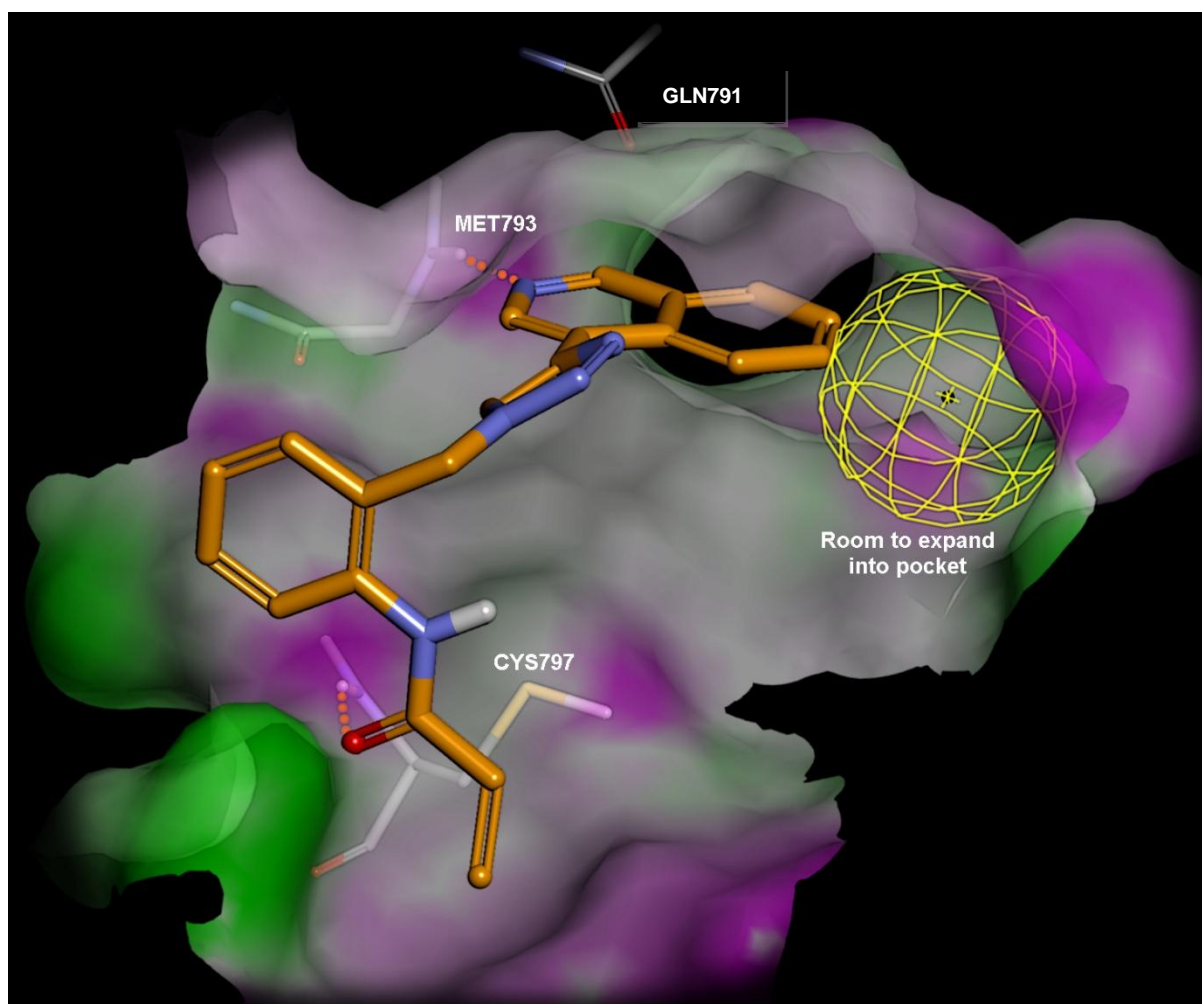


Figure 36

Illustration of possible sites for further synthetic investigation and modification.

As can be seen in Figure 36, there is a considerable amount of space between the carbon *alpha* to the nitrogen of the isoquinoline ring and the carbonyl bond of GLN791. This space, whilst large enough to warrant the introduction of a functional group, is also small enough to maintain a hydrogen bond effect. Thus we hypothesize the introduction of a hydrogen bond donor group, such as a hydroxyl or amine moiety at this position of the isoquinoline driving group, could result in higher efficacy and selectivity for member of a 2nd generation library. Secondly, on the right side of the scaffold there exists a large open hydrophobic pocket, shown by a yellow caged sphere in Figure 36. It is our belief that functionalizing the isoquinoline core at relevant positions to extend into this hydrophobic pocket would increase the inhibitor selectivity profile and possibly the potency.

To test this hypothesis docking calculations were undertaken with a large group of potential second generation inhibitors. These included the addition of the amine and hydroxyl hinge binding motif *ortho* to the isoquinoline nitrogen at **R**₁, as well as various functional groups on position **R**₂ and **R**₃ of the isoquinoline ring in different combinations. This included a methyl, ethyl, methoxy and cyano functional group for possible space filling. The results were promising and showed the highest score and visual impression with the groups illustrated in Figure 37 below. The synthesis of a 2nd generation library could thus yield compounds with increased efficacy and selectivity profiles for these irreversible inhibitors.

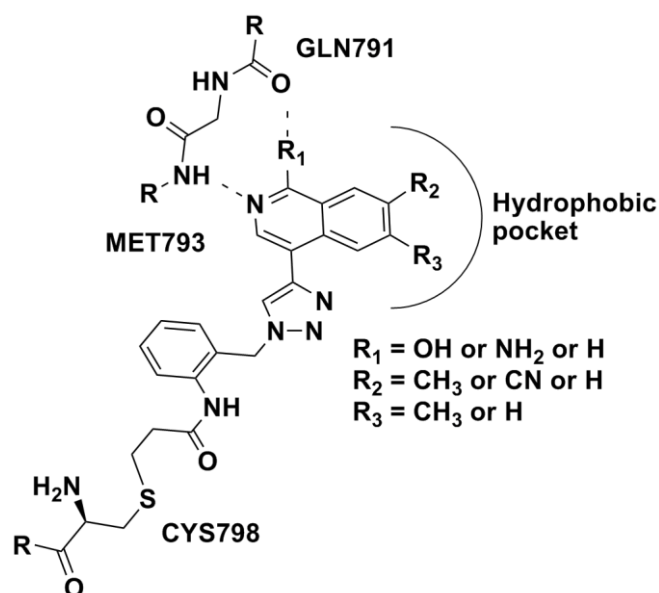
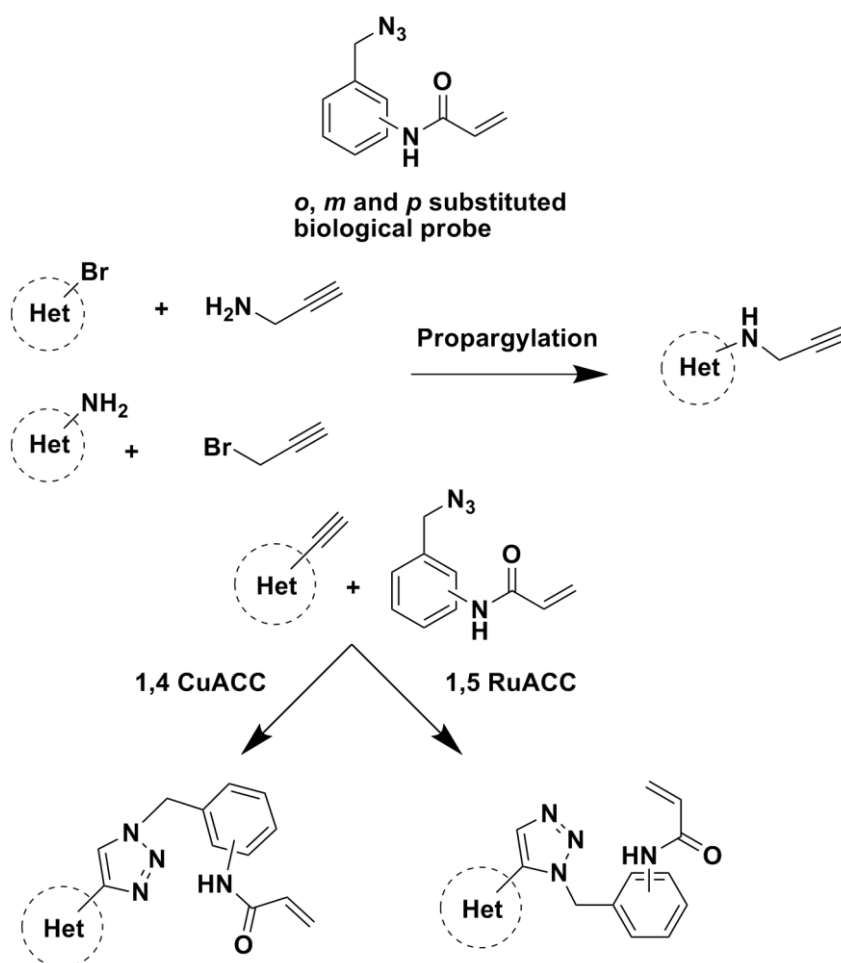


Figure 37
Possible structures for 2nd generation library of AT5.

6.1.2 Biological Space Filling and Cysteine Targeting Probes.

As was shown in the proposed synthesis of our irreversible compounds in Section 4.1.2, the benefits of using a benzyl azide with an *o*-, *m*- and *p*- substituted functional group, which would later become an electrophilic warhead capable of forming covalent bond interactions with the cysteine residue in the active site, is a largely untapped potential biological probe. If the synthetic methodology and route developed and employed in our synthesis of irreversible inhibitors were to be shortened and simplified to have the *o*-, *m*- and *p*- substituted electrophilic warhead already in place on the benzyl azide moiety, as shown in Scheme 12 below, this would open the door to a vast number of possibilities that these moieties could be used as biological probes of the kinase active site. Through the use of both CuAAC and RuAAC click chemistry as we have shown in our synthesis, a potentially wide ranging library could probe a significant amount of space in the active site; in addition, this library could be synthesized simply and effectively.

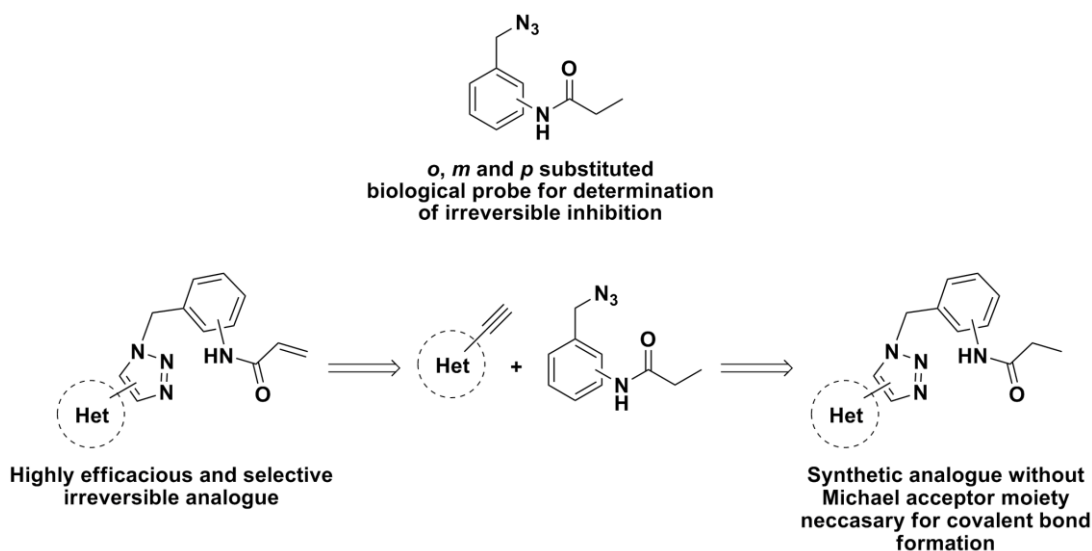


Scheme 12

Proposed synthetic plan for use of biological space probes to generate a large library of compounds.

This could be done by propargylation, or the addition of an alkyne group to heterocycles or driving groups that are known to form hydrogen bond interactions effectively with the hinge region of kinases, followed by subsequent coupling through both the 1,4-substituted CuAAC and the 1,5-substituted RuAAC with the *o*-, *m*- and *p*- substituted electrophilic warhead moieties as shown in Scheme 12. This would generate a large number of different spatial and space probing conformations from one heterocycle or driving group and thus a large library of potential irreversible inhibitors targeting the cysteine residue across a broad panel of kinases. From this library biological assays will hopefully lead to a few compounds that show high efficacy and selectivity for a certain kinase, and further synthetic modifications could result in an extremely potent and selective inhibitor.

Furthermore, if a certain compound generated through the use of this synthetic methodology shows promise by displaying high efficacy and potent selectivity, a simple and effective way to give an indication of whether or not this is through covalent bond formation with the cysteine residue would be to synthesize an analogue of the compound with the saturated propionamide probe derivative as shown in Scheme 13. This will afford critical information on whether or not the compounds inhibit irreversibly or not, as a large drop in the efficacy of the compound would be expected without the necessary Michael acceptor moiety. With the use of these both of these biological probes a large amount of information regarding the targeting of the cysteine residue, chemical space probed in the active site of the kinase as well as the type of inhibition that is undertaken by these synthesized compound will be afforded.



Scheme 13

Proposed synthetic method for insight into compounds mechanism of inhibition.

CHAPTER 7 – EXPERIMENTAL

7.1 GENERAL PROCEDURES

7.1.1 Purification of solvents and reagents.

Chemicals used in these experiments were purchased from Merck or Sigma Aldrich. Solvents used for chromatographic purposes were distilled by means of conventional distillation procedures. Solvents used for reaction purposes were dried over the appropriate drying agents and then distilled under N₂ gas. Tetrahydrofuran was distilled from sodium metal, using benzophenone as indicator. Dichloromethane, dichloroethane, dimethylformamide and acetonitrile were distilled from calcium hydride. Ethanol was distilled from magnesium turnings and iodine. Diethyl ether was bought with a $\geq 98\%$ purity grade from Sigma Aldrich and then dried on activated 3Å molecular sieves. Other reagents requiring purification were purified according to standard procedures.

7.1.2 Chromatography

Thin layer chromatography was performed using Merck silica gel 60 F254 coated on aluminium sheets. Visualization was performed with a UV lamp, using iodine on silica, or by spraying with a Cerium Ammonium Molybdate (CAM) or ninhydrin (NIN) or potassium permanganate (KMnO₄) solution followed by heating.

All column chromatography was performed on Merck silica gel 60 (particle size 0.040-0.063 mm) using one of or combinations of petroleum ether, EtOAc, toluene, dichloromethane, ethanol and/or MeOH as a solvent.

7.1.3 Spectroscopic and physical data

NMR spectra (¹H, ¹³C) were recorded on a 300 MHz Varian VNMRS (75 MHz for ¹³C), a 400 MHz Varian Unity Inova (101 MHz for ¹³C), or a 600 MHz Varian Unity Inova (150 MHz for ¹³C). Chemical shifts (δ) are reported in ppm and J-values are given in Hz. Chemical shifts were recorded using the residual solvent peak or external reference. All spectra were obtained at 25 °C unless otherwise reported. Data was processed using MestReNova.

Mass spectrometry was performed on a Waters SYNAPT G2. Infrared spectra were recorded on a Thermo Nicolet Nexus 470 by means of Attenuated Total Reflectance (ATR) mode.

Melting points were obtained using a Gallenkamp Melting Point Apparatus and are uncorrected.

7.1.4 Other general procedures

All reactions were performed under a positive pressure of 5.0 grade N₂ or Ar unless water was used as a solvent. The glassware was flame-dried while under vacuum before being purged with N₂ gas. Condensers were pre-dried at 120 °C for a minimum of two hours. Standard Schlenk techniques were employed when necessary.

Solvents were removed *in vacuo*, where we are referring to removal of the solvent using a rotary evaporator followed by removal of trace amounts of solvent using a high vacuum pump at *ca.* 0.08 mm Hg.

7.2 SYNTHESIS PERTAINING TO CHAPTER 3.

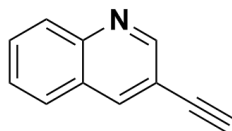
7.2.1 Compounds 2a-b.

General Procedure for Sonogashira Coupling of Quinoline Alkynes

A dry Schlenk tube was evacuated under high vacuum and filled with Ar (3×). To this Schlenk tube was added by syringe, under Ar, in anhydrous THF (15 mL). The solvent was then degassed by 3 - 5 cycles of freeze-pump-thaw technique. The solvent was subsequently degassed for 15 min with Ar purge. This was followed by the addition of the catalysts, PdCl₂(PPh₃)₂ (4 mol. %) and CuI (4 mol. %), under positive pressure Ar. Et₃N (2 equiv) was then added by syringe and the mixture was allowed to stir for 5 min. Following this, trimethylsilylacetylene (TMSA) (1.5 equiv) was added by syringe. A colour change from yellow to black was witnessed, indicating the consumption of the catalyst and that the reaction was working. The reaction mixture was allowed to stir at rt, under N₂, for up to 6 h or until complete consumption of the starting materials (monitored by TLC). This resulted in the intermediate TMS-protected quinoline alkyne, requiring no characterisation or purification, which allowed for *in situ* deprotection. To the reaction mixture was added liquid TBAF - or CsF - (1.5 equiv.), which was then left to stir for 0.5 h until the deprotection was complete (monitored by TLC). The reaction mixture was then filtered through Celite, followed by removal of the Et₃N *in vacuo*. The reaction mixture was then diluted with EtOAc (30 mL) and washed with a saturated NH₄Cl solution (60 mL). The layers were then separated and the organic layer was rinsed with a saturated solution of brine (50 mL), dried over MgSO₄ and filtered. After removal of the solvents *in vacuo*, the residue was purified by

flash column chromatography over silica gel eluted first with EtOAc and hexane (EtOAc:Hexane, 5:95) and then (EtOAc:Hexane, 60:40). This afforded the pure product as a white solid. The details for the compounds synthesized are described below.

3-ethynylquinoline - 2a

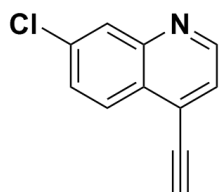


Scale: 3-bromoquinoline (800 mg, 3.84 mmol)

This compound was synthesized following the general procedure for Sonogashira coupling of quinoline alkynes. The compound was purified by silica gel column chromatography, eluted first with EtOAc and hexane (EtOAc:Hexane, 5:95) and then (EtOAc:Hexane, 60:40). This afforded the pure product as a white solid (500 mg, 3.26 mmol, 85%).

R_f = 0.3 (EtOAc:Hexane, 5:95) ; **Mp** 73-75 °C; **IR (ATR, cm⁻¹)**:3159(s, stretch, -C≡C-H), 2092(w, stretch, -C≡C-), 1120 (s, stretch, C-N); **¹H NMR (400 MHz, CDCl₃)** δ 8.94 (d, *J* = 2.1 Hz, 1H, ArH), 8.28 (d, *J* = 1.9 Hz, 1H, ArH), 8.12 – 8.05 (m, 1H, ArH), 7.79 – 7.75 (m, 1H, ArH), 7.73 (ddd, *J* = 8.4, 6.9, 1.5 Hz, 1H, ArH), 7.56 (ddd, *J* = 8.1, 7.0, 1.1 Hz, 1H, ArH), 3.28 (s, 1H, CCH); **¹³C NMR (101 MHz, CDCl₃)** δ 152.4 (ArC), 147.2 (ArC), 139.4 (ArC), 130.5 (ArC), 129.6 (ArC), 127.7 (ArC), 127.5 (ArC), 127.1 (ArC), 116.4 (ArC), 81.1(CCH), 80.6 (CCC); **HRMS-TOF MS ES⁺: *m/z* [M+H]⁺** calcd for C₁₁H₈N: 154.0657; found: 154.0657

7-chloro-4-ethynylquinoline - 2b



Scale: 7-chloro-4-iodoquinoline (1500 mg, 5.18 mmol)

This compound was synthesized following the general procedure for Sonogashira coupling of quinoline alkynes. However, CsF (1.2 equiv) was used as the deprotecting agent for the synthesis of this compound. The compound was purified by silica gel column chromatography, eluted first with EtOAc and hexane (EtOAc:Hexane, 5:95) and then (EtOAc:Hexane, 60:40). This afforded the pure product as a white solid (603 mg, 3.21 mmol, 62%).

R_f = 0.33 (EtOAc:Hexane, 5:95) ; **Mp** 109-111 °C; **IR (ATR, cm⁻¹)**:3170 (s, stretch, -C≡C-H), 2097(w, stretch, -C≡C-), 1151 (s, stretch, C-N); **¹H NMR (400 MHz, CDCl₃)** δ 8.87 (d, *J* = 4.4 Hz, 1H, ArH), 8.19 (t, *J* = 8.6 Hz, 1H, ArH), 8.11 (d, *J* = 2.0 Hz, 1H, ArH), 7.56 (dd, *J*

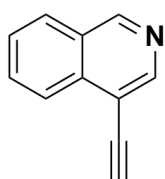
= 8.9, 2.1 Hz, 1H,ArH), 7.52 (d, $J = 4.4$ Hz, 1H,ArH), 3.68 (s, 1H,CCH); ^{13}C NMR (101 MHz,CDCl₃) δ 150.8 (ArC), 148.4 (ArC), 136.1 (ArC), 128.8 (ArC), 128.8 (ArC), 128.5 (ArC), 127.3 (ArC), 126.4 (ArC), 124.6 (ArC), 87.1 (CCH), 78.9 (CCC); HRMS-TOF MS ES+: m/z [M+H]⁺ calcd for C₁₁H₇ClN: 188.0267; found: 188.0265

7.2.2 Compounds 2c-d.

General procedure for Sonogashira coupling of isoquinoline alkynes

A dry Schlenk tube was evacuated under high vacuum and filled with Ar (3×). To this Schlenk tube was added by syringe, under Ar, anhydrous Et₃N (15 mL). The solvent was then degassed by 3 to 5 cycles of freeze-pump-thaw technique. The solvent was subsequently degassed for 15 min with Ar purge. This was followed by the addition of the catalysts, PdCl₂(PPh₃)₂(4 mol. %) and CuI (4 mol. %), under positive pressure Ar. The reaction mixture was then allowed to stir for 5 min. Following this, TMSA (1.5 equiv) was added by syringe. The reaction mixture was placed in an oil bath heated to 65 °C and a colour change from yellow to black was witnessed, indicating the consumption of the catalyst and that the reaction was working. The reaction mixture was allowed to stir at 65 °C, under N₂, for up to 8 h or until complete consumption of the starting materials (monitored by TLC). This resulted in the intermediate TMS-protected quinoline alkyne, requiring no characterisation or purification, which allowed for *in situ* deprotection. To the reaction mixture was added liquid TBAF (1.5 equiv.), which was then left to stir for 0.5 h until the deprotection was complete (monitored by TLC). The reaction mixture was then filtered through celite, followed by removal of the Et₃N *in vacuo*. The reaction mixture was then diluted with EtOAc (30 mL) and washed with a saturated ammonium chloride solution (60 mL). The layers were then separated and the organic layer was rinsed with a saturated solution of brine (50 mL), dried over MgSO₄ and filtered. After removal of the solvents *in vacuo*, the residue was purified by flash column chromatography over silica gel eluted first with EtOAc and hexane (EtOAc:Hexane, 5:95), then (EtOAc:Hexane, 60:40). This afforded the pure product as a brown solid. The details for the compounds synthesized are described below.

4-ethynylisoquinoline - 2c



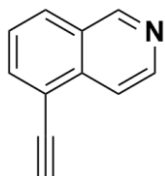
Scale: 4-bromoisoquinoline (800 mg, 3.84 mmol)

This compound was synthesized following the general procedure for Sonogashira coupling of isoquinoline alkynes. The compound was purified by

silica gel column chromatography, eluted first with EtOAc and hexane (EtOAc:Hexane, 5:95) and then (EtOAc:Hexane, 60:40). This afforded the pure product as a brown solid (491 mg, 3.22 mmol, 84%).

R_f = 0.31 (EtOAc:Hexane, 5:95); **Mp** 70-72 °C; **IR (ATR, cm^{-1})**: 3157(s, stretch, $-\text{C}\equiv\text{C}-\text{H}$), 2086 (w, stretch, $-\text{C}\equiv\text{C}-$), 1166 (s, stretch, $\text{C}-\text{N}$); **^1H NMR (400 MHz, CDCl_3) δ** 9.21 (s, 1H, *ArH*), 8.72 (d, J = 4.9 Hz, 1H, *ArH*), 8.25 (dd, J = 8.4, 0.7 Hz, 1H, *ArH*), 7.98 (t, J = 7.6 Hz, 1H, *ArH*), 7.82 – 7.74 (m, 1H, *ArH*), 7.65 (ddd, J = 8.1, 7.0, 1.1 Hz, 1H, *ArH*), 3.55 (s, 1H, *CCH*); **^{13}C NMR (101 MHz, CDCl_3) δ** 152.7 (*ArC*), 147.4 (*ArC*), 136.0 (*ArC*), 131.4 (*ArC*), 128.1 (*ArC*), 128.1 (*ArC*), 127.8 (*ArC*), 125.0 (*ArC*), 114.9 (*ArC*), 84.6 (*CCH*), 79.0 (*CCC*); **HRMS-TOF MS ES+**: m/z [$\text{M}+\text{H}$] $^+$ calcd for $\text{C}_{11}\text{H}_8\text{N}$: 154.0657; found: 154.0656

5-ethynylisoquinoline - 2d



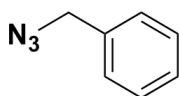
Scale: 5-bromoisoquinoline (600 mg, 2.88 mmol)

This compound was synthesized following the general procedure for Sonogashira coupling of isoquinoline alkynes. The compound was purified by silica gel column chromatography, eluted first with EtOAc and hexane (EtOAc:Hexane, 5:95) and then (EtOAc:Hexane, 60:40). This afforded the pure product as a brown solid (390 mg, 2.54 mmol, 88%).

R_f = 0.31 (EtOAc:Hexane, 5:95); **Mp** 79-81 °C; **IR (ATR, cm^{-1})**: 3185 (s, stretch, $-\text{C}\equiv\text{C}-\text{H}$), 2098(w, stretch, $-\text{C}\equiv\text{C}-$), 1145 (s, stretch, $\text{C}-\text{N}$); **^1H NMR (400 MHz, CDCl_3) δ** 9.26 (s, 1H, *ArH*), 8.61 (s, 1H, *ArH*), 8.09 (s, 1H, *ArH*), 8.01 – 7.93 (m, 1H, *ArH*), 7.90 (d, J = 5.0 Hz, 1H, *ArH*), 7.54 (s, 1H, *ArH*), 3.52 (s, 1H, *CCH*); **^{13}C NMR (101 MHz, CDCl_3) δ** 152.7 (*ArC*), 144.0 (*ArC*), 136.4 (*ArC*), 135.2 (*ArC*), 128.7 (*ArC*), 128.3 (*ArC*), 126.8 (*ArC*), 119.3 (*ArC*), 118.8 (*ArC*), 83.4 (*CCH*), 80.2 (*CCC*); **HRMS-TOF MS ES+**: m/z [$\text{M}+\text{H}$] $^+$ calcd for $\text{C}_{11}\text{H}_8\text{N}$: 154.0657; found: 154.0655

7.2.2 Compounds 3a-b.

(azidomethyl)benzene - 3a

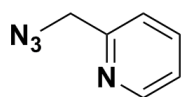


To a stirred solution of benzyl bromide (1.39 mL, 11.7 mmol) in a water/acetone mixture (50 mL, 1:4) was added NaN_3 (1.14g, 17.5 mmol, 1.5 equiv.) The resulting suspension was then stirred at rt, under N_2 , for 24 h. The acetone was removed under reduced pressure and then diluted with DCM (30 mL) and deionised water

(30 mL) and the organic layer was separated. The aqueous layer was extracted with aliquots of DCM (3 × 20 mL) and the combined organic layers were then rinsed with a saturated solution of brine (50 mL), dried over MgSO₄ and filtered. The solvent was removed under reduced pressure and the product 4a (1.55g, 10.7 mmol) was afforded in quantitative yield as a yellow oil. The product **3a** was sufficiently pure to use without further work up or purification. FTIR analysis was used to confirm product formation which correlated well with the literature.¹⁷³

IR (ATR, cm⁻¹): 2089 (s, assym. stretch, N₃), 1252 (s, symm. stretch, N₃)

2-(azidomethyl)pyridine - **3b**



A dry, 2-neck round-bottomed flask charged with 2-(bromomethyl)pyridine hydrobromide (1.20 g, 4.74 mmol), 18-crown-6 (cat.) and tetrabutylammonium iodide (cat.) was evacuated under high vacuum and filled with Ar(3×). DMF (2 mL) was added through a septum by syringe, under positive pressure (Ar) and to this stirred solution was added diisopropylethylamine (1 mL). Lastly, NaN₃ (0.30g, 4.7 mmol, 1.2 equiv.) was added and the solution was left to stir at rt, under N₂, for 24 h. The solution was then diluted with EtOAc (20 mL), rinsed with basic brine (20 mL×3, pH > 10) followed by washing with an NH₄Cl solution (30 mL, 1M). The organic layer was then dried over MgSO₄ and filtered. The solvent was removed under reduced pressure to afford the pure product 4b as a yellow-brown oil (496mg, 3.35 mmol, 78%). The product **3b** was sufficiently pure to use without further work up or purification. FTIR analysis confirmed product formation which correlated well with the literature.¹⁷⁴

IR (ATR, cm⁻¹): 2093 (s, assym. stretch, N₃), 1270 (s, symm. stretch, N₃).

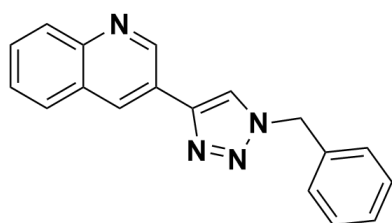
7.2.2 Compounds 4a-d.

General procedure for the copper-mediated azide alkyne cycloaddition reactions (CuAAC)

A dry, 2-neck round bottom flask charged with alkyne (1 equiv) and azide (1.2 equiv) was evacuated under high vacuum and filled with Ar(3×). A solution of MeOH/water (30 mL, 2:1) was added through a septum by syringe, under positive pressure (Ar). To this stirred solution was added copper acetate hydrate (10 mol. %) and the solution was left to stir at rt, under N₂, for 36h or until complete consumption of the starting material (monitored by TLC).

The MeOH was removed under reduced pressure and the reaction mixture was diluted with EtOAc (30 mL) and washed with an NH₄Cl solution (60 mL, 1 M). The layers were then separated and the aqueous layer was washed with successive portions of EtOAc (3×20 mL). The combined organic layers were then rinsed with a saturated solution of brine (60 mL), dried over MgSO₄ and filtered. After removal of the solvents *in vacuo*, the residue was purified by flash column chromatography over silica gel, eluted first with EtOAc and hexane (EtOAc:Hexane, 60:40), followed by MeOH and EtOAc (MeOH:EtOAc, 5:95). This afforded the pure product as a white solid. The details for the compounds synthesized are described below.

3-(1-benzyl-1H-1,2,3-triazol-4-yl)quinoline - 4a

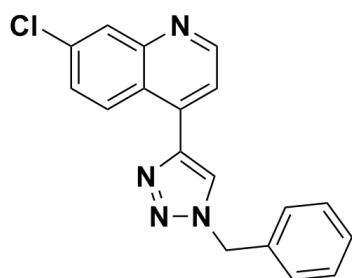


Scale: 3-ethynylisoquinoline (0.1 g, 0.65 mmol)

This compound was synthesized following the general procedure for CuAAC. The compound was purified by silica gel column chromatography, eluted first with EtOAc and hexane (EtOAc:Hexane, 60:40), followed by MeOH and EtOAc (MeOH:EtOAc, 5:95). This afforded the pure product as a white solid (0.14g, 0.47 mmol, 73%).

R_f = 0.31 (EtOAc:Hexane, 60:40); **Mp** 157-159 °C; **IR (ATR, cm⁻¹)**: 3064 (s, stretch, =C–H), 2922 (m, stretch, CH₂), 1046 (s, stretch, C–N), 813 (s, oop, C–H); **¹H NMR (300 MHz, CDCl₃)** δ 9.26 (s, 1H, ArH), 8.61 (d, *J* = 2.0 Hz, 1H, ArH), 8.09 (d, *J* = 8.4 Hz, 1H, ArH), 7.86 (s, 1H, CCHN), 7.84 (dd, *J* = 8.2, 1.1 Hz, 1H, ArH), 7.69 (ddd, *J* = 8.4, 6.9, 1.5 Hz, 1H, ArH), 7.54 (ddd, *J* = 8.0, 7.0, 1.1 Hz, 1H, ArH), 7.47 – 7.29 (m, 5H, ArH), 5.61 (s, 2H, CH₂); **¹³C NMR (75 MHz, CDCl₃)** δ 148.4 (ArC), 147.9 (ArC), 145.5 (NCCH), 134.5 (ArC), 132.0 (ArC), 129.7 (ArC), 129.4 (ArC), 129.3 (CCHN), 129.1 (ArC), 128.3 (ArC), 128.2 (ArC), 128.0 (ArC), 127.3 (ArC), 123.9 (ArC), 120.1 (ArC), 54.5 (CH₂); **HRMS-TOF MS ES+**: *m/z* [M+H]⁺ calcd for C₁₈H₁₅N₄: 287.1297; found: 287.1297

4-(1-benzyl-1H-1,2,3-triazol-4-yl)-7-chloroquinoline - 4b



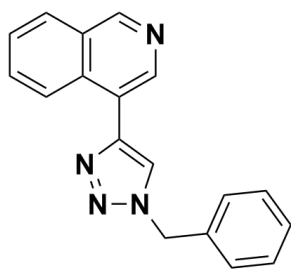
Scale: 7-chloro-4-ethynylquinoline (0.10 g, 0.53 mmol)

This compound was synthesized following the general procedure for CuAAC. The compound was purified by silica gel column chromatography, eluted first with EtOAc and hexane

(EtOAc:Hexane, 60:40), followed by MeOH and EtOAc (MeOH:EtOAc, 5:95). This afforded the pure product as a white solid (0.12 g, 0.29 mmol, 55%).

R_f = 0.32 (EtOAc:Hexane, 60:40); **Mp** 123-127 °C; **IR (ATR, cm^{-1})**: 3071 (s, stretch, =C–H), 2920 (m, stretch, CH_2), 1054 (s, stretch, C–N), 824 (s, oop, C–H); **^1H NMR (300 MHz, CDCl_3)** δ 8.91 (d, J = 4.5 Hz, 1H, ArH), 8.61 (d, J = 9.1 Hz, 1H, ArH), 8.14 (d, J = 2.2 Hz, 1H, ArH), 7.86 (s, 1H, CCHN), 7.57 – 7.51 (m, 2H, ArH), 7.47 – 7.34 (m, 5H, ArH), 5.67 (s, 2H, CH_2); **^{13}C NMR (75 MHz, CDCl_3)** δ 151.1 (ArC), 149.6 (ArC), 145.3 (NCCH), 136.2 (ArC), 135.7 (ArC), 134.3 (ArC), 129.5 (CCHN), 129.3 (ArC), 129.0 (ArC), 128.4 (ArC), 128.3 (ArC), 127.6 (ArC), 124.1 (ArC), 123.3 (ArC), 120.5 (ArC), 54.7 (CH_2); **HRMS-TOF MS ES+**: m/z [$\text{M}+\text{H}$] $^+$ calcd for $\text{C}_{18}\text{H}_{14}\text{N}_4\text{Cl}$: 321.0907; found: 321.0904

4-(1-benzyl-1*H*-1,2,3-triazol-4-yl)isoquinoline - 4c

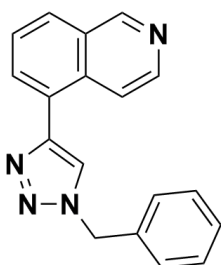


Scale: 4-ethynylisoquinoline (0.10 g, 0.65 mmol)

This compound was synthesized following the general procedure for CuAAC. The compound was purified by silica gel column chromatography, eluted first with EtOAc and hexane (EtOAc:Hexane, 60:40), followed by MeOH and EtOAc (MeOH:EtOAc, 5:95). This afforded the pure product as a white solid (0.12 g, 0.33 mmol, 51%).

R_f = 0.31 (EtOAc:Hexane, 60:40); **Mp** 111-113 °C; **IR (ATR, cm^{-1})**: 3069 (s, stretch, =C–H), 2925 (m, stretch, CH_2), 1059 (s, stretch, C–N), 827 (s, oop, C–H); **^1H NMR (400 MHz, DMSO-d_6)** δ 9.34 (s, 1H, ArH), 8.85 (s, 1H, ArH), 8.78 (s, 1H, ArH), 8.62 (d, J = 8.5 Hz, 1H, ArH), 8.22 (d, J = 8.1 Hz, 1H, ArH), 7.87 (t, J = 7.7 Hz, 1H, ArH), 7.76 (t, J = 7.5 Hz, 1H, ArH), 7.46 – 7.39 (m, 4H, ArH, CCHN), 7.39 – 7.32 (m, 1H, ArH), 5.75 (s, 2H, CH_2); **^{13}C NMR (101 MHz, DMSO-d_6)** δ 152.6 (ArC), 143.3 (NCCH), 142.4 (ArC), 135.9 (ArC), 132.3 (ArC), 131.3 (CCHN), 128.8 (ArC), 128.2 (ArC), 128.2 (ArC), 128.0 (ArC), 127.6 (ArC), 124.5 (ArC), 121.4 (ArC), 53.1 (CH_2); **HRMS-TOF MS ES+**: m/z [$\text{M}+\text{H}$] $^+$ calcd for $\text{C}_{18}\text{H}_{15}\text{N}_4$: 287.1297; found: 287.1293

5-(1-benzyl-1*H*-1,2,3-triazol-4-yl)isoquinoline - 4d



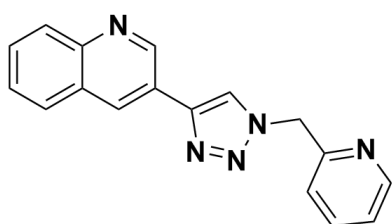
Scale: 5-ethynylisoquinoline (0.10 g, 0.65 mmol)

This compound was synthesized following the general procedure for CuAAC. The compound was purified by silica gel column chromatography, eluted first with EtOAc and hexane (EtOAc:Hexane, 60:40), followed by MeOH and EtOAc (MeOH:EtOAc, 5:95). This afforded the pure product as a white solid (0.13 g, 0.33 mmol, 51%).

R_f = 0.30 (EtOAc:Hexane, 60:40); **Mp** 131-132 °C; **IR (ATR, cm⁻¹)**:3103 (s, stretch, =C–H), 2925 (m, stretch, CH₂),1071 (s, stretch, C–N), 831 (s, oop, C–H); **¹H NMR (400 MHz, DMSO-d₆)** δ 9.38 (s, 1H,ArH), 8.81 (s, 1H,ArH), 8.57 (d, *J* = 6.0 Hz, 1H,ArH), 8.46 (d, *J* = 6.0 Hz, 1H,ArH), 8.16 (d, *J* = 8.0 Hz, 1H,ArH), 8.08 (d, *J* = 7.2 Hz, 1H,ArH), 7.76 (t, *J* = 7.7 Hz, 1H,ArH), 7.41 (dd, *J* = 8.5, 5.3 Hz, 4H,ArH,CCHN), 7.36 (dd, *J* = 8.8, 3.0 Hz, 1H,ArH), 5.73 (s, 2H, CH₂); **¹³C NMR (101 MHz, DMSO-d₆)** δ 153.0 (ArC), 144.9 (NCCH), 143.7 (ArC), 135.9 (ArC), 132.3 (ArC), 131.5 (ArC), 130.5 (CCHN), 128.8 (ArC), 128.7 (ArC), 128.2 (ArC), 128.0 (ArC), 127.2 (ArC), 126.7 (ArC), 124.3 (ArC), 118.1 (ArC), 53.1 (CH₂); **HRMS-TOF MS ES⁺: *m/z* [M+H]⁺** calcd for C₁₈H₁₅N₄: 287.1297; found: 287.1292

7.2.3 Compounds 5a-d.

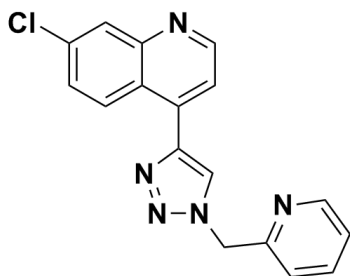
3-[1-(pyridin-2-ylmethyl)-1H-1,2,3-triazol-4-yl]quinoline - 5a



Scale: 3-ethynylisoquinoline (0.10 g, 0.65 mmol)

This compound was synthesized following the general procedure for CuAAC. The compound was purified by silica gel column chromatography, eluted first with EtOAc and hexane (EtOAc:Hexane, 60:40), followed by MeOH and EtOAc (MeOH:EtOAc, 5:95). This afforded the pure product as a white solid (0.13 g, 0.36 mmol, 56%).

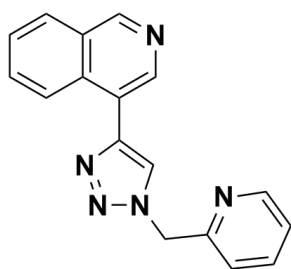
R_f = 0.24 (EtOAc:Hexane, 60:40); **Mp** 137-139 °C; **IR (ATR, cm⁻¹)**:3131 (s, stretch, =C–H), 2918 (m, stretch, CH₂),1045 (s, stretch, C–N), 844 (s, oop, C–H); **¹H NMR (400 MHz, DMSO-d₆)** δ 9.41 (d, *J* = 2.1 Hz, 1H,ArH), 8.91 (s, 1H,ArH), 8.81 (d, *J* = 1.8 Hz, 1H,ArH), 8.57 (d, *J* = 4.7 Hz, 1H,ArH), 8.04 (dd, *J* = 7.8, 4.5 Hz, 2H,ArH), 7.85 (td, *J* = 7.7, 1.8 Hz, 1H,ArH), 7.78 – 7.72 (m, 1H,ArH), 7.63 (t, *J* = 7.5 Hz, 1H,ArH), 7.43 – 7.39 (m, 1H,ArH,CCHN), 7.37 (dd, *J* = 7.5, 4.9 Hz, 1H,ArH), 5.83 (s, 2H, CH₂); **¹³C NMR (101 MHz, DMSO-d₆)** δ 154.8 (ArC), 149.5 (ArC), 148.2 (ArC), 147.1 (ArC), 143.9 (NCCH), 137.4 (ArC), 130.9 (CCHN), 129.6 (ArC), 128.8 (ArC), 128.3 (ArC), 127.6 (ArC), 127.2 (ArC), 124.0 (ArC), 123.4 (ArC), 123.2 (ArC), 122.4 (ArC), 54.7 (CH₂); **HRMS-TOF MS ES⁺: *m/z* [M+H]⁺** calcd for C₁₇H₁₄N₅: 287.1249; found: 287.1250

7-chloro-4-[1-(pyridin-2-ylmethyl)-1H-1,2,3-triazol-4-yl]quinoline - 5b

Scale: 7-chloro-4-ethynylquinoline (0.10 g, 0.53 mmol)

This compound was synthesized following the general procedure for CuAAC. The compound was purified by silica gel column chromatography, eluted first with EtOAc and hexane (EtOAc:Hexane, 60:40), followed by MeOH and EtOAc (MeOH:EtOAc, 5:95). This afforded the pure product as a white solid (0.12 g, 0.36 mmol, 68%).

R_f = 0.23 (EtOAc:Hexane, 60:40); **Mp** 122-123 °C; **IR (ATR, cm^{-1})**: 3120 (s, stretch, =C–H), 2980 (m, stretch, CH_2), 1048 (s, stretch, C–N), 840 (s, oop, C–H); **^1H NMR (400 MHz, CDCl_3)** δ 8.93 (d, J = 4.5 Hz, 1H, ArH), 8.65 – 8.61 (m, 2H, ArH), 8.21 (s, 1H, CCHN), 8.14 (d, J = 2.2 Hz, 1H, ArH), 7.75 (td, J = 7.7, 1.8 Hz, 1H, ArH), 7.61 (d, J = 4.5 Hz, 1H, ArH), 7.54 (dd, J = 9.1, 2.2 Hz, 1H, ArH), 7.37 (d, J = 7.8 Hz, 1H, ArH), 7.31 (ddd, J = 7.6, 4.9, 1.0 Hz, 1H, ArH), 5.78 (s, 2H, CH_2); **^{13}C NMR (101 MHz, CDCl_3)** δ 153.9 (ArC), 151.2 (ArC), 150.2 (ArC), 149.6 (ArC), 145.2 (NCCH), 137.7 (ArC), 136.3 (ArC), 135.7 (ArC), 129.0 (CCHN), 128.3 (ArC), 127.6 (ArC), 124.2 (ArC), 124.1 (ArC), 123.9 (ArC), 123.0 (ArC), 120.5 (ArC), 56.0 (CH_2); **HRMS-TOF MS ES+**: m/z [$\text{M}+\text{H}$] $^+$ calcd for $\text{C}_{17}\text{H}_{13}\text{N}_5$: 322.0854; found: 322.0851

4-[1-(pyridin-2-ylmethyl)-1H-1,2,3-triazol-4-yl]isoquinoline - 5c

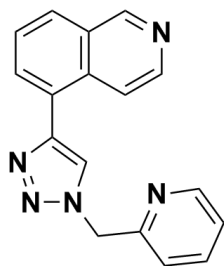
Scale: 4-ethynylisoquinoline (0.10 mg, 0.65 mmol)

This compound was synthesized following the general procedure for CuAAC. The compound was purified by silica gel column chromatography, eluted first with EtOAc and hexane (EtOAc:Hexane, 60:40), followed by MeOH and EtOAc (MeOH:EtOAc, 5:95). This afforded the pure product as a white solid (0.13 mg, 0.45 mmol, 69%).

R_f = 0.23 (EtOAc:Hexane, 60:40); **Mp** 110-112 °C; **IR (ATR, cm^{-1})**: 3120 (s, stretch, =C–H), 2920 (m, stretch, CH_2), 1049 (s, stretch, C–N), 840 (s, oop, C–H); **^1H NMR (400 MHz, CDCl_3)** δ 9.25 (s, 1H, ArH), 8.72 (s, 1H, ArH), 8.63 (d, J = 4.2 Hz, 1H, ArH), 8.56 (d, J = 8.5 Hz, 1H, ArH), 8.09 (s, 1H, CCHN), 8.01 (d, J = 8.2 Hz, 1H, ArH), 7.78 – 7.70 (m, 2H, ArH),

7.64 (ddd, $J = 8.0, 6.9, 1.0$ Hz, 1H,ArH), 7.34 (d, $J = 7.8$ Hz, 1H,ArH), 7.32 – 7.27 (m, 1H,ArH), 5.79 (s, 2H, CH₂); ¹³C NMR (101 MHz,CDCl₃) δ 154.3 (ArC), 153.1 (ArC), 150.1 (ArC), 144.9 (NCCH), 143.0 (ArC), 137.6 (ArC), 133.6 (ArC), 131.2 (CCHN), 128.1 (ArC), 127.6 (ArC), 125.1 (ArC), 123.7 (ArC), 123.3 (ArC), 122.8 (ArC), 56.0 (CH₂); HRMS-TOF MS ES+: m/z [M+H]⁺ calcd for C₁₇H₁₃N₅: 287.1249; found: 287.1242

5-[1-(pyridin-2-ylmethyl)-1H-1,2,3-triazol-4-yl]isoquinoline - 5d



Scale: 5-ethynylisoquinoline (0.10 g, 0.65 mmol)

This compound was synthesized following the general procedure for CuAAC. The compound was purified by silica gel column chromatography, eluted first with EtOAc and hexane (EtOAc:Hexane, 60:40), followed by MeOH and EtOAc (MeOH:EtOAc, 5:95). This afforded the pure product as a white solid (0.12g, 0.43 mmol, 66%).

R_f = 0.22 (EtOAc:Hexane, 60:40); **Mp** 128-130 °C; **IR** (ATR, cm⁻¹):3130 (s, stretch, =C–H), 2929 (m, stretch,CH₂),1050 (s, stretch, C–N), 824 (s, oop, C–H); ¹H NMR (300 MHz, CDCl₃) δ 8.63 (d, $J = 3.4$ Hz, 1H,ArH), 8.34 (s, 1H,ArH), 8.08 (s, 1H,CCHN), 7.98 (t, $J = 7.6$ Hz, 2H,ArH), 7.74 (td, $J = 7.7, 1.7$ Hz, 1H,ArH), 7.69 – 7.60 (m, 1H,ArH), 7.40 – 7.26 (m, 2H,ArH), 5.78 (s, 2H, CH₂); ¹³C NMR (75 MHz,CDCl₃) δ 154.3 (ArC), 153.0 (ArC), 150.1 (ArC), 146.3 (ArC), 143.9 (NCCH), 137.6 (ArC), 133.6 (ArC), 130.9 (CCHN), 128.6 (ArC), 127.3 (ArC), 127.0 (ArC), 123.7 (ArC), 123.2 (ArC), 122.8 (ArC), 56.0 (CH₂); HRMS-TOF MS ES+: m/z [M+H]⁺ calcd for C₁₇H₁₃N₅: 287.1249; found: 287.1247

7.3 SYNTHESIS PERTAINING TO CHAPTER 4.

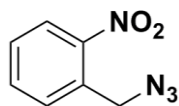
7.3.1 Compounds 6a-c.

General Procedure for Synthesis of Nitrobenzyl Azides

To a stirred solution of nitrobenzyl bromide (1 equiv) in a round bottom flask, in a water/acetone mixture (50 mL, 1:4) was added NaN₃ (1.5 equiv.) The resulting suspension was then stirred at rt, under N₂, for 24 h. The acetone was removed under reduced pressure and then diluted with DCM (30 mL) and deionised water (30 mL) and the organic layer was separated. The aqueous layer was extracted with aliquots of DCM (3×10 mL) and the combined organic layers were then rinsed with a saturated solution of brine (50 mL), dried over MgSO₄ and filtered. The solvent was removed under reduced pressure to afford the

product which was sufficiently pure to use without further work up or purification. FTIR analysis was used to confirm product formation.

1-(azidomethyl)-2-nitrobenzene - 6a

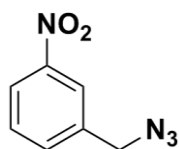


Scale: 2-nitrobenzyl bromide (1.00 g, 4.62 mmol)

This compound was synthesized following the general procedure nitrobenzyl azides. This afforded the pure product in quantitative yield as a brown oil (0.82 g, 4.26 mmol).

$R_f = 0.64$ (EtOAc:Hexane, 60:40); **IR (ATR, cm^{-1}):**3074 (s, stretch, ArC–H),2916 (m, stretch, CH_2), 2091 (s, assym. stretch, N_3), 1523 (s, assym. stretch, N-O), 1254 (s, symm. stretch, N_3)

1-(azidomethyl)-3-nitrobenzene - 6b

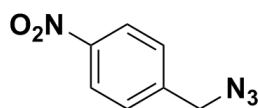


Scale: 3-nitrobenzyl bromide (1.00 g, 4.62 mmol)

This compound was synthesized following the general procedure nitrobenzyl azides. This afforded the pure product as a brown oil (0.81 g, 4.53 mmol, 98%).

$R_f = 0.54$ (EtOAc:Hexane, 60:40); **IR (ATR, cm^{-1}):**3072 (s, stretch, ArC–H), 2970 (m, stretch, CH_2),2091 (s, assym. stretch, N_3), 1523 (s, assym. stretch, N-O), 1252 (s, symm. stretch, N_3)

1-(azidomethyl)-4-nitrobenzene - 6c



Scale: 4-nitrobenzyl bromide (1.00 g, 4.62 mmol)

This compound was synthesized following the general procedure nitrobenzyl azides. This afforded the pure product as a white solid (0.81 g, 4.52 mmol, 98%).

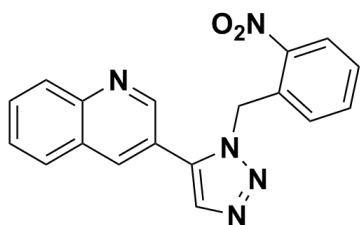
$R_f = 0.46$ (EtOAc:Hexane, 10:90); **IR (ATR, cm^{-1}):**3079 (s, stretch, ArC–H), 2920(m, stretch, CH_2),2093 (s, assym. stretch, N_3), 1515 (s, assym. stretch, N-O), 1251 (s, symm. stretch, N_3)

7.3.1 Compounds 7a-l.

**General procedure for the ruthenium-mediated azide alkyne cycloaddition reactions
(RuAAC)**

A dry Schlenk tube was evacuated under high vacuum and filled with Ar(3×). To this Schlenk tube was added by syringe, under Ar, anhydrous toluene (15 mL). The solvent was subsequently degassed for 1 h with Ar purge. After degassing, the catalyst Cp*RuCl(COD) (4 mol. %) and alkyne **4a-d** (1 equiv) were added under positive pressure Ar and the mixture was allowed to stir for 5 min under Ar. Following this, the azide **6a-c** (1.2 equiv) was also added under positive pressure Ar. In all reactions the alkyne was added first, followed by the azide. The reaction mixture was then placed in an oil bath heated to 80 °C and was allowed to stir under N₂ for 24 h or until complete consumption of starting materials (monitored by TLC). The reaction mixture was then absorbed directly onto silica gel and purified by flash column chromatography over silica gel eluting with EtOAc and hexane (EtOAc:Hexane, 70:30) to yield the pure product as a yellow/orange brown solid. The details for the compounds synthesized are described below.

3-[1-(2-nitrobenzyl)-1H-1,2,3-triazol-5-yl]quinoline - 7a



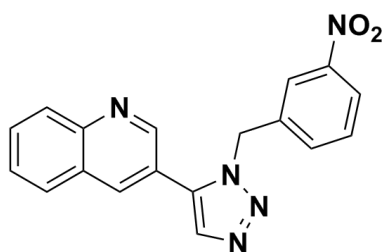
Scale: 3-ethynylquinoline (0.15 g, 0.98 mmol)

This compound was synthesized following the general procedure for RuAAC. The compound was purified by silica gel column chromatography, eluted with EtOAc and hexane (EtOAc:Hexane, 70:30). This afforded the pure product as a yellow brown solid (0.28 g, 0.83 mmol, 85%).

R_f = 0.45 (EtOAc:Hexane, 70:30); **Mp** 99-101 °C; **IR (ATR, cm⁻¹)**: 3110 (s, stretch, ArC-H), 2963 (m, stretch, CH₂), 1520 (s, assym. stretch, N-O), 1122 (s, stretch, C-N), 855 (s, oop, C-H); **¹H NMR (400 MHz, CDCl₃)** δ 8.77 (d, *J* = 2.3 Hz, 1H, ArH), 8.16 (dd, *J* = 8.2, 1.3 Hz, 1H, ArH), 8.12 (dd, *J* = 8.4, 0.8 Hz, 1H, ArH), 8.07 (d, *J* = 2.2 Hz, 1H, ArH), 8.00 (s, 1H, CCHN), 7.84 – 7.76 (m, 2H, ArH), 7.67 – 7.58 (m, 2H, ArH), 7.56 – 7.48 (m, 1H, ArH), 6.87 (dd, *J* = 7.8, 1.0 Hz, 1H, ArH), 6.07 (s, 2H, CH₂); **¹³C NMR (101 MHz, CDCl₃)** δ 148.9 (ArC), 148.3 (ArC), 147.0 (ArC), 136.1 (NCCH), 135.9 (ArC), 134.7 (ArC), 134.3 (ArC), 131.5 (CCHN), 131.3 (ArC), 129.6 (ArC), 129.6 (ArC), 128.9 (ArC), 128.2 (ArC), 128.1

(ArC), 127.2 (ArC), 125.8 (ArC), 119.8 (ArC), 49.6 (CH₂); **HRMS-TOF MS ES+**: *m/z* [M+H]⁺ calcd for C₁₈H₁₄N₅O₂: 332.1147; found: 332.1156

3-[1-(3-nitrobenzyl)-1*H*-1,2,3-triazol-5-yl]quinoline - 7b

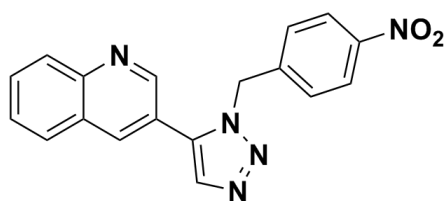


Scale: 3-ethynylquinoline (0.15 g, 0.98 mmol)

This compound was synthesized following the general procedure for RuAAC. The compound was purified by silica gel column chromatography, eluted with EtOAc and hexane (EtOAc:Hexane, 70:30). This afforded the pure product as a yellow brown solid (0.30 g, 0.9 mmol, 92%)

R_f = 0.45 (EtOAc:Hexane, 70:30); **Mp** 142-144 °C; **IR (ATR, cm⁻¹)**: 3070 (s, stretch, ArC–H), 2901(m, stretch, CH₂), 1521 (s, assym. stretch, N–O), 1125 (s, stretch, C–N), 837 (s, oop, C–H); **¹H NMR (400 MHz, CDCl₃)** δ 8.78 (d, *J* = 2.2 Hz, 1H, Ar*H*), 8.15 (d, *J* = 9.1 Hz, 2H, Ar*H*), 8.05 (d, *J* = 2.1 Hz, 1H, Ar*H*), 7.99 – 7.94 (m, 1H, Ar*H*), 7.93 (s, 1H, CCHN), 7.82 (m, 2H, Ar*H*), 7.69 – 7.61 (m, 1H, Ar*H*), 7.55 – 7.42 (m, 2H, Ar*H*), 5.72 (s, 2H, CH₂); **¹³C NMR (101 MHz, CDCl₃)** δ 149.1 (ArC), 148.6 (ArC), 148.3 (ArC), 137.1 (NCCH), 136.4 (ArC), 135.4 (ArC), 134.5 (ArC), 133.3 (ArC), 131.4 (CCHN), 130.4 (ArC), 129.7 (ArC), 128.3 (ArC), 128.1 (ArC), 127.1 (ArC), 123.7 (ArC), 122.39 (ArC), 119.92 (ArC), 51.4 (CH₂); **HRMS-TOF MS ES+**: *m/z* [M+H]⁺ calcd for C₁₈H₁₄N₅O₂: 332.1147; found: 332.1152

3-[1-(4-nitrobenzyl)-1*H*-1,2,3-triazol-5-yl]quinoline - 7c



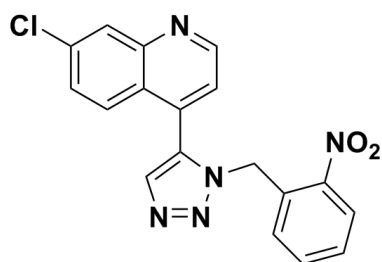
Scale: 3-ethynylquinoline (0.15 g, 0.98 mmol)

This compound was synthesized following the general procedure for RuAAC. The compound was purified by silica gel column chromatography, eluted with EtOAc and hexane (EtOAc:Hexane, 70:30). This afforded the pure product as a brown solid (0.27g, 0.82 mmol, 83%)

R_f = 0.43 (EtOAc:Hexane, 70:30); **Mp** 144-146 °C; **IR (ATR, cm⁻¹)**: 3060 (s, stretch, ArC–H), 2912(m, stretch, CH₂), 1508 (s, assym. stretch, N–O), 1141 (s, stretch, C–N), 836 (s, oop, C–H); **¹H NMR (400 MHz, CDCl₃)** δ 8.77 (d, *J* = 2.3 Hz, 1H, Ar*H*), 8.16 (dt, *J* = 9.1, 2.4 Hz,

3H,ArH), 8.00 (t, $J = 4.1$ Hz, 1H,ArH), 7.94 (s, 1H,CCHN), 7.83 (ddd, $J = 8.4, 6.9, 1.5$ Hz, 1H,ArH), 7.78 (dd, $J = 8.0, 0.6$ Hz, 1H,ArH), 7.64 (ddd, $J = 8.1, 6.9, 1.1$ Hz, 1H,ArH), 7.29 – 7.28 (m, 1H,ArH), 7.27 – 7.25 (m, 1H,ArH), 5.72 (s, 2H, CH₂); ¹³C NMR (101 MHz,CDCl₃) δ 149.0 (ArC), 148.3 (ArC), 148.1 (ArC), 142.1 (ArC), 136.3 (NCCH), 135.5 (ArC), 134.5 (ArC), 131.4 (CCHN), 129.7 (ArC), 128.3 (ArC), 128.1 (ArC), 128.1 (ArC), 127.1 (ArC), 124.4 (ArC), 119.9 (ArC); 51.5 (CH₂); HRMS-TOF MS ES+: m/z [M+H]⁺ calcd for C₁₈H₁₄N₅O₂: 332.1147; found: 332.1150

7-chloro-4-[1-(2-nitrobenzyl)-1H-1,2,3-triazol-5-yl]quinoline - 7d

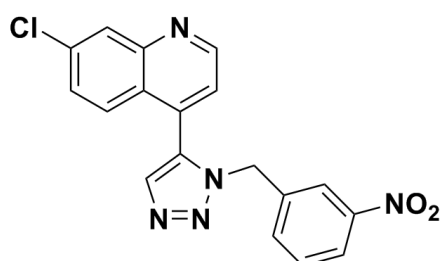


Scale: 7-chloro-4-ethynylquinoline (0.15 g, 0.8 mmol)

This compound was synthesized following the general procedure for RuAAC. The compound was purified by silica gel column chromatography, eluted with EtOAc and hexane (EtOAc:Hexane, 70:30). This afforded the pure product as an orange brown solid (0.23 g, 0.64 mmol, 81%)

R_f = 0.46 (EtOAc:Hexane, 70:30); **Mp** 173-175 °C; **IR (ATR, cm⁻¹)**: 3148 (s, stretch, ArC–H), 2901(m, stretch, CH₂), 1524 (s, assym. stretch, N–O), 1244 (s, stretch, C–N), 882 (s, oop, C–H); ¹H NMR (400 MHz, CDCl₃) δ 8.93 (d, $J = 4.1$ Hz, 1H,ArH), 8.19 (s, 1H,ArH), 8.01 (d, $J = 8.0$ Hz, 1H,ArH), 7.96 (s, 1H,CCHN), 7.51 (m, 5H,ArH), 7.19 (d, $J = 4.1$ Hz, 1H,ArH), 6.94 (d, $J = 7.6$ Hz, 1H,ArH), 5.90 (d, $J = 50.3$ Hz, 2H, CH₂); ¹³C NMR (101 MHz,CDCl₃) δ 150.9 (ArC), 149.1 (ArC), 147.2 (ArC), 136.7 (NCCH), 135.3 (ArC), 134.3 (ArC), 133.9 (ArC), 133.0 (ArC), 130.5 (CCHN), 129.7 (ArC), 129.7 (ArC), 129.5 (ArC), 129.3 (ArC), 125.7 (ArC), 125.6 (ArC), 124.8 (ArC), 122.3 (ArC), 49.6 (CH₂); HRMS-TOF MS ES+: m/z [M+H]⁺ calcd for C₁₈H₁₃ClN₅O₂: 366.0758; found: 366.0759

7-chloro-4-[1-(3-nitrobenzyl)-1H-1,2,3-triazol-5-yl]quinoline - 7e

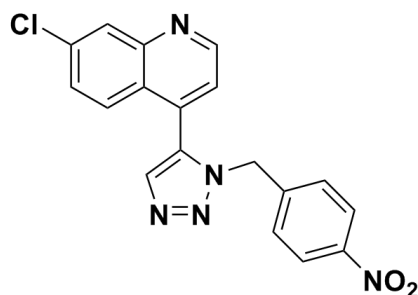


Scale: 7-chloro-4-ethynylquinoline (0.15 g, 0.8 mmol)

This compound was synthesized following the general procedure for RuAAC. The compound was purified by silica gel column chromatography, eluted with EtOAc and hexane (EtOAc:Hexane, 70:30). This afforded the pure product as an orange brown solid (0.24 g, 0.66 mmol, 83%)

R_f = 0.48 (EtOAc:Hexane, 70:30); **Mp** 176-178 °C; **IR (ATR, cm⁻¹)**:3076 (s, stretch, ArC–H), 2961(m, stretch, CH₂),1524 (s, assym. stretch, N–O), 1259 (s, stretch, C–N), 819 (s, oop, C–H); **¹H NMR (400 MHz, CDCl₃) δ** 8.99 (d, *J* = 4.0 Hz, 1H,ArH), 8.22 (s, 1H,ArH), 8.09 (d, *J* = 7.9 Hz, 1H,ArH), 7.94 (s, 1H,CCHN), 7.71 (s, 1H,ArH), 7.47 (d, *J* = 8.6 Hz, 1H,ArH), 7.39 (t, *J* = 7.9 Hz, 1H,ArH), 7.33 (d, *J* = 8.9 Hz, 1H,ArH), 7.28 (d, *J* = 7.6 Hz, 1H,ArH), 7.21 (d, *J* = 4.0 Hz, 1H,ArH), 5.52 (s, 2H, CH₂); **¹³C NMR (101 MHz,CDCl₃) δ** 150.8 (ArC), 148.9 (ArC), 148.4 (ArC), 136.8 (NCCH), 136.2 (ArC), 135.3 (ArC), 133.6 (ArC), 133.2 (ArC), 130.1 (CCHN), 129.4 (ArC), 129.3 (ArC), 125.7 (ArC), 124.8 (ArC), 123.7 (ArC), 122.7 (ArC), 122.6 (ArC), 51.7 (CH₂); **HRMS-TOF MS ES+**: *m/z* [M+H]⁺ calcd for C₁₈H₁₃ClN₅O₂: 366.0758; found: 366.0757

7-chloro-4-[1-(4-nitrobenzyl)-1H-1,2,3-triazol-5-yl]quinoline - 7f

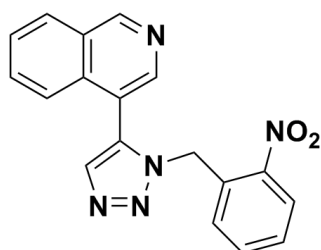


Scale: 7-chloro-4-ethynylquinoline (0.15 g, 0.8 mmol)

This compound was synthesized following the general procedure for RuAAC. The compound was purified by silica gel column chromatography, eluted with EtOAc and hexane (EtOAc:Hexane, 70:30). This afforded the pure product as a brown solid (0.24 g, 0.65 mmol, 82%)

R_f = 0.46 (EtOAc:Hexane, 70:30); **Mp** 181-189 °C; **IR (ATR, cm⁻¹)**:3115 (s, stretch, ArC–H), 2903(m, stretch, CH₂),1516 (s, assym. stretch, N–O), 1285 (s, stretch, C–N), 856 (s, oop, C–H); **¹H NMR (400 MHz, CDCl₃) δ** 8.94 (d, *J* = 4.1 Hz, 1H,ArH), 8.21 (s, 1H,ArH), 8.04 (d, *J* = 8.4 Hz, 2H,ArH), 7.92 (s, 1H,CCHN), 7.47 (d, *J* = 8.5 Hz, 1H,ArH), 7.33 (d, *J* = 8.9 Hz, 1H,ArH), 7.11 (t, *J* = 8.1 Hz, 1H,ArH), 7.05 (d, *J* = 8.3 Hz, 2H,ArH), 5.49 (s, 2H, CH₂); **¹³C NMR (101 MHz,CDCl₃) δ** 150.8 (ArC), 149.0 (ArC), 148.0 (ArC), 141.2 (ArC), 136.8 (NCCH), 135.31 (ArC), 133.3 (ArC), 133.2 (ArC), 129.5 (CCHN), 129.4 (ArC), 128.5 (ArC), 125.7 (ArC), 124.8 (ArC), 124.2 (ArC), 122.5 (ArC), 51.7 (CH₂); **HRMS-TOF MS ES+**: *m/z* [M+H]⁺ calcd for C₁₈H₁₃ClN₅O₂: 366.0758; found: 366.0759

4-[1-(2-nitrobenzyl)-1H-1,2,3-triazol-5-yl]isoquinoline - 7g



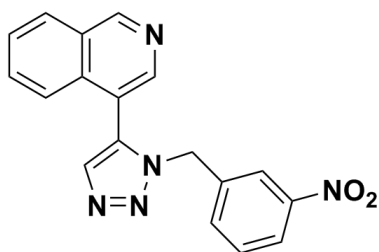
Scale: 4-ethynylisoquinoline (0.15 g, 0.98 mmol)

This compound was synthesized following the general procedure for RuAAC. The compound was purified by silica gel column

chromatography, eluted with EtOAc and hexane (EtOAc:Hexane, 70:30). This afforded the pure product as a yellow brown solid (0.16 g, 0.5 mmol, 54%)

R_f = 0.44 (EtOAc:Hexane, 70:30); **Mp** 129-131 °C; **IR (ATR, cm⁻¹)**:3055 (s, stretch, ArC–H), 2961(m, stretch, CH₂),1523 (s, assym. stretch, N–O), 1260 (s, stretch, C–N), 861 (s, oop, C–H); **¹H NMR (400 MHz, CDCl₃)** δ 9.32 (s, 1H,ArH), 8.27 (s, 1H,ArH), 8.07 (dt, *J* = 7.1, 3.0 Hz, 1H,ArH), 8.01 – 7.93 (m, 2H,ArH,CCHN), 7.78 – 7.65 (m, 2H,ArH), 7.55 (td, *J* = 7.7, 1.2 Hz, 1H,ArH), 7.50 (dd, *J* = 8.1, 6.2 Hz, 1H,ArH), 7.46 – 7.37 (m, 1H,ArH), 6.89 (d, *J* = 7.3 Hz, 1H,ArH), 5.83 (s, 2H, CH₂); **¹³C NMR (101 MHz,CDCl₃)** δ 154.9 (ArC), 147.1 (ArC), 143.0 (ArC), 135.7 (NCCH), 134.3 (ArC), 133.8 (ArC), 132.2 (ArC), 131.1 (CCHN), 129.4 (ArC), 129.3 (ArC), 128.6 (ArC), 128.5 (ArC), 125.5 (ArC), 123.4 (ArC), 118.1 (ArC), 49.3 (CH₂); **HRMS-TOF MS ES⁺: *m/z* [M+H]⁺** calcd for C₁₈H₁₄N₅O₂: 332.1147; found: 332.1150

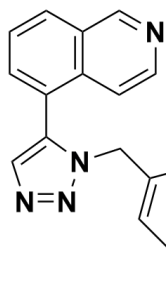
4-[1-(3-nitrobenzyl)-1*H*-1,2,3-triazol-5-yl]isoquinoline - 7h



Scale: 4-ethynylisoquinoline (0.15 g, 0.98 mmol)

This compound was synthesized following the general procedure for RuAAC. The compound was purified by silica gel column chromatography, eluted with EtOAc and hexane (EtOAc:Hexane, 70:30). This afforded the pure product as an orange brown solid (0.17 g, 0.51 mmol, 55%)

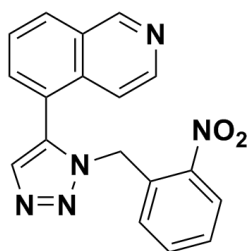
R_f = 0.44 (EtOAc:Hexane, 70:30); **Mp** 131-133 °C;**IR (ATR, cm⁻¹)**:3034 (s, stretch, ArC–H), 2916(m, stretch, CH₂),1525 (s, assym. stretch, N–O), 1161 (s, stretch, C–N), 907 (s, oop, C–H); **¹H NMR (400 MHz, CDCl₃)** δ 9.35 (s, 1H,ArH), 8.32 (s, 1H,ArH), 8.09 – 8.04 (m, 1H,ArH), 7.97 (ddd, *J* = 8.0, 2.1, 1.4 Hz, 1H,ArH), 7.90 (s, 1H,CCHN), 7.64 (m, 2H,ArH), 7.52 (t, *J* = 1.7 Hz, 1H,ArH), 7.33 (t, *J* = 7.8 Hz, 1H,ArH), 7.27 (ddd, *J* = 12.6, 7.0, 4.7 Hz, 2H,ArH), 5.50 (s, 2H, CH₂); **¹³C NMR (101 MHz,CDCl₃)** δ 154.9 (ArC), 148.2 (ArC), 144.1 (ArC), 136.4 (NCCH), 135.8 (ArC), 134.4 (ArC), 133.8 (ArC), 133.0 (ArC), 132.0 (ArC), 130.0 (CCHN), 128.5 (ArC), 128.5 (ArC), 123.5 (ArC), 123.3 (ArC), 122.9 (ArC), 118.4 (ArC), 51.7 (CH₂);**HRMS-TOF MS ES⁺: *m/z* [M+H]⁺** calcd for C₁₈H₁₄N₅O₂: 332.1147; found: 332.1145

4-[1-(4-nitrobenzyl)-1*H*-1,2,3-triazol-5-yl]isoquinoline - 7i

Scale: 4-ethynylisoquinoline (0.15 g, 0.98 mmol)

This compound was synthesized following the general procedure for RuAAC. The compound was purified by silica gel column chromatography, eluted with EtOAc and hexane (EtOAc:Hexane, 70:30). This afforded the pure product as an orange brown solid (0.18 g, 0.55 mmol, 60%)

R_f = 0.43 (EtOAc:Hexane, 70:30); **Mp** 214-216 °C; **IR (ATR, cm⁻¹)**: 3140 (s, stretch, ArC–H), 2935(m, stretch, CH₂), 1517 (s, assym. stretch, N–O), 1163 (s, stretch, C–N), 928 (s, oop, C–H); **¹H NMR (400 MHz, CDCl₃)** δ 9.38 (s, 1H, ArH), 8.32 (s, 1H, ArH), 8.05 (t, *J* = 12.7 Hz, 1H, ArH), 7.96 (d, *J* = 8.7 Hz, 2H, ArH), 7.91 (s, 1H, CCHN), 7.66 (m, 2H, ArH), 7.29 (d, *J* = 8.1 Hz, 1H, ArH), 7.02 (d, *J* = 8.7 Hz, 2H, ArH), 5.50 (s, 2H, CH₂); **¹³C NMR (101 MHz, CDCl₃)** δ 154.8 (ArC), 147.8 (ArC), 144.1 (ArC), 141.5 (ArC), 135.8 (NCCH), 134.36 (ArC), 133.1 (ArC), 132.0 (CCHN), 128.6 (ArC), 128.5 (ArC), 128.5 (ArC), 124.0 (ArC), 123.4 (ArC), 51.6 (CH₂); **HRMS-TOF MS ES⁺: *m/z* [M+H]⁺** calcd for C₁₈H₁₄N₅O₂: 332.1147; found: 332.1147

5-[1-(2-nitrobenzyl)-1*H*-1,2,3-triazol-5-yl]isoquinoline - 7j

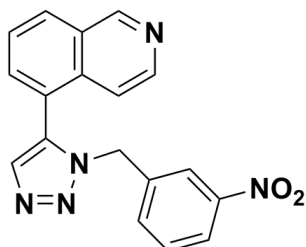
Scale: 5-ethynylisoquinoline (0.1 g, 0.65 mmol)

This compound was synthesized following the general procedure for RuAAC. The compound was purified by silica gel column chromatography, eluted with EtOAc and hexane (EtOAc:Hexane, 70:30). This afforded the pure product as an orange brown solid (0.11 g, 0.34 mmol, 53%)

R_f = 0.29 (EtOAc:Hexane, 80:20); **Mp** 194-196 °C; **IR (ATR, cm⁻¹)**: 3128 (s, stretch, ArC–H), 2922(m, stretch, CH₂), 1524 (s, assym. stretch, N–O), 1105 (s, stretch, C–N), 869 (s, oop, C–H); **¹H NMR (400 MHz, CDCl₃)** δ 9.35 (s, 1H, ArH), 8.52 (s, 1H, ArH), 8.13 (d, *J* = 8.2 Hz, 1H, ArH), 7.95 (d, *J* = 6.1 Hz, 2H, ArH, CCHN), 7.65 (t, *J* = 7.7 Hz, 1H, ArH), 7.61 – 7.50 (m, 2H, ArH), 7.43 (t, *J* = 7.8 Hz, 1H, ArH), 7.28 (s, 1H, ArH), 7.00 (d, *J* = 7.7 Hz, 1H, ArH), 5.83 (s, 2H, CH₂); **¹³C NMR (101 MHz, CDCl₃)** δ 153.2 (ArC), 147.3 (ArC), 144.5 (ArC), 135.3 (NCCH), 135.2 (ArC), 134.6 (ArC), 134.2 (ArC), 132.6 (ArC), 130.9 (ArC), 130.4

(CCHN), 129.7 (ArC), 129.4 (ArC), 126.8 (ArC), 125.3 (ArC), 123.2 (ArC), 117.1(ArC), 77.36 (ArC), 49.0 (CH₂); **HRMS-TOF MS ES⁺**: *m/z* [M+H]⁺ calcd for C₁₈H₁₄N₅O₂: 332.1147; found: 332.1151

5-[1-(3-nitrobenzyl)-1*H*-1,2,3-triazol-5-yl]isoquinoline - 7k

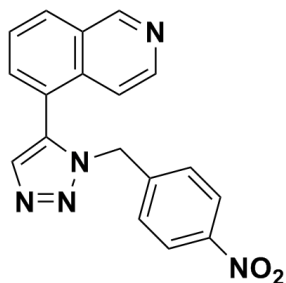


Scale: 5-ethynylisoquinoline (0.15 g, 0.98 mmol)

This compound was synthesized following the general procedure for RuAAC. The compound was purified by silica gel column chromatography, eluted with EtOAc and hexane (EtOAc:Hexane, 70:30). This afforded the pure product as an orange brown solid (0.18 g, 0.53 mmol, 54%)

R_f = 0.3 (EtOAc:Hexane, 80:20); **Mp** 130-132 °C; **IR (ATR, cm⁻¹)**:3074 (s, stretch, ArC–H), 2904(m, stretch, CH₂),1522 (s, assym. stretch, N–O), 1105 (s, stretch, C–N), 832 (s, oop, C–H); **¹H NMR (400 MHz, CDCl₃)** δ 9.37 (s, 1H), 8.45 (d, *J* = 5.4 Hz, 1H,Ar*H*), 8.19 (t, *J* = 9.9 Hz, 1H,Ar*H*), 8.00 (d, *J* = 7.9 Hz, 1H,Ar*H*), 7.85 (s, 1H,CCHN), 7.74 – 7.64 (m, 1H,Ar*H*), 7.53 (d, *J* = 7.2 Hz, 2H,Ar*H*), 7.40 – 7.30 (m, 1H,Ar*H*), 7.27 (d, *J* = 5.9 Hz, 1H,Ar*H*), 7.14 (d, *J* = 5.8 Hz, 1H,Ar*H*), 5.47 (s, 2H, CH₂); **¹³C NMR (101 MHz,CDCl₃)** δ 152.8 (ArC), 148.2 (ArC), 143.8 (ArC), 136.5 (NCCH), 135.3 (ArC), 134.8 (ArC), 134.4 (ArC), 133.8 (ArC), 133.3 (ArC), 130.7 (CCHN), 130.0 (ArC), 127.0 (ArC), 123.5 (ArC), 123.4 (ArC), 122.8 (ArC), 117.3 (ArC), 51.6 (CH₂); **HRMS-TOF MS ES⁺**: *m/z* [M+H]⁺ calcd for C₁₈H₁₄N₅O₂: 332.1147; found: 332.1145

5-[1-(4-nitrobenzyl)-1*H*-1,2,3-triazol-5-yl]isoquinoline - 7l



Scale: 5-ethynylisoquinoline (0.15 g, 0.98 mmol)

This compound was synthesized following the general procedure for RuAAC. The compound was purified by silica gel column chromatography, eluted with EtOAc and hexane (EtOAc:Hexane, 70:30). This afforded the pure product as an orange brown solid (0.20 g, 0.58 mmol, 60%)

R_f = 0.3 (EtOAc:Hexane, 80:20); **Mp** 169-171 °C;**IR (ATR, cm⁻¹)**:3123 (s, stretch, ArC–H), 2961(m, stretch, CH₂),1515 (s, assym. stretch, N–O), 1258 (s, stretch, C–N), 793 (s, oop, C–

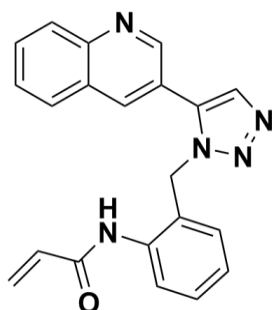
H); ^1H NMR (400 MHz, CDCl_3) δ 9.37 (s, 1H,ArH), 8.49 (d, $J = 5.3$ Hz, 1H,ArH), 8.16 (d, $J = 8.2$ Hz, 1H,ArH), 7.98 (t, $J = 9.3$ Hz, 2H,ArH), 7.87 (s, 1H,CCHN), 7.65 (t, $J = 7.7$ Hz, 1H,ArH), 7.44 (t, $J = 9.5$ Hz, 1H,ArH), 7.19 (d, $J = 5.8$ Hz, 1H,ArH), 7.02 (d, $J = 8.5$ Hz, 2H,ArH), 5.46 (s, 2H, CH_2); ^{13}C NMR (101 MHz, CDCl_3) δ 153.0 (ArC), 147.9 (ArC), 144.1 (ArC), 141.6 (ArC), 135.3 (NCCH), 134.7 (ArC), 134.6 (ArC), 133.2 (ArC), 130.5 (CCHN), 128.5 (ArC), 126.9 (ArC), 124.0 (ArC), 123.3 (ArC), 117.3 (ArC), 51.51 (CH_2); HRMS-TOF MS ES+: m/z [$\text{M}+\text{H}$] $^+$ calcd for $\text{C}_{18}\text{H}_{14}\text{N}_5\text{O}_2$: 332.1147; found: 332.1146

7.3.2 Compounds 8a-l.

General Procedure for Reduction of Aromatic Nitro Groups and Acylation with Acryloyl Chloride

To a 2 neck round bottom flask was added a solution of the aromatic nitro "clicked" compound **7a-l** (1 equiv) in anhydrous DCM (15 mL) under N_2 . A hydrogen balloon was attached to one neck and Pd/C (10 mol. % on C) (5 mol. %) was added to the reaction mixture. The N_2 was evacuated through a tap on the other neck, creating a hydrogen atmosphere in the reaction vessel under atmospheric pressure. The resulting suspension was then stirred at rt for 6 hours or until complete reduction of the nitro moiety to the amine (monitored by TLC). The reaction mixture was then filtered through Celite and the solvent was removed under reduced pressure to afford the product as a white foam, which was sufficiently pure to use without further purification. To a dry round bottom flask was then directly added a solution of the crude reduced aromatic amine (1 equiv) in anhydrous DCM (15 mL) under N_2 . The reaction mixture was placed in an ice bath and cooled to 0°C , where after Et_3N (12 equiv) was added slowly by syringe and allowed to stir for 5 min. Acryloyl chloride (1.2 equiv) was then added drop-wise and a colour change from colourless to yellow was seen immediately. The ice bath was then removed and the reaction mixture was allowed to stir at rt for up to 4 hours or until complete consumption of the starting material (monitored by TLC). After removal of the solvent *in vacuo*, the residue was purified by flash column chromatography over silica gel, eluting first with EtOAc and hexane (EtOAc:Hexane, 90:10), then EtOAc. This afforded the pure product as a white foam/solid.

N-{2-[[5-(quinolin-3-yl)-1*H*-1,2,3-triazol-1-yl]methyl]phenyl}acrylamide - **8a**

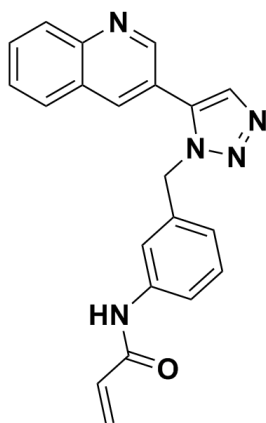


Scale: 3-(1-(2-nitrobenzyl)-1*H*-1,2,3-triazol-5-yl)quinoline (200 mg, 0.604 mmol)

This compound was synthesized following the general procedure for reduction of aromatic nitro and acylation with acryloyl chloride. The compound was purified by silica gel column chromatography, eluted first with EtOAc and hexane (EtOAc:Hexane, 90:10) and then EtOAc. This afforded the pure product as a white foam (131 mg, 0.37 mmol, 61%)

R_f = 0.44 (EtOAc:Hexane, 90:10); **Mp** 185-187 °C; **IR (ATR, cm⁻¹)**: 3247 (m, stretch, N–H), 3120 (s, stretch, ArC–H), 1652 (s, stretch, –C=C–), 1208 (s, stretch, C–N), 803 (s, oop, C–H); **¹H NMR (400 MHz, DMSO-d₆)** δ 9.84 (s, 1H, NH), 8.94 (d, *J* = 2.2 Hz, 1H, ArH), 8.40 (d, *J* = 2.1 Hz, 1H, ArH), 8.24 (s, 1H, CCHN), 8.05 (d, *J* = 8.3 Hz, 1H, ArH), 7.96 (d, *J* = 8.4 Hz, 1H, ArH), 7.88 – 7.78 (m, 1H, ArH), 7.68 (t, *J* = 7.1 Hz, 1H, ArH), 7.39 – 7.22 (m, 2H, ArH), 7.11 (t, *J* = 7.5 Hz, 1H, ArH), 6.73 (d, *J* = 7.3 Hz, 1H, ArH), 6.28 (s, 1H, CCHC), 6.12 (dd, *J* = 17.1, 2.0 Hz, 1H, CCH₂), 5.77 (s, 2H, CH₂), 5.70 – 5.59 (m, 1H, CCH₂); **¹³C NMR (101 MHz, DMSO-d₆)** δ 163.5 (HNCO), 149.3 (ArC), 147.1 (ArC), 135.2 (NCCH), 135.0 (ArC), 135.0 (ArC), 133.9 (ArC), 131.2 (CCCH₂), 130.7 (CCHN), 130.5 (ArC), 128.7 (ArC), 128.5 (ArC), 128.3 (ArC), 127.5 (ArC), 127.4 (ArC), 126.8 (CCH₂), 126.8 (ArC), 126.0 (ArC), 125.7 (ArC), 119.96 (ArC), 48.83 (CH₂); **HRMS-TOF MS ES+**: *m/z* [M+H]⁺ calcd for C₂₁H₁₈N₅O: 356.1511; found: 356.1510

***N*-{3-[[5-(quinolin-3-yl)-1*H*-1,2,3-triazol-1-yl]methyl]phenyl}acrylamide - 8b**



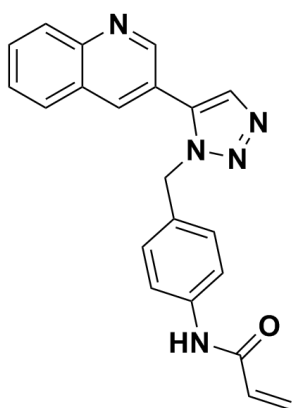
Scale: 3-(1-(3-nitrobenzyl)-1*H*-1,2,3-triazol-5-yl)quinoline (200 mg, 0.604 mmol)

This compound was synthesized following the general procedure for reduction of aromatic nitro and acylation with acryloyl chloride. The compound was purified by silica gel column chromatography, eluted first with EtOAc and hexane (EtOAc:Hexane, 90:10) and then EtOAc. This afforded the pure product as a white foam (132 mg, 0.37 mmol, 62%)

R_f = 0.44 (EtOAc:Hexane, 90:10); **Mp** 122-124 °C; **IR (ATR, cm⁻¹)**: 3259 (m, stretch, N–H), 1667 (s, stretch, –C=C–), 1202 (s, stretch, C–N), 747 (s, oop, C–H); **¹H NMR (400 MHz, DMSO-d₆)** δ 10.12 (s, 1H, NH), 8.95 (d, *J* = 2.2 Hz, 1H, ArH), 8.51 (dd, *J* = 9.0, 1.9 Hz, 1H, ArH), 8.21 (d, *J* = 8.7 Hz, 1H, CCHN), 8.05 (d, *J* = 8.5 Hz, 1H, ArH), 7.97 (t, *J* = 7.2 Hz, 1H, ArH), 7.90 – 7.79 (m, 1H, ArH), 7.68 (t, *J* = 7.4 Hz, 1H, ArH), 7.55 (d, *J* = 8.3 Hz, 1H, ArH), 7.39 (s, 1H, ArH), 7.21 (t, *J* = 7.9 Hz, 1H, ArH), 6.94 – 6.72 (m, 1H, CCHC), 6.46 – 6.30 (m,

1H, CCH₂), 6.29 – 6.13 (m, 1H, CCH₂), 5.88 – 5.62 (m, 3H, CH₂); ¹³C NMR (101 MHz, DMSO-d₆) δ 163.1 (HNCO), 149.3 (ArC), 147.2 (ArC), 139.5 (NCCH), 136.5 (ArC), 135.6 (ArC), 134.8 (ArC), 134.2 (ArC), 131.7 (CCCH₂), 130.7 (CCHN), 129.2 (ArC), 128.8 (ArC), 128.5 (ArC), 127.6 (ArC), 127.0 (ArC), 126.8 (CCH₂), 122.0 (ArC), 120.0 (ArC), 118.7 (ArC), 117.5 (ArC), 51.5 (CH₂); HRMS-TOF MS ES+: *m/z* [M+H]⁺ calcd for C₂₁H₁₈N₅O: 356.1511; found: 356.1520

***N*-{4-[[5-(quinolin-3-yl)-1*H*-1,2,3-triazol-1-yl]methyl]phenyl}acrylamide - 8c**



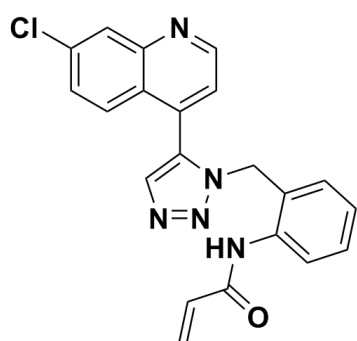
Scale: 3-(1-(4-nitrobenzyl)-1*H*-1,2,3-triazol-5-yl)quinoline (200 mg, 0.604 mmol)

This compound was synthesized following the general procedure for reduction of aromatic nitro and acylation with acryloyl chloride. The compound was purified by silica gel column chromatography, eluted first with EtOAc and hexane (EtOAc:Hexane, 90:10) and then EtOAc. This afforded the pure product as a white foam (134

mg, 0.38 mmol, 62%)

R_f = 0.43 (EtOAc:Hexane, 90:10); **Mp** 178-180 °C; **IR (ATR, cm⁻¹)**: 3239 (m, stretch, N–H), 1679 (s, stretch, –C=C–), 1254 (s, stretch, C–N), 790 (s, oop, C–H); **¹H NMR (400 MHz, DMSO-d₆) δ** 10.12 (s, 1H, NH), 8.95 (d, *J* = 2.2 Hz, 1H, ArH), 8.54 (d, *J* = 2.1 Hz, 1H, ArH), 8.19 (s, 1H, CCHN), 8.06 (d, *J* = 8.5 Hz, 1H, ArH), 8.00 (d, *J* = 8.1 Hz, 1H, ArH), 7.84 (t, *J* = 7.0 Hz, 1H, ArH), 7.69 (t, *J* = 7.5 Hz, 1H, ArH), 7.54 (d, *J* = 8.5 Hz, 2H, ArH), 7.01 (d, *J* = 8.5 Hz, 2H, ArH), 6.37 (dd, *J* = 17.0, 10.1 Hz, 1H, CCHC), 6.21 (dd, *J* = 17.0, 2.0 Hz, 1H, CCH₂), 5.79 (s, 2H, CH₂), 5.76 – 5.69 (m, 1H, CCH₂); **¹³C NMR (101 MHz, DMSO-d₆) δ** 163.1 (HNCO), 149.4 (ArC), 147.2 (ArC), 138.6 (NCCH), 135.6 (ArC), 134.7 (ArC), 134.2 (ArC), 131.7 (CCCH₂), 130.8 (ArC), 130.6 (CCHN), 128.8 (ArC), 128.5 (ArC), 127.7 (ArC), 127.6 (ArC), 127.0 (ArC), 126.8 (CCH₂), 120.1 (ArC), 119.4 (ArC), 51.3 (CH₂); **HRMS-TOF MS ES+**: *m/z* [M+H]⁺ calcd for C₂₁H₁₈N₅O: 356.1511; found: 356.1521

***N*-{2-[[5-(7-chloroquinolin-4-yl)-1*H*-1,2,3-triazol-1-yl]methyl]phenyl}acrylamide - 8d**

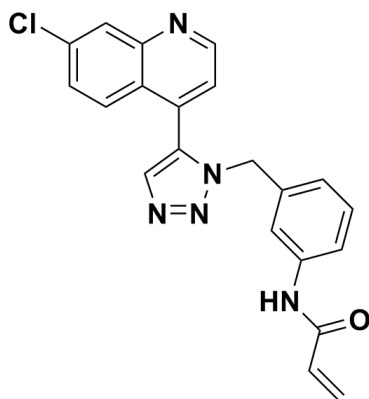


Scale: 7-chloro-4-(1-(2-nitrobenzyl)-1*H*-1,2,3-triazol-5-yl)quinoline (140 mg, 0.38 mmol)

This compound was synthesized following the general procedure for reduction of aromatic nitro and acylation with acryloyl chloride. The compound was purified by silica gel column chromatography, eluted first with EtOAc and hexane (EtOAc:Hexane, 90:10) and then EtOAc. This afforded the pure product as a white foam (90 mg, 0.23 mmol, 61%)

R_f = 0.41 (EtOAc:Hexane, 90:10); **Mp** 154-156 °C; **IR (ATR, cm⁻¹)**:3249 (m, stretch, N–H), 1665 (s, stretch, –C=C–), 1186 (s, stretch, C–N), 876 (s, oop, C–H); **¹H NMR (400 MHz, CDCl₃)** δ 9.09 (s, 1H, NH), 9.03 (d, *J* = 4.3 Hz, 1H, ArH), 8.25 (d, *J* = 1.9 Hz, 1H, ArH), 7.89 (t, *J* = 8.3 Hz, 1H, ArH), 7.85 (s, 1H, CCHN), 7.46 (dd, *J* = 8.9, 2.0 Hz, 1H, ArH), 7.28 – 7.25 (m, 3H, ArH), 6.79 (t, *J* = 7.4 Hz, 1H, ArH), 6.47 (t, *J* = 3.7 Hz, 1H, ArH), 6.46 – 6.40 (m, 1H, CCHC), 6.31 (d, *J* = 7.4 Hz, 1H, CCH₂), 5.85 (d, *J* = 10.8 Hz, 1H, CCH₂), 5.30 (s, 2H, CH₂); **¹³C NMR (101 MHz, CDCl₃)** δ 164.3 (HNCO), 150.9 (ArC), 148.9 (ArC), 137.0 (NCCH), 136.9 (ArC), 135.1 (ArC), 133.5 (ArC), 133.2 (ArC), 131.4 (CCCH₂), 130.4 (CCHN), 130.2 (ArC), 129.4 (ArC), 129.3 (ArC), 128.2 (ArC), 125.9 (CCH₂), 125.1 (ArC), 124.94 (ArC), 123.05 (ArC), 50.1 (CH₂); **HRMS-TOF MS ES⁺: *m/z* [M+H]⁺** calcd for C₂₁H₁₇ClN₅O: 390.1122; found: 390.1120

***N*-{3-[[5-(7-chloroquinolin-4-yl)-1*H*-1,2,3-triazol-1-yl]methyl]phenyl}acrylamide - 8e**



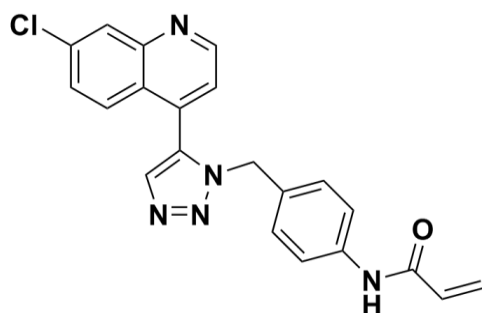
Scale: 7-chloro-4-(1-(3-nitrobenzyl)-1*H*-1,2,3-triazol-5-yl)quinoline (190 mg, 0.52 mmol)

This compound was synthesized following the general procedure for reduction of aromatic nitro and acylation with acryloyl chloride. The compound was purified by silica gel column chromatography, eluted first with EtOAc and hexane (EtOAc:Hexane, 90:10) and then EtOAc. This afforded the pure product as a white foam (113 mg, 0.29 mmol, 56%)

R_f = 0.41 (EtOAc:Hexane, 90:10); **Mp** 128-131 °C; **IR (ATR, cm⁻¹)**:3271 (m, stretch, N–H), 2920 (m, stretch, CH₂), 1668 (s, stretch, –C=C–), 1169 (s, stretch, C–N), 877 (s, oop, C–H); **¹H NMR (400 MHz, CDCl₃)** δ 8.94 (s, 1H, NH), 8.16 (s, 1H, ArH), 7.88 (d, *J* = 24.5 Hz, 1H, CCHN), 7.65 (s, 1H, ArH), 7.48 – 7.36 (m, 2H, ArH), 7.35 – 7.27 (m, 1H, ArH), 7.18 (d, *J* = 4.3 Hz, 1H, ArH), 7.15 – 6.99 (m, 2H, ArH), 6.56 (t, *J* = 7.9 Hz, 1H, ArH), 6.45 – 6.35 (m, 1H, CCHC), 6.29 – 6.15 (m, 1H, CCH₂), 5.75 (d, *J* = 10.3 Hz, 1H, CCH₂), 5.40 (d, *J* = 20.4 Hz, 2H, CH₂); **¹³C NMR (101 MHz, CDCl₃)** δ 163.6 (HNCO), 150.8 (ArC), 149.6

(ArC), 148.8 (ArC), 138.6 (NCCH), 136.5 (ArC), 135.3 (ArC), 135.1 (ArC), 133.6 (CCCH₂), 131.0 (CCHN), 129.6 (ArC), 129.1 (ArC), 129.0 (ArC), 128.3 (ArC), 126.0 (CCH₂), 125.1 (ArC), 123.4 (ArC), 122.9 (ArC), 120.0 (ArC), 119.0 (ArC), 52.6 (CH₂); **HRMS-TOF MS ES+**: m/z [M+H]⁺ calcd for C₂₁H₁₇ClN₅O: 390.1122; found: 390.1118

***N*-{4-[[5-(7-chloroquinolin-4-yl)-1*H*-1,2,3-triazol-1-yl]methyl]phenyl}acrylamide - 8f**

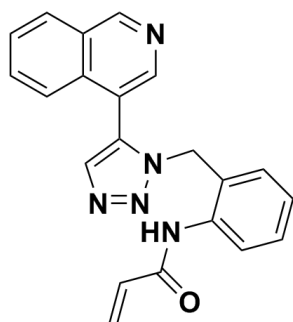


Scale: 7-chloro-4-(1-(4-nitrobenzyl)-1*H*-1,2,3-triazol-5-yl)quinoline (190 mg, 0.52 mmol)

This compound was synthesized following the general procedure for reduction of aromatic nitro and acylation with acryloyl chloride. The compound was purified by silica gel column chromatography, eluted first with EtOAc and hexane (EtOAc:Hexane, 90:10) and then EtOAc. This afforded the pure product as a white foam (116 mg, 0.30 mmol, 57%)

R_f = 0.4 (EtOAc:Hexane, 90:10); **Mp** 161-173 °C; **IR (ATR, cm⁻¹)**: 3287 (m, stretch, N-H), 2850 (m, stretch, CH₂), 1675 (s, stretch, -C=C-), 1242 (s, stretch, C-N), 877 (s, oop, C-H); **¹H NMR (400 MHz, CDCl₃)** δ 8.92 (s, 1H, NH), 8.19 (t, *J* = 6.1 Hz, 1H, ArH), 7.85 (s, 1H, CCHN), 7.47 (d, *J* = 8.5 Hz, 1H, ArH), 7.43 (dd, *J* = 8.9, 1.6 Hz, 1H, ArH), 7.36 (d, *J* = 8.0 Hz, 2H, ArH), 7.30 (d, *J* = 8.9 Hz, 1H, ArH), 7.12 (d, *J* = 4.2 Hz, 1H, ArH), 6.79 (d, *J* = 8.3 Hz, 2H, ArH), 6.42 (d, *J* = 16.8 Hz, 1H, CCHC), 6.24 (dd, *J* = 16.8, 10.2 Hz, 1H, CCH₂), 5.77 (d, *J* = 10.2 Hz, 1H, CCH₂), 5.36 (s, 2H, CH₂); **¹³C NMR (101 MHz, CDCl₃)** δ 163.6 (HNCO), 150.8 (ArC), 148.9 (ArC), 138.3 (NCCH), 136.5 (ArC), 135.2 (ArC), 133.7 (ArC), 133.0 (CCCH₂), 131.0 (CCHN), 130.2 (ArC), 129.2 (ArC), 129.1 (ArC), 128.57 (ArC), 128.42 (ArC), 126.0 (CCH₂), 125.1 (ArC), 122.7 (ArC), 120.1v, 52.4 (CH₂); **HRMS-TOF MS ES+**: m/z [M+H]⁺ calcd for C₂₁H₁₇ClN₅O: 390.1122; found: 390.1111

***N*-{2-[[5-(isoquinolin-4-yl)-1*H*-1,2,3-triazol-1-yl]methyl]phenyl}acrylamide - 8g**



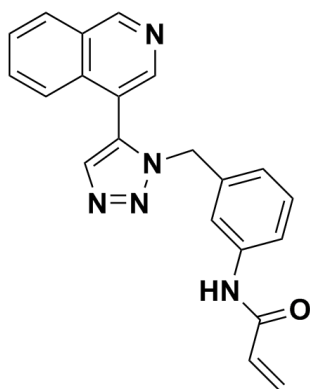
Scale: 4-(1-(2-nitrobenzyl)-1*H*-1,2,3-triazol-5-yl)isoquinoline (108 mg, 0.33 mmol)

This compound was synthesized following the general procedure for reduction of aromatic nitro and acylation with acryloyl chloride. The compound was purified by silica gel column chromatography, eluted

first with EtOAc and hexane (EtOAc:Hexane, 90:10) and then EtOAc. This afforded the pure product as a white foam (68 mg, 0.19 mmol, 59%)

R_f = 0.24 (EtOAc:Hexane, 90:10); **Mp** 189-191 °C; **IR (ATR, cm⁻¹)**: 3224 (m, stretch, N–H), 2919(m, stretch, CH₂), 1673 (s, stretch, –C=C–), 1205 (s, stretch, C–N), 749 (s, oop, C–H); **¹H NMR (400 MHz, CDCl₃)** δ 9.43 (s, 1H, NH), 8.41 (s, 1H, ArH), 8.13 (d, *J* = 7.9 Hz, 1H, ArH), 7.92 (d, *J* = 7.8 Hz, 1H, ArH), 7.84 (s, 1H, CCHN), 7.76 – 7.63 (m, 2H, ArH), 7.28 (d, *J* = 8.3 Hz, 1H, ArH), 7.22 (d, *J* = 7.2 Hz, 1H, ArH), 6.76 (t, *J* = 7.4 Hz, 1H, CCHC), 6.55 – 6.44 (m, 2H, ArH), 6.34 (d, *J* = 7.4 Hz, 1H, CCH₂), 5.84 (dd, *J* = 8.9, 2.3 Hz, 1H, CCH₂), 5.28 (s, 2H, CH₂); **¹³C NMR (101 MHz, CDCl₃)** δ 164.3 (HNCO), 155.0 (ArC), 144.5 (ArC), 137.1 (NCCH), 135.5 (ArC), 134.6 (ArC), 133.4 (ArC), 132.2 (ArC), 131.6 (CCCH₂), 130.4 (CCHN), 130.2 (ArC), 128.5 (ArC), 128.4 (ArC), 127.9 (ArC), 125.3 (CCH₂), 124.9 (ArC), 124.8 (ArC), 123.6 (ArC), 118.2 (ArC), 49.7 (CH₂); **HRMS-TOF MS ES⁺: *m/z* [M+H]⁺** calcd for C₂₁H₁₈N₅O: 356.1511; found: 356.1515

***N*-{3-[[5-(isoquinolin-4-yl)-1*H*-1,2,3-triazol-1-yl]methyl]phenyl}acrylamide - 8h**



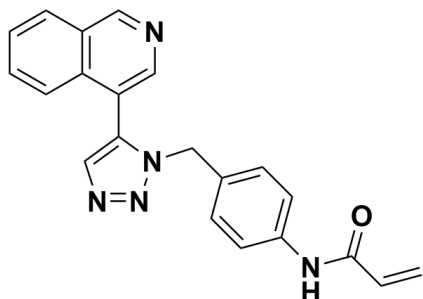
Scale: 4-(1-(3-nitrobenzyl)-1*H*-1,2,3-triazol-5-yl)isoquinoline (131 mg, 0.4 mmol)

This compound was synthesized following the general procedure for reduction of aromatic nitro and acylation with acryloyl chloride. The compound was purified by silica gel column chromatography, eluted first with EtOAc and hexane (EtOAc:Hexane, 90:10) and then EtOAc. This afforded the pure product as a white foam (91 mg, 0.26 mmol, 64%)

R_f = 0.24 (EtOAc:Hexane, 90:10); **Mp** 126-128 °C; **IR (ATR, cm⁻¹)**: 3266 (m, stretch, N–H), 1667 (s, stretch, –C=C–), 1207 (s, stretch, C–N), 747 (s, oop, C–H); **¹H NMR (400 MHz, CDCl₃)** δ 9.32 (s, 1H, NH), 8.29 (d, *J* = 5.0 Hz, 1H, ArH), 8.08 – 8.02 (m, 2H, ArH), 7.85 (s, 1H, CCHN), 7.68 – 7.59 (m, 2H, ArH), 7.54 (d, *J* = 8.0 Hz, 1H, ArH), 7.35 – 7.30 (m, 1H, ArH), 7.10 (s, 1H, ArH), 7.02 (t, *J* = 7.9 Hz, 1H, ArH), 6.52 (d, *J* = 7.7 Hz, 1H, ArH), 6.38 (dd, *J* = 16.9, 1.4 Hz, 1H, CCHC), 6.24 (dd, *J* = 16.9, 10.1 Hz, 1H, CCH₂), 5.72 (dd, *J* = 10.1, 1.4 Hz, 1H, CCH₂), 5.37 (s, 2H, CH₂); **¹³C NMR (101 MHz, CDCl₃)** δ 163.7 (HNCO), 154.6 (ArC), 144.2 (ArC), 138.7 (NCCH), 135.5 (ArC), 135.4 (ArC), 134.6 (ArC), 133.1 (ArC), 131.9 (CCCH₂), 131.2 (CCHN), 129.5 (ArC), 128.3 (ArC), 128.3 (ArC), 128.0 (ArC), 123.7

(CCH₂), 123.4 (ArC), 120.0 (ArC), 119.0 (ArC), 118.7 (ArC), 52.4 (CH₂); **HRMS-TOF MS ES+**: *m/z* [M+H]⁺ calcd for C₂₁H₁₈N₅O: 356.1511; found: 356.1511

***N*-{4-[[5-(isoquinolin-4-yl)-1*H*-1,2,3-triazol-1-yl]methyl]phenyl}acrylamide - 8i**

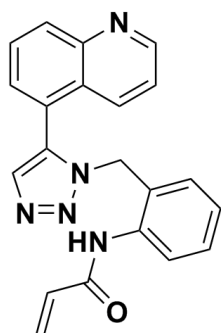


Scale: 4-(1-(4-nitrobenzyl)-1*H*-1,2,3-triazol-5-yl)isoquinoline (155 mg, 0.47 mmol)

This compound was synthesized following the general procedure for reduction of aromatic nitro and acylation with acryloyl chloride. The compound was purified by silica gel column chromatography, eluted first with EtOAc and hexane (EtOAc:Hexane, 90:10) and then EtOAc. This afforded the pure product as a white foam (95 mg, 0.27 mmol, 57%)

R_f = 0.26 (EtOAc:Hexane, 90:10); **Mp** 179-181 °C; **IR (ATR, cm⁻¹)**: 3224 (m, stretch, N–H), 2960(m, stretch, CH₂), 1681 (s, stretch, –C=C–), 1250 (s, stretch, C–N), 752 (s, oop, C–H); **¹H NMR (400 MHz, CDCl₃) δ** 9.36 (s, 1H, NH), 8.25 (s, 1H, ArH), 8.09 (dd, *J* = 17.8, 11.4 Hz, 2H, ArH), 7.86 (s, 1H, CCHN), 7.74 – 7.63 (m, 2H, ArH), 7.36 (d, *J* = 6.8 Hz, 3H, ArH), 6.76 (t, *J* = 13.9 Hz, 2H, ArH), 6.47 – 6.21 (m, 2H, CCHC, CCH₂), 5.73 (d, *J* = 10.1 Hz, 1H, CCH₂), 5.42 – 5.28 (m, 2H, CH₂); **¹³C NMR (101 MHz, CDCl₃) δ** 163.7 (HNCO), 154.6 (ArC), 144.17 (ArC), 138.3 (NCCH), 135.5 (ArC), 134.6 (ArC), 132.9 (ArC), 132.0 (CCCH₂), 131.2 (CCHN), 130.3 (ArC), 128.6 (ArC), 128.4 (ArC), 128.3 (ArC), 128.2 (ArC), 128.1 (ArC), 123.7 (CCH₂), 120.1 (ArC), 118.7 (ArC), 52.2 (CH₂); **HRMS-TOF MS ES+**: *m/z* [M+H]⁺ calcd for C₂₁H₁₈N₅O: 356.1511; found: 356.1516

***N*-{2-[[5-(quinolin-5-yl)-1*H*-1,2,3-triazol-1-yl]methyl]phenyl}acrylamide - 8j**

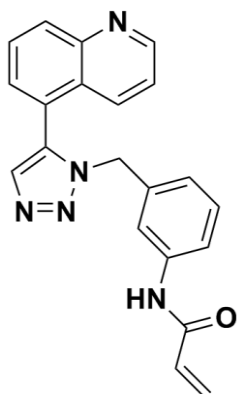


Scale: 5-(1-(2-nitrobenzyl)-1*H*-1,2,3-triazol-5-yl)isoquinoline (140 mg, 0.42mmol)

This compound was synthesized following the general procedure for reduction of aromatic nitro and acylation with acryloyl chloride. The compound was purified by silica gel column chromatography, eluted with EtOAc and MeOH (EtOAc:MeOH, 95:5). This afforded the pure product as a white foam (91 mg, 0.26 mmol, 61%)

R_f = 0.38 (EtOAc:MeOH, 95:5) ; **Mp** 193-195 °C; **IR (ATR, cm⁻¹)**: 3222 (m, stretch, N–H), 1673 (s, stretch, –C=C–), 1245 (s, stretch, C–N), 827 (s, oop, C–H); **¹H NMR (400 MHz, CDCl₃) δ** 9.39 (s, 2H, NH), 8.49 (s, 1H, ArH), 8.19 (dd, *J* = 22.3, 7.6 Hz, 1H, ArH), 7.97 (d, *J* = 7.6 Hz, 1H, ArH), 7.83 (s, 1H, CCHN), 7.75 (t, *J* = 7.6 Hz, 1H, ArH), 7.66 – 7.57 (m, 1H, ArH), 7.26 (t, *J* = 7.7 Hz, 1H, ArH), 7.08 (d, *J* = 5.6 Hz, 1H, ArH), 6.75 (t, *J* = 7.3 Hz, 1H, CCHC), 6.49 (q, *J* = 17.2 Hz, 2H, ArH), 6.23 (d, *J* = 7.2 Hz, 1H, CCH₂), 5.84 (t, *J* = 12.6 Hz, 1H, CCH₂), 5.28 (d, *J* = 12.7 Hz, 2H, CH₂); **¹³C NMR (101 MHz, CDCl₃) δ** 164.3 (HNCO), 153.2 (ArC), 144.7 (ArC), 137.3 (NCCH), 135.1 (ArC), 134.9 (ArC), 134.9 (ArC), 133.4 (ArC), 131.65 (CCCH₂), 130.6 (CCHN), 130.3 (ArC), 130.3 (ArC), 128.0 (ArC), 126.8 (CCH₂), 125.1 (ArC), 124.8 (ArC), 123.1 (ArC), 117.3 (ArC), 49.7 (CH₂); **HRMS-TOF MS ES+**: *m/z* [M+H]⁺ calcd for C₂₁H₁₈N₅O: 356.1511; found: 356.1515

***N*-{2-[[5-(quinolin-5-yl)-1*H*-1,2,3-triazol-1-yl]methyl]phenyl}acrylamide - 8k**

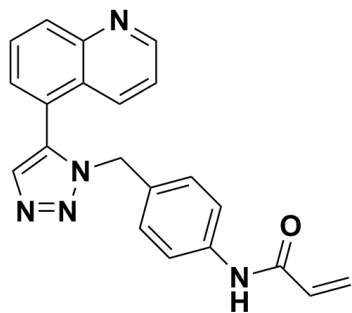


Scale: 5-(1-(3-nitrobenzyl)-1*H*-1,2,3-triazol-5-yl)isoquinoline (150 mg, 0.45 mmol)

This compound was synthesized following the general procedure for reduction of aromatic nitro and acylation with acryloyl chloride. The compound was purified by silica gel column chromatography, eluted with EtOAc and MeOH (EtOAc:MeOH, 95:5). This afforded the pure product as a white foam (93 mg, 0.26 mmol, 58%)

R_f = 0.37 (EtOAc:MeOH, 95:5); **Mp** 134-136 °C; **IR (ATR, cm⁻¹)**: 3262 (m, stretch, N–H), 2960 (m, stretch, CH₂), 1611 (s, stretch, –C=C–), 1257 (s, stretch, C–N), 792 (s, oop, C–H); **¹H NMR (400 MHz, CDCl₃) δ** 9.30 (s, 1H, NH), 8.40 (s, 1H, ArH), 8.10 (d, *J* = 8.3 Hz, 1H), 7.83 (s, 1H, CCHN), 7.65 (t, *J* = 7.7 Hz, 1H, ArH), 7.57 – 7.47 (m, 2H, ArH), 7.36 (d, *J* = 8.0 Hz, 1H, ArH), 7.14 – 7.02 (m, 3H, ArH), 6.58 (d, *J* = 7.8 Hz, 1H, ArH), 6.40 (d, *J* = 16.9 Hz, 1H, CCHC), 6.21 (dd, *J* = 16.8, 10.2 Hz, 1H, CCH₂), 5.76 (d, *J* = 10.2 Hz, 1H, CCH₂), 5.34 (s, 2H, CH₂); **¹³C NMR (101 MHz, CDCl₃) δ** 163.5 (HNCO), 152.9 (ArC), 144.1 (ArC), 138.4 (NCCH), 135.6 (ArC), 135.1 (ArC), 134.9 (ArC), 134.5 (ArC), 133.2 (ArC), 131.1 (CCCH₂), 130.1 (CCHN), 129.5 (ArC), 128.6 (ArC), 128.2 (ArC), 126.9 (CCH₂), 123.7 (ArC), 123.6 (ArC), 119.8 (ArC), 119.2 (ArC), 117.4 (ArC), 52.4 (CH₂); **HRMS-TOF MS ES+**: *m/z* [M+H]⁺ calcd for C₂₁H₁₈N₅O: 356.1511; found: 356.1512

***N*-{2-[[5-(quinolin-5-yl)-1*H*-1,2,3-triazol-1-yl]methyl]phenyl}acrylamide - 8l**



Scale: 5-(1-(4-nitrobenzyl)-1H-1,2,3-triazol-5-yl)isoquinoline
(140 mg, 0.42 mmol)

This compound was synthesized following the general procedure for reduction of aromatic nitro and acylation with acryloyl chloride. The compound was purified by silica gel column chromatography, eluted with EtOAc and MeOH (EtOAc:MeOH, 95:5). This afforded the pure product as a white foam (99 mg, 0.28 mmol, 66%)

R_f = 0.36 (EtOAc:MeOH, 95:5); **Mp** 196-198 °C; **IR (ATR, cm^{-1})**: 3274 (m, stretch, N–H), 2960 (m, stretch, CH_2), 1664 (s, stretch, $\text{C}=\text{C}$), 1256 (s, stretch, C–N), 760 (s, oop, C–H); **^1H NMR (400 MHz, CDCl_3) δ** 9.33 (s, 1H, NH), 8.45 (d, J = 5.8 Hz, 1H, ArH), 8.12 (d, J = 8.3 Hz, 1H, ArH), 7.82 (s, 1H, CCHN), 7.65 (dd, J = 18.5, 11.2 Hz, 1H, ArH), 7.51 (s, 1H, ArH), 7.46 (d, J = 6.6 Hz, 1H, ArH), 7.34 (d, J = 8.1 Hz, 2H, ArH), 7.13 (d, J = 5.9 Hz, 1H, ArH), 6.78 (d, J = 8.4 Hz, 2H, ArH), 6.42 (d, J = 16.8 Hz, 1H, CCHC), 6.30 – 6.17 (m, 1H, CCH_2), 5.84 – 5.71 (m, 1H, CCH_2), 5.32 (s, 2H, CH_2); **^{13}C NMR (101 MHz, CDCl_3) δ** 153.1 (HNCO), 144.5 (ArC), 138.1 (NCCH), 135.1 (ArC), 134.8 (ArC), 134.4 (ArC), 133.0 (ArC), 131.1 (CCCH_2), 130.6 (CCHN), 130.1 (ArC), 128.6 (ArC), 128.3 (ArC), 126.7 (CCH_2), 123.7 (ArC), 120.0 (ArC), 117.4 (ArC), 52.1 (CH_2); **HRMS-TOF MS ES⁺: m/z [$\text{M}+\text{H}$]⁺** calcd for $\text{C}_{21}\text{H}_{18}\text{N}_5\text{O}$: 356.1511; found: 356.151

CHAPTER 8 – REFERENCES

References for Chapters 1-7 follow. Figures, diagrams and schemes taken directly from the source are referenced accordingly in the title of the corresponding figure, diagram or scheme.

1. Cancer Mortality and Morbidity *Situation and Trends* [Online], 2013. http://www.who.int/gho/ncd/mortality_morbidity/cancer_text/en/ (accessed 14/01).
2. Parkin, D. M.; Bray, F.; Ferlay, J.; Pisani, P., Global cancer statistics, 2002. *Ca-A Cancer Journal for Clinicians* **2005**,55 (2), 74-108.
3. Global Cancer Facts & Figures 2nd Edition. American Cancer Society: Atlanta, 2011.
4. Parkin, D. M.; Pisani, P.; Ferlay, J., Global Cancer Statistics. *Ca-A Cancer Journal for Clinicians* **1999**,49 (1), 33-64.
5. World Cancer Factsheet. International Agency for Research on Cancer and Cancer Research UK: London, 2012.
6. Ferlay, J., Soerjomataram, I., Ervik, M., Dikshit, R., Eser, S., Mathers, C., Rebelo, M., Parkin, D. M., Forman, D., Bray, F. GLOBOCAN 2012 v1.0, Cancer Incidence and Mortality Worldwide 2013. <http://globocan.iarc.fr> (accessed 14/01/14).
7. Bray, F.; Ren, J. S.; Masuyer, E.; Ferlay, J., Global estimates of cancer prevalence for 27 sites in the adult population in 2008. *International Journal of Cancer* **2013**,132 (5), 1133-1145.
8. Ferlay, J.; Shin, H. R.; Bray, F.; Forman, D.; Mathers, C. D.; Parkin, D. GLOBOCAN 2008, Cancer Incidence and Mortality Worldwide 2010. <http://globocan.iarc.fr> (accessed 14/01/14).
9. Jemal, A.; Bray, F.; Forman, D.; O'Brien, M.; Ferlay, J.; Center, M.; Parkin, D. M., Cancer burden in Africa and opportunities for prevention. *Cancer* **2012**,118 (18), 4372-4384.
10. Cancer Fact sheet N°297 2013. <http://www.who.int/mediacentre/factsheets/fs297/en/> (accessed 15/01/14).
11. Dangoor, N. E. How many different types of cancer are there? 2013. <http://www.cancerresearchuk.org/cancer-help/about-cancer/cancer-questions/how-many-different-types-of-cancer-are-there> (accessed 15/01/14).
12. Hajdu, S. I., A note from history: Landmarks in history of cancer, part 1. *Cancer* **2011**,117 (5), 1097-1102.
13. The History of Cancer 2012. <http://www.cancer.org/cancer/cancerbasics/thehistoryofcancer/> (accessed 15/01/14).
14. Hajdu, S. I., A note from history: Landmarks in history of cancer, part 3. *Cancer* **2012**,118 (4), 1155-1168.

15. Robinson, D. H.; Toledo, A. H., Historical development of modern anesthesia. *Journal of Investigative Surgery* **2012**,*25* (3), 141-149.
16. Miller, J. T.; Rahimi, S. Y.; Lee, M., History of infection control and its contributions to the development and success of brain tumor operations. *Neurosurgical focus* **2005**,*18* (4), 1-5.
17. Young, R. E., The history of breast cancer surgery: Halsted's radical mastectomy and beyond. *Australian Medical Student Journal* **2013**,*4* (1), 53-55.
18. Hajdu, S. I., A note from history: Landmarks in history of cancer, part 4. *Cancer* **2012**,*118* (20), 4914-4928.
19. DeVita Jr, V. T.; Rosenberg, S. A., Two hundred years of cancer research. *New England Journal of Medicine* **2012**,*366* (23), 2207-2214.
20. Hajdu, S. I.; Darvishian, F., A note from history: Landmarks in history of cancer, part 5. *Cancer* **2013**,*119* (8), 1450-1466.
21. Rous, P., A transmissible avian neoplasm. (Sarcoma of the common fowl). *Journal of Experimental Medicine* **1979**,*150* (4), 738-753.
22. Boveri, T., Concerning the origin of malignant tumours by Theodor Boveri. Translated and annotated by Henry Harris. *Journal of Cell Science* **2008**,*121* (SUPPL. 1), 1-84.
23. Wagener, D. J. T., The History of Oncology. Springer Uitgeverij: Netherlands, 2009; pp. 19, 25.
24. Olson, J. S., Bathsheba's breast: women, cancer & history. The Johns Hopkins University Press: Baltimore, 2002; pp. 32-33.
25. Hajdu, S. I., A note from history: Landmarks in history of cancer, part 2. *Cancer* **2011**,*117* (12), 2811-2820.
26. Fenster, J. M. Hazardous to Your Health: The Surgeon General Makes His Case *American Heritage* [Online], 2006, p. 62-64.
27. Gordon, R., The Alarming History of Medicine. St Martin's Press: New York, 1993.
28. Hajdu, S. I.; Vadmal, M., A note from history: Landmarks in history of cancer, Part 6. *Cancer* **2013**,*119* (23), 4058-4082.
29. Nordling, C. O., A New Theory on the Cancer-inducing Mechanism. *British Journal of Cancer* **1953**,*7* (1), 68-72.
30. Knudson Jr, A. G., Mutation and cancer: statistical study of retinoblastoma. *Proceedings of the National Academy of Sciences of the United States of America* **1971**,*68* (4), 820-823.

31. Huebner, R. J.; Todaro, G. J., Oncogenes of RNA tumor viruses as determinants of cancer. *Proceedings of the National Academy of Sciences of the United States of America* **1969**,*64* (3), 1087-1094.
32. Martin, G. S., The hunting of the Src. *Nature Reviews Molecular Cell Biology* **2001**,*2* (6), 467-474.
33. Todd, R.; Wong, D. T. W., Oncogenes. *Anticancer Research* **1999**,*19* (6 A), 4729-4746.
34. Barillot, E.; Calzone, L.; Hupe, P.; Vert, J.-P.; Zinovyev., A., *Computational Systems Biology of Cancer*. Chapman & Hall/CRC Mathematical & Computational Biology: 2012.
35. Croce, C. M., Oncogenes and cancer. *New England Journal of Medicine* **2008**,*358* (5), 502-511.
36. Sabin, A. B., Suppression of malignancy in human cancer cells: issues and challenges. *Proceedings of the National Academy of Sciences of the United States of America* **1981**,*78* (11), 7129-7133.
37. Sherr, C. J., Principles of Tumor Suppression. *Cell* **2004**,*116* (2), 235-246.
38. Hanahan, D.; Weinberg, R. A., Hallmarks of cancer: The next generation. *Cell* **2011**,*144* (5), 646-674.
39. Anand, P.; Kunnumakkara, A. B.; Sundaram, C.; Harikumar, K. B.; Tharakan, S. T.; Lai, O. S.; Sung, B.; Aggarwal, B. B., Cancer is a preventable disease that requires major lifestyle changes. *Pharmaceutical research* **2008**,*25* (9), 2097-2116.
40. Ribatti, D.; Mangialardi, G.; Vacca, A., Stephen Paget and the 'seed and soil' theory of metastatic dissemination. *Clinical and Experimental Medicine* **2006**,*6* (4), 145-149.
41. Stockwell, S., Classics in oncology. George Thomas Beatson, M.D. (1848-1933). *Ca-A Cancer Journal for Clinicians* **1983**,*33* (2), 105-121.
42. Classics in oncology. Charles Brenton Huggins. *Ca-A Cancer Journal for Clinicians* **1972**,*22* (4), 230-231.
43. Thomsen, V., Wilhelm Conrad Röntgen and the discovery of X-rays. *Spectroscopy (Santa Monica)* **2008**,*23* (7), 31-34.
44. Pioneer in x-ray therapy. *Science* **1957**,*125* (3236), 18.
45. Thwaites, D. I.; Tuohy, J. B., Back to the future: The history and development of the clinical linear accelerator. *Physics in Medicine and Biology* **2006**,*51* (13), R343-R362.
46. Ginzton, E. L.; Nunan, C. S., History of microwave electron linear accelerators for radiotherapy. *International Journal of Radiation Oncology Biology Physics* **1985**,*11* (2), 205-216.
47. Johnston, T. A cannon for oncologists *Stanford Alumni* [Online], 2011. https://alumni.stanford.edu/get/page/magazine/article/?article_id=28139 (accessed 20/01/15).

48. Kaufmann, S. H. E., Immunology's foundation: The 100-year anniversary of the Nobel Prize to Paul Ehrlich and Elie Metchnikoff. *Nature Immunology* **2008**,9 (7), 705-712.
49. Chabner, B. A.; Roberts Jr, T. G., Chemotherapy and the war on cancer. *Nature Reviews Cancer* **2005**,5 (1), 65-72.
50. DeVita Jr, V. T.; Chu, E., A history of cancer chemotherapy. *Cancer Research* **2008**,68 (21), 8643-8653.
51. Torchilin, V. P., Recent advances with liposomes as pharmaceutical carriers. *Nature Reviews Drug Discovery* **2005**,4 (2), 145-160.
52. Rabik, C. A.; Dolan, M. E., Molecular mechanisms of resistance and toxicity associated with platinating agents. *Cancer Treatment Reviews* **2007**,33 (1), 9-23.
53. Strebhardt, K.; Ullrich, A., Paul Ehrlich's magic bullet concept: 100 Years of progress. *Nature Reviews Cancer* **2008**,8 (6), 473-480.
54. Rosenberg, S. A.; Restifo, N. P.; Yang, J. C.; Morgan, R. A.; Dudley, M. E., Adoptive cell transfer: A clinical path to effective cancer immunotherapy. *Nature Reviews Cancer* **2008**,8 (4), 299-308.
55. Takayama, T.; Sekine, T.; Makuuchi, M.; Yamasaki, S.; Kosuge, T.; Yamamoto, J.; Shimada, K.; Sakamoto, M.; Hirohashi, S.; Ohashi, Y.; Kakizoe, T., Adoptive immunotherapy to lower postsurgical recurrence rates of hepatocellular carcinoma: A randomised trial. *Lancet* **2000**,356 (9232), 802-807.
56. Fujita, K.; Ikarashi, H.; Takakuwa, K.; Kodama, S.; Tokunaga, A.; Takahashi, T.; Tanaka, K., Prolonged disease-free period in patients with advanced epithelial ovarian cancer after adoptive transfer of tumor-infiltrating lymphocytes. *Clinical Cancer Research* **1995**,1 (5), 501-507.
57. Kimura, H.; Yamaguchi, Y., A phase III randomized study of interleukin-2 lymphokine-activated killer cell immunotherapy combined with chemotherapy or radiotherapy after curative or noncurative resection of primary lung carcinoma. *Cancer* **1997**,80 (1), 42-49.
58. Kantoff, P. W.; Higano, C. S.; Shore, N. D.; Berger, E. R.; Small, E. J.; Penson, D. F.; Redfern, C. H.; Ferrari, A. C.; Dreicer, R.; Sims, R. B.; Xu, Y.; Frohlich, M. W.; Schellhammer, P. F., Sipuleucel-T immunotherapy for castration-resistant prostate cancer. *New England Journal of Medicine* **2010**,363 (5), 411-422.
59. Pfisterer, P. H.; Wolber, G.; Efferth, T.; Rollinger, J. M.; Stuppner, H., Natural products in structure-assisted design of molecular cancer therapeutics. *Current Pharmaceutical Design* **2010**,16 (15), 1718-1741.
60. Siegel, R.; Ma, J.; Zou, Z.; Jemal, A., Cancer Statistics, 2014. *CA-A Cancer Journal for Clinicians* **2014**, 9-29.
61. Kidwai, M.; Venkataramanan, R.; Mohan, R.; Sapra, P., Cancer chemotherapy and heterocyclic compounds. *Current Medicinal Chemistry* **2002**,9 (12), 1209-1228.

62. Craig Venter, J.; Adams, M. D.; Myers, E. W.; Li, P. W.; Mural, R. J.; Sutton, G. G.; Smith, H. O.; Yandell, M.; Evans, C. A.; Holt, R. A.; Gocayne, J. D.; Amanatides, P.; Ballew, R. M.; Huson, D. H.; Wortman, J. R.; Zhang, Q.; Kodira, C. D.; Zheng, X. H.; Chen, L.; Skupski, M.; Subramanian, G.; Thomas, P. D.; Zhang, J.; Gabor Miklos, G. L.; Nelson, C.; Broder, S.; Clark, A. G.; Nadeau, J.; McKusick, V. A.; Zinder, N.; Levine, A. J.; Roberts, R. J.; Simon, M.; Slayman, C.; Hunkapiller, M.; Bolanos, R.; Delcher, A.; Dew, I.; Fasulo, D.; Flanigan, M.; Florea, L.; Halpern, A.; Hannenhalli, S.; Kravitz, S.; Levy, S.; Mobarry, C.; Reinert, K.; Remington, K.; Abu-Threideh, J.; Beasley, E.; Biddick, K.; Bonazzi, V.; Brandon, R.; Cargill, M.; Chandramouliswaran, I.; Charlab, R.; Chaturvedi, K.; Deng, Z.; di Francesco, V.; Dunn, P.; Eilbeck, K.; Evangelista, C.; Gabrielian, A. E.; Gan, W.; Ge, W.; Gong, F.; Gu, Z.; Guan, P.; Heiman, T. J.; Higgins, M. E.; Ji, R. R.; Ke, Z.; Ketchum, K. A.; Lai, Z.; Lei, Y.; Li, Z.; Li, J.; Liang, Y.; Lin, X.; Lu, F.; Merkulov, G. V.; Milshina, N.; Moore, H. M.; Naik, A. K.; Narayan, V. A.; Neelam, B.; Nusskern, D.; Rusch, D. B.; Salzberg, S.; Shao, W.; Shue, B.; Sun, J.; Yuan Wang, Z.; Wang, A.; Wang, X.; Wang, J.; Wei, M. H.; Wides, R.; Xiao, C.; Yan, C.; Yao, A.; Ye, J.; Zhan, M.; Zhang, W.; Zhang, H.; Zhao, Q.; Zheng, L.; Zhong, F.; Zhong, W.; Zhu, S. C.; Zhao, S.; Gilbert, D.; Baumhueter, S.; Spier, G.; Carter, C.; Cravchik, A.; Woodage, T.; Ali, F.; An, H.; Awe, A.; Baldwin, D.; Baden, H.; Barnstead, M.; Barrow, I.; Beeson, K.; Busam, D.; Carver, A.; Center, A.; Lai Cheng, M.; Curry, L.; Danaher, S.; Davenport, L.; Desilets, R.; Dietz, S.; Dodson, K.; Doup, L.; Ferriera, S.; Garg, N.; Gluecksmann, A.; Hart, B.; Haynes, J.; Haynes, C.; Heiner, C.; Hladun, S.; Hostin, D.; Houck, J.; Howland, T.; Ibegwam, C.; Johnson, J.; Kalush, F.; Kline, L.; Koduru, S.; Love, A.; Mann, F.; May, D.; McCawley, S.; McIntosh, T.; McMullen, I.; Moy, M.; Moy, L.; Murphy, B.; Nelson, K.; Pfannkoch, C.; Pratts, E.; Puri, V.; Qureshi, H.; Reardon, M.; Rodriguez, R.; Rogers, Y.-H.; Romblad, D.; Ruhfel, B.; Scott, R.; Sitter, C.; Smallwood, M.; Stewart, E.; Strong, R.; Suh, E.; Thomas, R.; Ni Tint, N.; Tse, S.; Vech, C.; Wang, G.; Wetter, J.; Williams, S.; Williams, M.; Windsor, S.; Winn-Deen, E.; Wolfe, K.; Zaveri, J.; Zaveri, K.; Abril, J. F.; Guigo, R.; Campbell, M. J.; Sjolander, K. V.; Karlak, B.; Kejariwal, A.; Mi, H.; Lazareva, B.; Hatton, T.; Narechania, A.; Diemer, K.; Muruganujan, A.; Guo, N.; Sato, S.; Bafna, V.; Istrail, S.; Lippert, R.; Schwartz, R.; Walenz, B.; Yooseph, S.; Allen, D.; Basu, A.; Baxendale, J.; Blick, L.; Caminha, M.; Carnes-Stine, J.; Caulk, P.; Chiang, Y. H.; Coyne, M.; Dahlke, C.; Deslattes Mays, A.; Dombroski, M.; Donnelly, M.; Ely, D.; Esparham, S.; Fosler, C.; Gire, H.; Glanowski, S.; Glasser, K.; Glodek, A.; Gorokhov, M.; Graham, K.; Gropman, B.; Harris, M.; Heil, J.; Henderson, S.; Hoover, J.; Jennings, D.; Jordan, C.; Jordan, J.; Kasha, J.; Kagan, L.; Kraft, C.; Levitsky, A.; Lewis, M.; Liu, X.; Lopez, J.; Ma, D.; Majoros, W.; McDaniel, J.; Murphy, S.; Newman, M.; Nguyen, T.; Nguyen, N.; Nodell, M.; Pan, S.; Peck, J.; Peterson, M.; Rowe, W.; Sanders, R.; Scott, J.; Simpson, M.; Smith, T.; Sprague, A.; Stockwell, T.; Turner, R.; Venter, E.; Wang, M.; Wen, M.; Wu, D.; Wu, M.; Xia, A.; Zandieh, A.; Zhu, X., The sequence of the human genome. *Science* **2001**,*291* (5507), 1304-1351.
63. Pierotti, M. A.; Negri, T.; Tamborini, E.; Perrone, F.; Pricl, S.; Pilotti, S., Targeted Therapies: The Rare Cancer Paradigm. *Molecular Oncology* **2010**,*4* (1), 19-37.
64. Cancer Drugs & Treatments Market - Data, Analysis and Forecasts to 2023 2013. <http://www.reportlinker.com/p01889380-summary/The-Cancer-Drugs-Treatments-Market-Data-Analysis-Forecasts-to-.html> (accessed 23/01/14).
65. Bolten, B. M.; Drapeau, M.; Grubert, N.; Pickering, L.; Vora, P.; Mack, G. S. Strategic Overview of the Targeted Cancer Therapies Marketplace 2010.

- <http://www.decisionresources.com/Products-and-Services/Report?r=spech60110> (accessed 23/01/14).
66. Aloe, L., Rita Levi-Montalcini: The discovery of nerve growth factor and modern neurobiology. *Trends in Cell Biology* **2004**,14 (7), 395-399.
67. Carpenter, G.; Cohen, S., Epidermal Growth Factor. *Annual Review of Biochemistry* **1979**,48, 193-216.
68. Signal transduction as a drug-discovery platform. *Nature biotechnology* **2000**,18 Suppl, IT37-39.
69. Abou-Jawde, R.; Choueiri, T.; Alemany, C.; Mekhail, T., An overview of targeted treatments in cancer. *Clinical Therapeutics* **2003**,25 (8), 2121-2137.
70. Jordan, V. C., Tamoxifen: Catalyst for the change to targeted therapy. *European Journal of Cancer* **2008**,44 (1), 30-38.
71. Jordan, V. C., Tamoxifen: A most unlikely pioneering medicine. *Nature Reviews Drug Discovery* **2003**,2 (3), 205-213.
72. Cole, M. P.; Jones, C. T.; Todd, I. D., A new anti-oestrogenic agent in late breast cancer. An early clinical appraisal of ICI46474. *British Journal of Cancer* **1971**,25 (2), 270-275.
73. Wang, D. Y.; Fulthorpe, R.; Liss, S. N.; Edwards, E. A., Identification of Estrogen-Responsive Genes by Complementary Deoxyribonucleic Acid Microarray and Characterization of a Novel Early Estrogen-Induced Gene: EEIG1. *Molecular Endocrinology* **2004**,18 (2), 402-411.
74. Bange, J.; Zwick, E.; Ullrich, A., Molecular targets for breast cancer therapy and prevention. *Nature Medicine* **2001**,7 (5), 548-552.
75. Hudis, C. A., Trastuzumab - Mechanism of action and use in clinical practice. *New England Journal of Medicine* **2007**,357 (1), 39-51.
76. Lemonick, M. D.; Park, A. New Hope for Cancer *Time Magazine US Edition* [Online], 2001. <http://content.time.com/time/magazine/article/0,9171,999978,00.html> (accessed 24/01/14).
77. Goldman, J. M.; Melo, J. V., Mechanisms of disease: Chronic myeloid leukemia - Advances in biology and new approaches to treatment. *New England Journal of Medicine* **2003**,349 (15), 1451-1464.
78. Capdeville, R.; Buchdunger, E.; Zimmermann, J.; Matter, A., Glivec (ST1571, imatinib), a rationally developed, targeted anticancer drug. *Nature Reviews Drug Discovery* **2002**,1 (7), 493-502.
79. Druker, B. J.; Guilhot, F.; O'Brien, S. G.; Gathmann, I.; Kantarjian, H.; Gattermann, N.; Deininger, M. W. N.; Silver, R. T.; Goldman, J. M.; Stone, R. M.; Cervantes, F.; Hochhaus, A.; Powell, B. L.; Gabilove, J. L.; Rousselot, P.; Reiffers, J.; Cornelissen, J. J.; Hughes, T.; Agis, H.; Fischer, T.; Verhoef, G.; Shepherd, J.; Saglio, G.; Gratwohl, A.;

Nielsen, J. L.; Radich, J. P.; Simonsson, B.; Taylor, K.; Baccarani, M.; So, C.; Letvak, L.; Larson, R. A., Five-year follow-up of patients receiving imatinib for chronic myeloid leukemia. *New England Journal of Medicine* **2006**,355 (23), 2408-2417.

80. Folkman, J., Tumor angiogenesis: therapeutic implications. *New England Journal of Medicine* **1971**,285 (21), 1182-1186.

81. Ribatti, D., Judah Folkman, a pioneer in the study of angiogenesis. *Angiogenesis* **2008**,11 (1), 3-10.

82. Zetter, B. R., The scientific contributions of M. Judah Folkman to cancer research. *Nature Reviews Cancer* **2008**,8 (8), 647-654.

83. Folkman, J., Angiogenesis. *Annual Review of Medicine* **2006**,57, 1-18.

84. Weinstein, I. B., Cancer: Addiction to oncogenes - The Achilles heel of cancer. *Science* **2002**,297 (5578), 63-64.

85. Fernandez, A.; Udagawa, T.; Schwesinger, C.; Beecken, W. D.; Achilles-Gerte, E.; McDonnell, T. J.; D'Amato, R. J., Angiogenic potential of prostate carcinoma cells overexpressing bcl-2. *Journal of the National Cancer Institute* **2001**,93 (3), 208-213.

86. Ferrara, N.; Henzel, W. J., Pituitary follicular cells secrete a novel heparin-binding growth factor specific for vascular endothelial cells. *Biochemical and Biophysical Research Communications* **1989**,161 (2), 851-858.

87. Ferrara, N.; Hillan, K. J.; Gerber, H. P.; Novotny, W., Discovery and development of bevacizumab, an anti-VEGF antibody for treating cancer. *Nature Reviews Drug Discovery* **2004**,3 (5), 391-400.

88. Kerbel, R.; Folkman, J., Clinical translation of angiogenesis inhibitors. *Nature Reviews Cancer* **2002**,2 (10), 727-739.

89. Cao, Y.; Langer, R., A review of Judah Folkman's remarkable achievements in biomedicine. *Proceedings of the National Academy of Sciences of the United States of America* **2008**,105 (36), 13203-13205.

90. Brown, J. M.; Attardi, L. D., The role of apoptosis in cancer development and treatment response. *Nature Reviews Cancer* **2005**,5 (3), 231-237.

91. Richardson, P. G.; Barlogie, B.; Berenson, J.; Singhal, S.; Jagannath, S.; Irwin, D.; Rajkumar, S. V.; Srkalovic, G.; Alsina, M.; Alexanian, R.; Siegel, D.; Orlovski, R. Z.; Kuter, D.; Limentani, S. A.; Lee, S.; Hideshima, T.; Esseltine, D. L.; Kauffman, M.; Adams, J.; Schenkein, D. P.; Anderson, K. C., A phase 2 study of Bortezomib in relapsed, refractory myeloma. *New England Journal of Medicine* **2003**,348 (26), 2609-2617.

92. Richardson, P. G.; Sonneveld, P.; Schuster, M. W.; Irwin, D.; Stadtmauer, E. A.; Facon, T.; Harousseau, J. L.; Ben-Yehuda, D.; Lonial, S.; Goldschmidt, H.; Reece, D.; San-Miguel, J. F.; Bladé, J.; Boccadoro, M.; Cavenagh, J.; Dalton, W. S.; Boral, A. L.; Esseltine, D. L.; Porter, J. B.; Schenkein, D.; Anderson, K. C., Bortezomib or high-dose dexamethasone for relapsed multiple myeloma. *New England Journal of Medicine* **2005**,352 (24), 2487-2498.

93. Adams, J.; Kauffman, M., Development of the proteasome inhibitor Velcade™ (Bortezomib). *Cancer Investigation* **2004**,*22* (2), 304-311.
94. Taberero, J.; Shapiro, G. I.; LoRusso, P. M.; Cervantes, A.; Schwartz, G. K.; Weiss, G. J.; Paz-Ares, L.; Cho, D. C.; Infante, J. R.; Alsina, M.; Gounder, M. M.; Falzone, R.; Harrop, J.; White, A. C. S.; Toudjarska, I.; Bumcrot, D.; Meyers, R. E.; Hinkle, G.; Svrzikapa, N.; Hutabarat, R. M.; Clausen, V. A.; Cehelsky, J.; Nochur, S. V.; Gamba-Vitalo, C.; Vaishnav, A. K.; Sah, D. W. Y.; Gollob, J. A.; Burris Iii, H. A., First-in-humans trial of an RNA interference therapeutic targeting VEGF and KSP in cancer patients with liver involvement. *Cancer Discovery* **2013**,*3* (4), 406-417.
95. Graziani, G.; Szabó, C., Clinical perspectives of PARP inhibitors. *Pharmacological Research* **2005**,*52* (1 SPEC. ISS.), 109-118.
96. Sandhu, S. K.; Yap, T. A.; de Bono, J. S., Poly(ADP-ribose) polymerase inhibitors in cancer treatment: A clinical perspective. *European Journal of Cancer* **2010**,*46* (1), 9-20.
97. Golub, T. R.; Slonim, D. K.; Tamayo, P.; Huard, C.; Gaasenbeek, M.; Mesirov, J. P.; Coller, H.; Loh, M. L.; Downing, J. R.; Caligiuri, M. A.; Bloomfield, C. D.; Lander, E. S., Molecular classification of cancer: Class discovery and class prediction by gene expression monitoring. *Science* **1999**,*286* (5439), 531-527.
98. Blackstock, W. P.; Weir, M. P., Proteomics: Quantitative and physical mapping of cellular proteins. *Trends in Biotechnology* **1999**,*17* (3), 121-127.
99. Gerber, D. E., Targeted therapies: A new generation of cancer treatments. *American Family Physician* **2008**,*77* (3), 311-319.
100. Society, A. C. Carl and Gerty Cori and Carbohydrate Metabolism. <http://www.acs.org/content/acs/en/education/whatischemistry/landmarks/carbohydratemetabolism.html> (accessed 01/25/14).
101. Cohen, P., The origins of protein phosphorylation. *Nature Cell Biology* **2002**,*4* (5), E127-E130.
102. Fischer, E. H.; Krebs, E. G., Conversion of phosphorylase B to phosphorylase A in muscle extracts. *The Journal of Biological Chemistry* **1955**,*216* (1), 121-132.
103. Krebs, E. G.; Fischer, E. H., The phosphorylase b to a converting enzyme of rabbit skeletal muscle. *BBA - General Subjects* **1956**,*20* (C), 150-157.
104. Fischer, E. H.; Graves, D. J.; Crittenden, E. R.; Krebs, E. G., Structure of the site phosphorylated in the phosphorylase B to A reaction. *The Journal of Biological Chemistry* **1959**,*234* (7), 1698-1704.
105. Ingebritsen, T. S.; Cohen, P., The protein phosphatases involved in cellular regulation: 1. Classification and substrate specificities. *European Journal of Biochemistry* **1983**,*132* (2), 255-261.
106. Shoji, S.; Parmelee, D. C.; Wade, R. D.; Kumar, S.; Ericsson, L. H.; Walsh, K. A.; Neurath, H.; Long, G. L.; Demaille, J. G.; Fischer, E. H.; Titani, K., Complete amino acid

sequence of the catalytic subunit of bovine cardiac muscle cyclic AMP-dependent protein kinase. *Proceedings of the National Academy of Sciences of the United States of America* **1981**,78 (2 II), 848-851.

107. Collett, M. S.; Erikson, R. L., Protein kinase activity associated with the avian sarcoma virus src gene product. *Proceedings of the National Academy of Sciences of the United States of America* **1978**,75 (4), 2021-2024.

108. Hunter, T.; Sefton, B. M., Transforming gene product of Rous sarcoma virus phosphorylates tyrosine. *Proceedings of the National Academy of Sciences of the United States of America* **1980**,77 (3 I), 1311-1315.

109. Hunter, T., Tony Hunter: kinase king. Interview by Ruth Williams. *The Journal of Cell Biology* **2008**,181 (4), 572-573.

110. Ushiro, H.; Cohen, S., Identification of phosphotyrosine as a product of epidermal growth factor-activated protein kinase in A-431 cell membranes. *Journal of Biological Chemistry* **1980**,255 (18), 8363-8365.

111. Ubersax, J. A.; Ferrell Jr, J. E., Mechanisms of specificity in protein phosphorylation. *Nature Reviews Molecular Cell Biology* **2007**,8 (7), 530-541.

112. Nobelprize.org. "The Nobel Prize in Physiology or Medicine 1992". <http://www.nobelprize.org/nobel_prizes/medicine/laureates/1992/index.html> (accessed 28/01/14).

113. (a) Hanks, S. K., Genomic analysis of the eukaryotic protein kinase superfamily: A perspective. *Genome Biology* **2003**,4 (5);(b) Stout, T. J.; Foster, P. G.; Matthews, D. J., High-throughput structural biology in drug discovery: Protein kinases. *Current Pharmaceutical Design* **2004**,10 (10), 1069-1082;(c) Hunter, T., Protein kinases and phosphatases: The yin and yang of protein phosphorylation and signaling. *Cell* **1995**,80 (2), 225-236;(d) Manning, G.; Whyte, D. B.; Martinez, R.; Hunter, T.; Sudarsanam, S., The protein kinase complement of the human genome. *Science* **2002**,298 (5600), 1912-1934.

114. Hanks, S. K.; Hunter, T., The eukaryotic protein kinase superfamily: Kinase (catalytic) domain structure and classification. *FASEB Journal* **1995**,9 (8), 576-596.

115. Cohen, P., The regulation of protein function by multisite phosphorylation - A 25 year update. *Trends in Biochemical Sciences* **2000**,25 (12), 596-601.

116. Echols, N.; Harrison, P.; Balasubramanian, S.; Luscombe, N. M.; Bertone, P.; Zhang, Z.; Gerstein, M., Comprehensive analysis of amino acid and nucleotide composition in eukaryotic genomes, comparing genes and pseudogenes. *Nucleic Acids Research* **2002**,30 (11), 2515-2523.

117. Human Protein Kinases Overview. <http://www.cellsignal.com/reference/kinase/overview.html> (accessed 29/01/14).

118. Ghose, A. K.; Herbertz, T.; Pippin, D. A.; Salvino, J. M.; Mallamo, J. P., Knowledge based prediction of ligand binding modes and rational inhibitor design for kinase drug discovery. *Journal of Medicinal Chemistry* **2008**,51 (17), 5149-5171.

-
119. Kritikou, E. Phosphorylate and Conquer *Nature Milestones Cancer* [Online], 2006, p. S17. <http://www.nature.com/milestones/milecancer/full/milecancer16.html> (accessed 03/02/14).
120. Goymer, P. An Important Difference *Nature Milestones Cancer* [Online], 2006, p. S18. <http://www.nature.com/milestones/milecancer/full/milecancer17.html> (accessed 03/01/02).
121. Zhang, J.; Yang, P. L.; Gray, N. S., Targeting cancer with small molecule kinase inhibitors. *Nature Reviews Cancer* **2009**,9 (1), 28-39.
122. Blume-Jensen, P.; Hunter, T., Oncogenic kinase signalling. *Nature* **2001**,411 (6835), 355-365.
123. Paul, M. K.; Mukhopadhyay, A. K., Tyrosine kinase – Role and significance in Cancer. *International Journal of Medical Sciences* **2004**,1 (2), 101-115.
124. Krause, D. S.; Van Etten, R. A., Tyrosine kinases as targets for cancer therapy. *New England Journal of Medicine* **2005**,353 (2), 172-187.
125. Roskoski, R. USFDA Approved Protein Kinase Inhibitors 2013. <http://www.brimr.org/PKI/PKIs.htm> (accessed 04/02/14).
126. Fedorov, O.; Müller, S.; Knapp, S., The (un)targeted cancer kinome. *Nature Chemical Biology* **2010**,6 (3), 166-169.
127. Davies, S. P.; Reddy, H.; Caivano, M.; Cohen, P., Specificity and mechanism of action of some commonly used protein kinase inhibitors. *Biochemical Journal* **2000**,351 (1), 95-105.
128. Shaw, A. T.; Kim, D. W.; Nakagawa, K.; Seto, T.; Crinó, L.; Ahn, M. J.; De Pas, T.; Besse, B.; Solomon, B. J.; Blackhall, F.; Wu, Y. L.; Thomas, M.; O'Byrne, K. J.; Moro-Sibilot, D.; Camidge, D. R.; Mok, T.; Hirsh, V.; Riely, G. J.; Iyer, S.; Tassell, V.; Polli, A.; Wilner, K. D.; Jänne, P. A., Crizotinib versus chemotherapy in advanced ALK-positive lung cancer. *New England Journal of Medicine* **2013**,368 (25), 2385-2394.
129. Geyer, C. E.; Forster, J.; Lindquist, D.; Chan, S.; Romieu, C. G.; Pienkowski, T.; Jagiello-Gruszfeld, A.; Crown, J.; Chan, A.; Kaufman, B.; Skarlos, D.; Campone, M.; Davidson, N.; Berger, M.; Oliva, C.; Rubin, S. D.; Stein, S.; Cameron, D., Lapatinib plus capecitabine for HER2-positive advanced breast cancer. *New England Journal of Medicine* **2006**,355 (26), 2733-2743.
130. Cappuzzo, F., SATURN: A double-blind, randomized, phase III study of maintenance erlotinib versus placebo following nonprogression with first-line platinum-based chemotherapy in patients with advanced NSCLC. *Journal of Clinical Oncology* **2009**,27, 15.
131. Lynch, T. J.; Bell, D. W.; Sordella, R.; Gurubhagavatula, S.; Okimoto, R. A.; Brannigan, B. W.; Harris, P. L.; Haserlat, S. M.; Supko, J. G.; Haluska, F. G.; Louis, D. N.; Christiani, D. C.; Settleman, J.; Haber, D. A., Activating Mutations in the Epidermal Growth Factor Receptor Underlying Responsiveness of Non-Small-Cell Lung Cancer to Gefitinib. *New England Journal of Medicine* **2004**,350 (21), 2129-2139.

132. Kobayashi, S.; Boggon, T. J.; Dayaram, T.; Jänne, P. A.; Kocher, O.; Meyerson, M.; Johnson, B. E.; Eck, M. J.; Tenen, D. G.; Halmos, B., EGFR mutation and resistance of non-small-cell lung cancer to gefitinib. *New England Journal of Medicine* **2005**,*352* (8), 786-792.
133. Daub, H.; Specht, K.; Ullrich, A., Strategies to overcome resistance to targeted protein kinase inhibitors. *Nature Reviews Drug Discovery* **2004**,*3* (12), 1001-1010.
134. (a) Bogoyevitch, M. A.; Fairlie, D. P., A new paradigm for protein kinase inhibition: blocking phosphorylation without directly targeting ATP binding. *Drug Discovery Today* **2007**,*12* (15-16), 622-633;(b) Garuti, L.; Roberti, M.; Bottegoni, G., Irreversible protein kinase inhibitors. *Current Medicinal Chemistry* **2011**,*18* (20), 2981-2994.
135. Thaimattam, R.; Banerjee, R.; Miglani, R.; Iqbal, J., Protein kinase inhibitors: Structural insights into selectivity. *Current Pharmaceutical Design* **2007**,*13* (27), 2751-2765.
136. Carmi, C.; Mor, M.; Petronini, P. G.; Alfieri, R. R., Clinical perspectives for irreversible tyrosine kinase inhibitors in cancer. *Biochemical Pharmacology* **2012**,*84* (11), 1388-1399.
137. Leproult, E.; Barluenga, S.; Moras, D.; Wurtz, J. M.; Winssinger, N., Cysteine mapping in conformationally distinct kinase nucleotide binding sites: Application to the design of selective covalent inhibitors. *Journal of Medicinal Chemistry* **2011**,*54* (5), 1347-1355.
138. Merkul, E.; Klukas, F.; Dorsch, D.; Grädler, U.; Greiner, H. E.; Müller, T. J. J., Rapid preparation of triazolyl substituted NH-heterocyclic kinase inhibitors via one-pot Sonogashira coupling-TMS-deprotection-CuAAC sequence. *Organic and Biomolecular Chemistry* **2011**,*9* (14), 5129-5136.
139. Buckle, D. R.; Rockell, C. J. M.; Smith, H.; Spicer, B. A., Studies on 1,2,3-triazoles. 13. (Piperazinylalkoxy)[1]benzopyrano[2,3-d]-1,2,3-triazol-9(1H)-ones with combined H1-antihistamine and mast cell stabilizing properties. *Journal of Medicinal Chemistry* **1986**,*29* (11), 2262-2267.
140. Bourne, Y.; Kolb, H. C.; Radić, Z.; Sharpless, K. B.; Taylor, P.; Marchot, P., Freeze-frame inhibitor captures acetylcholinesterase in a unique conformation. *Proceedings of the National Academy of Sciences of the United States of America* **2004**,*101* (6), 1449-1454.
141. Fan, W.-Q.; Katritzky, A. R., 4.01 - 1,2,3-Triazoles. In *Comprehensive Heterocyclic Chemistry II*, Katritzky, A. R.; Rees, C. W.; Scriven, E. F. V., Eds. Pergamon: Oxford, 1996; pp 1-126.
142. Potratz, S.; Mishra, A.; Bäuerle, P., Thiophene-based donor-acceptor co-oligomers by copper-catalyzed 1,3-dipolar cycloaddition. *Beilstein Journal of Organic Chemistry* **2012**,*8*, 683-692.
143. Collin, M. P.; Hobbie, S. N.; Böttger, E. C.; Vasella, A., Synthesis of 1,2,3-triazole analogues of lincomycin. *Helvetica Chimica Acta* **2008**,*91* (10), 1838-1848.

144. Irie, T.; Fujii, I.; Sawa, M., Design and combinatorial synthesis of a novel kinase-focused library using click chemistry-based fragment assembly. *Bioorganic and Medicinal Chemistry Letters* **2012**,*22* (1), 591-596.
145. Dempke, W. C. M.; Suto, T.; Reck, M., Targeted therapies for non-small cell lung cancer. *Lung Cancer* **2010**,*67* (3), 257-274.
146. Sharma, S. V.; Bell, D. W.; Settleman, J.; Haber, D. A., Epidermal growth factor receptor mutations in lung cancer. *Nature Reviews Cancer* **2007**,*7* (3), 169-181.
147. (a) Mendelsohn, J.; Baselga, J., The EGF receptor family as targets for cancer therapy. *Oncogene* **2000**,*19* (56), 6550-6565;(b) Olayioye, M. A.; Neve, R. M.; Lane, H. A.; Hynes, N. E., The ErbB signaling network: Receptor heterodimerization in development and cancer. *EMBO Journal* **2000**,*19* (13), 3159-3167;(c) Klapper, L. N.; Waterman, H.; Sela, M.; Yarden, Y., Tumor-inhibitory antibodies to HER-2/ErbB-2 may act by recruiting c-Cbl and enhancing ubiquitination of HER-2. *Cancer Research* **2000**,*60* (13), 3384-3388.
148. Normanno, N.; De Luca, A.; Bianco, C.; Strizzi, L.; Mancino, M.; Maiello, M. R.; Carotenuto, A.; De Feo, G.; Caponigro, F.; Salomon, D. S., Epidermal growth factor receptor (EGFR) signaling in cancer. *Gene* **2006**,*366* (1), 2-16.
149. Kumar, S.; Bawa, S.; Gupta, H., Biological activities of quinoline derivatives. *Mini-Reviews in Medicinal Chemistry* **2009**,*9* (14), 1648-1654.
150. Karunakaran, C. S., A clinical trial of malaria prophylaxis using a single dose of chloroquine at different intervals in an endemic malarious area. *Journal of Tropical Medicine and Hygiene* **1980**,*83* (5), 195-201.
151. Rowland, M.; Durrani, N., Randomized controlled trials of 5- and 14-days primaquine therapy against relapses of vivax malaria in an Afghan refugee settlement in Pakistan. *Transactions of the Royal Society of Tropical Medicine and Hygiene* **1999**,*93* (6), 641-643.
152. Harinasuta, T.; Bunnag, D.; Wernsdorfer, W. H., A phase II clinical trial of mefloquine in patients with chloroquine-resistant falciparum malaria in Thailand. *Bulletin of the World Health Organization* **1983**,*61* (2), 299-305.
153. Senthilkumar, P.; Dinakaran, M.; Yogeewari, P.; Sriram, D.; China, A.; Nagaraja, V., Synthesis and antimycobacterial activities of novel 6-nitroquinolone-3-carboxylic acids. *European Journal of Medicinal Chemistry* **2009**,*44* (1), 345-358.
154. Sadana, A. K.; Mirza, Y.; Aneja, K. R.; Prakash, O., Hypervalent iodine mediated synthesis of 1-aryl/hetryl-1,2,4-triazolo[4,3-a] pyridines and 1-aryl/hetryl 5-methyl-1,2,4-triazolo[4,3-a]quinolines as antibacterial agents. *European Journal of Medicinal Chemistry* **2003**,*38* (5), 533-536.
155. Guo, L. J.; Wei, C. X.; Jia, J. H.; Zhao, L. M.; Quan, Z. S., Design and synthesis of 5-alkoxy-[1,2,4]triazolo[4,3-a]quinoline derivatives with anticonvulsant activity. *European Journal of Medicinal Chemistry* **2009**,*44* (3), 954-958.

156. Clemence, F.; Le Martret, O.; Delevallee, F.; Benzoni, J.; Jouanen, A.; Jouquey, S.; Mouren, M.; Deraedt, R., 4-Hydroxy-3-quinolinecarboxamides with antiarthritic and analgesic activities. *Journal of Medicinal Chemistry* **1988**,*31* (7), 1453-1462.
157. McCall, J. M.; TenBrink, R. E.; Kamdar, B. V.; Skaletzky, L. L.; Perricone, S. C.; Piper, R. C.; Delehanty, P. J., 7-(Trifluoromethyl)-4-aminoquinoline hypotensives: Novel peripheral sympatholytics. *Journal of Medicinal Chemistry* **1986**,*29* (1), 133-137.
158. (a) Wang, Y. D.; Miller, K.; Boschelli, D. H.; Ye, F.; Wu, B.; Floyd, M. B.; Powell, D. W.; Wissner, A.; Weber, J. M.; Boschelli, F., Inhibitors of Src tyrosine kinase: The preparation and structure-activity relationship of 4-anilino-3-cyanoquinolines and 4-anilinoquinazolines. *Bioorganic and Medicinal Chemistry Letters* **2000**,*10* (21), 2477-2480;(b) Mettey, Y.; Vierfond, J. M.; Baudry, M.; Cochet, C.; Sarrouilhe, D., Benzo[c]quinoliziniums: A new family of inhibitors for protein kinase CKII. *Bioorganic and Medicinal Chemistry Letters* **1997**,*7* (8), 961-964.
159. (a) Gentry, C. L.; Lukas, R. J., Local anesthetics noncompetitively inhibit function of four distinct nicotinic acetylcholine receptor subtypes. *Journal of Pharmacology and Experimental Therapeutics* **2001**,*299* (3), 1038-1048;(b) Falkner, B.; Daniels, S. R.; Flynn, J. T.; Gidding, S.; Green, L. A.; Ingelfinger, J. R.; Lauer, R. M.; Morgenstern, B. Z.; Portman, R. J.; Prineas, R. J.; Rocchini, A. P.; Rosner, B.; Sinaiko, A. R.; Stettler, N.; Urbina, E.; Roccella, E. J.; Hoke, T.; Hunt, C. E.; Pearson, G.; Karimbakas, J.; Horton, A., The fourth report on the diagnosis, evaluation, and treatment of high blood pressure in children and adolescents. *Pediatrics* **2004**,*114* (2 III), 555-576;(c) Liu, J. K.; Couldwell, W. T., Intra-arterial papaverine infusions for the treatment of cerebral vasospasm induced by aneurysmal subarachnoid hemorrhage. *Neurocritical Care* **2005**,*2* (2), 124-132.
160. Iwasa, K.; Moriyasu, M.; Tachibana, Y.; Kim, H. S.; Wataya, Y.; Wiegrebe, W.; Bastow, K. F.; Cosentino, L. M.; Kozuka, M.; Lee, K. H., Simple isoquinoline and benzyloisoquinoline alkaloids as potential antimicrobial, antimalarial, cytotoxic, and anti-HIV agents. *Bioorganic and Medicinal Chemistry* **2001**,*9* (11), 2871-2884.
161. Rode, H. B.; Sos, M. L.; Grütter, C.; Heynck, S.; Simard, J. R.; Rauh, D., Synthesis and biological evaluation of 7-substituted-1-(3-bromophenylamino) isoquinoline-4-carbonitriles as inhibitors of myosin light chain kinase and epidermal growth factor receptor. *Bioorganic and Medicinal Chemistry* **2011**,*19* (1), 429-439.
162. Chinchilla, R.; Nájera, C., Recent advances in Sonogashira reactions. *Chemical Society Reviews* **2011**,*40* (10), 5084-5121.
163. Sonogashira, K.; Tohda, Y.; Hagihara, N., A convenient synthesis of acetylenes: catalytic substitutions of acetylenic hydrogen with bromoalkenes, iodoarenes and bromopyridines. *Tetrahedron Letters* **1975**,*16* (50), 4467-4470.
164. Heravi, M. M.; Sadjadi, S., Recent advances in the application of the Sonogashira method in the synthesis of heterocyclic compounds. *Tetrahedron* **2009**,*65* (37), 7761-7775.
165. Chinchilla, R.; Nájera, C., The Sonogashira reaction: A booming methodology in synthetic organic chemistry. *Chemical Reviews* **2007**,*107* (3), 874-922.

166. Xue, L.; Lin, Z., Theoretical aspects of palladium-catalysed carbon-carbon cross-coupling reactions. *Chemical Society Reviews* **2010**,39 (5), 1692-1705.
167. Schelhaas, M.; Waldmann, H., Protecting group strategies in organic synthesis. *Angewandte Chemie - International Edition in English* **1996**,35 (18), 2056-2083.
168. Greene, T. W.; Wuts, P. G. M., *Protective Groups in Organic Synthesis*. John Wiley & Sons: New York, 1991.
169. Palmer, C. J.; Casida, J. E., Selective catalytic hydrogenation of an olefin moiety in the presence of a terminal alkyne function. *Tetrahedron Letters* **1990**,31 (20), 2857-2860.
170. Freeze-Pump-Thaw Degassing of Liquids.
http://depts.washington.edu/eoopic/linkfiles/Freeze_Pump_Thaw.pdf (accessed 10/02/14).
171. Van Aeken, S.; Verbeeck, S.; Deblander, J.; Maes, B. U. W.; Abbaspour Tehrani, K., Synthesis of 3-substituted benzo[g]isoquinoline-5,10-diones: A convenient one-pot Sonogashira coupling/iminoannulation procedure. *Tetrahedron* **2011**,67 (12), 2269-2278.
172. Hosmane, R. S.; Liebman, J. F., Paradoxes and paradigms: Why is quinoline less basic than pyridine or isoquinoline? A classical organic chemical perspective. *Structural Chemistry* **2009**,20 (4), 693-697.
173. Campbell-Verduyn, L. S.; Mirfeizi, L.; Dierckx, R. A.; Elsinga, P. H.; Feringa, B. L., Phosphoramidite accelerated copper(I)-catalyzed [3 + 2] cycloadditions of azides and alkynes. *Chemical Communications* **2009**, (16), 2139-2141.
174. Brotherton, W. S.; Michaels, H. A.; Tyler Simmons, J.; Clark, R. J.; Dalai, N. S.; Zhu, L., Apparent copper(II)-accelerated azide - alkyne cycloaddition. *Organic Letters* **2009**,11 (21), 4954-4957.
175. Steed, J. W.; Atwood, J. L., *Supramolecular Chemistry*. 2nd ed.; Wiley: West Sussex, England.
176. Kolb, H. C.; Finn, M. G.; Sharpless, K. B., Click Chemistry: Diverse Chemical Function from a Few Good Reactions. *Angewandte Chemie - International Edition* **2001**,40 (11), 2004-2021.
177. Hoyle, C. E.; Bowman, C. N., Thiol-ene click chemistry. *Angewandte Chemie - International Edition* **2010**,49 (9), 1540-1573.
178. Blackman, M. L.; Royzen, M.; Fox, J. M., Tetrazine ligation: Fast bioconjugation based on inverse-electron-demand Diels-Alder reactivity. *Journal of the American Chemical Society* **2008**,130 (41), 13518-13519.
179. Kashemirov, B. A.; Bala, J. L. F.; Chen, X.; Ebetino, F. H.; Xia, Z.; Russell, R. G. G.; Coxon, F. P.; Roelofs, A. J.; Rogers, M. J.; McKenna, C. E., Fluorescently labeled risedronate and related analogues: "Magic linker" synthesis. *Bioconjugate Chemistry* **2008**,19 (12), 2308-2310.

180. Stöckmann, H.; Neves, A. A.; Stairs, S.; Brindle, K. M.; Leeper, F. J., Exploring isonitrile-based click chemistry for ligation with biomolecules. *Organic and Biomolecular Chemistry* **2011**,*9* (21), 7303-7305.
181. Spiteri, C.; Moses, J. E., Copper-catalyzed azide-alkyne cycloaddition: Regioselective synthesis of 1,4,5-trisubstituted 1,2,3-triazoles. *Angewandte Chemie - International Edition* **2010**,*49* (1), 31-33.
182. Boren, B. C.; Narayan, S.; Rasmussen, L. K.; Zhang, L.; Zhao, H.; Lin, Z.; Jia, G.; Fokin, V. V., Ruthenium-catalyzed azide-alkyne cycloaddition: Scope and mechanism. *Journal of the American Chemical Society* **2008**,*130* (28), 8923-8930.
183. Moses, J. E.; Moorhouse, A. D., The growing applications of click chemistry. *Chemical Society Reviews* **2007**,*36* (8), 1249-1262.
184. Iha, R. K.; Wooley, K. L.; Nyström, A. M.; Burked, D. J.; Kade, M. J.; Hawker, C. J., Applications of orthogonal "Click" Chemistries in the synthesis of functional soft materials. *Chemical Reviews* **2009**,*109* (11), 5620-5686.
185. Angell, Y. L.; Burgess, K., Peptidomimetics via copper-catalyzed azide-alkyne cycloadditions. *Chemical Society Reviews* **2007**,*36* (10), 1674-1689.
186. Chouhan, G.; James, K., Efficient construction of proline-containing β -turn mimetic cyclic tetrapeptides via CuAAC macrocyclization. *Organic Letters* **2013**,*15* (6), 1206-1209.
187. Wu, P.; Feldman, A. K.; Nugent, A. K.; Hawker, C. J.; Scheel, A.; Voit, B.; Pyun, J.; Fréchet, J. M. J.; Sharpless, K. B.; Fokin, V. V., Efficiency and fidelity in a click-chemistry route to triazole dendrimers by the copper(I)-catalyzed ligation of azides and alkynes. *Angewandte Chemie - International Edition* **2004**,*43* (30), 3928-3932.
188. Kolb, H. C.; Sharpless, K. B., The growing impact of click chemistry on drug discovery. *Drug Discovery Today* **2003**,*8* (24), 1128-1137.
189. (a) Baskin, J. M.; Prescher, J. A.; Laughlin, S. T.; Agard, N. J.; Chang, P. V.; Miller, I. A.; Lo, A.; Codelli, J. A.; Bertozzi, C. R., Copper-free click chemistry for dynamic in vivo imaging. *Proceedings of the National Academy of Sciences of the United States of America* **2007**,*104* (43), 16793-16797;(b) Jewett, J. C.; Bertozzi, C. R., Cu-free click cycloaddition reactions in chemical biology. *Chemical Society Reviews* **2010**,*39* (4), 1272-1279.
190. Rostovtsev, V. V.; Green, L. G.; Fokin, V. V.; Sharpless, K. B., A stepwise Huisgen cycloaddition process: Copper(I)-catalyzed regioselective "ligation" of azides and terminal alkynes. *Angewandte Chemie - International Edition* **2002**,*41* (14), 2596-2599.
191. Tornøe, C. W.; Christensen, C.; Meldal, M., Peptidotriazoles on solid phase: [1,2,3]-Triazoles by regiospecific copper(I)-catalyzed 1,3-dipolar cycloadditions of terminal alkynes to azides. *Journal of Organic Chemistry* **2002**,*67* (9), 3057-3064.
192. Himo, F.; Lovell, T.; Hilgraf, R.; Rostovtsev, V. V.; Noodleman, L.; Sharpless, K. B.; Fokin, V. V., Copper(I)-catalyzed synthesis of azoles. DFT study predicts unprecedented reactivity and intermediates. *Journal of the American Chemical Society* **2005**,*127* (1), 210-216.

193. Hein, J. E.; Fokin, V. V., Copper-catalyzed azide-alkyne cycloaddition (CuAAC) and beyond: New reactivity of copper(i) acetylides. *Chemical Society Reviews* **2010**,39 (4), 1302-1315.
194. Bernard, S.; Defoy, D.; Dory, Y. L.; Klarskov, K., Efficient synthesis of nevirapine analogs to study its metabolic profile by click fishing. *Bioorganic and Medicinal Chemistry Letters* **2009**,19 (21), 6127-6130.
195. Kamata, K.; Nakagawa, Y.; Yamaguchi, K.; Mizuno, N., 1,3-Dipolar cycloaddition of organic azides to alkynes by a dicopper-substituted silicotungstate. *Journal of the American Chemical Society* **2008**,130 (46), 15304-15310.
196. Katayama, T.; Kamata, K.; Yamaguchi, K.; Mizuno, N., A supported copper hydroxide as an efficient, ligand-free, and heterogeneous precatalyst for 1,3-dipolar cycloadditions of organic azides to terminal alkynes. *ChemSusChem* **2009**,2 (1), 59-62.
197. Singh, J.; Petter, R. C.; Kluge, A. F., Targeted covalent drugs of the kinase family. *Current Opinion in Chemical Biology* **2010**,14 (4), 475-480.
198. Singh, J.; Petter, R. C.; Baillie, T. A.; Whitty, A., The resurgence of covalent drugs. *Nature Reviews Drug Discovery* **2011**,10 (4), 307-317.
199. Barf, T.; Kaptein, A., Irreversible protein kinase inhibitors: Balancing the benefits and risks. *Journal of Medicinal Chemistry* **2012**,55 (14), 6243-6262.
200. Ou, S. H. I., Second-generation irreversible epidermal growth factor receptor (EGFR) tyrosine kinase inhibitors (TKIs): A better mousetrap? A review of the clinical evidence. *Critical Reviews in Oncology/Hematology* **2012**,83 (3), 407-421.
201. (a) Wissner, A.; Fraser, H. L.; Ingalls, C. L.; Dushin, R. G.; Floyd, M. B.; Cheung, K.; Nittoli, T.; Ravi, M. R.; Tan, X.; Loganzo, F., Dual irreversible kinase inhibitors: Quinazoline-based inhibitors incorporating two independent reactive centers with each targeting different cysteine residues in the kinase domains of EGFR and VEGFR-2. *Bioorganic and Medicinal Chemistry* **2007**,15 (11), 3635-3648;(b) Mi, Y. C.; Lee, K. O.; Jong, W. K.; Chang, G. L.; Ji, Y. S.; Young, H. K.; Gwan, S. L.; Seung, B. P.; Maeng, S. K., Discovery of a novel Her-1/Her-2 dual tyrosine kinase inhibitor for the treatment of Her-1 selective inhibitor-resistant non-small cell lung cancer. *Journal of Medicinal Chemistry* **2009**,52 (21), 6880-6888;(c) Zhou, W.; Ercan, D.; Chen, L.; Yun, C. H.; Li, D.; Capelletti, M.; Cortot, A. B.; Chirieac, L.; Iacob, R. E.; Padera, R.; Engen, J. R.; Wong, K. K.; Eck, M. J.; Gray, N. S.; Jänne, P. A., Novel mutant-selective EGFR kinase inhibitors against EGFR T790M. *Nature* **2009**,462 (7276), 1070-1074;(d) Chang, S.; Zhang, L.; Xu, S.; Luo, J.; Lu, X.; Zhang, Z.; Xu, T.; Liu, Y.; Tu, Z.; Xu, Y.; Ren, X.; Geng, M.; Ding, J.; Pei, D.; Ding, K., Design, synthesis, and biological evaluation of novel conformationally constrained inhibitors targeting epidermal growth factor receptor threonine 790 → methionine 790 mutant. *Journal of Medicinal Chemistry* **2012**,55 (6), 2711-2723;(e) Zhou, W.; Ercan, D.; Jänne, P. A.; Gray, N. S., Discovery of selective irreversible inhibitors for EGFR-T790M. *Bioorganic and Medicinal Chemistry Letters* **2011**,21 (2), 638-643.
202. Carmi, C.; Cavazzoni, A.; Vezzosi, S.; Bordi, F.; Vacondio, F.; Silva, C.; Rivara, S.; Lodola, A.; Alfieri, R. R.; Monica, S. L.; Galetti, M.; Ardizzoni, A.; Petronini, P. G.; Mor,

- M., Novel irreversible epidermal growth factor receptor inhibitors by chemical modulation of the cysteine-trap portion. *Journal of Medicinal Chemistry* **2010**,*53* (5), 2038-2050.
203. Zhang, L.; Chen, X.; Xue, P.; Sun, H. H. Y.; Williams, I. D.; Sharpless, K. B.; Fokin, V. V.; Jia, G., Ruthenium-catalyzed cycloaddition of alkynes and organic azides. *Journal of the American Chemical Society* **2005**,*127* (46), 15998-15999.
204. Ykman, P.; L'Abbé, G.; Smets, G., Reactions of α -keto- and α -ester phosphorus ylides with carbonyl azides. Isomerization of the reaction products. *Tetrahedron Letters* **1970**,*11* (60), 5225-5228.
205. Krasinski, A.; Fokin, V. V.; Sharpless, K. B., Direct synthesis of 1,5-disubstituted-4-magnesio-1,2,3-triazoles, revisited. *Organic Letters* **2004**,*6* (8), 1237-1240.
206. Fioravanti, S.; Pellacani, L.; Ricci, D.; Tardella, P. A., Stereoselective azide cycloaddition to chiral cyclopentanone enamines. *Tetrahedron Asymmetry* **1997**,*8* (13), 2261-2266.
207. Hou, D. R.; Kuan, T. C.; Li, Y. K.; Lee, R.; Huang, K. W., Electronic effects of ruthenium-catalyzed [3+2]-cycloaddition of alkynes and azides. *Tetrahedron* **2010**,*66* (48), 9415-9420.
208. Majireck, M. M.; Weinreb, S. M., A study of the scope and regioselectivity of the ruthenium-catalyzed [3 + 2]-cycloaddition of azides with internal alkynes. *Journal of Organic Chemistry* **2006**,*71* (22), 8680-8683.
209. Salmon, A. J.; Williams, M. L.; Maresca, A.; Supuran, C. T.; Poulsen, S. A., Synthesis of glycoconjugate carbonic anhydrase inhibitors by ruthenium-catalysed azide-alkyne 1,3-dipolar cycloaddition. *Bioorganic and Medicinal Chemistry Letters* **2011**,*21* (20), 6058-6061.
210. Zhang, J.; Kemmink, J.; Rijkers, D. T. S.; Liskamp, R. M. J., Synthesis of 1,5-triazole bridged vancomycin CDE-ring bicyclic mimics using RuAAC macrocyclization. *Chemical Communications* **2013**,*49* (40), 4498-4500.
211. Johansson, J. R.; Lincoln, P.; Nordén, B.; Kann, N., Sequential one-pot ruthenium-catalyzed azide-alkyne cycloaddition from primary alkyl halides and sodium azide. *Journal of Organic Chemistry* **2011**,*76* (7), 2355-2359.
212. Naota, T.; Takaya, H.; Murahashi, S. L., Ruthenium-catalyzed reactions for organic synthesis. *Chemical Reviews* **1998**,*98* (7), 2599-2660.
213. Bruneau, C.; Dixneuf, P. H., Metal vinylidenes in catalysis. *Accounts of Chemical Research* **1999**,*32* (4), 311-323.
214. Trost, B. M.; Toste, F. D.; Pinkerton, A. B., Non-metathesis ruthenium-catalyzed C-C bond formation. *Chemical Reviews* **2001**,*101* (7), 2067-2096.
215. Boz, E.; Tüzün, N. Ş., Reaction mechanism of ruthenium-catalyzed azide-alkyne cycloaddition reaction: A DFT study. *Journal of Organometallic Chemistry* **2013**,*724*, 167-176.

216. Vanier, G. S., Simple and efficient microwave-assisted hydrogenation reactions at moderate temperature and pressure. *Synlett* **2007**, (1), 131-135.
217. Chandrasekhar, S.; Prakash, S. J.; Rao, C. L., Poly(ethylene glycol) (400) as superior solvent medium against ionic liquids for catalytic hydrogenations with PtO₂. *Journal of Organic Chemistry* **2006**, *71* (5), 2196-2199.
218. Xu, L.; Li, X.; Zhu, Y.; Xiang, Y., One-pot synthesis of *N,N*-dimethylaniline from nitrobenzene and methanol. *New Journal of Chemistry* **2009**, *33* (10), 2051-2054.
219. Xing, W. K.; Ogata, Y., Effect of *meta* and *para* substituents on the stannous chloride reduction of nitrobenzenes in aqueous ethanol. *Journal of Organic Chemistry* **1983**, *48* (15), 2515-2520.
220. Porzelle, A.; Woodrow, M. D.; Tomkinson, N. C. O., Facile procedure for the synthesis of *N*-aryl-*N*-hydroxy carbamates. *Synlett* **2009**, (5), 798-802.
221. Korich, A. L.; Hughes, T. S., A facile, one-pot procedure for forming diarylimines from nitroarenes and benzaldehydes. *Synlett* **2007**, (16), 2602-2604.
222. Pogorelić, I.; Filipan-Litvić, M.; Merkaš, S.; Ljubić, G.; Capanec, I.; Litvić, M., Rapid, efficient and selective reduction of aromatic nitro compounds with sodium borohydride and Raney nickel. *Journal of Molecular Catalysis A: Chemical* **2007**, *274* (1-2), 202-207.
223. Mozingo, R. Catalyst, Raney Nickel, W-2 *Organic Synthesis Collections* [Online], 1955, p. 181. <http://www.orgsyn.org/demo.aspx?prep=cv3p0181> (accessed 08/02/14).
224. Simard, J. R.; Getlik, M.; Grütter, C.; Pawar, V.; Wulfert, S.; Rabiller, M.; Rauh, D., Development of a fluorescent-tagged kinase assay system for the detection and characterization of allosteric kinase inhibitors. *Journal of the American Chemical Society* **2009**, *131* (37), 13286-13296.
225. Schneider, R.; Beumer, C.; Simard, J. R.; Grütter, C.; Rauh, D., Selective detection of allosteric phosphatase inhibitors. *Journal of the American Chemical Society* **2013**, *135* (18), 6838-6841.
226. Schneider, R.; Gohla, A.; Simard, J. R.; Yadav, D. B.; Fang, Z.; van Otterlo, W. A. L.; Rauh, D., Overcoming compound fluorescence in the FLiK screening assay with red-shifted fluorophores. *Journal of the American Chemical Society* **2013**, *135* (22), 8400-8408.
227. Getlik, M.; Simard, J. R.; Termathe, M.; Grütter, C.; Rabiller, M.; van Otterlo, W. A. L.; Rauh, D., Fluorophore labeled kinase detects ligands that bind within the MAPK insert of p38 α kinase. *PLoS ONE* **2012**, *7* (7).
228. Schneider, R.; Becker, C.; Simard, J. R.; Getlik, M.; Bohlke, N.; Janning, P.; Rauh, D., Direct binding assay for the detection of type IV allosteric inhibitors of Abl. *Journal of the American Chemical Society* **2012**, *134* (22), 9138-9141.

229. Simard, J. R.; Klüter, S.; Grütter, C.; Getlik, M.; Rabiller, M.; Rode, H. B.; Rauh, D., A new screening assay for allosteric inhibitors of cSrc. *Nature Chemical Biology* **2009**, *5* (6), 394-396.
230. Pawar, V. G.; Sos, M. L.; Rode, H. B.; Rabiller, M.; Heynck, S.; van Otterlo, W. A. L.; Thomas, R. K.; Rauh, D., Synthesis and biological evaluation of 4-anilinoquinolines as potent inhibitors of epidermal growth factor receptor. *Journal of Medicinal Chemistry* **2010**, *53* (7), 2892-2901.